Roles of Sphingolipids in the Interaction between *Arabidopsis thaliana* and *Pseudomonas syringae*

Eloïse Huby

2022

Roles of Sphingolipids in the Interaction between
Arabidopsis thaliana & *Pseudomonas syringae*

Eloïse HUBY

Original dissertation presented to obtain the degree of doctor in agricultural sciences and biological engineering

- April 2022 –

JURY

Résumé

Les sphingolipides (SLs) sont des molécules ubiquitaires diverses constituant au moins 40% des membranes plasmiques (PM) végétales, initialement connus comme modulateurs de l'intégrité membranaire. Ils sont aujourd'hui décrits chez *Arabidopsis thaliana* comme des acteurs importants dans les réponses aux stress (a)biotiques, les mutants dans la biosynthèse des SLs étant par exemple plus sensibles à *Pseudomonas syringae*. L'immunité innée des plantes repose sur la reconnaissance de motifs d'invasion des agents pathogènes par des récepteurs protéiques. L'interaction incompatible entre *Arabidopsis* et *P. syringae* pv. *tomato* (*Pst*) produisant un effecteur d'avirulence déclenche la réponse hypersensible (HR), une mort cellulaire programmée au site d'infection empêchant la propagation de la bactérie. Nous avons ici mis en évidence que la co-infiltration de *Pst* produisant soit l'effecteur AvrRpm1, AvrB ou AvrPphB et de la sphinganine (SL, d18:0) n'induit pas de HR chez Arabidopsis, en corrélation avec la sous-expression du gène codant la N-myristoyltransférase responsable de l'ajout d'un acide gras sur ces effecteurs dans le cytoplasme de l'hôte. De plus, le d18:0 n'a pas eu d'effet antibactérien direct et les plantes co-infiltrées n'ont pas montré de signes typiques de réponse immunitaire tels que l'augmentation de la production d'acide salicylique et de ROS extracellulaires. Des études biophysiques ont montré que le d18:0 interagissait avec les lipides des PM de plantes et de bactéries. Le SL pourrait donc perturber la composition et l'organisation des PM des plantes, suggérant que cette interaction physique modifierait la reconnaissance des plantes ou leur réponse aux bactéries.

Abstract

  Sphingolipids (SLs) are ubiquitous, highly diverse molecules constituting at least 40% of plant plasma membranes (PM). Initially known as modulators of membrane integrity, they now emerge as important players in plant responses to (a)biotic stresses. It was notably reported that *Arabidopsis thaliana* mutants in SLs biosynthesis were more susceptible to *Pseudomonas syringae*. Plant innate immunity mostly relies on the recognition of invasion patterns stemming from pathogens by proteinaceous receptors. In the incompatible interaction between *Arabidopsis* and *P. syringae* pv. *tomato* producing the effector AvrRpm1 (*Pst AvrRpm1*), this recognition quickly triggers the hypersensitive response (HR), a rapid programmed cell death at the site of infection preventing the spread of the bacterium. In this thesis, we highlighted that the co-infiltration of *Pst AvrRpm1* and the SL sphinganine (d18:0) suppressed HR on *Arabidopsis* leaves, which was also observable with two other bacteria carrying the effectors AvrB and AvrPphB. Such SL-induced HR suppression was correlated with the down-regulation of the gene encoding the N-myristoyltransferase responsible for fatty acylation of these effectors in the host cytoplasm. In addition, d18:0 did not have a direct antibacterial effect and co-infiltrated plants did not display typical signs of immune response such as increased salicylic acid and extracellular ROS production. Biophysical studies showed that d18:0 interacted with plant and bacterial PM lipids. More specifically, it would seem that the SL could disturb plant PM composition and organization suggesting that this physical interaction could alter plant recognition of, or response to the bacteria.

Remerciements

J'adresse de sincères remerciements au Pr. Monica Höfte, au Dr. Sonia Rippa, au Dr. Stephan Dorey, au Dr. Marc Ongena et au Pr. Philippe Jacques pour avoir accepté d'évaluer ces travaux de thèse et ainsi me faire bénéficier de leurs expertises.

Je remercie également le Dr. Laurent Deslandes et le Dr. Laurence Lins, membres de mon Comité de Suivi de Thèse, pour avoir su porter un regard critique pertinent à l'égard de ces travaux et avoir également permis leur bonne avancée.

Merci également au Pr. Ivo Feussner et au Dr. Cornelia Herrfurth de l'Université de Göttingen pour leur contribution et leur expertise pour le dosage des hormones.

Ces travaux de thèse ont été réalisés au sein de deux laboratoires d'accueil, le laboratoire de Résistance Induite et Bioprotection des Plantes, à Reims, et le laboratoire de Biophysique Moléculaire aux Interfaces, à Gembloux. J'exprime donc ma plus grande gratitude, à ma directrice de thèse, Fabienne Baillieul, à mon encadrante Sandrine Dhondt-Cordelier et à ma promotrice de thèse Magali Deleu. Je vous remercie de m'avoir accordé votre temps, votre patience, votre énergie et vos compétences, indispensables à la réalisation de cette thèse. Votre encadrement et la confiance que vous avez placé en moi a su m'apporter l'autonomie et a sans aucun doute contribué à mon évolution en tant que jeune chercheuse.

La réussite de ces travaux n'a été possible que grâce au concours de l'ensemble du personnel technique de mes deux laboratoires. Je remercie donc chaleureusement Sandra Villaume et Catherine Chemotti, pour le temps précieux qu'elles m'ont consacré, aussi bien pour l'aide technique que pour la formation aux techniques indispensables à la réalisation des expériences présentées dans ce manuscrit. Je remercie également Jeff Guise, pour ses conseils d'expert sur la culture de plantes et, entre autres, son aide pour leur entretien pendant mes deux années à Reims. Ma gratitude va aussi à Sébastien Steel, pour son aide technique et pour avoir facilité mes expérimentations (pas nécessairement fructueuses) au TERRA. J'adresse enfin mes remerciements à Marc Ongena pour m'avoir permis l'accès aux ressources du TERRA, à Qassim Esmaeel et Lisa Sanchez pour le partage de leur maitrise de la microbiologie, à Jérôme Crouzet pour m'avoir fait découvrir l'AFM, ainsi qu'à l'ensemble des équipes du RIBP et du LBMI.

Bien entendu, j'adresse un remerciement tout particulier à mes « camarades de classe » français et belges. Marion et Matthieu, les Rémois d'adoption, Aurélien, Willy et Yoann, les post-docs aux connaissances infinies et aux goûts musicaux douteux, Guillaume aka Guillaumpédia, Manon, Katia, Aurélie et Arianne, merci pour votre soutien et votre aide, au labo comme en dehors. Ces quatre années de thèse n'auraient certainement pas été les mêmes sans vous.

Merci à mes parents de m'avoir permis de terminer ces études, aussi longues soient elles, ainsi qu'à l'ensemble de mon entourage le plus proche (même toi Guillaume !) ayant sans équivoque contribué, plus que je ne puis l'exprimer ou l'imaginer, au bon déroulement de cette thèse.

Ces derniers mots iront à Robert, Francine et Véronique, j'aurai voulu célébrer ce diplôme avec vous.

Summary

Scientific valorisation

Oral communications:

- **9th European Symposium on Plant lipids** – Marseille, France – Juillet 2019

Huby, E., Deleu M., Clément C., Baillieul F., and Dhondt-Cordelier S. (2019).

The roles of sphingolipids in the interaction between *Pseudomonas syringae* and *Arabidopsis thaliana*

- **14èmes rencontres Plantes – Bactéries** – Aussois, France – Janvier 2020

Huby, E., Dhondt-Cordelier S., Clément C., Baillieul F., and Deleu M. (2019).

The roles of sphingolipids in the interaction between *Pseudomonas syringae* and *Arabidopsis thaliana*

Flash communications:

- **Journées Jeunes Chercheurs Condorcet 2021** – Online – Janvier 2021

2ème Prix « com flash »

Huby, E., Dhondt-Cordelier S., Clément C., Baillieul F., and Deleu M. (2021).

Le rôle des sphingolipides dans l'interaction entre *Pseudomonas syringae* et *Arabidopsis thaliana*

Poster :

- **Journées transfrontalières, École doctorale URCA** – Reims – Mars 2019

Huby, E., Deleu M., Clément C., Baillieul F., and Dhondt-Cordelier S. (2019).

The roles of sphingolipids in the interaction between *Pseudomonas syringae* and *Arabidopsis thaliana*

Publications :

- Huby, E., Napier, J.A., Baillieul, F., Michaelson, L.V., and Dhondt-Cordelier, S. (2020). Sphingolipids: towards an integrated view of metabolism during the plant stress response. New Phytol *225*, 659–670.

- Huby, E.*, Gilliard, G.*, Cordelier, S., Ongena, M., Dhondt-Cordelier, S., and Deleu, M. (2021). Protoplast: A Valuable Toolbox to Investigate Plant Stress Perception and Response. Front. Plant Sci. *12*, 749581.

List of abbreviations

3-KSR : 3-Ketosphinganine reductase

ABA : Abscisic acid

ACD5 : Accelerated cell death 5

ACER : Alkaline ceramidase

AFM : Atomic force microscopy

Avr : Avirulence

BI-1 : Bax-inhibitor 1

CAC : Critical aggregation concentration

CC : Coiled coil

CDPK : Calcium-dependent protein kinase

CEL : Conserved effector locus

Cer : Ceramide

CERK : Ceramide kinase

CERK1 : Chitin elicitor receptor kinase 1

CFU : Colony forming unit

CL : Cardiolipine

CMC : Critical micellar concentration

Cer-P : Ceramide phosphate

coA : CoenzymeA

Col-0 : Columbia-0

CW : Cell wall

DAG : Diacylglycerol

DAMP : Damage-associated molecular pattern

DhCer : Dihydroceramide

DLS : Dynamic light scattering

DPL1 : Dihydrosphingosine-phosphate lyase

EDS1 : Enhanced disease susceptibility1

EEL : Exchangeable effector locus

EFR : Elongation factor-Tu receptor

EGF : Epidermal growth factor

ET : Ethylene

ETI : Effector triggered immunity

EtOH : Ethanol

ETS : Effector triggered susceptibility

FA : Fatty acid

FAO : Food and agriculture organization

FAH : Fatty acid hydroxylase

FB1 : Fumonisine B1

FLS2 : Flagellin insensitive 2

FW : Fresh weight

GINT1 : Glucosamine inositolphosphorylceramide transferase 1

GIPC : Glycosyl inositol phosphocéramide

GluCer : Glucosylceramide

GMT1 : GIPC mannosyl-transferase 1

GONST1 : Golgi localized nucleotide sugar transporter1

GUV : Giant unilamellar vesicle

Hop : Hrp-dependent outer proteins

Hpi : Hours post inoculation

HR : Hypersensitive response

Hrc : HR conserved

Hrp : HR and pathogenicity

IP : Invasion pattern

IPCS : Inositol phosphorylceramide synthase

IPR : Invasion pattern receptor

IPUT : Inositol phosphorylceramide glucuronosyltransferase

JA : Jasmonate

LB : Lysogeny broth

LCB : Long chain base

LCB-P : Long chain base phosphate

LCB1,2 : Subunit of serine palmitoyltransferase 1 and 2

LCFA : Long chain fatty acid

LOH : Lag one homolog

LORE: Lipooligosaccharide- specific reduced elicitation

LPS : Lipopolysaccharide

LRR : Leucine rich repeat

LUV : Large unilamellar vesicle

MLV : Multilamellar vesicle

M/PAMP : Microbial- / pathogen- associated molecular pattern

M/PTI : MAMP / PAMP /pattern-triggered immunity

MAPK : Mitogen-activated protein kinase

NB : Nucleotide-binding

NCER : Neutral ceramidase

NLP : Necrosis and ethylene-inducing peptide 1-like protein

NLR : nucleotide-binding site leucine-rich repeat

NMT : N-myristoyltransferase

NO : Nitric oxide

OD : Optical density

OPDA : Jasmonate 12-oxo-phytodienoic acid

ORM : Orosomucoid-like protein

PA : Phosphatidic acid

PAI : Pathogenicity island

PC : Phosphatidylcholine

PCD : Programmed cell death

PDF1.2 : Plant defensin 1.2

PE : Phosphatidylethanolamine

PG : Phosphatidylglycerols

PI : Phosphoinositol

PLC : Phospholipase C

PLD : Phospholipase D

PLPC : palmitoyl-linoleoyl-phosphatidylcholine

PM : Plasma membrane

POPE : palmitoyl-oleoyl-phosphatidylethanolamine

POPG : palmitoyl-oleoyl-phosphatidylglycerol

PR : Pathogenesis related

PRR : Pattern recognition receptors

PS : Phosphatidylserine

PTI : Pattern-triggered immunity

Pv. : Pathovar

qRT-PCR : Quantitative reverse transcription polymerase chain reaction

RBOH : Respiratory burst oxidase homolog

RIN4 : RPM1 interacting protein4

RLK : Receptor-like kinase

RLP : Receptor-like protein

RLU : Relative light unit

ROS : Reactive oxygen species

RPM : Resistance to *P. syringae* pv. *maculicola*

RPS : Resistance to *P. syringae*

SA : Salicylic acid

SBH : Sphingoid base hydroxylase

SDN : Stimulateur des défenses naturelles

Sito : Sitosterol

SL : Sphingolipide

SLD : Sphingolipid Δ8 long-chain base desaturase

SPHK : Sphingosine kinase

SPT : Serine palmitoyl transferase

ssSPT : Small subunit of serine palmitoyl transferase

SUV : Small unilamellar vesicles

T3SS : Type III secretion system / Système de sécrétion de type III

TIR : Toll-Interleukin 1 receptor

UBQ5 : Ubiquitin 5

VLCFA : Very long chain fatty acid

VSP1 : Vegetative storage protein 1

WT : Wild type

YEM : Yeast extract medium

List of figures

List of tables

Foreword

Since the settlement of populations and the beginnings of agriculture, humans have had to deal with numerous pests that have had a direct impact not only on people and their nutrition but also on the economy.

The latest IPCC (Intergovernmental Panel on Climate Change) report predicts that the increase in global temperature will lead to an increase in the number and intensity of heat waves with devastating effects on human health, ecosystems and consequently on agriculture (IPCC, 2021). A recent joint report by the IPCC and the FAO (Food and Agriculture Organisation of the United Nation, www.fao.org) also states that climate change will lead to an increase in plant health problems in agrosystems, while highlighting the lack of scientific research on the impact of climate change on pests and their effects on cropping practices (Gullino *et al.*, 2021). In 2019, the FAO already estimated that pests and diseases were responsible for 20-40% of annual losses in agricultural production worldwide, amounting to some US$ 290 billion. With the population expected to grow to between 8 and 10.4 billion people by 2050, the FAO predicts that global agricultural production will need to increase by 70% to meet needs, which means increasing yields while adapting to a changing climate.

Currently, the main way to control these pests is through the use of conventional plant protection products, or pesticides. Some 44 036 tonnes of pesticides were sold in 2020, an increase of 23% compared to the previous year, but still 20% less than between 2015 and 2017 (www.agriculture.gouv.fr). However, more and more resistance to these molecules is being reported (Hawkins *et al.*, 2019) and a decline in their effectiveness has also been highlighted, notably due to changing climatic conditions (Matzrafi, 2019). Furthermore, pesticides have also been widely criticised for their effects on human health (Sabarwal *et al.*, 2018) and the environment (Tang *et al.*, 2021).

Various directives have been put in place to counter the problems caused by conventional plant protection products, such as the ECOPHYTO (I, II & II+) plan in France, which aims to reduce their use by 50% by 2025. The use of biocontrol products, alone or in combination with other plant protection products, is supposed to be more environmentally friendly and is also encouraged by the regulations. Indeed, in order to promote their development in France, these products benefit from accelerated procedures for their marketing and reduced taxes. This alternative to conventional products is

therefore increasingly popular and their sales are constantly increasing: 20% more in 2020 than between 2015 and 2017 (www.ecologie.gouv.fr). These products include macro- and micro-organisms, chemical mediators and natural substances of animal, plant, or mineral origin, of which plant defence stimulators (PDS) or elicitors can be part (www.agriculture.gouv.fr).

Numerous studies show that sphingolipids (SLs) play an important role in both human and plant metabolism. In addition to their important roles in signalling, growth and cell death (Hannun and Obeid, 2008), several benefits of their addition to the human diet have also been put forward, such as the prevention of certain diseases, including skin diseases, bacterial infections, cancers, and neurodegenerative diseases (Wang *et al.*, 2021). In plants, their structural and biological roles, both during development and in response to stress, are well known and widely studied (Ali *et al.*, 2018; Faure and Molino, 2017; Markham *et al.*, 2013). Nevertheless, little research reports the effects of their exogenous application on plants.

Although far from the technical aspect and applied research related to alternatives to pesticides, understanding the interaction between a pathogen, its host and a molecule of interest is complementary to them. It is in this context that this thesis was written, with the aim of deciphering the mechanisms of action of exogenous SLs and more particularly sphinganine in the *Pseudomonas syringae / Arabidopsis thaliana* pathosystem.

General Introduction

I.   Plant immunity

Plants are immobile organisms, constantly exposed to climatic variations, at the base of the food chain and targets of many pathogens and other pests. These can be of various kinds: viruses, bacteria, fungi, insects, nematodes, or even parasitic plants. Plants have therefore developed extremely complex and effective defence mechanisms to survive in this hostile environment (**Figure 1.**) (Bigeard *et al.*, 2015). There are constitutive defences (spines, cuticles, resins, wall…), naturally present in the plant, and induced defences, resulting from their innate immune system.

As plants do not have mobile defence cells or an adaptive immune system, the effectiveness of their resistance to their aggressors is therefore based on the innate immunity of each cell and the perception of signals emanating from the detection of pathogens (Couto and Zipfel, 2016; Jones and Dangl, 2006). In some cases, however, the set of systemic responses developed during an infection can constitute an immunological memory that will allow the plant to prepare its defences and improve its resistance to the pathogen (Martinez-Medina *et al.*, 2016; Reimer-Michalski and Conrath, 2016).

1. Innate immunity

Several types of molecular patterns can be recognised by the plant immune system, PAMPs (Pathogen-associated molecular pattern), MAMPs (Microbe-associated molecular pattern), HAMPs (Herbivory-associated molecular pattern) or DAMPs (Damage-associated molecular pattern) (Boller and He, 2009). These are globally conserved between microorganisms, whether they are pathogenic or not. For example, flg22, a flagellin peptide making up the bacterial flagellum, the lipopolysaccharides (LPS) of bacterial membranes, or the chitin of fungal walls, are among the most studied DAMPs (Jones and Dangl, 2006; Ranf *et al.*, 2015).
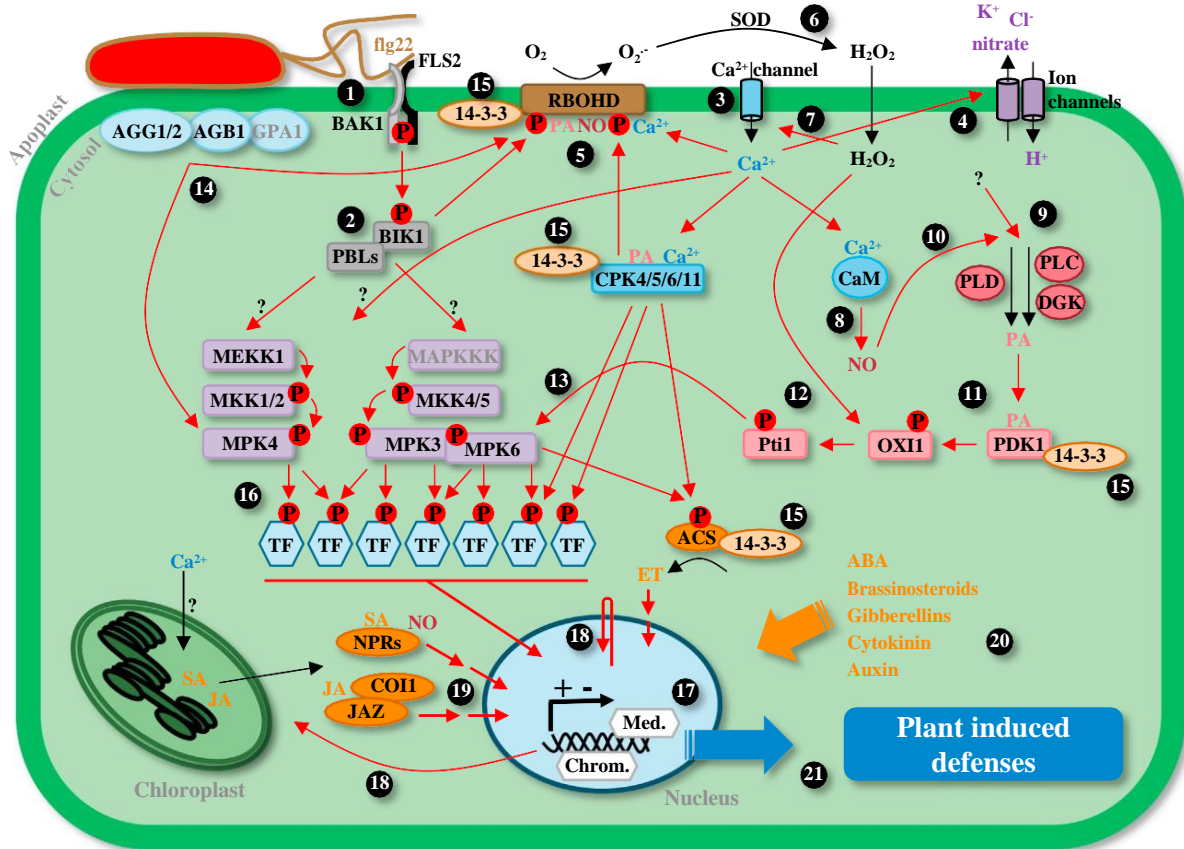
Figure 1: PTI signalling mechanisms (from Bigeard *et al.*, 2015)

Illustration of the complexity of the mechanisms involved in the perception of Flg22 by the PRR FLS2 involving notably a Ca^{2+} burst, the opening of other membrane channels (H^+ influx, K^+, Cl^- and nitrate efflux), a production of ROS via RBOHD regulated by PA and NO the expression of genes involved in SA, JA and ET signalling, the synthesis of antimicrobial compounds. This complex signalling network ultimately leads to the implementation of plant-induced defences. Black arrows indicate enzymatic pathways or transport, and red arrows indicate regulation (direct or indirect activation/inhibition). Question marks indicate unidentified or unclear events. ABA: abscisic acid, ACS: 1-aminocyclopropane-1-carboxylic acid synthase, AGB1: Gβ subunit, AGG1/2: Gγ subunit, BAK1: BRI1-associated receptor kinase, BIK1: *Botrytis*-induced kinase, Chrom: chromatin remodelers/modifiers, COI1: coronatine-insensitive 1, CPK: calcium-dependent protein kinase, DGK: diacylglycerol kinase, ET: ethylene, FLS2: Flagellin-sensitive 2, GPA1: Gα subunit; Med: mediator subunits, JA: jasmonic acid, JAZ: jasmonate ZIM domain, MEKK: MAPK kinase kinase, MKK: MAPK kinase, MPK: mitogen-activated protein kinase, NO: nitric oxide OXI1: oxidative-signal inducible 1 ,PA: phosphatidic acid, PBL: PBS1-like ,PLC: phospholipase C, PLD: phospholipase D, Pti1: Pto-interacting 1, RBOHD: Respiratory burst homolog D ,SA: salicylic acid, SOD: superoxide dismutase, TF: transcription factor.

The zig-zag coevolutionary model divides plant molecular defence strategies in two phases (**Figure 2**) (Jones and Dangl, 2006). The first uses the recognition of MAMP, PAMP or DAMP through plant cell surface-anchored pattern recognition receptors (PRRs) to induce a set of responses such as MAMP-triggered immunity (MTI), PAMP-triggered immunity (PTI), and DAMP-triggered immunity which are collectively referred to as pattern-triggered immunity (PTI; Saijo *et al.*, 2018). The second requires the recognition of microbial effectors, or virulence factors that suppress PTI, through resistance (R) proteins which initiates effector-triggered immunity (ETI). PTI and ETI share many signals and components but their pathways are induced at a different scale and timing (Bjornson and Zipfel, 2021; Yuan *et al.*, 2021a), although some recent studies are finding that PTI is required for full ETI induction and that ETI can in turn induce and stabilize some components of PTI (Ngou *et al.*, 2021; Yuan *et al.*, 2021b; Pruitt *et al.*, 2021), also suggesting a mechanistic link between PTI signalling and ETI activation (Bjornson and Zipfel, 2021).

Although the "zig-zag" model has long been used and accepted by the scientific community, it does not include all the mechanisms involved in plant immunity, particularly the fact that some effectors are recognised by PRRs and not NLRs. In 2015, Cook *et al.* therefore proposed a new model grouping MAMPs, DAMPs and effectors under the term invasion factors (IP, Invasion pattern). The term IP includes for example double-stranded viral RNA and molecular signals from arbuscular mycorrhizal fungi and nitrogen-fixing rhizobia (van der Burgh and Joosten, 2019). According to this model, PTI and ETI become a single process that relies on the perception of IPs by IPRs (Invasion pattern receptors) and results in the induction of the plant immune response.

a. PTI

PTI is based on the recognition of molecular patterns by plasma membrane (PM)-associated pattern recognition receptors (PRRs). PRRs usually are receptor-like kinases (RLKs), which are the most numerous, and receptor-like proteins (RLPs), which do not have an intracellular kinase domain (Bentham *et al.*, 2020; Couto and Zipfel, 2016; Ngou *et al.*, 2021). These PRRs can be further subdivided according to the nature of their extracellular domain, among others (Zipfel, 2014):
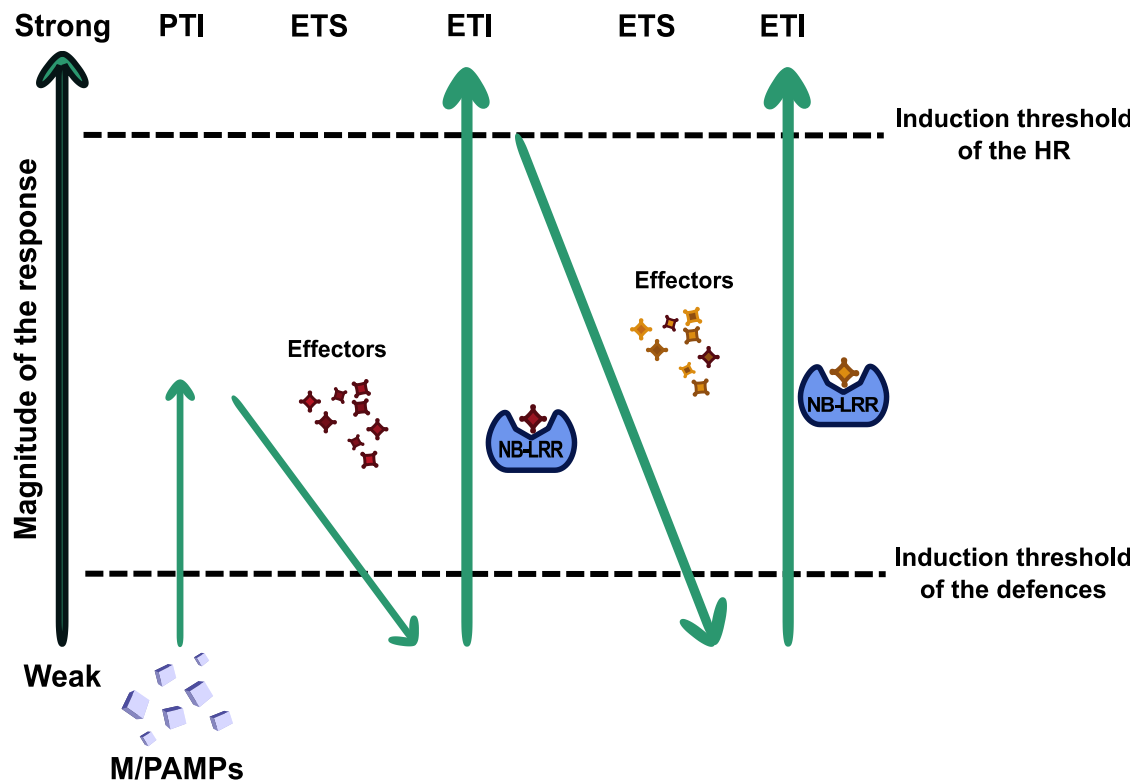
Figure 2. The zig-zag model of plant immunity (adapted from Jones & Dangl 2006)

Phase 1: M/PAMPs (Pathogen/Microbial-Associated Molecular Patterns) are perceived by PRRs (Pattern recognition receptors), induce PTI (PAMP/MAMP-triggered immunity). **Phase 2:** the pathogen translocates effectors into the target cell which alter the M/PTI, giving ETS (Effector-triggered sensitivity). **Phase 3:** an effector is recognised by an NLR (Nucleotide binding-leucine rich repeat) protein triggering ETI (Effector triggered immunity), an accelerated and amplified version of PTI, resulting in HR (Hypersensitive response). **Phase 4:** Other effectors will block the ETI, leading once again to the ETS and if the plant has the NB-LRR corresponding to the effector, triggering a new ETI.

- Leucine rich repeat: preferentially bind proteins or peptides such as flagellin
- Lysin motif: preferentially bind carbohydrate-containing molecules, such as chitin or bacterial peptidoglycans.
- Lectin-type: bind ATP and bacterial lipids.
- Epidermal growth factor (EGF): recognise oligogalacturonide derivatives of the plant cell wall (CW).

PRRs specifically interact with several types of molecules to trigger defence mechanisms in plants, for instance, FLAGELLIN INSENSITIVE 2 (FLS2) and elongation factor-Tu receptor (EFR) are PRRs that recognize flg22 (Bauer *et al.*, 2001) and the bacterial elongation factor-Tu (Zipfel *et al.*, 2006), respectively. The chitin elicitor receptor kinase 1 (CERK1) perceives chitin and peptidoglycan (Miya *et al.*, 2007) and the *Arabidopsis* PRR, LIPOOLIGOSACCHARIDE-SPECIFIC REDUCED ELICITATION (LORE) perceives medium-chain 3-hydroxy fatty acid, the building block of bacterial LPS (Kutschera *et al.*, 2019). Most non-adapted plant pathogens will not be able to pass this first line of defence (Couto and Zipfel, 2016).

b. ETI

In some cases, pathogens will have adapted and will be able to secrete effectors that interfere with the PTI. These effectors have various effects on the host plant cells and aim to hijack its metabolism to promote the growth of the pathogen. *Pseudomonas syringae* (*P. syringae*), for example, produces several of them, such as HopZ1 which targets tubulin or AvrPto which targets multiple kinases (Deslandes and Rivas, 2012). These effectors and their effects will be discussed in more detail in section **VI.** of the Introduction to this manuscript.

In response, some plants have developed intracellular immune receptors, namely nucleotide binding (NB) leucine rich repeat (LRR) receptor (NLR) proteins, encoded by resistance (R) genes that recognize effectors or their activity to trigger the effector-triggered immunity (ETI) and thus restore an effective immune response (Couto and Zipfel, 2016; Jones and Dangl, 2006; Nguyen *et al.*, 2021). Two main classes of NLRs can be distinguished, CC-NLRs, containing an N-terminal coiled-coil domain (CC) and TIR-NLRs, containing an N-terminal toll-interleukin 1 receptor (TIR) domain (Coll *et al.*, 2011). NLR can induce ETI either by directly recognizing effectors or by indirectly recognizing host proteins that have been modified by effector activity (Ade *et al.*, 2007; Wang *et al.*, 2019). In indirect recognition model, NLR protein either recognize effector modified host target protein known as guardee, that is bound to and monitored by NLR protein, or recognize effectors modified plant decoy protein that mimic host target protein (Bentham *et al.*, 2020; Block and Alfano, 2011). This phenomenon will be discussed in part **VII.** of the Introduction.

If the plant has receptors adapted to the effectors of the pathogen, it will be qualified as "resistant", and the pathogen will not develop. On the other hand, if the plant does not have the appropriate receptors and the pathogen can develop in it, it will be called "susceptible" (Jones and Dangl, 2006; Katagiri *et al.*, 2002). Natural selection will cause pathogens to develop effectors that suppress or bypass the ETI, thus causing plants to co-evolve in parallel.

2. Signalling and defence responses

a. Constitutive defences

These defences constitute the first obstacle that pathogens will face. They are both physical and biochemical barriers that limit their entry into the plant. Physical barriers include spines, trichomes, hairs on the surface of the aerial parts, the cuticle, which is partly composed of waxes, and the plant wall (Bacete *et al.*, 2018; Domínguez *et al.*, 2017). Biochemical defences include compounds that serve to defend against herbivores or have antimicrobial activities, such as phytoanticipins (VanEtten *et al*, 1994). This includes odorous triterpenes (limonene, geraniol, etc.), whose role is to repel insects, alkaloids such as caffeine or nicotine, and other compounds resulting from the secondary metabolism of plants (Bennett and Wallsgrove, 1994; Kaplan *et al.*, 2008; Moore and Johnson, 2017).

b. Signalling and inducible responses

Several types of responses can be mounted by the plant to respond to pathogen attacks. These can be classified into two categories, early responses that occur within seconds to minutes of the perception of a MAMP, and late responses, which follow several hours later.

Signalling phenomena and early responses

Although their roles are not yet fully understood, signalling phenomena will first act as messengers and allow the modification of the plant's immune status in order to trigger underlying defence phenomena.

The first observable phenomenon, triggered 30 seconds to 2 minutes after the perception of the pathogen by the plant, is an induction of ion flows in the cytosol, particularly calcium ions. Crucial for the continuation of the immune response, this influx will lead to the activation of multiple kinases, including calcium-dependent protein kinases (CDPK) (Coca and San Segundo, 2010; Singh *et al.*, 2017). Several isoforms of CDPKs exist and allow the regulation of plant immunity through the production and accumulation of phytohormones followed by transcriptional reprogramming of defence genes (Bredow and Monaghan, 2019; Singh *et al.*, 2017). For example, overexpression of *AtCDPK1* is linked to an increase in the amount of the hormone salicylic acid (SA), followed by induction of the expression of SA-regulated defence genes, leading to increased resistance to *Botrytis cinerea* (*B. cinerea*) and the bacterium *P. syringae* (Coca and San Segundo, 2010).

This is followed by the production of reactive oxygen species (ROS), which starts 4-6 minutes after the perception of the pathogen. ROS have not only major roles in plant adaptation to stress but also in plant development and growth (Qi *et al.*, 2017). This class of molecules includes hydrogen peroxide (H_2O_2), superoxide anions ($O_2.^-$) and hydroxyl radicals ($\cdot OH$). Of these, H_2O_2 is the most stable and often acts as an intra- and intercellular signal (Baxter *et al.*, 2014). ROS are produced in different cellular compartments such as the CW, PM, mitochondria or even chloroplasts and peroxisomes (Qi *et al.*, 2017). Under normal conditions, these ROS are natural by-products of plant metabolism and are detoxified to protect cellular functions from their powerful antioxidant capacities (Halliwell, 2006). Under stress conditions, ROS production is predominantly apoplastic, rapid and transient (Kadota *et al.*, 2015; Yu *et al.*, 2017). It acts either directly, as an anti-microbial agent (O'Brien *et al.*, 2012) and in CW reinforcement (Kärkönen and Kuchitsu, 2015), or indirectly as a signalling agent during HR (Torres, 2010). This production is dependent on PM-related NADPH oxidases, known as Rboh (Respiratory burst oxidase homolog). In *Arabidopsis thaliana* (*Arabidopsis*), 10 members of this family have been identified and RbohD and F appear to be mainly responsible for the oxidative peaks observed in response to MAMPs and microbial agents (Sagi and Fluhr, 2006). Their localisation at the PM is well known (Simon-Plas *et al.*, 2011) and other studies have specified their organisation in clusters at the microdomain level (Hao *et al.*, 2014; Mongrand *et al.*, 2004). Rbohs also possess a calcium-binding domain, suggesting regulation of ROS production by the calcium influx caused by pathogen perception (Kadota *et al.*, 2015). Their signalling activity has also been shown to be dependent on nitric oxide (NO). Indeed, NO is synthesised by the plant at the same time as ROS after pathogen detection (Huang *et al.*, 2019). It has been shown that a balanced synthesis of these two types of molecules is necessary for the triggering of the HR (Delledonne *et al.*, 2001) and that NO-mediated S-nitrosylation of *AtRbohD* governs a negative feedback loop limiting ROS production and consequently HR (Yun *et al.*, 2011).

After this production of ROS and NO follows the production of phosphatidic acid (PA). PA synthesis can be achieved either by phospholipid cleavage by an enzyme of the phospholipase D family or by phosphorylation of diacylglycerol (DAG) by the DAG kinase. DAG itself being produced by phospholipase C mediated degradation of phosphoinositide (Johansson *et al.*, 2014; Li and Wang, 2019). PA is present in low proportions in PM under controlled conditions, but its content increases sharply in response to many stresses, including PTI and ETI (Bargmann and Munnik, 2006). This phospholipid is thought to play several roles in the regulation of the plant's immune defences, including an impact on hormone signalling and ROS production (Li and Wang, 2019).

Finally, a few minutes after the perception of the pathogen, a phosphorylation cascade is triggered to transmit the information to the nucleus. These cascades are dependent on three kinds of kinases: MAPKKKs (Mitogen-activated protein kinase kinase kinases), MAPKKs and MAPKs (Asai *et al.*, 2002; Yu *et al.*, 2017).

Signalling phenomena and late responses

Transcription factors control many processes involved in plant immunity all the while maintaining the balance between growth and optimal defence. As such, they are subject to transcriptional and post-transcriptional control as well as post-translational modifications (Singh *et al.*, 2002). In plants, there are several families of transcription factors involved in responses to biotic stresses, including bHLH (basic helix-loop-helix), MYB (myeloblastosis related), WRKY or NAC (No apical meristem, *Arabidopsis* transcription activation factor, cup-shaped cotyledon) (Ng *et al.*, 2018). In response to biotic stresses, transcription factors transform external signals into intracellular signals, triggering hormonal signalling pathways and gene expression cascades for the activation and regulation of defence-related genes (Singh *et al.*, 2002).

Thus, a few tens of minutes after the triggering of early responses, the levels of phytohormones involved in defence phenomena are modulated (Yu *et al.*, 2017). The two most studied hormones in plant defence phenomena are SA and jasmonic acid (JA). Numerous studies prove that SA and JA pathways communicate with each other and are even thought to be antagonistic (Li *et al.*, 2019; Shigenaga *et al.*, 2017; Zhou and Zhang, 2020). In *Arabidopsis*, SA is responsible for plant resistance to biotrophic pathogens that colonise living cells, while JA is associated with resistance to necrotrophic pathogens that invade dead cells (Betsuyaku *et al.*, 2018). Often, when JA is involved in resistance phenomena, ethylene (ET) seems to enhance its action and thus increases resistance to necrotrophs (Penninckx *et al.*, 1998). Other hormones are involved in plant defence phenomena and act by modulating the SA / JA - ET pathways, such as abscisic acid (ABA), auxin, brassinosteroids, gibberellic acid, cytokinins or strigolactones (Li *et al.*, 2019).

Variations in hormone content will lead, under the control of transcription factors, to changes in the expression of many genes, particularly those encoding PR (Pathogenesis related) proteins and peptides (Bari and Jones, 2009). This is the case, for example, for the genes *PR1* and *PR5*, overexpressed in response to SA, *PDF1.2* (Plant defensin 1.2), overexpressed in response to JA and ET and *VSP1* (Vegetative storage protein 1) overexpressed in response to JA (Glazebrook, 2005; Guerineau *et al.*, 2003). Finally, phytoalexins with antimicrobial properties can also be produced, such as camalexin by *Arabidopsis* (Zhang *et al.*, 2014). One to several hours after pathogen perception, other responses are initiated, such as the deposition of callose (a β1-3 glucan polymer)

between the CW and the PM, as well as stomata closure to limit their entry into the plant (Yu *et al.*, 2017).

Finally, as mentioned earlier, the specific effector/NLR recognition during ETI can result in a HR (Hypersensitive response), a form of programmed cell death (PCD) that aims to prevent the spread of the pathogen (Coll *et al.*, 2011; Heath, 2000). As a result, this mode of defence is effective against (hemi)biotrophic pathogens but much less so against necrotrophs such as *B. cinerea* (Govrin and Levine, 2000).

II. Plasma membranes of plants and bacteria

PMs, whether of plants or bacteria, are much more complex entities than the simple model of lipid bilayers with embedded proteins. They are the point of exchange and communication between a cell and its environment and therefore have a major role in their functioning and adaptation to external changes. As the PM is a dynamic structure, any change resulting from the activity of a molecule, whether from a pathogen or not, will have repercussions on its function and integrity and consequently on its membrane proteins. Composed of a hydrophilic head and a hydrophobic body, the lipids of PMs are arranged in two sheets forming a bilayer and the lipid content of these sheets varies between organisms (van Meer *et al.*, 2008).

1. In plants

The plant PM constitutes a physical barrier that is selectively permeable to certain solutes and macromolecules, allowing, among other things, the maintenance of cell homeostasis and acting as a platform for signal transduction, particularly in defence phenomena (Gronnier *et al.*, 2016). The PM is extremely complex, composed of lipids and a large diversity of proteins, and must be stable but also fluid and adaptable (Mamode Cassim *et al.*, 2019). Its organisation, originally proposed in 1972 by Singer and Nicholson as a 'fluid mosaic' (Nicolson, 2014; Singer and Nicolson, 1972), has in fact been shown to be much more complex, with proteins and lipids being able to segregate to form heterogeneous asymmetric domains (Mamode Cassim *et al.*, 2019).

a. Lipid composition

Plant PM is partly composed of glycerophospholipids, whose basic backbone is composed of a glycerol attached to two esterified fatty acid chains, and a phosphate moiety to which a specific

moiety is attached. Phosphatidylcholines (PC) and phosphatidylethanolamines (PE) alone represent nearly 50% of the total membrane lipids, making them the major phospholipids of the PM. Phosphatidylserines (PS), phosphatidylinositols (PI), phosphatidylglycerols (PG) and PA are present in the PM in a minority (**Figure 3.**) (Furt *et al.*, 2011; Mamode Cassim *et al.*, 2019; van Meer *et al.*, 2008).

SLs, especially their glycosylated forms, such as glucosylceramide (GluCer) or glycosyl inositol phosphoceramides (GIPC) (**Figure 3.**), are mainly concentrated in the outer leaflet of the PM and account for up to 40 mol% of the PM lipids in tobacco (Mamode Cassim *et al.*, 2019). Their major structural and biological roles will be developed later (see **IV.**).

Phytosterols, free or conjugated, whose quantity is relatively stable between species, accumulate in the PM, to represent up to 30% of its total lipids (Cacas *et al.*, 2016). In plants there are many species, unlike the single sterols in animals, cholesterol, and in fungi, ergosterol. However, sitosterol (**Figure 3.**) appears as the main one in most species, including *Arabidopsis*. There are also glycosylated forms of sterols, steryl glucosides and their acylated forms, which are derivatives of membrane sterols and their amounts in plant cells vary greatly depending on the species and growth conditions (Mamode Cassim *et al.*, 2019). Their role as structural components of the membrane has only recently been highlighted and not all their functions have yet been elucidated (Moreau *et al.*, 2018). Phytosterols are the major contributors to PM stiffness, although each phytosterol contributes in different ways. For exemple stigmasterol, found in tobacco, shows a lower capacity to stiffen the PM than sitosterol. These molecules, in free and conjugated form, work synergistically within the membrane to order it (Grosjean *et al.*, 2015).
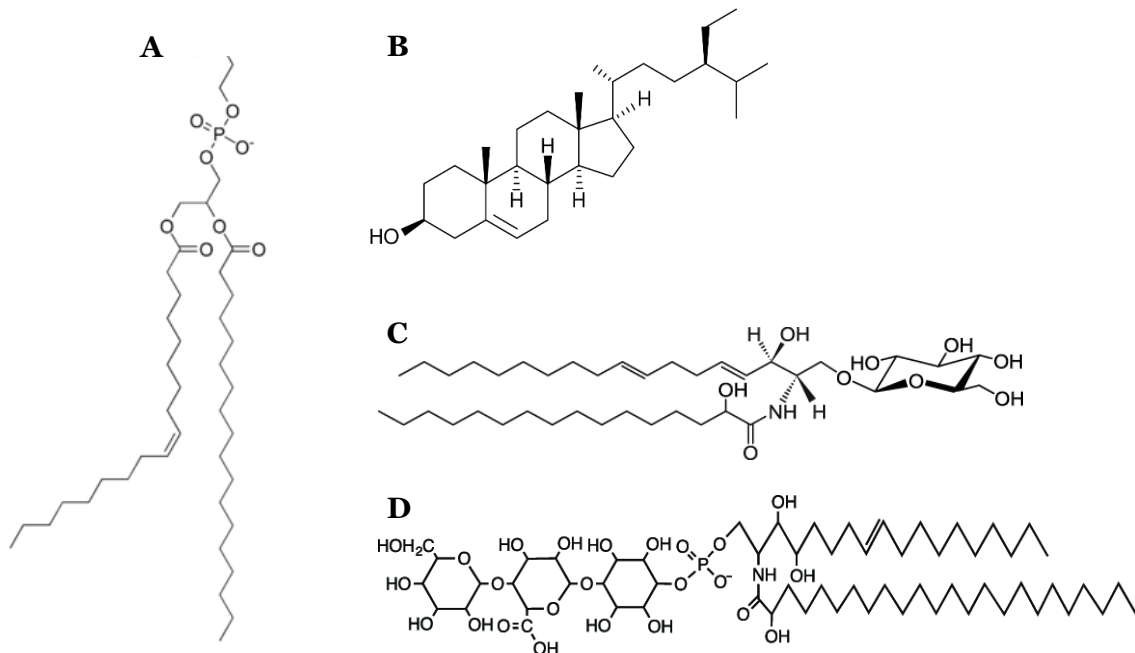
Figure 3: Structure of major lipids in *Arabidopsis*

A. Basic phospholipid skeleton. The R-radical can correspond to choline (PC), ethanolamine (PE), serine (PS), inositol (PI) or glycerol (PG) (adapted from Furt *et al.* 2011). **B.** Structure of sitosterol **C.** Structure of a glucosylceramide (Ceramide 4,8-sphingadiene alpha-hydroxypalmite). **D.** Structure of a glycosyl inositol phosphoceramide (GIPC).

b. Organisation

In terms of lipid composition, eukaryotic PMs are asymmetric (**Figure 4.**). In plants, the outer leaflet is mainly composed of SL and phytosterols while the inner leaflet comprises more phospholipids (Gronnier *et al.*, 2018). These lipids can be in different states in the PM depending on the physiological conditions. In general, there are three distinct states (Mamode Cassim *et al.*, 2019):

- A liquid-disordered phase, characterised by the presence of glycerophospholipids with unsaturated chains. The lipids are not highly condensed, their acyl chains are mobile and lateral diffusion is important.
- A solid-gel phase, rich in SL, where the lipids are densely condensed and lateral diffusion is very slow.

- A liquid-ordered phase, formed by the association of SL and sterols, where the lipids are as condensed as in the solid-gel phase but with a lateral diffusion similar to that of the disordered liquid phase.

Within the PM coexist particular domains formed by an assembly of lipids and proteins. The nanodomains (size < 1 μm) and microdomains (size > 1 μm) which seem to carry multiple proteins (Grosjean *et al.*, 2015; Mongrand *et al.*, 2010), some of which are related to plant defence (Shahollari *et al.*, 2004), which will be developed later in this chapter (see **IV.**).
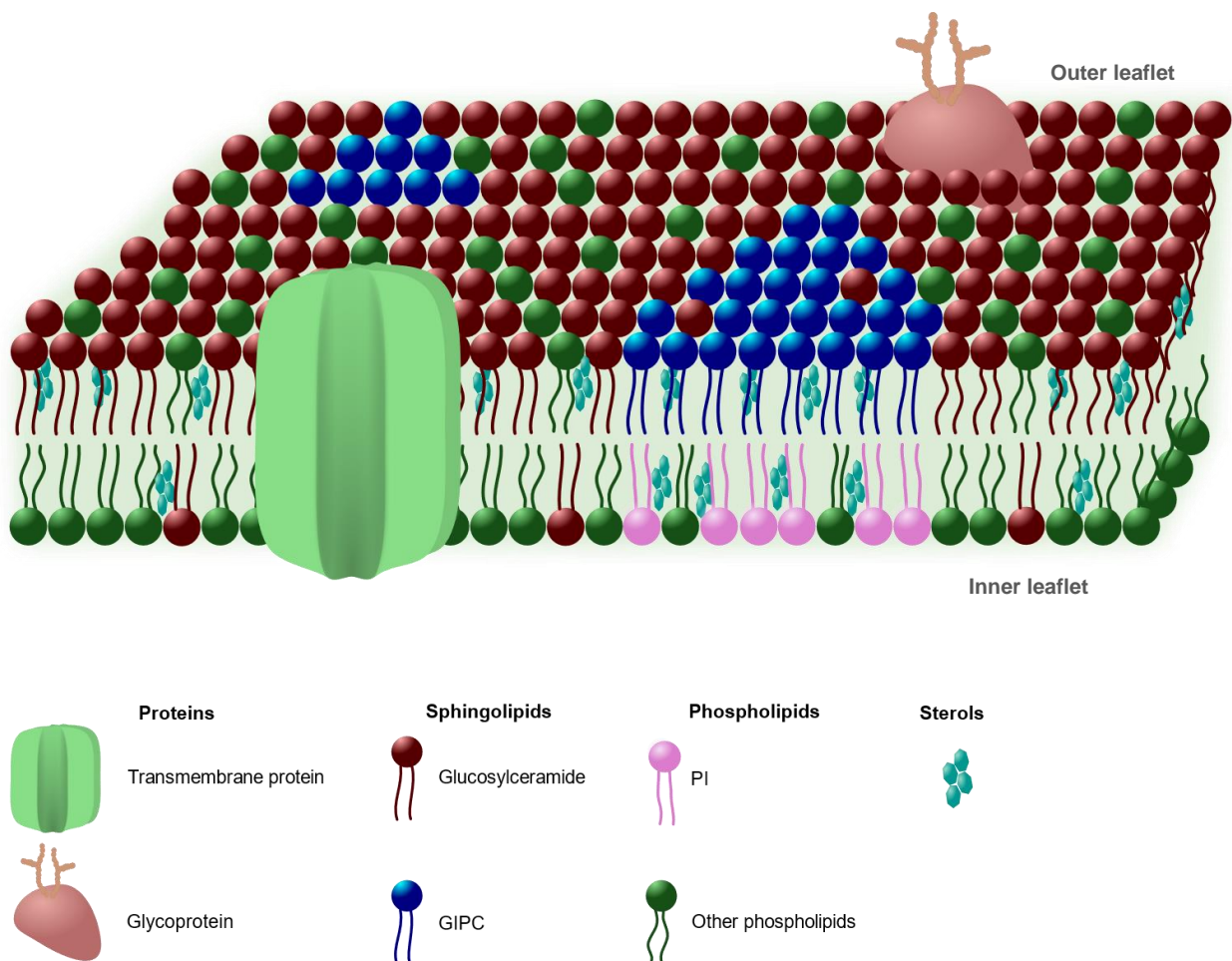
Figure 4: Schematic representation of a plant plasma membrane (adapted from Cacas *et al.*, 2016)

The lipids of plant plasma membranes are distributed asymmetrically between the cytosolic and apoplastic layers. Some of these lipids are grouped in microdomains composed mainly of sphingolipids and sterols. Various proteins, transmembrane or not, are distributed in this membrane.

2. In bacteria

Bacteria are generally divided into two categories according to their wall structure, Gram+ and Gram-. While Gram+ bacteria have a single PM surrounded by a thick wall of peptidoglycans, Gram- bacteria have two PMs, an inner and an outer, separated by a thin layer of peptidoglycans. The outer PM consists mainly of LPS. The inner PM is composed of glycerophospholipids, such as PS, PE, PG, PI, hopanoids or cardiolipin (CL) (Sohlenkamp and Geiger, 2016).

Classically, for Gram- bacteria, PE is the most abundant, representing up to 70 or even 80% of the total lipids of the internal PM, PG represents about 15-20% and CL about 5%. These amounts can vary depending on the mitotic stage of the bacteria and the environmental conditions (Le *et al.*, 2011). The presence of this outer membrane directly impacts the activity of certain antibacterial compounds, such as rhamnolipids, which would then be more effective on Gram+ bacteria (Naughton *et al.*, 2019).

III. Sphingolipids, ubiquitous and versatile molecules

SLs are ubiquitous lipids in eukaryotes and can also be found in some bacteria. In the animal kingdom, they are particularly present in PMs, the major SL of which is sphingomyelin, essential for many biological phenomena such as nerve signal transduction, apoptosis, cell ageing and development (Hannun and Obeid, 2008; Ramstedt and Slotte, 2002). In plants, they are also found in tonoplasts and endomembranes. They account for nearly 40% of the lipids in the PM, where they are particularly concentrated in the outer leaflet and play a role in its integrity and permeability to ions (Cacas *et al.*, 2016). In addition to their structural role, they also play a biological role, whether during PCD during plant development or immunity, ABA-dependent closure of stomatal guard cells or as mediators in (a)biotic stress responses (Ali *et al.*, 2018; Huby *et al.*, 2020; Markham *et al.*, 2013). The review article summarising and detailing the biosynthetic pathway and roles of SLs in biotic and abiotic stresses is available in **Appendix I** (Huby *et al.*, 2020).

1. Biosynthesis, structure, and occurrence of sphingolipids

a. Plant sphingolipids

This class of lipids shows a very high structural diversity. For example, up to 168 types of SLs have been identified in the model plant *Arabidopsis* (Markham and Jaworski, 2007). The basic skeleton of SLs is formed by long chain bases (LCBs) composed of carbon chains (typically 18 carbon atoms) characterised by the presence of a hydroxyl group in positions 1 and 4, and an amine group in position 2 (**Figure 5. and 6.**) (Merrill, 2011). This basic structure can be linked to a fatty acid (FA) to form ceramides. These FAs are separated into two categories, LCFAs (Long chain fatty acid: C14 to C20) or VLCFAs (Very long chain fatty acid: C20-36) (Lynch and Dunn, 2004; Markham *et al.*, 2013). Finally, a ceramide can be more complex, either by simple variations in chain length, by methylation, hydroxylation, or desaturation of the LCB and/or FA parts, or by conjugation with polar groups in position 1 of the LCB. These include phosphoryl groups, mono- or multi-hexoses (glucosylceramide) or inositol phosphate groups (**Figure 5.**) (Berkey *et al.*, 2012; Lynch and Dunn, 2004; Sperling and Heinz, 2003).
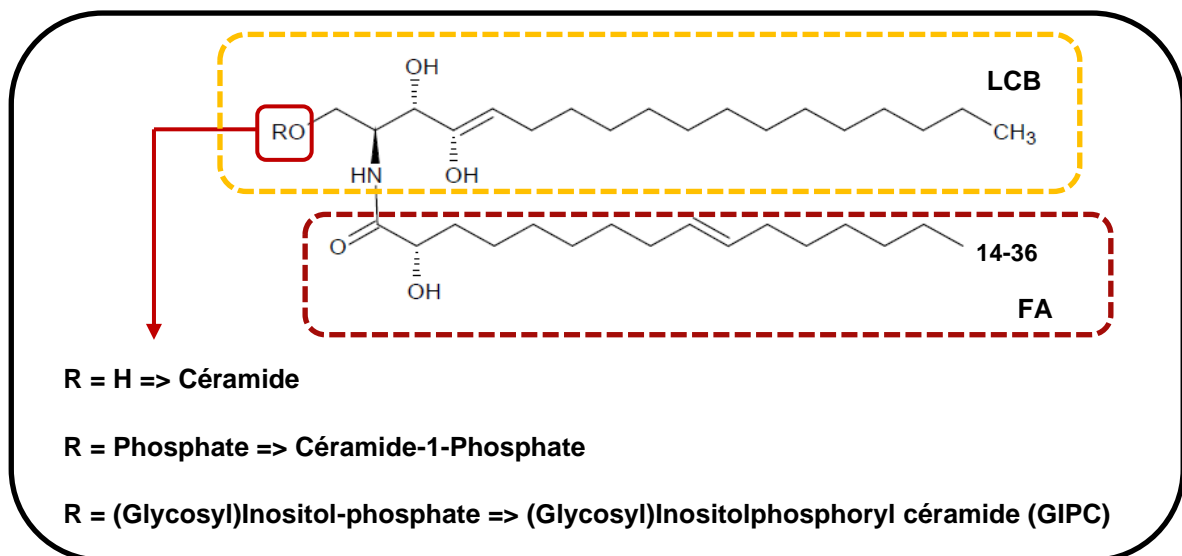
Figure 5. Ceramide, the basic structure of more complex sphingolipids (from Berkey *et al.*, 2012).

Ceramide is composed of two structures, a long chain base (LCB) and a fatty acid (FA) linked by an amide group. A LCB typically has an 18-carbon chain, which can be hydroxylated at the 4-position and can have a double bond at the 4- or 8-position. The FA has a chain of 14 to 36 carbons, which can be hydroxylated at position 1 and have a double bond at position 9. This ceramide can then be modified by substitution of the R group at position 1 of the LCB. Other residues can be added to the inositol phosphate groups and GluCer to form other more complex SLs.

Despite this great structural diversity, SLs are classified into four categories (Pata *et al.*, 2010):

- LCBs
- Ceramides (Cer)   In free or phosphorylated form (LCB-P, Cer-P)
- Glucosylceramides (GluCer)
- Glycosyl Inositol Phosphoceramides (GIPC)

In *Arabidopsis*, they represent 0.5%, 2%, 34% and 64% of total SLs respectively (Mamode Cassim *et al.*, 2019).
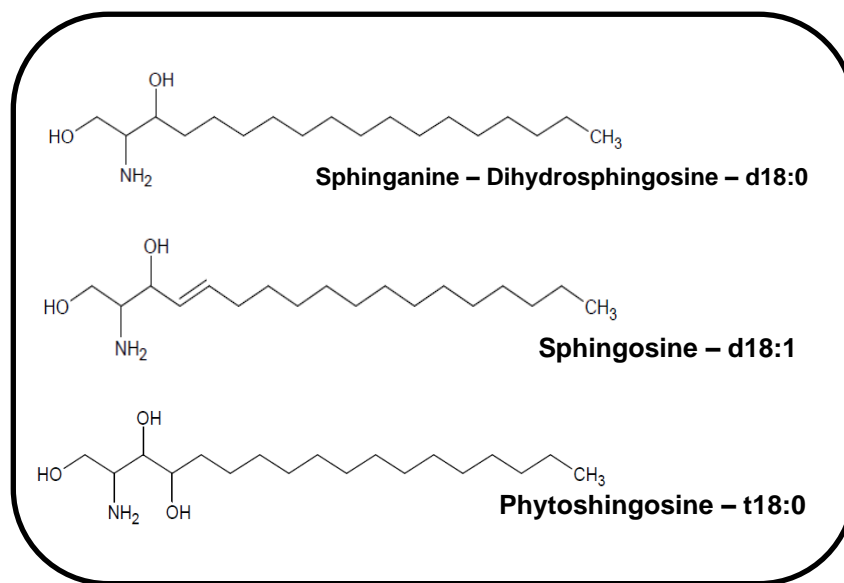
Figure 6. Example of LCB structure

The LCBs d18:0, d18:1 and t18:0 are made up of 18 carbon atoms. Dihydrosphingosine has two hydroxyl groups in positions 1 and 4, sphingosine has two hydroxyl groups in positions 1 and 4 and an unsaturation in position 4 and phytosphingosine has three hydroxyl groups in positions 1, 4 and 5.

Their biosynthesis (**Figure 7.**) is shared between the endoplasmic reticulum and the Golgi apparatus. This can take place in two ways (Hannun and Obeid, 2008):

- A *de novo* pathway, which starts with the condensation of a serine and a palmitoyl-CoA under the action of a key enzyme, serine palmitoyl transferase (SPT). Complete knockout of this gene results in lethality in mice, yeast, and plants (Chen *et al.*, 2006; Hojjati *et al.*, 2005).
- A "rescue" pathway that will allow the release and reuse of LCBs and ceramides from more complex SLs.
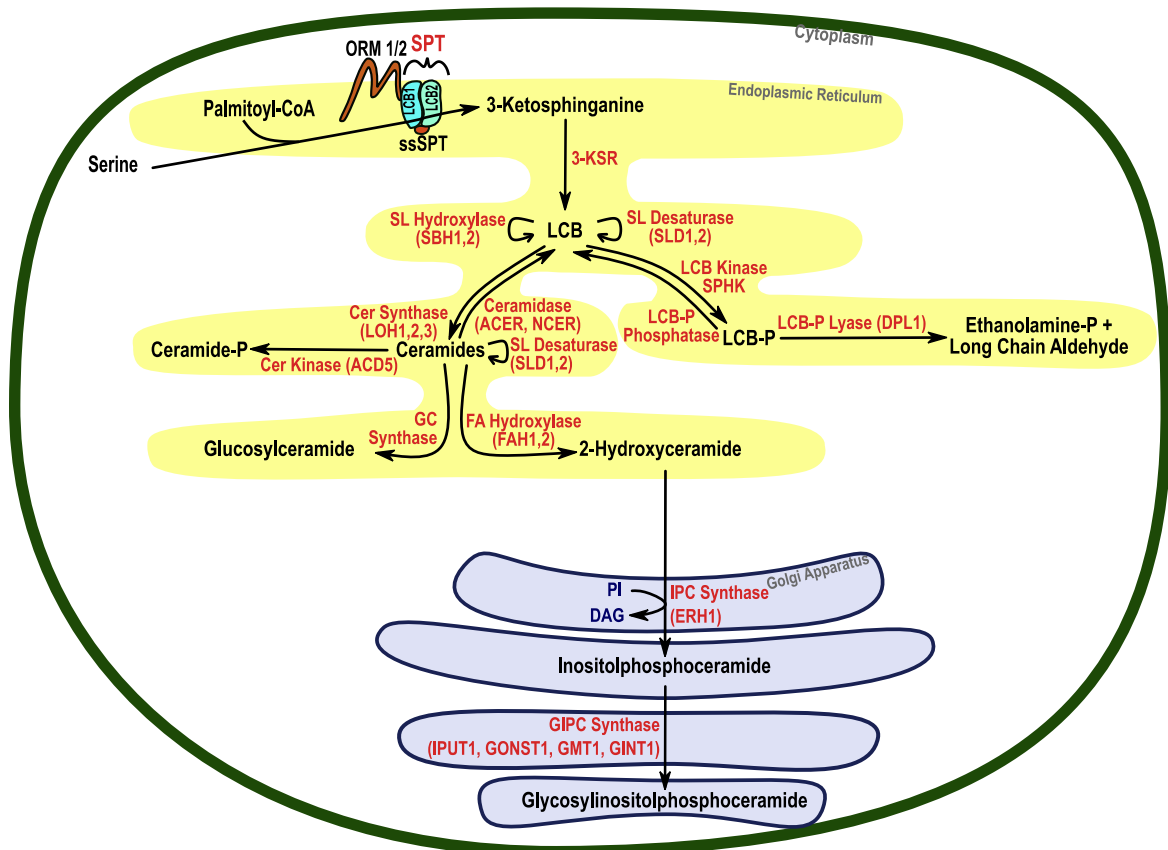
Figure 7. Schematic representation of the sphingolipid biosynthetic pathway in plants (from Huby *et al.*, 2020)

3-KSR, 3-Ketosphinganine Reductase; ACD5, Accelerated Cell Death 5; ACER, Alkaline Ceramidase; Cer, Ceramide; Ceramide-P, Ceramide-Phosphate; coA, CoenzymeA; DAG, Diacylglycerol; DPL1, Dihydrosphingosine-Phosphate Lyase; FA, Fatty Acid; FAH, Fatty Acid Hydroxylase; GC, Glucosylceramide; GINT1, Glucosamine Inositolphosphorylceramide Transferase 1; GIPC, Glycosyl Inositol Phospho Ceramide; GMT1, GIPC Mannosyl-Transferase 1; GONST1, Golgi Localized Nucleotide Sugar Transporter1; IPCS, Inositol Phosphorylceramide Synthase; IPUT, Inositol Phosphorylceramide Glucuronosyltransferase 1; LCB1,2, Subunit of Serine Palmitoyltransferase 1 and 2; LCB, Long-Chain Base; LCB-P, Long-Chain Base Phosphate; LOH, Lag One Homolog; NCER, Neutral Ceramidase; ORM, Orosomucoid-like Protein; PI, Phosphoinositol; SBH, Sphingoid Base Hydroxylase; SL, Sphingolipid; SLD, Sphingolipid Δ8 Long-Chain Base Desaturase; SPHK, Sphingosine Kinase; ssSPT, Small Subunit of Serine Palmitoyl Transferase; SPT, Serine Palmitoyl Transferase.

b. Bacterial sphingolipids

Bacterial SLs are predominantly present in the outer PM and, like plant SLs, have varied and complex structures whose base is also formed by LCBs. However, they are not universal in these organisms, as they have been identified in only a few groups of bacteria, such as Bacteroides, *Prevotella, Porphyromonas, Fusobacterium, Sphingomonas, Sphingobacterium, Bdellovibrio, Cystobacter, Mycoplasma* and *Flectobacillus* (Olsen and Jantzen, 2001). However, their biological role remains less known than in eukaryotes.

In *Pseudomonas*, the bacteria used in this thesis, the most common lipids are phospholipids, which constitute up to 40% of the PM (PE, PG and CL), glycolipids, fatty acids, LPS and ornithine lipids. SLs are therefore not found in these bacteria, either in their membranes or free in their cytoplasm (Pinkart and White, 1998).

2. Membrane role

As mentioned earlier, SLs are major components of microdomains. Those specific domain play an important role in many cellular processes, such as signalling, protein aggregation and stress responses, both through the proteins they carry and their lipid composition (Cacas *et al.*, 2012; Grennan, 2007; Pata *et al.*, 2010). Indeed, with the development of sphingolipidomics and the improvement of lipid quantification techniques, many studies have demonstrated the involvement of SLs in biotic and abiotic stress response, as well as in programmed cell death (Ali *et al.*, 2018; Berkey *et al.*, 2012; Huby *et al.*, 2020).

As SLs are key components of PMs, their regulation and their relationships to its other components is particularly important (Carmona-Salazar *et al.*, 2011). Indeed, some actors involved in cell death, such as Bax-inhibitor 1 (*AtBI-1*), interact with enzymes of the SL biosynthetic pathway (FAH1 and 2 - Fatty acid hydroxylase 1 and 2) (**Figure 7.**). Overexpression of the *AtBI-1* gene leads to an increased GluCer concentration in membrane microdomains. This causes the loss of proteins normally located at these microdomains and that are essential for plant defence, especially for cell death related to oxidative stress or to SA (Ishikawa *et al.*, 2015). The same is true in rice, where microdomains are less abundant in a knockout mutant *OsFAH1/2*, impaired in SL production. These mutant lines demonstrated that these microdomains, and consequently the proteins they contain such as the NADPH oxidase RbohB, were required for ROS production in response to the elicitor chitin in rice (Nagano *et al.*, 2016).

3. Response to biotic stresses

It has long been established that SLs play a role in both abiotic stresses (water, salt, cold, etc.), which will not be discussed here, and biotic stresses. Biotic stresses are caused by plant pathogens and are major threats to field crops. As mentioned earlier, plants have developed a defence arsenal to react to these attacks.

It has also recently been shown that the membrane GIPCs (outer leaflet) of eudicotyledons act as receptors for NLPs (Necrosis and ethylene-inducing peptide 1-like protein), produced by bacterial and fungal pathogens to promote infection. This recognition occurs via the terminal hexoses of the GIPC. The GIPCs of eudicotyledons have two, so that NLPs, by binding to them, can reach the PM and induce conformational changes in the plant, leading to cell death. The GIPCs of monocots have three hexoses and NLPs bind to them but cannot reach the PM and are therefore not active (Lenarcic *et al.*, 2017). SLs therefore play a role in plant defence and PCD through their structural role at the PM.

The use of fungal toxins, FB1 (Fumonisin B1) produced by *Fusarium monoliforme* and AAL produced by the necrotrophic agent *Alternaria alternata*, has highlighted the numerous roles of LCB and ceramides in the signalling and regulation of cell death, particularly during the stress response. Indeed, these two toxins are structural analogues of sphingosine (LCB, d18:1) and inhibit ceramide synthases (**Figure 7.**), the enzymes responsible for the transformation of LCB into ceramides. This inhibition results in the accumulation of d18:0 (sphinganine) and t18:0 (phytosphingosine) and subsequently PCD (Abbas *et al.*, 1994; Peer *et al.*, 2010; Saucedo-García *et al.*, 2011; Tsegaye *et al.*, 2007). Other studies using *Arabidopsis* mutants, such as CERK (Ceramide kinase) or ACD5 (Accelerated cell death 5), have also shown that the accumulation of free LCBs and ceramides, as well as the balance between phosphorylated and unphosphorylated forms, are associated with PCD (Liang, 2003; Simanshu *et al.*, 2014). Similarly, *Arabidopsis* lines overexpressing *AtORM1* & *2* (Orosomucoid-like protein, **Figure 7.**) proteins that negatively regulate SPT (Breslow and Weissman, 2010; Gururaj *et al.*, 2013), show increased resistance to FB1-induced PCD (Kimberlin *et al.*, 2016). Exogenous application of ceramides also correlates with PCD and is dependent on plant defence-related phenomena (ROS production, MPK6 activation), both in *Arabidopsis* and in tobacco cells (Lachaud *et al.*, 2010; Saucedo-García *et al.*, 2011; Shi *et al.*, 2007).

These studies have notably demonstrated the existence of a rheostat between LCBs/ceramides and their phosphorylated forms, showing their crucial role in PCD induction, determining cell fate, and linking SL metabolism to plant defence mechanisms (**Figure 8.**) (Alden *et al.*, 2011; Saucedo-Garcia *et al.*, 2015; Shi *et al.*, 2007; Townley *et al.*, 2005).
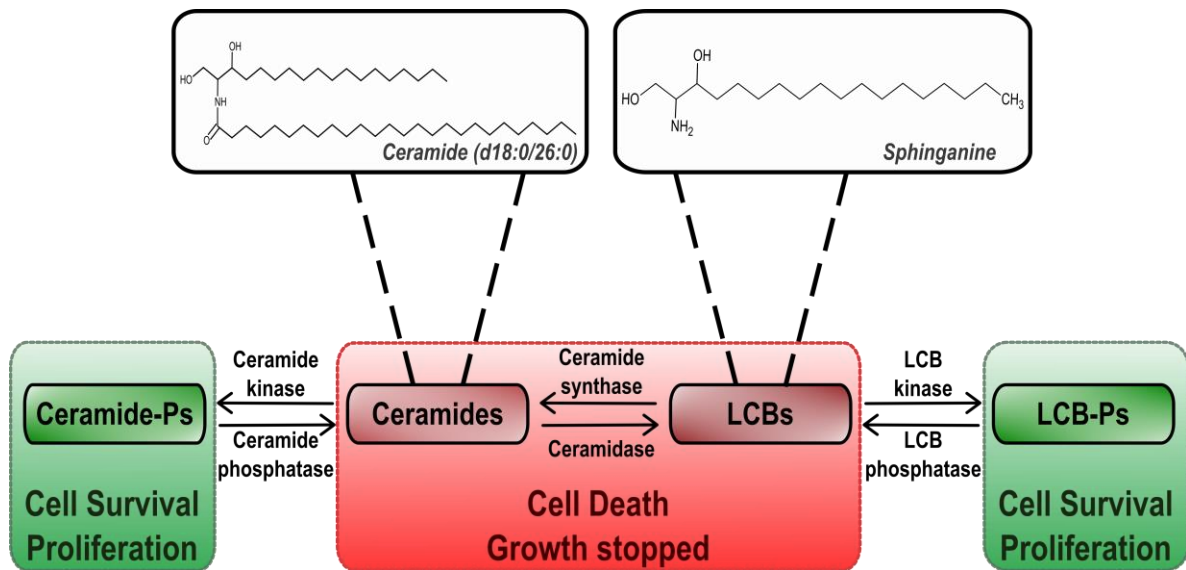
Figure 8. Representation of the sphingolipid rheostat (Huby *et al.* 2020)

The balance between LCBs/Ceramides and their phosphorylated derivatives determines cell fate.

In addition to their role as structural elements and in PCD via the LCB / long-chain base phosphate (LCB-P) and Cer / Cer-P rheostat, other studies have highlighted the relationship between SL and regulation of SA levels, a hormone involved in plant defence. For instance, the *Arabidopsis AtFAH1* & *2* mutants (**Figure 7.**) showed constitutively high levels of SA (König *et al.*, 2012; Shi *et al.*, 2015). The *fah1/fah2/loh2* triple mutant (Lag one homolog 1, **Figure 7.**), which accumulates ceramides and the LCB d18:0, also showed a PCD that was dependent on SA and EDS1 (Enhanced Disease Susceptibility1) and was probably linked to d18:0 accumulation (König *et al.*, 2021). Similarly, quadruple mutants that are impaired in both SL production (*fah1/fah2/loh1*) and SA production (*sid2-2*) or in SA-related signalling (*eds1-2*) suggest a reciprocal communication between these metabolites, as they accumulate less ceramide and LCB (König *et al.*, 2021). This communication could be due to an action of MPK6 or an accumulation of ROS/NO or calcium, but these hypotheses are currently uncertain (Coursol *et al.*, 2015; Sanchez-Rangel *et al.*, 2015). As SA is considered essential for plant resistance to (hemi)biotrophic pathogens, an alteration in SL metabolism also induces changes in the plant response to these microorganisms. For example, a loss of function of ORM1 & 2 proteins (**Figure 7.**), causes constitutive induction of SA-related genes and tolerance to *P. syringae* strain DG3 compared to the WT (Li *et al.*, 2016).

Similarly, while infection of *Arabidopsis* with an avirulent strain of *P. syringae* pathovar (pv.) *tomato* (*Pst*) causes an increase in intra-cellular t18:0 and high PCD related to a HR at the site of infection (Peer *et al.*, 2010), in an *Atdpl1-1* (Dihydrosphingosine-1-phosphate lyase1, **Figure 7.**) mutant, it is the t18:0-P that accumulates. This accumulation is accompanied by a repression of

the SA pathway in favour of the activation of the JA pathway, making the plants more susceptible to the pathogen (Magnin-Robert *et al.*, 2015).

IV. Elicitors and their perception by membrane lipids

Several studies suggest the perception of some elicitors *via* PM lipids, and not *via* protein receptors such as PRRs (Gerbeau-Pissot *et al.*, 2014; Lenarcic *et al.*, 2017; Nasir *et al.*, 2017; Xu *et al.*, 2001). By interacting with, or even inserting into, membrane lipids, these elicitors can induce changes in the physical properties of the membrane, in terms of composition and/or lateral (influence on lipid rafts) and/or transverse (effect on membrane asymmetry) organisation. These changes can influence the properties of multiple membrane proteins, such as ion channels, receptors, or enzymes thus leading to the establishment of plant defence phenomena (Cordelier *et al.*, 2021; Schellenberger *et al.*, 2019).

Most elicitors that interact with lipids are generally hydrophobic or amphiphilic in nature and have structures derived from lipids, proteins, or polysaccharides. Few elicitors of a purely lipidic nature, such as LCBs, are reported in the literature and their modes of action are even less described. Nevertheless, we can note the role of ergosterol, the major sterol of fungi, described as a general elicitor of plant defences (Klemptner *et al.*, 2014). It is believed to be able to modify the NADPH-oxidase of *Beta vulgaris* and also inhibit the activity of its H^+-ATPase. Due to its lipid nature and ability to form rafts, it is assumed that ergosterol would come into contact with or be adsorbed onto the PM, causing a modification of the plant's lipid rafts and consequently of the NADPH oxidases located there (Hao *et al.*, 2014; Rossard *et al.*, 2010). Several other elicitors are derived from lipids such as arachidonic acid or eicopolyenoic acid, produced by *Phytophtora infestans* (Bostock *et al.*, 1981, 2011) or cerebroside, a glycosphingolipid that induces defence phenomena in rice (Umemura *et al.*, 2002, 2004), but their modes of action are not yet elucidated.

Other elicitors of amphiphilic nature such as cyclic lipopeptides, produced by beneficial microorganisms such as *Streptomyces* or *Bacillus* could be able to interact with PM. Lipopeptides include the iturin family, fengycin (Deleu *et al.*, 2005, 2008; Ongena and Jacques, 2008) and surfactin (Henry *et al.*, 2011), all produced by *Bacillus subtilis*. It has also recently been shown that rhamnolipids, glycolipids notably produced by *Pseudomonas* and *Burkholderia* species, elicit defence reactions in grapevine, *Arabidopsis,* and oilseed rape (Monnier *et al.*, 2019; Sanchez *et al.*, 2012), and are capable of insertion into biomimetic artificial membranes of plants (Monnier *et al.*, 2019). Furthermore, these rhamnolipids have also proven to activate immune response influenced by the SL content of the PM (Schellenberger *et al.*, 2021).

Elicitors of a protein nature are also able to interact with PM lipids. For instance, harpins which are secreted by Gram- bacteria, and form pores in PMs (Choi *et al.*, 2013), cryptogein, secreted by the oomycete *Phytophtora cryptogea*, capable of increasing PM fluidity (Gerbeau-Pissot *et al.*, 2014) or NLPs, cytotoxins produced by bacteria, fungi, and oomycetes to facilitate their infection in plants. As mentioned earlier, these NLPs have been shown to bind to the terminal hexose part of GIPCs at the PM, which induces conformational changes in the NLP, allowing it to contact the membrane and become active (Lenarčič *et al.*, 2017).

V. Biophysical techniques applied to the study of plasma membrane/sphingolipid interaction

1. Membrane models

Both lipids and proteins of biological membranes are assembled in an extremely complex and asymmetric manner. Their organisation and composition vary according to time, environment, developmental stage of organisms and organs (Furt *et al.*, 2011). In order to study the effect of bioactive molecules on membrane lipids at the molecular level, it is necessary to simplify these biological membranes into model membranes. These artificial systems have the advantage of being versatile. They can be composed of a complex mixture of lipids to best mimic the composition and arrangement of biological membrane lipids but can also be composed of one or two lipids to study a particular aspect of PMs such as the presence of a specific lipid or a particular phase. They all allow fine control of the experimental conditions. Three systems are mainly used, lipid monolayers, supported bilayers and liposomes (**Figure 9.**) (Deleu *et al.*, 2014; Furlan *et al.*, 2020; Le *et al.*, 2011).
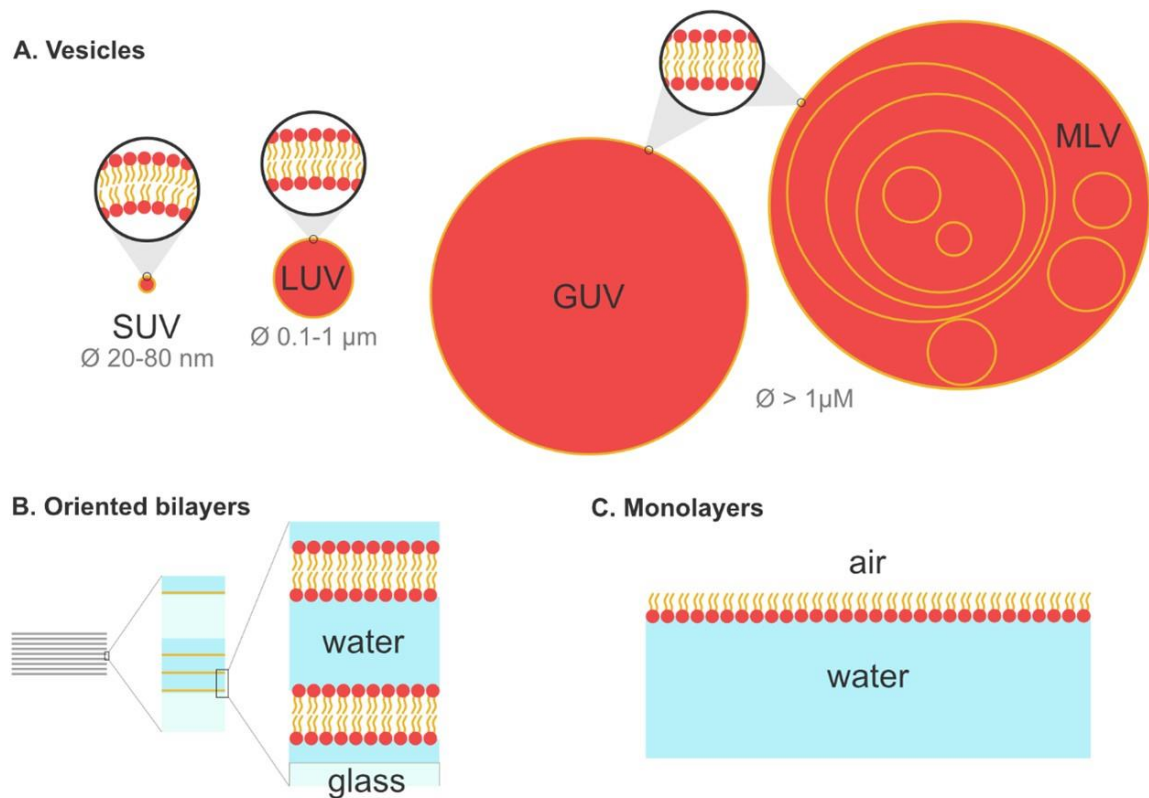
Figure 9. Schematic of membrane models used in biophysics (from Furlan *et al*. 2020)

A. The different types of liposomes, small unilamellar vesicle (SUV), large unilamellar vesicle (LUV), giant unilamellar vesicle (GUV) and multilamellar vesicle (MLV), and their diameters. This scaled representation allows the differences in membrane curvature to be highlighted. **B.** Oriented bilayers, where the lipid bilayers are supported on the glass slides and separated by thin layers of water. **C.** Orientation of lipids at the air-water interface forming monolayers.

Monolayers are simple models that aid to determine the ability of certain molecules to insert and interact with lipids of the outer leaflet of the membrane. Supported bilayers are flat bilayers spread on a solid support such as mica or glass. They are used, among other things, to study molecule / lipid head interactions and to predict the lateral and transverse molecular organisation of biological membranes. Finally, liposomes, which depending on the way they are prepared can be unilamellar (single bilayer) or multilamellar (multiple bilayers), can contain different types of aqueous contents, such as fluorophores. They are generally used to study various processes, such as membrane fusion, pore formation or cell adhesion (Deleu *et al*., 2014; Eeman and Deleu, 2010).

It is therefore possible to vary several parameters, such as the composition of the lipids and their proportions, as well as the model used, in order to obtain additional information on the mechanism of action at the molecular level.

2. Biophysical techniques and the information they provide

Langmuir trough

This technique aims to determine the adsorption or penetration capacity of a bioactive molecule on, or in, a monolayer of more or less ordered lipids. These measurements are based on lipids spread out in a monolayer at a given surface pressure (mN/m) on a buffer. The molecules of interest are injected into the subphase (the buffer), then a Wilhelmy plate tensiometer measures the surface pressure variations induced by the interaction of the bioactive molecule with the lipid monolayer at the air-liquid interface (**Figure 10.**) (Deleu *et al.*, 2014; Eeman *et al.*, 2006; Giner-Casares *et al.*, 2014). It is therefore possible to measure adsorption kinetics but also to evaluate the lipid specificity of the interaction by playing on the nature of the lipids deposited at the interface.
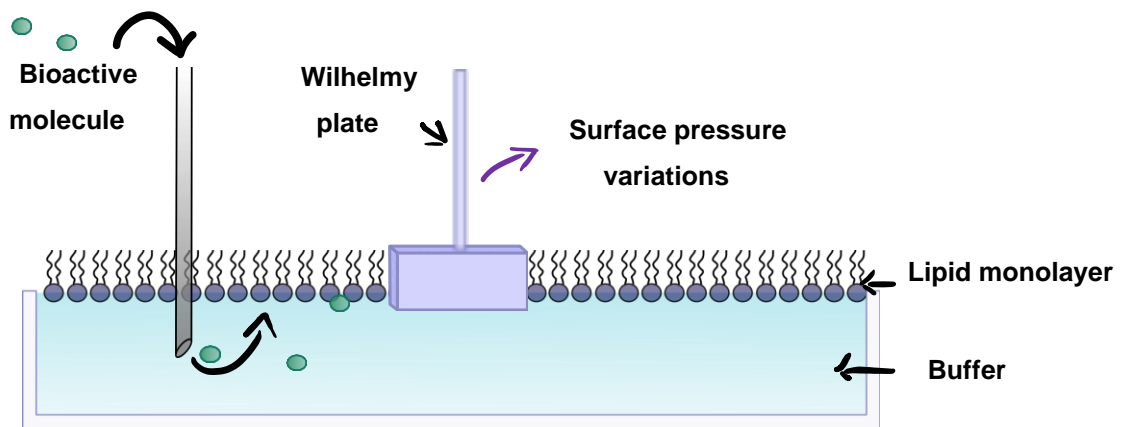
Figure 10. Schematic diagram of a Langmuir cell

This technique allows the measurement of variations in the surface pressure of a lipid monolayer, induced by the injection of a bioactive molecule.

Fluorescence spectroscopy

Study of membrane permeabilization

This technique requires the use of liposomes in which a hydrophilic fluorescent probe has previously been encapsulated. Calcein is often used and is self-quenched at high concentration (**Figure 11.**) (Maherani *et al.*, 2013; Shimanouchi *et al.*, 2009). The leakage of calcein from the liposomes to the medium caused by the addition of a bioactive molecule will induce an increase in fluorescence due to the dilution of the probe and its dequenching, thus determining the ability of the bioactive molecule to permeabilise or destabilise membranes (Deleu *et al.*, 2013).
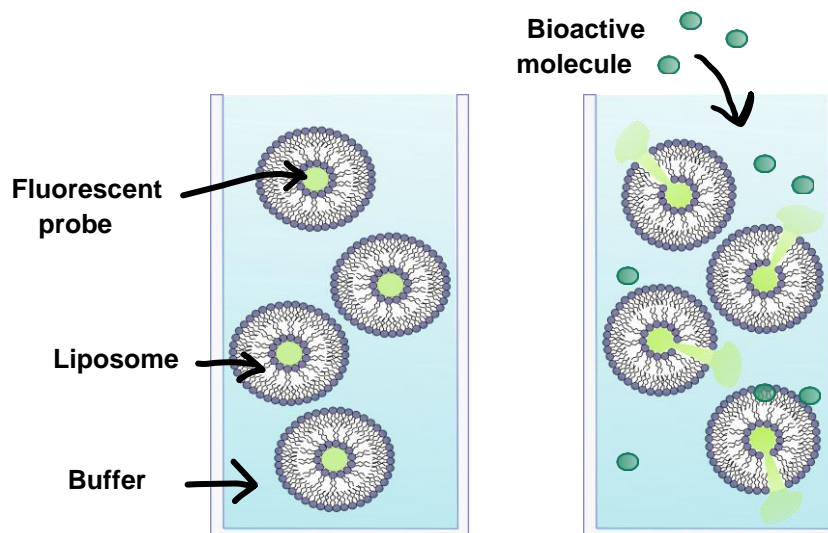
Figure 11. Schematic of the membrane permeabilization measurement

This technique allows to measure the variations in fluorescence of the medium induced by the addition of a molecule of interest. Depending on the action of the molecule on the membranes of the liposomes, these will release the hydrophilic fluorescent probe into the external environment to a greater or lesser extent.

Measurement of membrane fluidity

The use of fluorescent probes, such as Laurdan for example, can highlight changes in membrane fluidity and more particularly changes in the state of the lipids (gel, liquid-disordered, coexistence of phases) (Deleu *et al.*, 2013). Laurdan is added to a liposome solution and will insert itself into the bilayer uniformly within the outer and inner leaflet and without preference for the gel or fluid state of the lipids. The addition of a bioactive molecule can cause phase changes in the bilayer, thereby shifting the fluorescence emission spectrum of Laurdan (Parasassi and Gratton, 1995; Parasassi *et al.*, 1991). This can cause its dipole moment to increase significantly, and nearby water molecules will reorient themselves according to this new dipole. If the membrane is in the fluid state, the reorientation rate will be faster than the emission process, so the Laurdan emission spectrum will be red-shifted. Conversely, if the bilayer density increases toward a gel state, the dipolar relaxation of the water molecules will be slower and the emission spectrum of the probe will be less red-shifted (Deleu *et al.*, 2013).

Isothermal Titration Calorimetry (ITC)

ITC measures the heat released or absorbed when two compounds interact together in a given environment. One of the compounds is titrated into the solution containing the other compound and the heat fluxes associated with the interaction between the titrated and titrating solutions are determined as the titration proceeds, from which enthalpies changes can be determined. This

technique is widely used in the pharmaceutical field for ligand-receptor, enzyme-substrate, or antibody-antigen interactions (Deleu *et al.*, 2014). In the laboratory, it is typically used to study the interactions between a bioactive molecule of interest and liposomes. ITC provides a comprehensive characterisation of the thermodynamic parameters of the interaction between these two compounds, including binding affinities, enthalpy and entropy variations, stoichiometry parameters and critical membrane solubilisation concentrations (Deleu *et al.*, 2013). These data are then used to assess the nature of the interaction between the molecule of interest and artificial and biological membranes (Ghai *et al.*, 2012; Heerklotz and Seelig, 2000).

Atomic Force Microscopy (AFM)

Atomic force microscopy allows three-dimensional images to be obtained by scanning the surface of the sample using a lever fitted with a microscopic tip. In particular, this technique can image artificial samples (Morandat *et al.*, 2013), such as model membranes or biological samples, under specific physiological conditions allowing biological samples to remain viable (Alessandrini and Facci, 2005). These biological samples can be DNA, proteins, adherent mammalian cells, protoplasts (usually fixed) or bacteria (living or not) (Louise Meyer *et al.*, 2010; Yang *et al.*, 2015). In addition to surface topography, it is possible to observe changes in the resistance of a sample to deformation and thus study changes in the state (fluid or rigid) of membranes caused by the addition of a molecule of interest.

Dynamic Light Scattering (DLS)

This technique is based on the measurement of the variation in light scattering by particles in solution subjected to Brownian movements (random movements due to their interactions with the solvent). This variation is described by the autocorrelation function g(t) which corresponds to the differences in scattered intensities between a time x and time zero. Depending on the hydrodynamic radius of the particle under consideration, the shape of the autocorrelation function differs, and its mathematical smoothing allows an estimate of its size to be obtained. In the case of molecules self-aggregating in aqueous solution (lipids, surfactants), it is also possible to determine their aggregation states (monomer or aggregates) and to measure their critical micellar concentration (CMC) or critical aggregation concentration (CAC). For the latter, the variation of size particle is determined by the scattered intensity of the sample as a function of the concentration of the molecule. The size range of molecules that can be measured in DLS ranges from nanometre to micron (Furlan *et al.*, 2018; Topel *et al.*, 2013).

VI. *Pseudomonas syringae*, a versatile and adapted plant pathogen

The gamma subgroup of proteobacteria includes several important pathogens, including those infecting animals (*Escherichia*, *Salmonella*, *Shigella* and *Yersinia* spp.) or plants (*Erwinia*, *Pantoea*, *Xanthomonas*, *Xylella* and *Pseudomonas* spp.) (Buell *et al.*, 2003). The genus *Pseudomonas* is divided into two phylogenetic lineages, *Pseudomonas aeruginosa* and *Pseudomonas fluorescens*. The *P. fluorescens* lineage contains 6 phylogenetic groups including *P. syringae*, which regroups the majority of plant pathogens of the genus *Pseudomonas*. Within this group is the species *P. syringae*, which itself contains more than 60 pathovars (Gomila *et al.*, 2017). A table of many pathovars and their hosts is available in **Supplemental Table S1** (Hwang *et al.*, 2005).

P. syringae was first isolated from lilac (*Syringa vulgaris*) in 1902. It is a hemibiotrophic, rod-shaped, Gram-, motile with a flagellum, strictly aerobic bacterium that produces fluorescent pigments when in an iron-poor environment (Hirano, 1985). It is one of the most studied plant pathogens and serves as a model for the study and understanding of many biological phenomena such as bacterial pathogenicity, interaction molecular mechanisms between plants and micro-organisms, and microbial ecology and epidemiology. Each of the 60 identified pathovars infects a limited number of species or even only certain cultivars of a species (Gomila *et al.*, 2017). Collectively, *P. syringae* infect the majority of crops of economic interest, including many fruits, vegetables, and ornamentals, making this bacteria one of the most common and devastating plant pathogens (Xin *et al.*, 2018).

Although this species was initially identified on diseased plants and their pathogenicity has long remained their most studied aspect, it has since been shown that many isolates belonging to the species, such as *P. syringae* pv. *syringae* B728a, grow epiphytically and have a commensal relationship with plants (Hirano and Upper, 2000; Xin *et al.*, 2018).

1. Life cycle

The life cycle of *P. syringae* is generally divided into two phases, spatially and temporally connected. First, an epiphytic life phase, where the bacterium will grow on the surface of a healthy plant, followed by an endophytic phase where the bacterium will grow aggressively in the apoplast of the plant after entering through a natural opening or wound (Hirano and Upper, 2000). Most microorganisms fail in either of these phases, as the plant has developed effective strategies to restrict the entry and multiplication of these commensal bacteria.

a. Surviving as an epiphyte

The plant surface is commonly considered a hostile environment for microorganisms. Nutrients are limited, there is direct exposure to UV light, temperature and humidity variations are drastic and finally, bacteria are in competition with other epiphytic organisms (Beattie and Lindow, 1995; Lindow and Brandl, 2003). The phyllosphere is thus a very heterogeneous environment, although some nutrient-rich niches favourable to microorganisms exist, for example along veins, around trichomes or stomata (Hirano and Upper, 2000). Bacteria found on other parts of the plant have therefore developed processes to survive in this hostile environment, notably by creating their own "microenvironment". Some strains of *Pseudomonas* can, for example, produce surfactants to increase the wetting of leaves, while others live in large biofilm aggregates to resist desiccation (Bunster 1989, Hutchinson 1993). Bacteria must therefore face several challenges: crossing the epidermis, growing, spreading, etc. in order to continue their life cycle. Some micro-organisms will infect their hosts by using their natural openings, such as stomata, others through wounds, caused for example by frost (Melotto *et al.*, 2008).

- **<u>Crossing the epidermal barrier</u>**

Several factors favour the development of bacteria during their epiphytic life phase. For example, when a plant is weakened by another pathogen, or when environmental conditions are ideal for bacterial development (e.g., heavy rainfall, humidity, moderate temperatures). There are a number of natural openings through which bacteria can enter the plant. These include (Melotto *et al.*, 2008):

- Hydathodes, water-exuding pores at the leaf tips (by *Xanthomonas campestris* pv. *campestris*).
- Nectarthodes, nectar-secreting pores present at the emergence of the style and stamens (by *Erwinia amylovora*).
- Lenticels, pores used for respiration and present on stems and roots (by *Erwinia carotovora* var *Atroseptica*).
- Stomata, pores in the aerial parts of plants that control gas exchange and leaf transpiration. The closure of stomatal guard cells is regulated by the plant hormone ABA under water stress. These represent an ideal entry site for pathogens, notably *P. syringae*.

In response and in order to preserve their integrity, plants have developed defence mechanisms, such as closing the stomata after the perception of MAMPs (Melotto *et al.*, 2017). Bacteria in turn have developed attack strategies, notably via the secretion of phytotoxins such as coronatine, an analogue of OPDA (12-oxo-phytodienoic acid), a precursor of JA that can alter stomatal defence mechanisms thus allowing the reopening of stomata. Not all pathovars of *P. syringae* produce this

toxin, but some of them, such as *P. syringae* pv. *tabaci*, are still able to induce stomatal reopening after the initial defence reaction of the plant, suggesting that other mechanisms can bypass the stomatal defence (Melotto *et al.*, 2006).

In addition to these natural openings, bacteria may be satisfied with a wound on the plant to gain entry. These wounds can be mechanical or environmental, such as those caused by frost.

- **Inoculum sources**

The sources of inoculum, responsible for the appearance and spread of the bacteria, are many and varied, although their relative contributions to the occurrence of the disease remain unknown. Epiphytic bacteria may be a source of inoculum, as well as remnants of a systemic infection, or pre-existing cankers, localised necroses of the bark and cambium. *Pseudomonas* also exists on the surface of many weeds and non-hosts, which can serve as vectors. The bacterium can also be spread by rain, wind, insects, infected budwood, transport of infected nursery stock, and pruning and harvesting equipment.

b. Proliferating as an endophyte

After the bacteria have entered the apoplasm, they must continue to develop to ensure their virulence. Protein secretion plays a major role in the interaction between bacteria and their environment but transporting proteins across cell membranes is a real challenge. In order to achieve this, some bacteria, mainly Gram-, have developed secretion systems (type I to VII). More than twenty-five species of bacteria interacting with other organisms, whether pathogenic or not, are carriers of this system. These include many pathogens responsible for serious human diseases such as *Yersinia*, *Salmonella*, *Shigella* spp. or *Escherichia*, but also bacteria with disastrous agronomic consequences such as certain species of *Pseudomonas*, *Xanthomonas* or *Erwinia* (Xin and He, 2013).

The type III secretion system (T3SS) is the most studied and sophisticated. The first was identified in *Salmonella typhymurium* by Ginocchio *et al* (1994) who noted the formation of an appendage on the surface of the bacteria after its contact with a target cell. These are macro-molecular complexes, embedded in bacterial membranes, whose purpose is to initiate the infection process in their hosts. These molecules modulate crucial molecular functions of their hosts such as immune responses, cytoskeletal dynamics, transport vesicles or transduction signals (Alfano *et al.*, 2000). Despite the diversity of hosts and effectors, the secretion system remains relatively conserved, and the pathogenicity of these bacteria relies on a functional T3SS (Cornelis, 2006; Matteï *et al.*, 2011).

c. Structure of the T3SS

The T3SS, or "injectisome", is structurally linked to the bacterial flagellum and is widely conserved between bacterial species (Cornelis, 2006; Woestyn *et al.*, 1994). In animal biology, its structure is widely studied for therapeutic purposes, due to its predominant role in virulence, and has been characterised in some species, such as *Salmonella Typhimurium* (Hu *et al.*, 2018), which is not yet the case for plant pathogens.

The T3SS is composed of at least 20 distinct proteins that assemble into four major parts, the basal part, the cytosolic part, the export system and the needle or pilus (**Figure 12.**).

- The **basal part** of this system is formed by two ring structures that cross the inner and outer bacterial membrane from side to side (Hu *et al.*, 2018). At the outer membrane, the ring will be formed by proteins of the secretin family. Other proteins, the pilotins, facilitate the insertion, oligomerisation, and assembly of secretins (Diepold and Wagner, 2014).

- The **cytosolic complex** is associated with a membrane-associated ATPase in the bacterial cytoplasm. This is suspected to facilitate and regulate the entry of substrates to be exported into the secretory system (Diepold and Wagner, 2014).

- The **export system** is located in the basal part of the bacterial inner membrane and is composed of five highly conserved proteins that are essential for secretion, although their precise roles are not elucidated (Diepold *et al.*, 2011).

- The **needle**, called pilus in plant pathogens such as *P. syringae*, must be longer than in animal pathogens, as it must also pass through the plant CW (Jin and He, 2001). Upon infection, the pilus is polymerised and serves as a tunnel for effectors (**Figure 12.**). After contact with the target cell, components will be secreted to form a pore called translocon in the host PM. Without a translocon, effectors cannot be released into the target cell and the bacteria are non-pathogenic (Diepold and Armitage, 2015; Diepold and Wagner, 2014; Worrall *et al.*, 2011; Yip *et al.*, 2005).
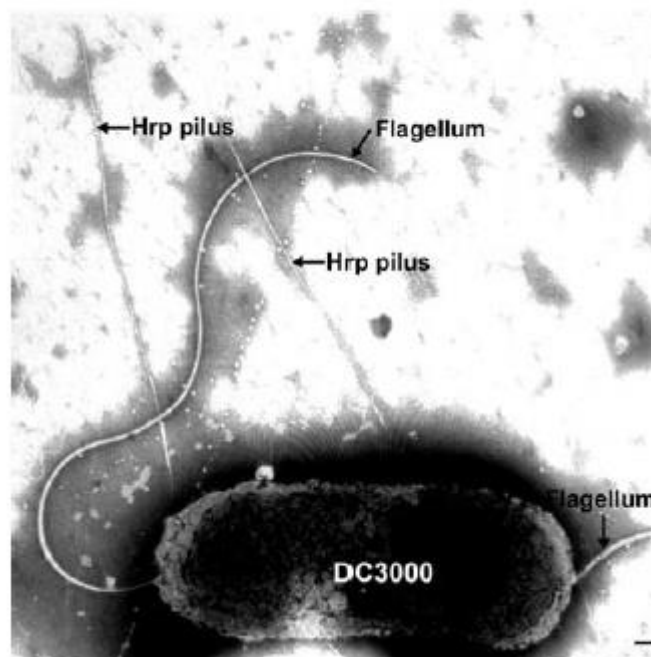
Figure 12: Transmission electron microscope image of *Pseudomonas syringae* pv. *tomato* DC3000 (Katagari *et al.*, 2002).

The bacterium has flagella of about 15 nm in diameter and several pili about 8 nm in diameter. These pili produced by the type III secretion system are involved in the translocation of virulent or avirulent effectors into the cytoplasm of host plant cells.

d. The Hrp/Hrc system and the notion of pathogenicity island

In *P. syringae*, the T3SS is encoded by the *hrp* (HR and pathogenicity) and *hrc* (HR conserved) genes assembled in a hrp/hrc cluster (Alfano and Collmer, 1997).

This hrp/hrc cluster, which is required for the production and regulation of a functional T3SS as well as for the secretion of protein effectors, is located within a chromosomal cluster named "Pathogenicity island" (PAI) (Waite *et al.*, 2017). The four most studied hrp clusters can be divided into two groups according to their gene similarity, operon structure and regulatory system (Alfano and Collmer, 1997). Group I is composed of the hrp clusters of *P. syringae* and *Erwinia amylovora*, and group II of those of *Ralstonia solanacearum* and *Xanthomonas campestris* (Alfano and Collmer, 1997).

Within this PAI, the hrp/hrc cluster is surrounded by the CEL (Conserved effector locus) and the EEL (Exchangeable effector locus). The CEL, which is conserved between species, contains genes that encode effectors important in virulence. The EEL contains genes that encode both effectors and genetic element sequences (Alfano *et al.*, 2000).

e. Proteins secreted by the T3SS

o **<u>Harpins and pilins</u>**

Harpins are extracellular proteins secreted by the T3SS and specific to phytopathogens. They are glycine-rich, cysteine-poor, and capable of inducing HR when infiltrated in high doses into plant tissues. Although their action is poorly understood, they are thought to contribute to the translocation of effectors into target cells (He and Collmer, 1993; Kvitko *et al.*, 2007).

Pilins are also essential molecules for bacterial virulence, since they constitute the pilus that carries the effectors.

o **<u>Effectors</u>**

These effectors, hop (Hrp-dependent outer proteins) or avr (avirulence), vary in number and function among bacterial species, reflecting the need for a specific (symbiotic or pathogenic) interaction with a particular host. These can have dramatic consequences on their target cells. Indeed, they possess a wide range of biochemical activities that can modulate the crucial molecular functions of their hosts in order to promote the survival and colonisation of the bacteria.

2. Symptoms and control

P. syringae is generally considered to be a hemibiotrophic pathogen of low virulence, locally infecting aerial plant parts. Infection is initially limited to a few millimetres, before spreading when the bacterium reaches its maximum growth, causing extensive cell death of the affected tissues (Xin and He, 2013). It is therefore an opportunistic bacterium, which targets particularly weakened plants.

The symptoms caused by *P. syringae* in host plants depend on the species and the part of the plant infected, the strain of the bacterium and the environmental conditions. Besides, more than one symptom can be observed on an affected plant. Symptoms are therefore most often observed on the aerial parts of the plant, including (Moore and Pscheidt, 2018):

- Flower scald: Flowers/buds turn brown to black
- Dead dormant buds: Common in cherries and apricots
- Necrotic spots on leaves
- Discoloured or blackened leaf veins due to systemic infection
- Fruit blotches and blisters
- Stem tip dieback, the most common symptom observed in 40 deciduous woody species from nurseries in the Pacific Northwest.

- Cankers on stems that appear as depressed areas in the bark that will darken over time. A gummy substance may exude from them if they are found on fruit.

One strategy for controlling bacterial populations on plants is the use of copper-containing bactericides which are toxic to bacterial cells in high doses. However, in the case of *Pst*, the massive use of these products has led to the appearance of resistant strains, such as *Pst* PT23.2 (Buell *et al.*, 2003).

VII. The *Pseudomonas syringae* pv. *tomato* – *Arabidopsis thaliana* pathosystem

Pst is a bacterium of agronomic interest that causes bacterial speck on its host, the tomato, making the fruit unfit for consumption. In the mid-1980s, after searching for a strain of *Pst* that could be transformed relatively easily, Dr. Cuppels generated a strain in his laboratory that was resistant to the antibiotic rifampicin, derived from *Pst* DC52, which he named DC3000 (Cuppels, 1986). After the discovery that this strain also had the ability to infect the model plant *Arabidopsis*, this bacterium became a model for the elucidation of plant / bacteria interactions (Whalen *et al.*, 1991), especially after the sequencing of its genome in 2003 (Buell *et al*, 2003).

1. Genetic potential

The complete genome of *Pst* DC3000 (Buell *et al.*, 2003), shows that it is composed of one circular chromosome and two plasmids, for a total of 5,763 ORFs classified in different categories. In total, 5% of its genome encodes genes involved in virulence. Some of which are related to toxin secretion, bacterial attachment, flagella, siderophores, UV, ROS and heavy metal resistance, and protein secretion systems (Buell *et al.*, 2003).

Although many strains of *P. syringae* are well adapted to the epiphytic lifestyle, it would appear that *Pst* DC3000 grows preferentially endophytically and that its survival on the leaf surface is limited in time (Boureau *et al.*, 2002). Indeed, other pathovars of *P. syringae* carry more genes related to DNA repair, UV resistance and the production of solutes associated with osmotolerance (Buell *et al.*, 2003; Feil *et al.*, 2005).

This bacterium has genes that encode type I to VI secretion systems. In *Pst* DC3000, the T3SS allows the secretion of at least 29 active effectors (Cunnac *et al.*, 2009). They participate in the virulence of the bacterium, by bypassing PTI, targeting phytoalexin or microtubule production

mechanisms, interfering with gene transcription and transport of immunity-related vesicles (Xin and He, 2013).

Many studies conducted with this bacterium use it transformed with genes encoding avirulent effectors that it does not naturally possess and that will cause ETI in plants that possess the ability to recognise them. Genes enabling the secretion of the effectors AvrRpm1 (*Pst AvrRpm1*), AvrB (*Pst AvrB*), AvrRpt2 (*Pst AvrRpt2*), AvrPphB (*Pst* AvrPphB) and AvrRps4 (*Pst AvrRps4*) are among the most common (Wei *et al.*, 2018).

2. Effectors of the pathosystem

a. AvrRpm1, AvrRpt2, AvrB and AvrPphB

The effector AvrRpm1 was originally identified in *P. syringae* pv. *maculicola* (*Psm*) strain m2 (Debener *et al.*, 1991), AvrB was isolated from *P. syringae* pv. *glycinea* and AvrRpt2 was originally identified in *Pst* strain JL1065 (Whalen *et al.*, 1991). In *Arabidopsis*, these effectors are recognised indirectly by the plant, as previously discussed with the "guard hypothesis" (**Figure 13. and 14.**). Indeed, the R genes of the plant encode the proteins associated with PM: RPM1 (Resistance to *P. syringae* pv. *maculicola*), and RPS2 (Resistance to *P. syringae*), are CC-NLRs associated at the PM with the RIN4 protein (RPM1 interacting protein4). In the absence of RPM1, phosphorylation of RIN4 would repress basal plant defences and promote pathogen growth (Mackey *et al.*, 2002).
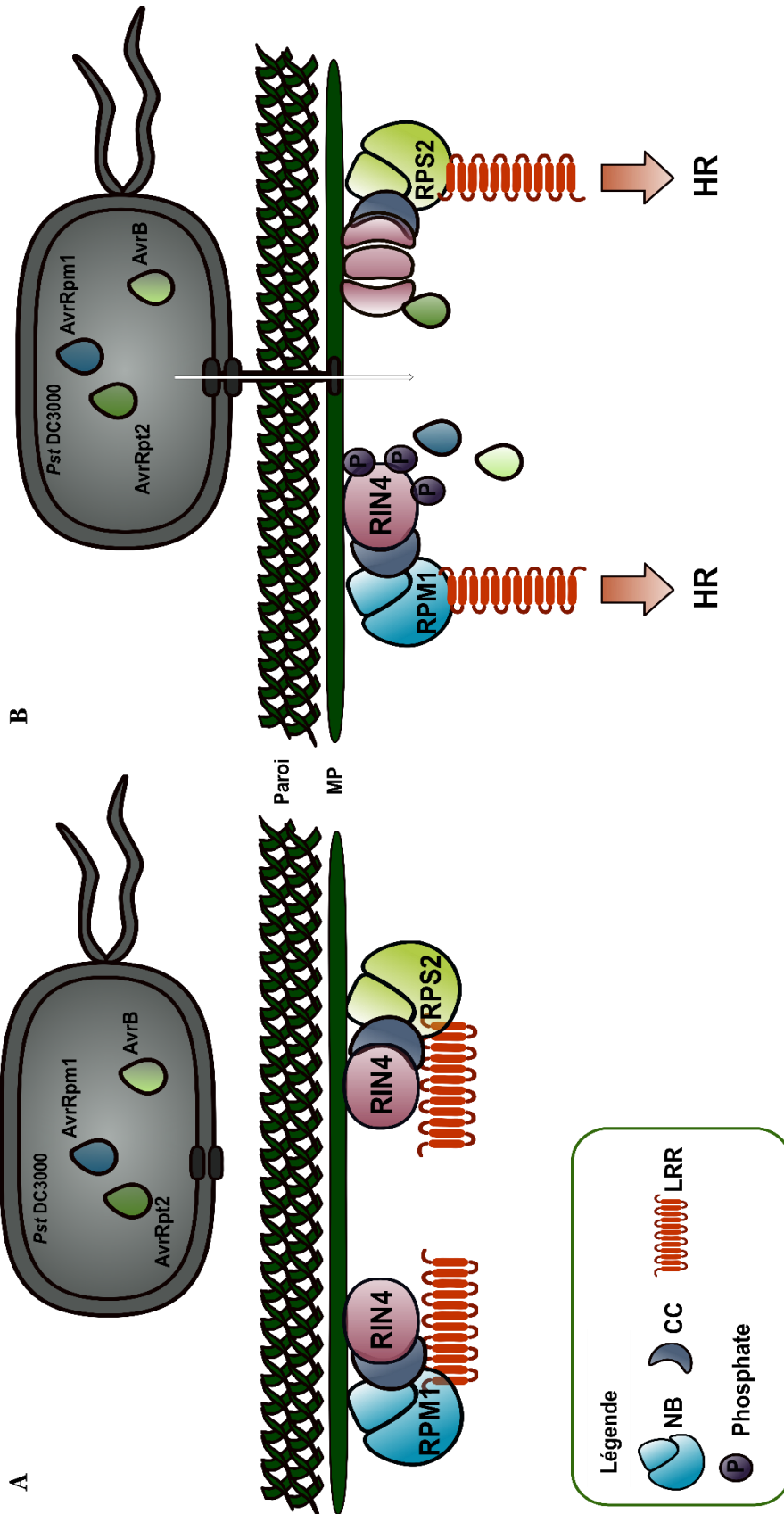
Figure 13. Schematic mode of action of AvrRpm1, AvrB and AvrRpt2 effectors in *Arabidopsis*

A. *Pst* DC3000 enters the apoplasm of plant tissues. The R proteins, RPM1 (CC-NLR), RPS2 (CC-NLR) and RIN4 are located at the membrane and are not activated. **B.** Upon contact with the plant cell, the bacterium will secrete the pilus of the type III secretion system in order to translocate effectors promulgating its virulence into the cytoplasm of host cells. In the case where *Pst* DC3000 is transformed with genes allowing the secretion of avirulent effectors, these will react with plant R-proteins which will become activated and trigger ETI in the form of HR (Hypersensitive Reaction). AvrRpm1 and AvrB will interact with RIN4, causing its phosphorylation, which will allow the activation of RPM1 and the HR. AvrRpt2 will interact with RIN4, causing its degradation, which will allow the activation of RPS2 and then the HR. The reaction is incompatible, and the plant is qualified as resistant.

Once translocated into the cytoplasm of the plant cell, the effectors AvrRpm1 and AvrB cause the phosphorylation of RIN4, inducing the activation of RPM1 and the triggering of the ETI leading to the HR (Nimchuk *et al.*, 2000). AvrRpt2 will cause degradation of RIN4 which in turn will allow activation of RPS2 leading to the HR (Boyes *et al.*, 1998; Chung *et al.*, 2011; Lee *et al.*, 2004; Mackey *et al.*, 2002; Xin *et al.*, 2018).

The effector AvrPphB was isolated from *P. syringae* pv. *phaseolicola*. It induces ETI in *Arabidopsis* by interacting indirectly, *via* the PBS1 protein, with the RPS5 protein (Resistance to *P. syringae* protein 5). The latter is a CC-NLR, which like RPM1, is located at the plant PM (Warren *et al.*, 1998) where it is associated with the PBS1 protein, a serine/threonine kinase (Ade *et al.*, 2007). AvrPphB will interact with PBS1 and cause its cleavage, inducing a conformational change in the protein which will then be recognised by RPS5, thus triggering the HR (Pottinger and Innes, 2020). AvrPphB is a cysteine protease, which will autolyse to reveal a myristoylation site (Puri, 1997), suggesting that the effector undergoes, like AvrRpm1 and AvrB, a myristoylation in the plant that allows it to be redirected to the PM, where RPS5 is located (Nimchuk *et al.*, 2000) (**Figure 14.**). AvrRpm1, AvrB and AvrPphB have no other similitude than their N-terminal sequence linked to myristoylation. This site would allow these effectors to be acylated by the plant, allowing them to be redirected to the membrane, where their target proteins, RIN4, RPM1 and PBS1, RPS5 are located (Nimchuk *et al.*, 2000) (**Table I.**).

Table I. *P. syringae* avirulence genes containing a consensus N-terminal sequence for fatty acid addition (from Nimchuck *et al.*, 2000)

	1 2 3 4 5 6 7 8 9
avrRpm1	M G C V S S T S R
avrB	M G C V S S K S T
avrPphB[a]	G C A S S G V S
SOS3 Ca sensor	M G C S V S K K K
avrC	M G N V C F R P S
avrPto	M G N I C V G G S
CPK1	M G N T C V G P S

References for each sequence are (top to bottom): Dangl et al., 1992; Tamaki et al., 1988; Jenner et al., 1991; J.-K. Zhu, personal communication; Tamaki et al., 1988; Salmeron and Staskawicz, 1993; Ellard-Ivey et al., 1999.
[a] Represents N terminus of processed AvrPphB protein as determined by Puri et al., 1997.
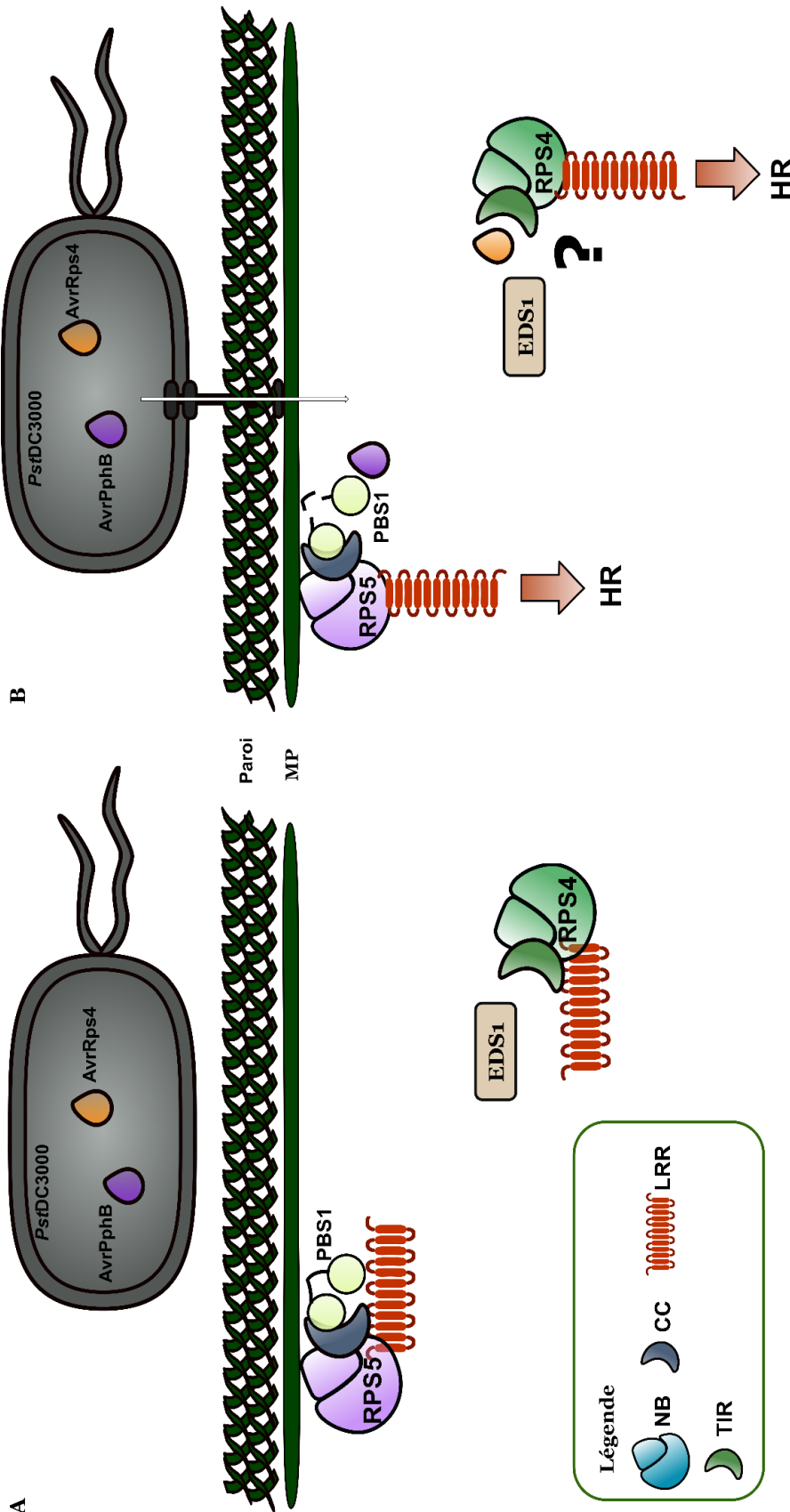
Figure 14. Schematic mode of action of AvrPphB and AvrRps4 effectors in *Arabidopsis*

A. *Pst* DC3000 enters the apoplasm of plant tissues. The proteins, RPS5 (CC-NLR) and PBS1 are located at the membrane. RPS4 (TIR-NLR) is located in the cytoplasm. The proteins are not activated. **B.** Upon contact with the plant cell, the bacterium will secrete the pilus of the type III secretion system in order to translocate effectors promulgating its virulence into the cytoplasm of host cells. In the case where *Pst* DC3000 is transformed with genes allowing the secretion of avirulent effectors, these will react with R proteins of the plant which will become activated and trigger ETI in the form of HR (Hypersensitive Reaction). AvrPphB will interact with PBS1, causing its cleavage, inducing a conformational change in PBS1 which will be detected by RPS5, allowing the subsequent triggering of the HR. The mechanism of AvrRps4 is less known, but it seems that it interacts with EDS1 (Enhanced Disease Suceptibility) in the cytoplasm, which causes the activation of RPS4 and then the HR. The reaction is incompatible, the plant is qualified as resistant.

b. AvrRps4

The effector AvrRps4, isolated from *P. syringae* pv. *phaseolicola*, also induces ETI in *Arabidopsis* (**Figure 14.**). It will interact with the RPS4 protein, a TIR-NLR first reported to be cytoplasmic (Gassmann *et al.*, 1999) and then nuclear, in an EDS1-dependent manner (Wirthmueller *et al.*, 2007). It appears that AvrRps4 breaks the physical interaction between EDS1 and RPS4, although one study showed that this interaction was not detectable *in planta* (Sohn *et al.*, 2012).

VIII. Thesis objectives and research strategies

Previous research by Magnin-Robert *et al.* (2015) has investigated interconnections between sphingolipids, cell death, and plant defence in response to hemibiotrophic and necrotrophic pathogens. More specifically, this report explored how altering SL metabolism can affect *Arabidopsis* resistance to *B. cinerea* and *Pst* DC3000 infection. To that end, LCB-P lyase (**Figure 7.**) *Arabidopsis* mutant (*AtDPL1*), disturbed in LCB/LCB-P accumulation, were analysed after infection. *B. cinerea*-inoculated *Atdpl1-1* plants showed an increase in t18:0-P and a decrease in d18:0 amounts. These SLs were therefore exogenously applied to further test their ability to modulate cell death and ROS production in response to *B. cinerea* and *Pst* DC3000. This experiment highlighted the absence of HR in WT *Arabidopsis* when *Pst AvrRpm1* was co-infiltrated with d18:0 (**Figure 15.**). These experiments also demonstrated that this co-infiltration caused a decrease in extracellular ROS production by the plant in response to *Pst AvrRpm1*. Furthermore, while there is a wealth of data on the links between LCBs and PCD (Ali *et al.*, 2018; Huby *et al*, 2020), very few report on the use of exogenously applied LCBs or their mode of action (Glenz *et al.*, 2019; Gutiérrez-Nájera *et al.*, 2020; Magnin-Robert *et al.*, 2015; Saucedo-García *et al.*, 2011; Shi *et al.*, 2007), which further prompted this research project. The aim of this thesis was therefore to clarify the mechanisms responsible for this absence of HR, in particular by elucidating the role and mode of action of exogenous SLs in this phenomenon.
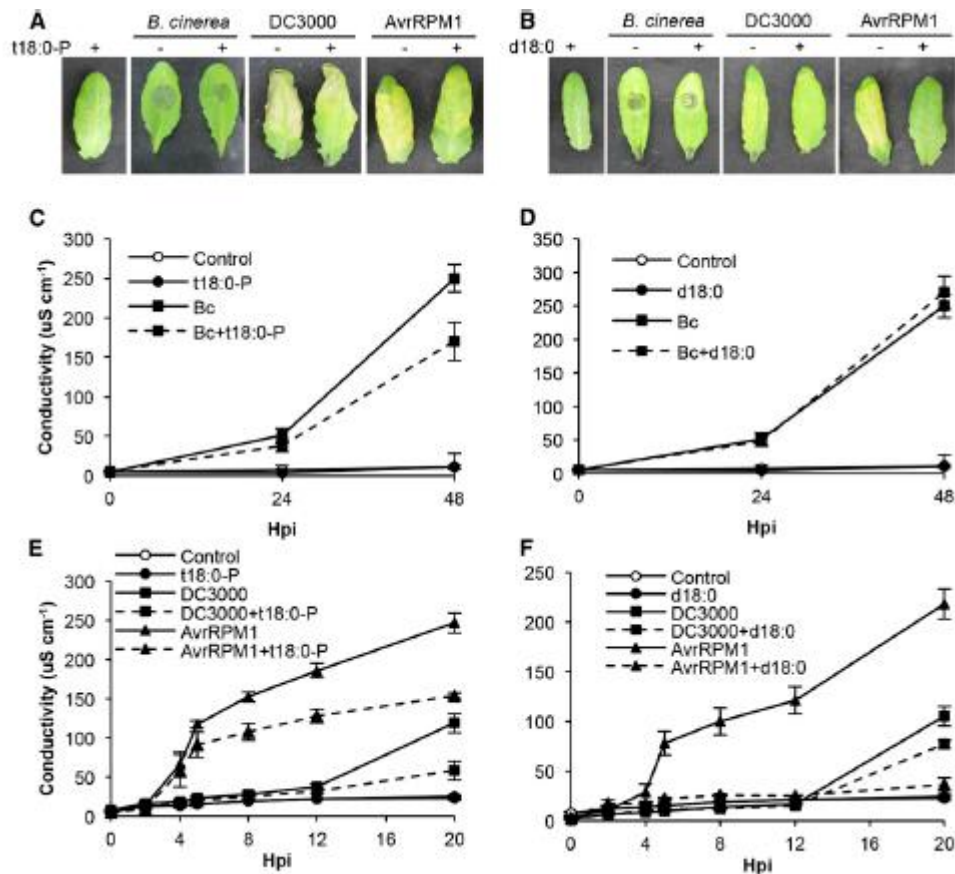
Figure 15. Exogenous effects of t18:0-P and d18:0 on electrolyte leakage in response to pathogen infection in wild-type *Arabidopsis* (from Magnin-Robert *et al.*, 2015)

A and B, *B. cinerea* conidia suspension was deposited on leaves of wild-type and *Atdpl1-1* mutant plants 15 min after infiltration of either t18-0-P or d18:0 solution. *Pst* and either t18-0-P or d18:0 solution were co-infiltrated into wild-type and *Atdpl1-1* leaves. Photographs represent symptoms observed 60 or 72 h after infection by the fungus or *Pst*, respectively. **C to F**, Conductivity (mS/cm^2) of solution containing t18:0-P- or d18:0-infiltrated leaf discs from the wild type inoculated by spraying *B. cinerea* (Bc) or PDB (Control) solution (C and D) or by infiltration of *Pst* DC3000, *Pst AvrRpm1*, or 10 mM MgCl$_2$ (E and F). Each value represents the mean ±SD of three replicates per experiment. The experiment was repeated three times with similar results.

The first two years of this thesis were spent at the University of Reims Champagne-Ardenne and allowed the biological characterisation of the specificity of the interaction between *Pst*, *Arabidopsis* and exogenous SLs and to determine the effect of the latter on the plant and the bacterium. The next two years were spent at Gembloux Agro-Biotech where biophysical experiments were carried out to characterise, at the molecular level, the interaction of sphinganine with plant and bacterial PM.

The results of this research work will be presented in four separate chapters, followed by a general discussion and conclusion.

Chapter 1, "Characterisation of the specificity of the interaction between *Pseudomonas syringae*, *Arabidopsis thaliana* and sphinganine", will focus on determining the key elements involved in the absence of HR observed during the *Pst AvrRpm1* / d18:0 co-infiltration. This will include the characterisation of the type of treatment, bacteria or SL used during this interaction.

Chapter 2, "*In vitro* and *in planta* effects of sphinganine on *Pseudomonas syringae*", will detail how sphinganine acts directly on the bacteria. Its effects on morphology and motility, as well as its antibacterial action and on the virulence of *P. syringae* will be discussed.

Chapter 3, "Effects of sphinganine and *Pseudomonas syringae* co-infiltration on defence mechanisms of *Arabidopsis thaliana*" will allow us to follow some defence parameters set up by *Arabidopsis* in response to *P. syringae* and how these are affected by the co-infiltration of sphinganine.

Finally, **Chapter 4** "Biophysical analysis of the interaction of sphinganine with lipids in plant and bacterial membranes" will focus on characterising the effect of sphinganine on PM, such as its ability to insert, permeabilise and modulate membrane fluidity. For this purpose, biomimetic membrane models representing lipid compositions of plant or bacterial membranes will be used.

54

1

Characterisation of the specificity of the interaction between *Pseudomonas syringae*, *Arabidopsis thaliana* and sphinganine

I. Context

The first part of this thesis aimed to determine if the absence of HR observed when *Pst AvrRpm1* and d18:0 were co-infiltrated in *Arabidopsis* leaves was specific to the experimental conditions. To that end, several approaches were employed to determine if this phenomenon was specific to the treatment method (co-infiltration), the plant (*Arabidopsis*), the SL (d18:0) or to the bacteria (*Pst AvrRpm1*) used.

There are several ways to inoculate a plant with bacteria: dipping, spraying and vacuum or syringe infiltration, to cite a few (Nimchuk *et al.*, 2000; Wirthmueller *et al.*, 2007; Jacob *et al.*, 2017). Here inoculation by spray were tested along with delayed infiltrations. The former, to experiment a type of infection requiring that bacteria go through the CW, unlike infiltration, and the later, to determine whether co-infiltration is paramount to the absence of HR.

Next, two other model plants, tomato and tobacco were selected to highlight if using *Arabidopsis* was a key factor in the phenomenon. The former is the primary host of *Pst* DC3000 and is therefore highly susceptible to the pathogen, the latter is a non-host plant that can detect *Pst* DC3000 and set up defences against it, including the HR notably through the SA pathway (Liu *et al.*, 2013).

To elucidate the specificity of d18:0 in the interaction, other molecules stemming from the SL metabolism were tested. Sphingosine (d18:1), phytosphingosine (t18:0), and phytosphingosine 1-phosphate (t18:0-P) were chosen to experiment on LCBs that possess or not a phosphate and a different hydroxylation and saturation degree. Two more complex SLs were selected based on their similarities of structure with d18:0. First dihydroceramide (DhCer - d18:0/18:0), to check whether adding a fatty acid could have an effect. Then glucosylceramide (GluCer - d18:2/16:0), to determine if adding a sugar could have an impact.

Finally, avirulent bacteria producing other effectors were tested to determine if the absence of HR was specific to *Pst AvrRpm1*. Among them, effectors AvrB and AvrRpt2 were chosen because their mode of action is somewhat similar to that of *Pst AvrRpm1*. Indeed, both interact with RIN4 and their corresponding R protein RPM1 and RPS2, respectively, are located at the PM (Boyes *et al.*, 1998; Mackey *et al.*, 2003; Xin *et al.*, 2018). AvrRps4 was tested because the location of its target, RPS4, is located within the cytoplasm, unlike RPM1 (Gassmann *et al.*, 1999; Wirthmueller *et al.*, 2007). Effector AvrPphB was in turn chosen because it shares an N-myristoylation sequence within AvrRpm1 and AvrB, which allows them to be redirected to the PM once they enter their host (Nimchuk *et al.*, 2000; Pottinger and Innes, 2020). Finally, two bacteria from the pathovar *maculicola,* closely related to the pathovar *tomato*, were picked to verify if the absence of HR was strain specific. The avirulent strain m2, which naturally produces AvrRpm1 (Debenert *et al.*, 1991), and the virulent strain ES4326 transformed to produce AvrRpm1 (Stahl *et al.*, 2016). Depending on whether the plant can recognize the bacterium or not, lesions are expected to appear at the

infiltration spot, either due to the HR or to the spread of the bacteria (Zipfel and Oldroyd, 2017). The two bacteria that should not be able to trigger a HR are *Pst* DC3000 and *Psm* ES4326, both carrying an empty vector.

II. Material and methods

1. Plant material and growth conditions

Wild type seeds of *Arabidopsis thaliana* Columbia-0 (Col-0) were obtained from the Nottingham *Arabidopsis* Stock Center (http://*Arabidopsis*.info) and grown in soil under 12 h-light/12 h-dark conditions (150 µmol/m²/s, 20°C, and 60% humidity) for 5 weeks. Tomato (*Solanum lycopersicum*) and tobacco (*Nicotiana tabacum*) seeds were grown in soil under 14 h-light/10 h-dark conditions (150 µmol/m²/s, 24°C, and 60% humidity) for up to 8 weeks.

2. Chemicals

Sphinganine (d18:0), sphingosine (d18:1), phytosphingosine (t18:0), Phytosphingosine 1-phosphate (t18:0-P), glucosylceramide (GluCer) and dihydroceramide (DhCer) were purchased from Avanti Polar Lipids, dissolved in ethanol (100%), and used without further purification.

3. Bacterial cultures

Pst DC3000 transformed to express the effectors AvrRpm1 (noted *Pst AvrRpm1*), AvrRpt2 (noted *Pst AvrRpt2*), AvrRps4 (noted *Pst AvrRps4*), AvrB (noted *Pst AvrB*) or AvrPphB (noted *Pst AvrPphB*) were provided by Prof. Jeff Dangl (University of North Carolina, USA) and Dr. Farid El-Kasmi (University of Tübingen, Germany), Prof. Brian Staskawicz (University of California, USA), Prof. Jane Parker (Max-Planck Institute, Cologne, Germany) and Dr. Brad Day (Michigan State university, USA), respectively. *Psm* m2, *Psm* ES4326, carrying an empty vector, and *Psm* ES4326 *AvrRpm1* were provided by Prof. Philippe Reymond (University of Lausanne, Switzerland), and Prof. Christiane Gatz (University of Göttingen, Germany), respectively.

Bacterial leaf pathogens *Pst* DC3000, *Pst AvrRpm1*, *Pst AvrRpt2*, *Pst AvrRps4*, *Pst AvrB* and *Pst AvrPphB*, were cultured overnight under agitation (180 rpm) at 28°C in liquid King's B medium, supplemented with rifampicin (50 µg/mL) and kanamycin (50 µg/mL). *Psm* m2, *Psm* ES4326 and *Psm* ES4326 *AvrRpm1*, were cultured overnight at 28°C in liquid King's B medium, supplemented

with streptomycin (50 μg/mL) for *Psm* m2, rifampicin (50 μg/mL) for *Psm* ES4326 and rifampicin and tetracycline (50 and 5 μg/mL, respectively) for *Psm* ES4326 *AvrRpm1*.

4. Inoculations

Upon treatments, bacterial cells were collected by centrifugation, washed two times, and resuspended in 10 mM MgCl$_2$ to reach different optical densities at 600 nm (OD$_{600}$). Final concentrations reached either 10^6, 10^7 or 10^8 CFU/mL, as specified further for each experiment. Bacterial solutions were either sprayed at 10^8 CFU/mL + 0.04% Silwet (v/v) or infiltrated (ca. 1 mL) at 10^6 or 10^7 CFU/mL on the abaxial side of *Arabidopsis* leaves using a 1 mL syringe without needle. Co-treatment of bacteria with sphinganine at 1, 10, 100 μM or 1 mM, as specified further for each experiment, were performed likewise. Control inoculations were conducted with 10 mM MgCl$_2$. At least four leaves per plant were treated for each condition on a minimum of three different plants. Each experiment was repeated at least three times. Lesions were estimated from pictures of the experiments that were taken 48 hours post infiltration (hpi), or 7 days post spraying.

III. Results

1. The absence of HR is dependent on co-infiltration

Bacterial infiltration, as used by Magnin-Robert *et al.* (2015), is a very specific treatment method and is far from representing a natural infection process. Indeed, here, bacteria are directly infiltrated into the apoplasm of plants and do not have an epiphytic life phase where they must penetrate the plant by their own means. Therefore, these first experiments aimed to determine if the absence of HR observed during the co-infiltration of *Pst AvrRpm1* and d18:0 was specific to this inoculation method.

Bacterial infection by spray were tested on *Arabidopsis* leaves. They were conducted with bacteria resuspended at 10^8 CFU/mL and d18:0 at 100 μM, and lesions were observed 7 days post treatment. None of the control treatments (MgCl$_2$ and ethanol) had an effect on the plant (data not shown). Spray bacterization with the bacteria alone or with d18:0 induced only a weak HR (**Figure 16A.**). Unfortunately, given the weak immune response of the plant to the bacteria alone, it was not possible to properly determine if this treatment method can replicate the results observed with co-infiltration. This could originate from the experimental conditions (e.g., temperature, humidity, age of plants).

Delayed infiltrations were also tested to determine whether co-infiltration is an important factor in the absence of HR. In all conditions, infiltrations were performed with bacteria resuspended at 10^7 CFU/mL and d18:0 at 100 µM, and lesions severity were estimated at 48 hpi. Once again, none of the control treatments (MgCl$_2$ and ethanol) had an effect on the plant (data not shown). Finally, the delayed infiltrations showed that even very short delays between d18:0 or bacterial infiltration can result in a HR, albeit moderate (**Figure 16B.**). A 5-minute delay between the two infiltrations was sufficient to obtain a moderate HR and a 30-minute delay for a full HR, indicating that co-infiltration of the bacteria and d18:0 appeared essential to the absence of HR.

A

	HR
AvrRpm1 sprayed	+
AvrRpm1+d18:0 sprayed	+
d18:0 infiltration then AvrRpm1 sprayed	+

B

	Infiltration delay (min)	HR
Pst AvrRpm1		+++
Pst AvrRpm1 followed by d18:0	5	++
	10	++
	30	+++
	60	+++
d18:0 followed by *Pst AvrRpm1*	5	++
	10	++
	30	+++
	60	+++
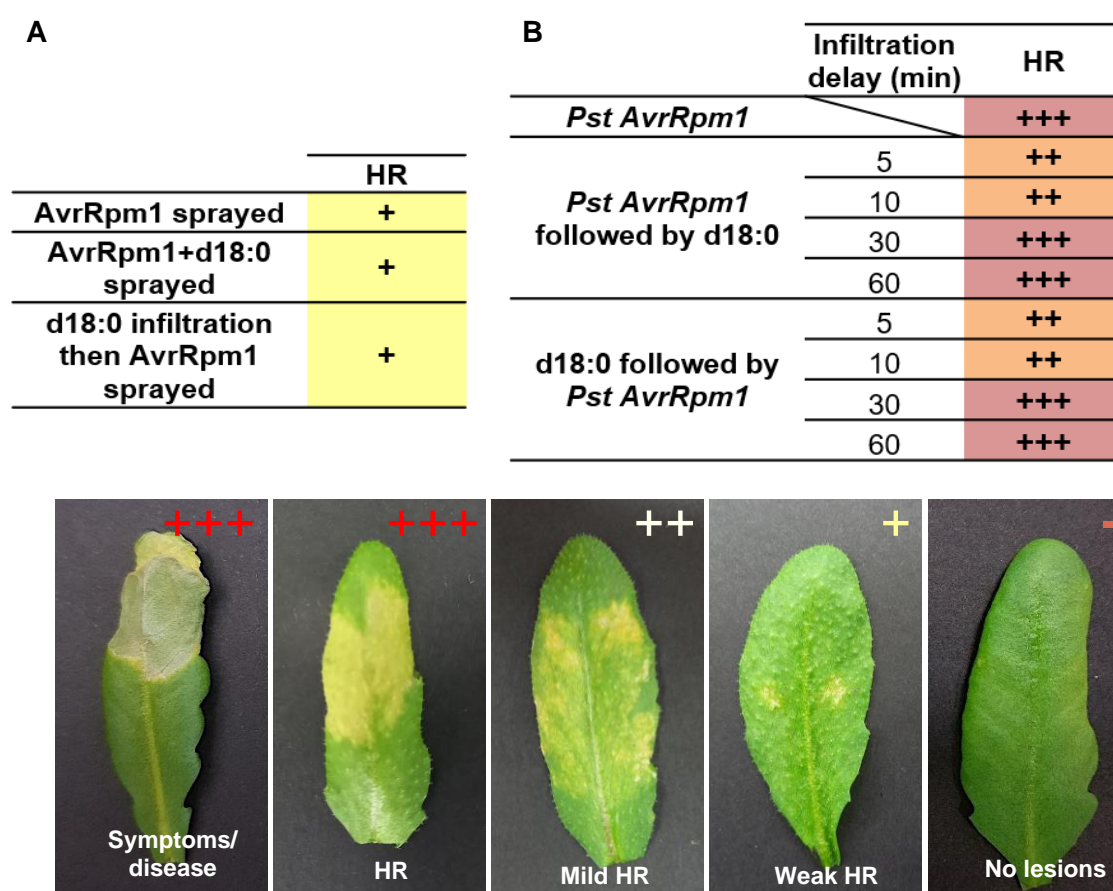
Figure 16. Phenotypes of *Arabidopsis* leaves after various treatments

Visual estimation of cell death severity of *Arabidopsis* WT Col-0 leaves. **A.** 7 days post spray treatment with *Pst AvrRpm1* (10^8 CFU/mL + 0,04% Silwet) and d18:0 (100 µM, ethanol 100%) **B.** 48 hours post delayed infiltration with *Pst AvrRpm1* (10^7 CFU/mL in 10 mM MgCl$_2$) and d18:0 (100 µM, ethanol 100%). Control inoculations were conducted with 10 mM MgCl$_2$ and ethanol (0,1%, v/v) and did not present cell death (data not shown). At least four leaves per plant were treated for each condition on a minimum of three different plants (n=3). Colors and symbols translate the estimated severity of visible cell death.

2. Co-infiltration provokes a reduced cell death in tomato and tobacco

Infiltration experiments were performed on both tomato and tobacco (**Figure 17.**). Tomato being the host of *Pst*, infiltration of the bacteria should cause necrosis due to its spreading. Tobacco being a non-host plant, it should be able to trigger defence phenomenon, including a HR at the site of infection. *Pst* DC3000 or *Pst AvrRpm1* were infiltrated on the abaxial face of tomato and tobacco leaves at 10^7 CFU/mL, either alone or with d18:0 at 100 µM. Lesions were estimated 96 hpi for tobacco and 48 hpi for tomato. Tomato leaves were observed earlier because as host plant, its reaction to the bacterium was faster and stronger than that of tobacco. None of the control treatments (MgCl$_2$ + ethanol) had an effect on the plant (data not shown).

	Tobacco	Tomato
Pst DC3000	+++	+++
Pst DC3000/d18:0	+++	+++
Pst AvrRpm1	++	+++
Pst AvrRpm1/d18:0	-	+

B.

C.

AvrRpm1 | AvrRpm1 /d18:0

AvrRpm1 | AvrRpm1/d18:0
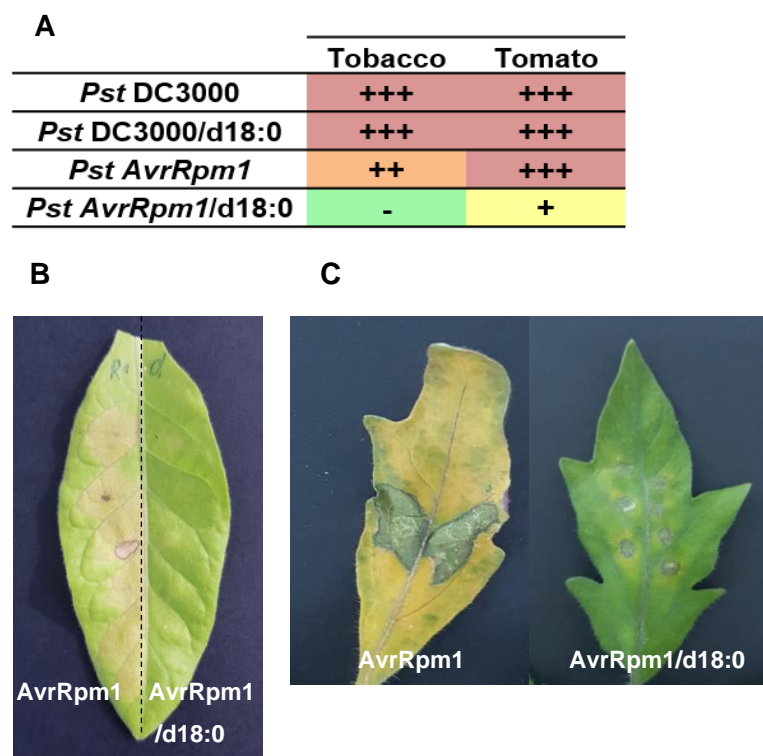
Figure 17. Summary of phenotypes of tobacco and tomato leaves after bacterial infiltration with or without d18:0

A. Visual estimation of cell death severity of tobacco and tomato leaves. Leaves were collected, 96 (tobacco) and 48 (tomato) hours post infiltration with *Pst* DC3000 or *Pst AvrRpm1* (10^7 CFU/mL in 10 mM MgCl$_2$) with or without d18:0 (100 µM, ethanol 100%). Control inoculations were conducted with 10 mM MgCl$_2$ and ethanol (0,1%, v/v) and did not present cell death (data not shown). At least four leaves per plant were treated for each condition on a minimum of three different plants (n=3). Colors and symbols translate the severity of visible cell death. **B.** Tobacco leaves and **C.** tomato leaves co-infiltrated with *Pst AvrRm1* and d18:0 show reduced necrosis.

Both plants strongly reacted to *Pst* DC3000 infiltrated alone or with d18:0 and showed extensive cell death (**Figure 17A.**). When infiltrated with *Pst AvrRpm1* they also both showed cell death although reduced in the case of tobacco (**Figure 17B.** and **C.**). However, when co-infiltrated with d18:0, both plants exhibited reduced cell death, suggesting the absence of HR might not be specific to *Arabidopsis*.

3. The absence of HR is linked to the type of sphingolipid used and is dose dependent

Experiments were performed to determine if the absence of HR previously observed by Magnin-Robert *et al.* (2015) could be obtained with other SLs and if this phenomenon was dose dependent. SLs were therefore co-infiltrated at various concentrations with either *Pst* DC3000 or *Pst AvrRpm1* on *Arabidopsis* leaves at 10^6 or 10^7 CFU/mL and lesions estimated 48 hpi.

None of the control treatments ($MgCl_2$ + ethanol) had a visible effect on the plant, neither did all the SLs infiltrated alone (data not shown).

Concerning the LCBs d18:1 and t18:0, all conditions tested yielded similar results to those observed with d18:0 (**Figure 18.**). Infiltration of *Pst* DC3000 alone or co-infiltrated with the LCBs provoked necrosis on *Arabidopsis* leaves. Co-infiltration of *Pst AvrRpm1* with either LCBs did not result in a visible HR from the plant. Concentrations of LCBs up to 10 μM were sufficient to suppress the HR, but symptoms started to appear at lower concentrations. The co-infiltration of *Pst AvrRpm1* and LCB-P, t18:0-P showed a completely different phenotype to that of LCBs. Even at a high concentration (100 μM), a strong HR was observable on treated leaves (**Figure 18.**).

The co-infiltration of the more complex SLs, DhCer and GluCer at 100 μM with *Pst* DC3000 or *Pst AvrRpm1* at 10^6 and 10^7 CFU/mL induced an HR on *Arabidopsis* leaves (**Figure 18.**). SLs were consequently co-infiltrated at a higher concentration (1 mM) with either bacterium at 10^6 or 10^7 CFU/mL. While no difference was noted at 10^7 CFU/mL, reduced HR were observed on the leaves for both bacteria at 10^6 CFU/mL.

		Pst DC3000		*Pst* AvrRpm1	
		10^6	10^7	10^6	10^7
Ctrl		+++	+++	++	+++
d18:0	1µM	+++	+++	++	++
	10µM	+++	+++	-	-
	100µM	+++	+++	-	-
d18:1	1µM	+++	+++	+	+
	10µM	+++	+++	-	-
	100µM	+++	+++	-	-
t18:0	1µM	+++	+++	+	+
	10µM	+++	+++	-	-
	100µM	+++	+++	-	-
t18:0-P	100µM	+++	+++	+++	+++
GluCer	100µM	+++	+++	++	+++
	1mM	+	+++	+	+++
DhCer	100µM	+++	+++	++	+++
	1mM	++	+++	+	+++

Figure 18. Summary of *Arabidopsis* leaves phenotypes after infiltration of *Pst* with or without sphingolipids at several concentrations

Visual estimation of cell death severity of *Arabidopsis* WT Col-0 leaves, 48 hours post infiltration with *Pst* DC3000 or *Pst* AvrRpm1 (10^6 or 10^7 CFU/mL in 10 mM $MgCl_2$) with or without sphingolipids (various concentrations, ethanol). Sphinganine (d18:0), sphingosine (d18:1), phytosphingosine (t18:0), phytosphingosine 1-phosphate (t18:0-P), dihydroceramide (DhCer) and glucosylceramide (GluCer) were tested. Control inoculations were conducted with 10 mM $MgCl_2$ and ethanol (0,1%, v/v) and did not present cell death (data not shown). At least four leaves per plant were treated for each condition on a minimum of three different plants (n=3). Colors and symbols translate the severity of visible cell death.

4. The absence of visible HR is not specific to *Pst AvrRpm1*

As effectors can function as both virulence and avirulence factors, they play deterministic roles in the outcome of plant–pathogen interactions (Alfano and Collmer, 2004). Here, *Pst* producing effectors other than AvrRpm1 and other pathovars of *P. syringae* producing AvrRpm1 have been selected to elucidate whether the absence of visible HR was dependent on the bacteria / effector used.

Experiments were carried out on *Arabidopsis* leaves with bacteria at 10^6 or 10^7 CFU/mL infiltrated either alone or with d18:0 at 100 µM. Lesions severity was estimated 48 hpi.

Once again, none of the $MgCl_2$ + ethanol control treatments led to visible cell death (data not shown). At 10^6 or 10^7 CFU/mL, all bacteria infiltrated alone led to cell death, except *Pst AvrB* at 10^6 CFU/mL, which we assumed was not concentrated enough to trigger a response from the plant (**Figure 19.**). *Pst AvrRpm1* at 10^6 CFU/mL, *Psm* ES4326 at 10^7 CFU/mL and *Pst AvrPphB* at both concentrations all showed mild cell death. Co-infiltration of d18:0 with *Pst* DC3000 and *Pst* ES4326 also resulted in cell death, as expected since *Arabidopsis* is susceptible to both bacteria. Similarly, co-infiltration of d18:0 with *Pst AvrRpt2*, *Pst AvrRps4* or *Psm* m2 had the same result as infiltration of the bacteria alone. Co-infiltration with *Pst AvrB*, *Pst AvrPphB* or *Psm* ES4326 *AvrRpm1*, did, however, affect the onset of the HR. Indeed, no cell death was observed for the first two bacteria and only minor lesions were observed on leaves infected with the latter. The absence of HR can therefore be observed with two more effectors, AvrB and AvrPphB. The results obtained with *Psm* ES4326 *AvrRpm1* suggest that the absence of HR is effector but not bacteria-dependent.

Bacteria	CFU/mL	Ctrl	d18:0
Pst DC3000	10^6	+++	+++
	10^7	+++	+++
Pst AvrRpm1	10^6	++	-
	10^7	+++	-
Pst AvrRpt2	10^6	+++	+++
	10^7	+++	+++
Pst AvrRps4	10^6	+++	+++
	10^7	+++	+++
Pst AvrB	10^6	-	-
	10^7	+++	-
Psm AvrPphB	10^6	++	-
	10^7	++	-
Psm ES	10^6	ND	ND
	10^7	+++	+++
Psm ES *AvrRpm1*	10^6	ND	ND
	10^7	++	+
Psm m2	10^6	+++	+++
	10^7	+++	+++

+++ Symptoms/disease   +++ HR   ++ Mild HR   + Weak HR   - No lesions
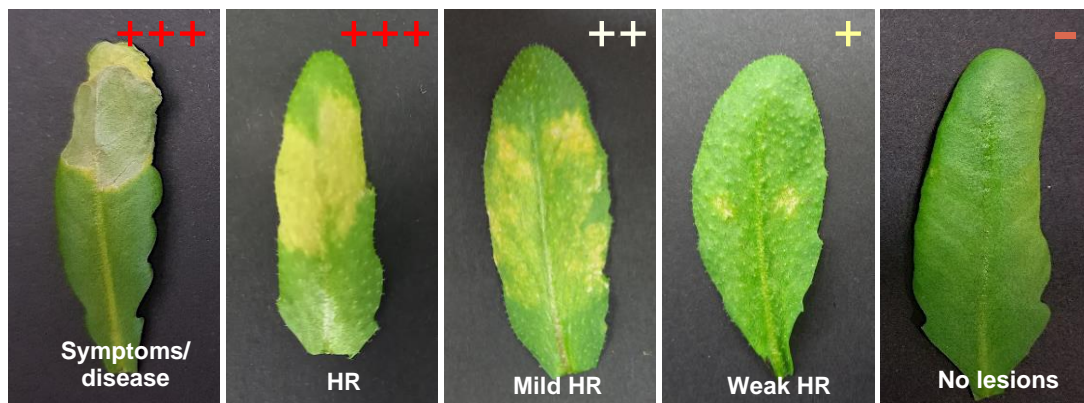
Figure 19. Summary of phenotypes of *Arabidopsis* leaves after infiltration of bacteria with or without d18:0

Visual estimation of cell death severity of *Arabidopsis* WT Col-0 leaves, 48 hours post infiltration. *Pst* DC3000, *Pst AvrRpm1*, *Pst AvrRpt2*, *Pst AvrRps4*, *Pst AvrB*, *Pst AvrPphB*, *Pst* ES4326 (noted ES), *Psm* ES4326 *AvrRpm1* (noted ES *AvrRpm1*) and *Psm* m2 were infiltrated (10^6 or 10^7 CFU/mL in 10mM $MgCl_2$) either with ethanol (0,1%, v/v) or with d18:0 (100 µM in ethanol). Control inoculations were conducted with 10 mM $MgCl_2$ and ethanol (0,1%, v/v) and did not present visible cell death (data not shown). At least four leaves per plant were treated for each condition on a minimum of three different plants (n=3). Colors and symbols translate the severity of visible cell death, ND (not determined).

IV. Discussion and conclusion

Pst DC3000 is a known poor epiphyte in the field (Katagiri *et al.*, 2002) and is therefore not considered a good model for the study of epiphytic interaction. This could explain why in our experiments, even when sprayed at high doses and in presence of a surfactant, only few symptoms were observable. Variations in the experimental setting (e.g., age of the plants, humidity…) might also be a possible explanation. The delayed treatments further confirmed that the absence of HR was specific to co-infiltration. Considering that even short infiltration delays have an impact on the onset of the HR, it would suggest that if d18:0 does have an effect on the bacteria and/or the plant, it must be very quick and / or transitory. Such rapid action can be observed in plant defence phenomena since some of them can be activated shortly after threat perception. The production of ROS or ion fluxes for instance occur within a few seconds (Bolwell and Wojtaszek, 1997) and it has already been shown in *Arabidopsis* cell cultures that the elicitor flagellin can induce phosphorylation of a protein within 30 seconds (Peck *et al.*, 2001). Similarly, transitory effect of elicitors have already been demonstrated such as cryptogein which triggers a massive transitory clathrin endocytosis from the PM of elicited tobacco BY-2 cells (Leborgne-Castel *et al.*, 2008).

The response of tomato and tobacco to *Pst* DC3000 is well-known and leads to necrosis due to the propagation of the bacteria or to the HR, respectively. However, co-infiltration of the bacterium with d18:0 on both plants provoked less extensive cell death. The fact that this can be observed in host (tomato) and tobacco plants that do not possess neither RPM1 nor RIN4 suggest these proteins are not necessarily involved in the absence of HR.

While some studies report LCBs can cause cell death at low concentrations on seedlings of *Arabidopsis* (Shi *et al.*, 2007; Saucedo-García *et al.*, 2011), such PCD was not observed with our experimental conditions. Furthermore, co-infiltration experiments with LCBs (d18:0, d18:1 and t18:0) suggest that carbon chain saturation and the number of hydroxyl groups does not alter their efficiency when co-infiltrated with *Pst AvrRpm1* in *Arabidopsis*, since no HR is observable with these molecules. However, co-infiltrations with t18:0-P does not stop the onset of the HR, which is consistent with co-infiltration experiments performed by Magnin-Robert *et al.* (2015). It would therefore seem that the addition of a phosphate, which renders the LCB charged, makes it inefficient. The two other SLs tested, GluCer and DhCer appear to be able to reduce symptoms caused by both *Pst* DC3000 and *Pst AvrRpm1*. However, such effect is only visible when SLs are highly concentrated (1 mM) and bacteria are infiltrated at low concentrations, which may indicate an antibacterial action of the molecules; such aspect will be covered in Chapter 2.

Concerning the different bacteria and effectors tested, the fact that a HR appeared when plants were treated with *Pst AvrRpt2* would first suggest that RIN4 is not directly involved in the

phenomenon, since both *Pst AvrRpt2* and *Pst AvrRpm1* interact with this protein. However, since the effector AvrRpm1 induces phosphorylation of RIN4 and AvrRpt2 its degradation, this different mode of action could explain the difference in the plant's response to *Pst AvrRpt2* (Boyes *et al.*, 1998; Mackey *et al.*, 2002). Absence of visible HR appeared with three of the tested bacteria. First with *Psm* ES4326 *AvrRpm1*, as expected since this bacterium produces the effector AvrRpm1. Since this result was observed with *Psm*, it suggests that *Pst* is not mandatory for the absence of HR. Then *Pst AvrB* and *Pst AvrPphB*, which, as previously mentioned, share an N-myristoylation sequence with AvrRpm1, allowing them to be redirected at the PM (Nimchuk *et al.*, 2000). These results would suggest that the myristoylation process is somehow involved in the absence of HR. However, these assumptions are challenged by the fact that co-infiltration of *Psm* m2 with d18:0 resulted in cell death while this strain is thought to naturally produce AvrRpm1 (Debenert *et al.*, 1991). This would suggest that there could be a redundancy mechanism between virulence factors that would allow *Psm* m2 to remain virulent. This has already been demonstrated in *Pst*, where effectors AvrPto and AvrPtoB both elicit a HR *via* their interaction with the tomato kinase Pto and thus both contribute to virulence (Lin and Martin, 2005; Cunnac *et al.*, 2009).

Other experiments have been conducted with *Arabidopsis* expressing dexamethasone (Dex)-inducible AvrRpm1 (Dex:AvrRpm1-HA Col-0). Unfortunately, none of the treatments tested were successful (data not shown). d18:0 was either infiltrated before spraying Dex or sprayed along with Dex. However, independently of the presence of d18:0, dexamethasone spraying on these plants triggered a strong induction of AvrRpm1, a rapid HR-like response within 6 hours and a complete drying of the plant within 24 hours. Several factor could explain why adding d18:0 to these plants did not reduce AvrRpm1-triggered cell death. We previously demonstrated that co-infiltration was a paramount factor to the absence of HR, and we could not replicate to treatment method here. The induction of AvrRpm1 has also previously been described as very strong and rapid (Mackey *et al.*, 2003; Kim *et al.*, 2009) and was perhaps too potent for d18:0 to have an effect on. Overall, these preliminary experiments highlighted key factors to replicate the absence of HR obtained when *Pst AvrRpm1* is co-infiltrated with d18:0. Among them, the SL used (LCBs), the method of treatment (co-infiltration) and the effectors employed (AvrRpm1, AvrB, AvrPphB).

Chapter 1 - Main Results

Key factors in the absence of visible HR:

- ✓ Specific to the LCBs: d18:0, d18:1, t18:0

- ✓ Co-infiltration of the bacteria and the LCB

- ✓ Efficient LCB concentrations range from 10 to 100 µM

- ✓ Three effectors involved: AvrRpm1, AvrB, and AvrPphB

2

The *in vitro* and *in planta* effects of
sphinganine on *Pseudomonas syringae*

I. Context

While the effect of bacteria on plant SL metabolism is well studied (Ali *et al.*, 2018; Huby *et al.*, 2020), exogen application of SLs on bacteria and its consequence on their metabolism and physiology is not well characterised. Various parameters were therefore followed to better decipher how d18:0 can affect *Pseudomonas*.

When exposed to certain molecules, bacteria can suffer a morphological dissociation, also called smooth-to-rough mutation. This phenomenon is irreversible and mutated bacteria often fail to survive in a host with an intact immune system (Sułowicz *et al.*, 2016; Butsenko *et al.*, 2020). Such mutations are therefore frequently associated with decreased virulence. Since it has already been demonstrated that pesticides, such as deltamethrin, can induce the appearance of mutated colonies of *Pst* (Butsenko *et al.*, 2020), a direct effect of d18:0 on the aspect of the bacteria could be envisaged. If such activity of d18:0 is expected, other factors linked to bacterial virulence that could be altered by d18:0 exposure are to be followed. Bacterial motility is one of these factors (Haefele and Lindow, 1987; Quiñones *et al.*, 2005), as motile bacteria are more likely to efficiently infect their hosts. Another important trait for epiphytic fitness and virulence is exopolysaccharide (EPS) production. EPS, are carbohydrate polymers produced by bacteria and secreted into the growth medium to form a biofilm facilitating water and nutrients accumulation, and protection against toxic macromolecules (Yu *et al.*, 1999). EPS production has proven to be paramount for virulence of *P. solanacearum* or *Xanthomonas campestris*, (Fett and Dunn, 1989; Arrebola *et al.*, 2015). While infection by leaf infiltration should bypass the epiphytic life phase, an action of d18:0 on EPS production by *Pst* should not be excluded.

As previously demonstrated, the absence of visible HR obtained when *Pst AvrRpm1* is co-infiltrated with d18:0 turned out to be dose dependent. This raised the question on a possible antibacterial and/or bacteriostatic effect of LCBs on *Pst*. Such activity has already been demonstrated against human pathogens (Fischer *et al.*, 2012; Becam *et al.*, 2017; Wu *et al.*, 2021). Indeed, through their structural and functional diversity, SLs have proven to be key players in infection prevention due to their antibacterial roles. For instance, the LCBs t18:0 and d18:1 were shown to have a strong effect on biofilm formation and adherence of *Streptococcus mutans*, which is responsible for dental caries (Cukkemane *et al.*, 2015). Besides, it was proven that d18:1 and synthetic short-chain ceramide analogue had a potent bactericidal activity against pathogenic *Neisseriae*, which can cause respiratory or sexual infections (Becam *et al.*, 2017). Other studies also pointed LCB protective functions, notably against lung infection in mice caused by *P. aeruginosa*, (Pewzner-Jung *et al.*, 2014), and SARS-CoV-2 (coronavirus-2) (Wu *et al.*, 2021). Considering these findings, *in vitro* bactericidal and bacteriostatic effects of d18:0 on *Pst* and *Psm* were therefore

tested. These results were completed by *in planta* studies to evaluate the presence and development of *Pst AvrRpm1* in *Arabidopsis* leaves after co-infiltration with d18:0.

The T3SS, as virulence apparatus embedded in the PM of *Pst*, could also be a target for exogenously added d18:0, especially since small molecules and antibodies capable of inhibiting the expression or function of the T3SS have already been discovered (Anantharajah *et al.*, 2016). Furthermore, since many T3SS knockout strains are incapable of causing systemic infection, it has emerged as an attractive anti-virulence target for therapeutic design (Hotinger *et al.*, 2021) and given the conserved nature of the T3SS and the *hrp/hrc* system among pathogens, redundancy between active molecules could be expected.

II. Materials and methods

1. Plant material and growth conditions

Wild type seeds of *Arabidopsis thaliana* Columbia-0 (Col-0) were obtained from the Nottingham *Arabidopsis* Stock Center (http://*Arabidopsis*.info) and grown in soil under 12 h-light/12 h-dark conditions (150 μmol/m²/s, 20°C, and 60% humidity) for 5 weeks.

2. Chemicals and culture medium

Composition of bacterial culture media King's B, LB, minimal medium m9, mannitol motility medium and yeast extract medium (YEM) is described in **Supplemental Table S2**. Chemical elements used for media and antibiotics were purchased from Sigma-Aldrich. Sphinganine (d18:0) was purchased from Avanti Polar Lipids, dissolved in ethanol (100%), and used without further purification. Extract-All was purchased from Eurobio Scientific. Verso cDNA synthesis kit and absolute blue SYBR Green Master Mix were purchased from Thermo Fisher Scientific.

3. Bacterial cultures

Pst DC3000, carrying an empty vector, *Pst AvrRpm1*, *Pst AvrRpt2*, *Pst AvrRps4*, *Pst AvrB* and *Pst AvrPphB*, were cultured overnight under agitation (180 rpm) at 28°C in liquid King's B medium, supplemented with rifampicin (50 μg/mL) and kanamycin (50 μg/mL). *Psm* m2, *Psm* ES4326 and *Psm* ES4326 *AvrRpm1*, were cultured overnight at 28°C in liquid King's B medium,

supplemented with streptomycin (50 μg/mL) for *Psm* m2, rifampicin (50 μg/mL) for *Psm* ES4326 and rifampicin and tetracycline (50 and 5 μg/mL, respectively) for *Psm* ES4326 *AvrRpm1*.

4. Morphological studies

To determine the effect of d18:0 on colony morphology of *Pst*, bacteria were either plated at 10^6 or 10^7 CFU/mL on King's B medium containing d18:0 (100 μM in ethanol) or mixed with d18:0 (100 μM in ethanol) prior to being plated. Morphology and structure of bacterial colonies were observed after a 48–72 hours incubation period at 28°C.

Mannitol motility medium was used to assess the motility of *Pst* and its ability to ferment mannitol. The medium is prepared in glass tubes and bacteria are vertically stabbed in the middle of the soft agar medium. Motile bacteria will have a diffuse growth along the inoculation line while non-motile bacteria will grow only along it. Phenol red acts as a pH indicator: if bacteria are able to ferment mannitol, it will turn yellow (Islam, 2017). *Pst* DC3000 and *Pst AvrRpm1* were inoculated as described at 10^6 or 10^7 CFU/mL either with ethanol (control) or with d18:0 (100 μM, ethanol 100%). Similar inoculations were also performed with medium containing d18:0 (100 μM, ethanol 100%). Tubes were observed after a 24-48 hours incubation period at 28°C.

Finally, YEM was used to study EPS production by *Pst* in response to d18:0 (Bonet *et al.*, 1993). *Pst* DC3000 and *Pst AvrRpm1* were plated at 10^6 or 10^7 CFU/mL, either on YEM containing d18:0 (100 μM, ethanol 100%) or mixed with d18:0 (100 μM, ethanol 100%) prior to being plated. EPS production in the different conditions was visually determined after a 48–72 hours incubation period at 28°C.

5. *In vitro* antibacterial assays

Bacteria were cultured as described (see **II.3**) before being distributed in 96 wells plates at 10^6, 10^7 or 10^8 CFU/mL in King's B medium supplemented with appropriate antibiotics, under agitation and at 28°C. Bacterium were plated either alone, with ethanol (0,1%, v/v) or with d18:0 (100 μM, ethanol 100%). The control was performed using culture medium and ethanol (0,1%, v/v). OD_{600} measurements were performed using the TECAN Spark® absorbance reader, every hour for 50h. The data presented are obtained solely from growth curve experiments, from which the growth rate was extracted

6. Inoculations and pathogen assay *in planta*

For bacterial count experiments, bacterial cells were cultured as described (see **II.3**), then collected by centrifugation, washed two times, and resuspended in 10 mM $MgCl_2$ to a final concentration of 10^7 CFU/mL (OD_{600} = 0.01). Bacterial solutions (ca. 1 mL) were then infiltrated on the abaxial side of *Arabidopsis* leaves using a 1 mL syringe without needle. Co-infiltration of bacteria with sphinganine (100 µM, ethanol 100%) were performed likewise. Control inoculations were conducted with 10 mM $MgCl_2$. At least four leaves per plant were treated for each condition on a minimum of three different plants. Inoculation pictures were taken, and lesion severity was estimated 48 hpi. Four inoculated leaves were weighted and ground in 1 mL of 10 mM $MgCl_2$ using a mortar and pestle. Appropriate dilutions were plated on King's B medium with suitable antibiotics, and bacterial colonies were counted. Data are reported as means ±SD of the log (CFU/mg fresh weight) of three replicates. Growth assays were performed three times with similar results.

For minimal medium experiments, bacterial cells were cultured as described (see **II.3**) then collected by centrifugation, washed two times, and resuspended in liquid m9 medium to a final concentration of 10^7 CFU/mL (OD_{600} = 0.01). They were subsequently incubated at 28°C for 16 hours before being collected by centrifugation, washed two times, and resuspended in 10 mM $MgCl_2$. Briefly, bacterial solutions were infiltrated into *Arabidopsis* leaves as previously described with ethanol (0,1%, v/v) or d18:0 (100 µM). Control inoculations were conducted with 10 mM $MgCl_2$ and ethanol (0,1%, v/v). Pictures of inoculated plants were taken 72 hpi. The experiment was repeated at least three times with similar results.

7. RNA extraction and qRT-PCR

For total RNA extraction, at least 3 leaves of 3 different inoculated plants were collected 6, 24 and 48 hpi. Fresh material was flash frozen in liquid nitrogen and conserved at -80°C until further use. RNA isolation was consequently performed with Extract-all from Eurobio Scientific, following recommendations from the manufacturer. For qRT-PCR, 1 µg RNA was used for reverse transcription using the Verso cDNA synthesis kit from Thermo Fisher Scientific (USA) following the supplier's recommendations. The transcripts were then quantified by qRT-PCR with a thermocycler CFX96 Real-Time system (Bio-Rad, USA) and the Absolute Blue SYBR Green Master Mis (Thermo Fisher Scientific, USA). Gene-specific primers are described in **Supplemental Table S3**. For each experiment, PCR was performed in duplicate. Transcript levels were normalized against those of the outer membrane porin F gene (*oprF*) and the 3-isopropylmalate

dehydratase small subunit gene (*leuD*), used as internal controls. Fold induction compared with sample treated with the bacterium alone was calculated using the ΔΔCt method:

$$(Ct_{GI[\text{unknown sample}]} - Ct_{GI[\text{reference sample}]}) - (Ct_{REF[\text{unknown sample}]} - Ct_{REF[\text{reference sample}]})$$

where GI is the gene of interest. Data were analysed with Bio-Rad CFX Manager software v2.0.

III. Results

1. Sphinganine addition did not highly modify the morphology or *in vitro* growth of *Pseudomonas*

Morphology of the colonies, motility of bacteria, ability to ferment mannitol or to produce EPS were tested on *Pst* DC3000, used as a control and *Pst AvrRpm1*, with or without d18:0. As results were similar for both bacteria at 10^6 and 10^7 CFU/mL, only results obtained at 10^7 CFU/mL are shown. Furthermore, adding d18:0 to the medium or to bacterial solutions prior to plating had no impact on any of the observed parameters, therefore, only results obtained with mixed bacteria / d18:0 solutions are shown (**Table II.**). Colonies of both treated and untreated *Pst* DC3000 and *Pst AvrRpm1* were round, small, smooth, and white, meaning d18:0 had no visible effect on the morphology of the colonies. Similarly, presence of d18:0 had no effect on bacteria motility as the mannitol motility medium was turbid only around the inoculation line, indicating that bacteria barely strayed from it. Moreover, it did not change colour, implying that bacteria did not ferment mannitol. Finally, EPS production did not seem altered by co-treatment with d8:0 (**Table II.**).

Table II. *In vitro* effects of d18:0 on *Pst* DC3000 and *Pst* AvrRpm1

Pst DC3000 and *Pst AvrRpm1* were plated (10^7 CFU/mL) on various media, either with ethanol (Ctrl - 0,1%, v/v) or with d18:0 (100 μM, ethanol 100%) and incubated at 28°C. Morphology of the colonies, motility, capacity to ferment mannitol and exopolysaccharide (EPS) production were observed between 24 and 72 hours post inoculation.

	Pst DC3000		*Pst* AvrRpm1	
d18:0	**-**	**+**	**-**	**+**
Morphology	Round, smooth, small, white	Round, smooth, small, white	Round, smooth, small, white	Round, smooth, small, white
Motility	+	+	+	+
Mannitol fermentation	-	-	-	-
EPS production	-	-	-	-

The anti-bacterial effect of d18:0 was tested *in vitro* on *Pst* DC3000, *Pst AvrRpm1*, *Pst AvrRpt2*, *Pst AvrRps4*, *Pst AvrB*, *Pst AvrPphB* and *Psm* m2, *Psm* ES4326 and *Psm* ES4326 *AvrRpm1* with or without d18:0 in the medium (**Figure 20.**). Ethanol had no effect on bacterial growth of all tested strains (data not shown). Out of all the bacteria tested, d18:0 significantly affected the growth rate of *Pst AvrRpt2*, *Psm* m2 and *Psm* ES4326. Surprisingly, all these bacteria do provoke cell death on leaves when co-infiltrated with d18:0. Interestingly, d18:0 had no antibacterial effect on bacteria that do not induce an HR when co-infiltrated, namely, *Pst AvrRpm1*, *Pst AvrB*, *Pst AvrPphB* and *Psm* ES4326 *AvrRpm1* (**Figure 20.**).
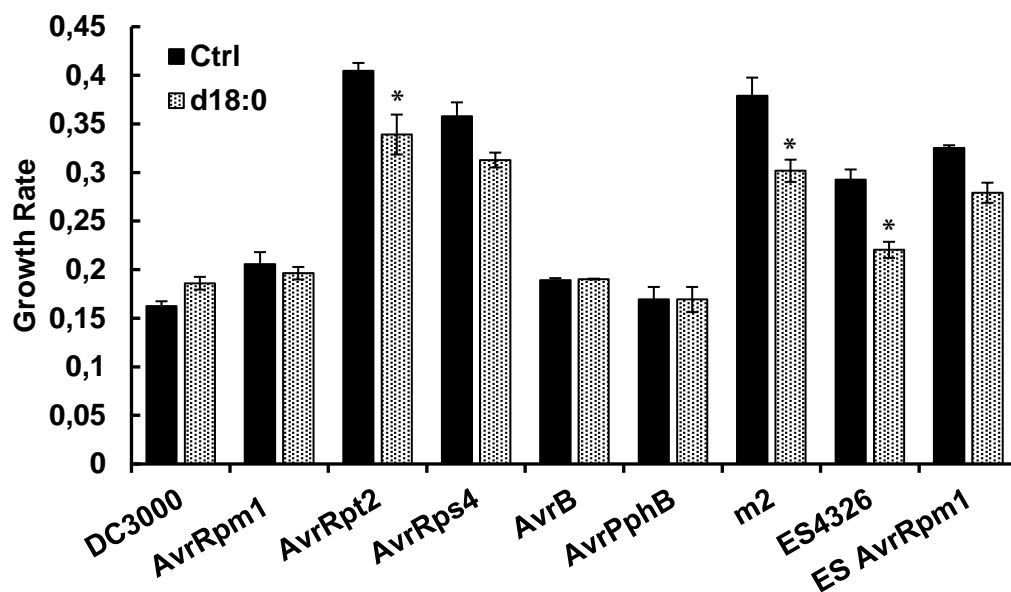
Figure 20. Effect of d18:0 on bacterial growth rates

Pst DC3000, *Pst AvrRpm1*, *Pst AvrRpt2*, *Pst AvrRps4*, *Pst AvrB*, *Pst AvrPphB*, *Psm* m2, *Psm* ES4326 and *Psm* ES4326 *AvrRpm1* (noted ES *AvrRpm1*) were cultivated at 28°C in King's B medium (10^8 CFU/mL) with appropriate antibiotics, either with ethanol (Ctrl – 0,1%, v/v) or with d18:0 (100 µM in ethanol). The growth rate was estimated from growth curve data (OD_{600}) over 48 hours, ±SD. Stars indicate statistical differences (t-test, p<0,05, n=3). Stars indicate statistical differences (Wilcoxon-Mann-Whitney, **, p<0,01; *, p<0,05).

2. Co-infiltration of sphinganine slightly reduced the growth of *Pst in planta*

To complete the *in vitro* data and determine the effect of the co-infiltration on bacterial growth *in planta*, bacterial populations were quantified 0 and 48 hpi (**Figure 21.**). *Arabidopsis* WT leaves were infiltrated with *Pst* DC3000 or *Pst AvrRpm1*, either with ethanol or d18:0. The growth of *Pst AvrRpm1*, the avirulent strain, was slightly reduced compared to the virulent strain, *Pst* DC3000.

Furthermore, while the co-infiltration had no consequence on the development of *Pst* DC3000, it slightly reduced *Pst AvrRpm1* growth at 0 and 48 hpi (**Figure 21.**). Interestingly, these results suggest that while *Pst AvrRpm1* continues its development on the plant, it is however incapable of triggering an HR from the plant.
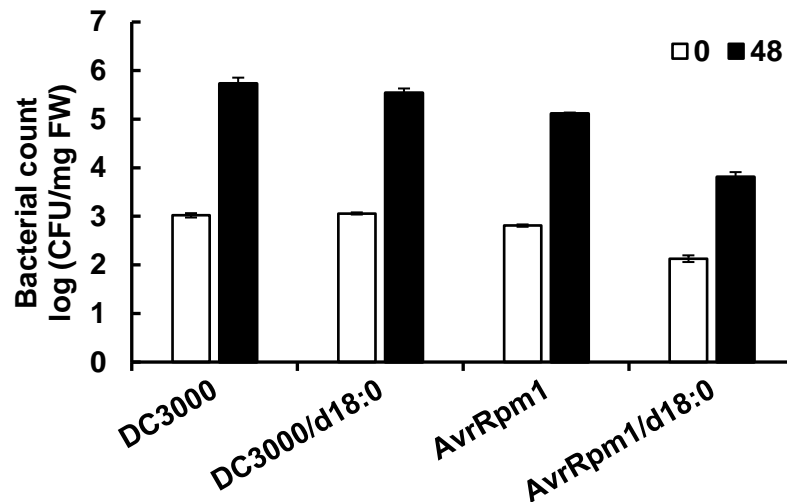
Figure 21. Effect of d18:0 on the development of *Pst* DC3000 and *Pst* AvrRpm1 in planta

Arabidopsis WT Col-0 leaves were harvested either directly or 48 hours post infiltration with *Pst* DC3000 or *Pst AvrRpm1* (10^7 CFU/mL, 10 mM $MgCl_2$) either with ethanol (Ctrl – 0,1%, v/v) or with d18:0 (100 µM, ethanol 100%). At least four leaves per plant were treated for each condition on a minimum of three different plants (n=3). Bacterial count and fresh weight of leaves were measured at each timing, ±SD. Control infiltration is performed with 10 mM $MgCl_2$, and ethanol (0,1%) and no bacterial growth was observable (data not shown).

3. Sphinganine could possibly interfere with the T3SS of *Pst*

Some minimum media are known to stimulate the expression of T3SS genes and effector production. They are believed to mimic *in planta* conditions therefore preparing the bacterium to be virulent (Jiang *et al.*, 2013). Here, we supposed that d18:0 could have an effect on the T3SS of *Pst AvrRpm1* and thus maybe on effector secretion in the plant cells, which could have caused the absence of HR on *Arabidopsis* leaves. Bacteria *Pst* DC3000 and *Pst AvrRpm1* were therefore grown in minimal medium m9 overnight before being infiltrated either with ethanol or d18:0. As expected, necrosis appeared due to the spread of the bacteria on leaves infiltrated with *Pst* DC3000 alone or co-infiltrated with d18:0 (**Figure 22.**). Surprisingly, co-infiltration of *Pst AvrRpm1* with d18:0 induced small symptoms on treated leaves, mostly at infiltration sites (**Figure 22.**).

Figure 22. Phenotypes of *Arabidopsis* leaves after infiltration of bacteria grown in minimal medium

Necrosis intensity of *Arabidopsis* WT Col-0 leaves, 72 hours post infiltration with *Pst* DC3000 or *Pst AvrRpm1*, grown overnight in minimal medium (10^7 CFU/mL, 10 mM $MgCl_2$), either with ethanol (0,1%, v/v) or with d18:0 (100 µM, ethanol 100%). Control infiltration is performed with 10 mM $MgCl_2$ and ethanol (0,1%, v/v). At least four leaves per plant were treated for each condition on a minimum of three different plants (n=3).

In order to further monitor the effect of d18:0 on the T3SS of *Pst*, several genes from the *hrp/hrc* system were selected for qRT-PCR (**Supplemental Table S4**). They were chosen based on their importance in the integrity of T3SS and in the virulence of the bacterium. Among all selected genes, suitable primers were found only for *hrpA1*, *hopB1*, *hrcC* and *hrpJ*. Issues stemmed from a lack of selectivity of the primers as well as the low amounts of bacterial DNA available *in planta*. Once again, *Pst* DC3000 was used as a control. Results are normalized on leaves treated with bacteria alone, meaning that the data reflect the difference in gene expression between bacteria alone and bacteria co-infiltrated with d18:0 (**Figure 23.**). For *Pst AvrRpm1*, co-infiltration induced an overexpression of *hrpA1* (at 6 and 24 hpi), *hrcC* and *hrpJ* (at 6 hpi). It also downregulated the expression of *hopB1* (at 6 and 24 hpi), and *hrpJ* (at 24 and 48 hpi). The expression pattern of these T3SS-associated genes seemed modified by d18:0 co-infiltration but data presented here are only preliminary as they originate from one experiment only. Therefore, further investigations would be needed to properly determine if d18:0 can affect the T3SS of *Pst AvrRpm1* (**Figure 23.**).
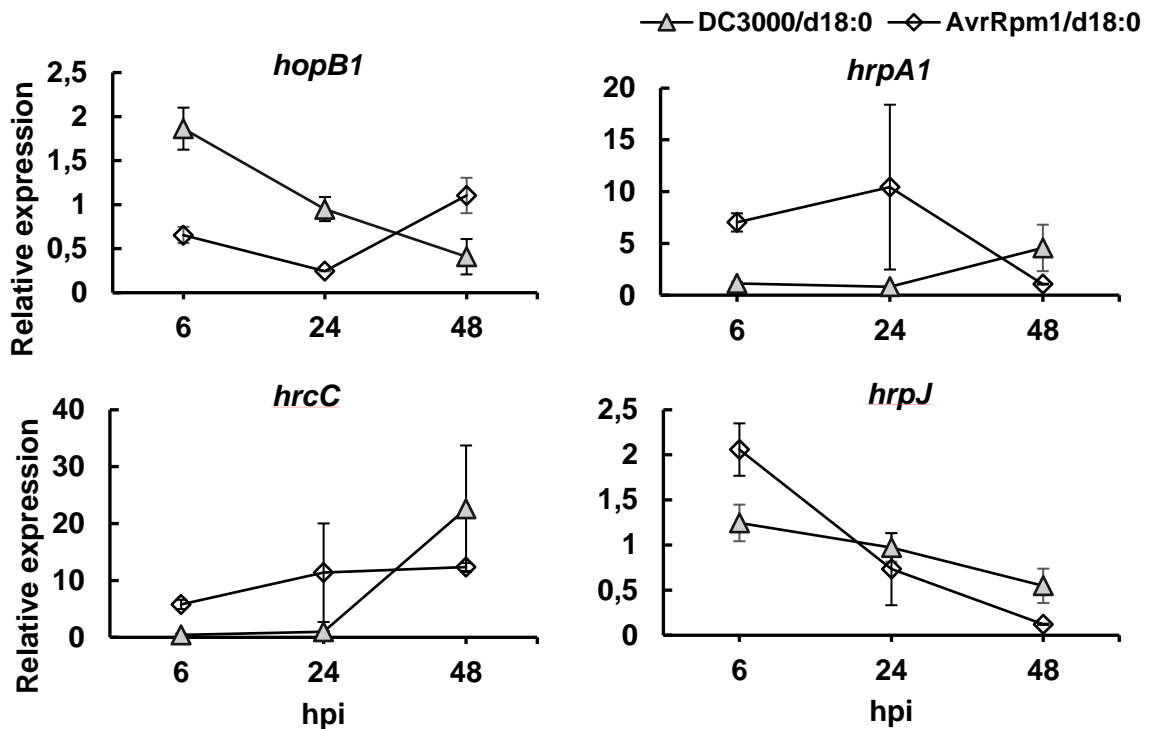
Figure 23. Effects of d18:0 on T3SS related genes of *Pst* in infected plants

Relative expression of T3SS related genes*: hopB1, hrpA1, hrcC* and *hrpJ* was followed. Leaves of *Arabidopsis* were harvested 6, 24 and 48 hours post infiltration with either *Pst* DC3000 or *Pst AvrRpm1* (10^7 CFU/mL, 10 mM $MgCl_2$) with ethanol (0,1%, v/v) or with d18:0 (100 µM, ethanol 100%). Results are normalized upon leaves treated with the bacterium alone.

IV. Discussion and conclusion

For both *Pst* strains, the morphology of their colonies, their motility and their inability to ferment mannitol was consistent with previous findings on *P. syringae* (Islam, 2017) and were unchanged by addition of d18:0. Although *Pst* DC3000 is thought to be a poor epiphyte (Boureau *et al.*, 2002), its EPS production remains important for host interaction and virulence (Farias *et al.*, 2019). Our results show that EPS production is equivalent between the two strains and was unaltered by the presence of d18:0. Overall, our analyses showed that if d18:0 has an effect on *Pst AvrRpm1* when co-infiltrated in *Arabidopsis* leaves, it is not visible in terms of morphology, motility, or capacity to produce EPS.

In vitro antibacterial tests showed that d18:0 significantly impacted the growth rates of three bacteria, *Pst AvrRpt2*, *Psm* m2 and *Psm* ES4326. Surprisingly, their co-infiltration with d18:0 *in planta* leads to cell death, whereas growth rates of bacteria that did not induce cell death, namely *Pst AvrRpm1*, *Pst AvrB*, *AvrPphB* and *Psm* ES4326 *AvrRpm1*, do not appear altered by the

presence of d18:0. LCBs and other SLs can have antibacterial effect on certain bacteria that infect humans (Dongfack *et al.*, 2012; Becam *et al.*, 2017; Wu *et al.*, 2021), and Glenz *et al.* (2022) showed that 25 and 50 µM of t18:0 were sufficient to reduce *Pst* survival by 50 and 95%, respectively. In our experimental conditions, however, d18:0 did not have such a potent effect on bacterial growth.

These *in vitro* data were subsequently completed by *in planta* experiments. Our results showed that even though *Pst AvrRpm1* is not capable of inducing an HR when co-infiltrated with d18:0, it is still present on the plant and continues its development over time without causing visible defence reactions from the plant. For co-infiltrated bacteria, at 0 hpi, there is less *Pst AvrRpm1* than *Pst* DC3000. Such diminution could perhaps be attributed to a slight antibacterial effect of d18:0 *in planta*. Considering this result, one might think that the absence of HR after co-infiltration could be due to the fact that the amount of bacteria present on the plant is not sufficient to trigger a HR. However, even when infected plants were cultivated for longer period than 48 hpi, no cell death could be observed.

Studies performed with *P. aeruginosa* have shown that the NH2 residue of d18:1 must be protonated for the molecule to have an antibacterial effect, which occurs under neutral and slightly acidic conditions (Wu *et al.*, 2021). It has also been demonstrated that the bactericidal activity of d18:1 relies on its binding to CL in the bacterial PM resulting in membrane permeabilization and thus death (Verhaegh *et al.*, 2020). These findings, although not directly transposable to *Pst,* highlighted a possible mode of action for d18:0, through its interaction with bacterial PM. Although this hypothesis will be discussed in Chapter 4, it led us to question whether d18:0 could have an effect on the T3SS since it is imbedded into the bacterial PM.

To explore this hypothesis, the first approach used was to stimulate the T3SS and effector production by incubating the bacteria in a minimal medium (Mudgett and Staskawicz, 1999; Jiang *et al.*, 2013). Most *hrp/hrc* genes are expressed at a very low level in standard, nutrient rich medium as their expression is induced only when infection of their host occurs (Wei *et al.*, 2000). Our experiments showed that incubation of *Pst AvrRpm1* in minimal media prior its co-infiltration with d18:0 was sufficient to observe cell death, although not important, on *Arabidopsis* leaves. The T3SS stimulation of *Pst AvrRpm1* was therefore sufficient to overcome the action that d18:0 might have had on the bacteria and / or the plant and to restore, at least partially, the HR. The two hypothesis that arose from this result were that this stimulation could either have reduce the direct effect of d18:0 on the T3SS of *Pst AvrRpm1* or have promoted the virulence of the bacterium sufficiently for it to overcome the effect of d18:0. The first hypothesis was tested by selecting genes of the *Pst* DC3000 T3SS (**Supplemental Table S4**). Among all genes selected, only four could be quantified by qRT-PCR. Their corresponding proteins were HrpA, the structural protein of the pilus, responsible for the formation of the pilus and required for virulence of *Pst* DC3000 and for HR elicitation (Wei *et al.*, 2000), HrcC and HrpJ, both located at the PM and required for virulence

and the secretion of some harpins (Deng and Huang, 1999) and HopB1, an effector that interacts with the host PM (Petnicki-Ocwieja *et al.*, 2005). So far, our experiments have shown that d18:0 co-infiltration modifies the expression levels of these genes. Particularly, the gene *hopB1,* which encodes an effector normally secreted through the T3SS, was down-regulated when *Pst* AvrRpm1 was co-infiltrated with d18:0 but not when *Pst* DC3000 was. It stands to assess the expression levels of the corresponding protein would enable to confirm that d18:0 alters its secretion.

Unfortunately, experiments on T3SS genes remained preliminary as qRT-PCR lacked specificity and very few data were available in the literature on the expression of these genes in bacteria, especially in *Pst* (Smith *et al.*, 2018). So far, no connection between exogenously applied SLs and T3SS perturbation has been put forward. Some human pathogenic bacteria however are known to use the SL pool of their host PM to cause infection (Rolando and Buchrieser, 2019). For instance, the translocon protein IpaB of *Shigella* interacts with cholesterol and SLs of their host cell lipid rafts to mediate infection (McShan and De Guzman, 2015). It could therefore be conceivable that d18:0 has an effect on *Pst AvrRpm1*, either by interacting directly with its PM or by modifying how the bacteria interact with the *Arabidopsis* PM.

Chapter 2 - Main Results

- ✓ d18:0 had no impact on morphology, motility, mannitol fermentation capacities and EPS production of *Pst* DC3000 and *Pst AvrRpm1*
- ✓ *In vitro* tests showed d18:0 did not have an antibacterial effect on *Pst AvrRpm1*, *Pst AvrB* and *Pst AvrPphB*.
- ✓ Co-infiltrated *Pst AvrRpm1* continues to develop *in planta* without causing an HR
- ✓ *Pst AvrRpm1* incubation in minimal media prior to co-infiltration allowed the apparition of small lesions

82

3

Effects of sphinganine and *Pseudomonas syringae* co-infiltration on *Arabidopsis* defence mechanisms

I. Context

Given the absence of HR when *Pst AvrRpm1* is co-infiltrated with d18:0, questions about the regulation of plant defence responses arose. The protein RIN4 is well conserved among land plants and is an important hub in plant defence response (Toruño *et al.*, 2019). It negatively regulates PTI since plant lacking or overexpressing RIN4 display enhanced or reduced defence responses, respectively (Kim *et al.*, 2005). In *Arabidopsis*, RIN4 is the target of no less than four bacterial effectors, AvrRpm1, AvrRpt2, AvrB and HopF2 (Afzal *et al.*, 2013) and has therefore been well characterised. In the "guard hypothesis", plant NLRs can recognize pathogens by monitoring effector-induced perturbations of the guard protein (Dangl and Jones, 2001). In resistant plants, RIN4 guards proteins RPM1 and RPS2, which upon perceiving RIN4 phosphorylation or degradation, respectively, can trigger ETI and the HR (Mackey *et al.*, 2002; Mackey *et al.*, 2003). In Chapter 1, we demonstrated that co-infiltration of *Pst AvrRpt2* with d18:0 induced PCD and that co-infiltration with *Pst AvrB* did not. While the first result led us to think RIN4 was not involved in the absence of HR, the latter suggested maybe RPM1 or the RPM1 / RIN4 complex was. Mutant approaches of RIN4, RPM1 and RPS2, have previously been used to decipher important plant defence signalling and response (Beckers *et al.*, 2009; Liu *et al.*, 2009; Lee *et al.*, 2015; El Kasmi *et al.*, 2017; Toruño *et al.*, 2019) and have been employed here to elucidate their role in the absence of HR.

Several markers of plant immunity were also followed. In particular, electrolyte leakage was studied to estimate plant cell death, as changes in conductivity may be associated with ion loss due to PM damages and thus cell death (Kawasaki *et al.*, 2005). Extracellular ROS production was also monitored as it is one of the hallmark of plant immunity, is linked to cell death and is mostly produced by RbohD located at the PM (Kadota *et al.*, 2015). Next, camalexin, the major phytoalexin of *Arabidopsis* was quantified since it has antifungal and antimicrobial activities (Zhang *et al.*, 2014). While camalexin is toxic to cultured cells of *Arabidopsis*, it does not contribute to cell death in bacteria-infected tissues (Rogers *et al.*, 1996). Furthermore, since ETI is thought to be regulated by a concentration gradient of SA (Betsuyaku *et al.*, 2018), we examined the expression of *PR1*, overexpressed in response to SA (Pieterse and van Loon, 1996; Glazebrook, 2005; Zienkiewicz *et al.*, 2020). To test whether the jasmonate signalling pathway was affected by sphinganine co-infiltration, the expression of *VSP1*, a JA-responsive gene (Guerineau *et al.*, 2003) was also followed. To complement these data, SA and JA-Isoleucine (JA-Ile), the active form of JA (Li *et al.*, 2019), were also quantified in *Arabidopsis* leaves.

In plants, myristoylation consists in the irreversible addition of a lipid, a myristate (C:14), on a specific protein sequence. This phenomenon concerns many proteins and aims to address them to

the PM. This reaction is catalysed by an enzyme, the N-myristoyltransferase (NMT). In *Arabidopsis*, two genes encode two homologs, namely *AtNMT1* and *AtNMT2* (Traverso *et al.*, 2008). In higher plants, as in mammals and fungus, determination of their localisation, roles at different developmental stages and whether these genes are redundant or not appeared difficult (Pierre *et al.*, 2007). It was although demonstrated in mouse that the *NMT* genes were nonredundant (Yang *et al.*, 2005). To our knowledge, myristoylation processes in plants are independent of SL metabolism. It can however be noted that in humans, part of the cardiac pool of the SLs, the d16:0, is synthesized from myristoyl-CoA instead of palmitoyl-CoA (Russo *et al.*, 2013). Results presented in Chapter 1 showed that co-infiltration of *Pst AvrB* and *Pst* AvrPphB with d18:0 did not induce a HR on *Arabidopsis* leaves, just like *Pst AvrRpm1*. Since the effectors AvrRpm1, AvrB, and AvrPphB each possess an amino acid N-myristoylation sequence that redirects them at the PM when inside their host (Nimchuk *et al.*, 2000), questions about the effect of sphinganine on this process arose.

II. Materials and methods

1. Plant material and growth conditions

Seeds of *Arabidopsis thaliana* reporter line *PR1::GUS*, T-DNA insertion mutants: *rpm1-3* (CS68739), *rpm1-rps2-rin4* (CS68760), and the transgenic line *RPM1-myc rpm1* (CS68778) were obtained from the Nottingham *Arabidopsis* Stock Center (http://*Arabidopsis*.info). Both mutants and wild type Columbia-0 were grown in soil under 12 h-light/12 h-dark conditions (150 µmol/m²/s, 20°C, and 60% humidity) for 5 weeks.

2. Chemicals and culture medium

Composition of bacterial culture media King's B is described in **Supplemental Table S2**. Chemical elements used for media, antibiotics, luminol and horseradish peroxidase were purchased from Sigma-Aldrich. Sphinganine (d18:0) was purchased from Avanti Polar Lipids, dissolved in ethanol (100%), and used without further purification. The flagellin-derived peptide flg22 was obtained from Proteogenix (France) and dissolved in distilled water. Extract-All was purchased from Eurobio Scientific. Verso cDNA synthesis kit and absolute blue SYBR Green Master Mix were purchased from Thermo Fisher Scientific.

3. Bacterial cultures and inoculations

Pst DC3000, carrying an empty vector, *Pst AvrRpm1*, *Pst AvrRpt2*, *Pst AvrRps4*, *Pst AvrB* and *Pst AvrPphB*, were cultured overnight under agitation (180 rpm) at 28°C in liquid King's B medium, supplemented with rifampicin (50 μg/mL) and kanamycin (50 μg/mL).

All strains were cultured overnight at 28°C in liquid King's B medium, supplemented with rifampicin (50 μg/mL) and kanamycin (50 μg/mL). Bacterial cells were then collected by centrifugation, washed, and resuspended in 10 mM $MgCl_2$ to a final concentration of 10^7 CFU/mL (OD_{600} = 0.01). Briefly, ca. 1 mL of bacterial solutions were infiltrated into *Arabidopsis* leaves as previously described with ethanol (0,1%, v/v) or d18:0 (100 μM). Control inoculations were conducted with 10 mM $MgCl_2$ and ethanol (0,1%, v/v). At least four leaves per plant were treated for each condition on a minimum of three different plants. Lesions were estimated from pictures of the experiments taken 48 hours post infiltration.

4. Immunoblotting assay

Extraction of total proteins were performed on pre-treated leaves of *RPM1-myc rpm1* plants collected 0, 2, 6 and 24 hpi. To that end, 20 mg of leaf tissues were ground in a homogenizer Potter-Elvehjem with 40 μL of extraction buffer (0.35 M Tris-HCl (pH 6.8), 30% (v/v) glycerol, 10% (v/v) SDS, 0.6 M DTT, 0.012% (w/v) bromophenol blue) and were denatured for 7 min at 95°C. Next, they were centrifuged at 11 000g for 5 min and 30 μL of supernatant were separated by 12% SDS-PAGE. Proteins were transferred onto PVDF membranes for 10 min at 25 V using iBLOT gel transfer system (Invitrogen). After 30 min in 5% saturation solution (50 g/L milk, TBS (137 mM NaCl, 2.7 mM KCl, 25 mM Tris-HCl), Tween20 0.05% (v/v)) and 3 times 5 min in 0.5% washing solution (5 g/L milk, TBS (137 mM NaCl, 2.7 mM KCl, 25 mM Tris-HCl), Tween 20 0.05% (v/v)). The membranes were incubated overnight with recombinant monoclonal Anti-c-myc epitope tag [Clone 9E10] Mouse IgG1 kappa (Cliniscience, 1:1000) at 4°C. Then, membranes were washed 3 times 5 min with the washing solution and incubated 1 h with anti-mouse IgG HRP-conjugated secondary antibodies (Bio-Rad, 1:3000) at room temperature. Finally, washed membranes were developed with SuperSignal® West Femto using an odyssey scanner (ODYSSEY® Fc Dual-Mode Imaging System, LI-COR).

To normalize protein loading, membranes were stripped 15 min with 0.25 M NaOH, blocked 30 min in 5% non-fat milk. Then, membranes were incubated at room temperature for 1 h with plant monoclonal anti-actin primary antibodies (CusAb, 1:1000) and 1 h with anti-mouse IgG HRP-conjugated secondary antibodies (Cell Signalling, 1:3000). Membranes were washed and

developed as previously described. Experiments were repeated at least three times with similar results.

5. Electrolyte leakage

To test the effect of d18:0 on ion leakage, bacteria were cultured and inoculated as described (see **II.3**), with or without d18:0 (100 µM). Ten minutes after bacteria inoculation, 9-mm-diameter leaf discs were collected using a cork borer from the infected area and washed extensively with distilled water for 1 hour. Two leaf discs were placed in each well of a 24 well plate containing 1 mL of distilled water. Conductivity measurements (three to four for each treatment) were then conducted over time using a B-771 LaquaTwin (Horiba) conductivity meter. Control inoculations were conducted with 10 mM $MgCl_2$ and ethanol (0,1%, v/v). Experiments were repeated at least three times with similar results.

6. Extracellular ROS production

Measurements of extracellular ROS production were adapted from Smith and Heese (2014). Briefly, single half leaf discs were placed in wells of a 96-well plate containing 150 mL of distilled water and incubated overnight at room temperature. Just before ROS quantification, distilled water was replaced by 150 mL of an elicitation solution containing 20 mg/mL horseradish peroxidase, 0.2 mM luminol, and bacteria or flagellin. Bacteria were added to a final concentration of 10^8 or 10^9 CFU/mL, as specified further. Flg22 was added to a final concentration of 1, 0,1 or 0.01 µM. In tests involving d18:0, the molecule was added at a final concentration of 100 µM concomitantly with the elicitation solution. Control inoculations were conducted with 10 mM $MgCl_2$ and ethanol (0,1%, v/v). Experiments were repeated at least three times with similar results.

7. RNA extraction and Real-Time RT-PCR

For total RNA extraction, at least 3 leaves of 3 different inoculated plants were collected 6 and 48 hpi. Fresh material was flash frozen in liquid nitrogen and conserved at -80°C until further use. RNA isolation was consequently performed with Extract-all from Eurobio Scientific, following recommendations from the manufacturer. For qRT-PCR, 1 µg RNA was used for reverse transcription using the Verso cDNA synthesis kit from Thermo Fisher Scientific (USA) following

the supplier's recommendations. The transcripts were then quantified by qRT-PCR with a thermocycler CFX96 Real-Time system (Bio-Rad, USA) and the Absolute Blue SYBR Green Master Mix (Thermo Fisher Scientific, USA). Gene-specific primers for PATHOGENESIS RELATED GENE 1 (*PR1*), VEGETATIVE STORAGE PROTEIN 1 (*VSP1*) and N-MYRISTOYLTRANSFERASE 1 (*NMT1*) are described in **Supplemental Table S3**. For each experiment, PCR was performed in triplicate or duplicate, as further specified. Transcript levels were normalized against those of the UBIQUITIN5 (*UBQ5*) gene, used as an internal control. Fold induction compared with untreated sample was calculated using the ΔΔCt method:

$$(Ct_{GI[unknown\ sample]}-Ct_{GI[reference\ sample]})-(Ct_{UBQ5[unknown\ sample]}-Ct_{UBQ5[reference\ sample]})$$

where GI is the gene of interest. Data were analysed with Bio-Rad CFX Manager software v2.0.

8. Phytohormone and camalexin quantifications

These experiments were conducted by Pr. Ivo Feussner and Dr. Cornelia Herrfurth (Alrbrecht von Haller Institute, Göttingen, Germany). The quantification of SA and JA-isoleucine and camalexin was performed at 0 and 48 hpi by UPLC-nano-ESI-MS/MS as previously described in Herrfurth and Feussner (2020).

9. GUS reporter assays

GUS enzyme activity of *PR1::GUS Arabidopsis* plants was determined histochemically on leaves of the reporter line, treated as previously described, collected at 48 hpi, placed in the GUS staining solution (50 mM sodium phosphate buffer - pH 7, 10mM EDTA, 1 mM $K_3Fe(CN)_6$, 2 mM X-GlcA, and 0,1% Triton X-100), vacuum infiltrated for 5 minutes and incubated for 4 hours at 37°C. Next, they were washed with milliQ water and put overnight at 4°C in a discoloration / fixation solution (ethanol:acetic acid, 3:1). Once the discoloration process was over, leaves were placed in 95% ethanol and observed.

10. Statistical analyses

Statistical analyses were performed in R (R Core Team, 2018). ANOVA and non-parametric tests, Kruskal-Wallis, and pair wise comparison Wilcoxon-Mann-Whitney, were conducted.

III. Results

1. RPM1 and RIN4 are not directly responsible for the absence of HR

It has been previously demonstrated that RPM1 is degraded within 4 to 6 hpi, coincidently with the onset of the HR (Boyes *et al.*, 1998). To elucidate if RPM1 and / or RIN4 were involved in the absence of HR, inoculations of *Pst AvrRpm1* on *rpm1-3, rpm1-rps2-rin4* mutant and *RPM1-myc rpm1* transgenic leaves were performed (**Figure 24A.**). Infiltration of the bacteria alone induced cell death, as expected. Despite lacking RPM1 and / or RIN4, all mutants showed the same phenotype as the WT when co-infiltrated with d18:0 as they did not exhibit visible cell death (**Figure 24A.**). To further elucidate the role of RPM1 and RIN4, *RPM1-myc rpm1* plant was used to monitor the *in planta* degradation of RPM1 following inoculation. Western blot analysis showed that while RPM1 was degraded around 4 to 6 hpi when *Pst AvrRpm1* was infiltrated alone, the protein was still intact 24 hpi when the bacteria is co-infiltrated (**Figure 24B.**). Collectively, these data suggest that neither RPM1 nor RIN4 are directly involved in the absence of HR observed during the co-infiltration of *Pst AvrRpm1* and d18:0.
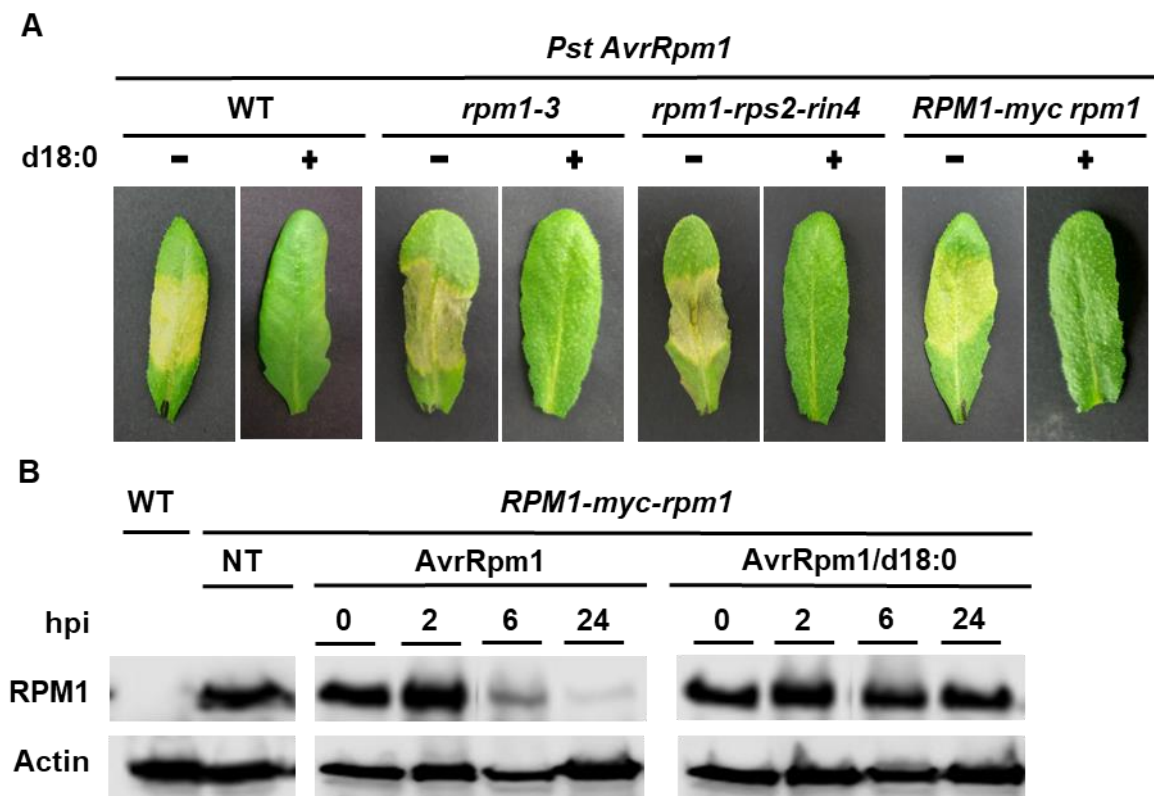
Figure 24. RPM1 is not involved in the absence of HR when *Pst AvrRpm1* is co-infiltrated with d18:0

A. Representative leaves of *Arabidopsis* WT Col-0 or mutants *rpm1-3, RPM1-myc rpm1*, and *rpm1-rps2-rin4* showing symptoms 72 hours post infiltration. *Pst AvrRpm1* was infiltrated (10^7 CFU/mL, 10 mM $MgCl_2$) either with ethanol (0,1%, v/v) or with d18:0 (100 μM, ethanol 100%). Control inoculations were conducted with 10 mM $MgCl_2$ and ethanol (0,1%, v/v) and did not result in visible cell death (data not shown). At least four leaves per plant were treated for each condition on a minimum of three different plants (n=3). **B.** To monitor the degradation of RPM1 following the inoculation with *Pst AvrRpm1*, leaves from WT Col-0 and *RPM1-myc rpm1* mutant were harvested either directly or 2, 6 or 24 hours post infiltration (hpi). NT refers to non-treated samples. Total proteins were then extracted, subjected to anti-myc antibodies, and put on a western blot. Actin was used as a loading control. All experiments were repeated at least 3 times with similar results.

2. Sphinganine co-infiltration with *Pst* modifies *Arabidopsis* defence responses

a. Co-infiltration with *Pst AvrRpm1* abolishes cell death linked to HR in *Arabidopsis*

Previous data showed that the co-infiltration of *Pst* DC3000 with d18:0 into leaves of WT *Arabidopsis* increased electrolyte leakage and was linked to cell death caused by the spread of the bacteria (Magnin-Robert *et al.*, 2015a). To further complete these data the experiment was repeated with *Pst AvrRpm1* and *Pst AvrRps4*, infiltrated either alone or with d18:0. *Pst AvrRps4* was here used as a control since its co-infiltration with d18:0 triggers a HR from the plant. Electrolyte leakage from control infiltration was constant around 150 µS/cm throughout the experiment (**Figure 25.**). Treatments with *Pst AvrRpm1* and *Pst AvrRps4* infiltrated alone, and *Pst AvrRps4* co-infiltrated with d18:0 provoked an increase in conductivity between 8 and 24 hpi. These findings were consistent with PCD previously observed on *Arabidopsis* leaves in the same conditions. No increase in electrolyte leakage was observed when *Pst AvrRpm1* was co-infiltrated with d18:0, also in accordance with the absence of visible HR on infiltrated leaves. Indeed, in this condition, medium conductivity was stable over time, between 80 and 97 µS/cm, while it reached 503 µS/cm at 24 hpi with *Pst AvrRpm1* infiltrated alone (**Figure 25.**). These findings therefore show that cell death, here linked to HR, is accompanied by increased medium conductivity and corroborates the absence of symptoms in *Pst AvrRpm1* co-infiltrated plants.
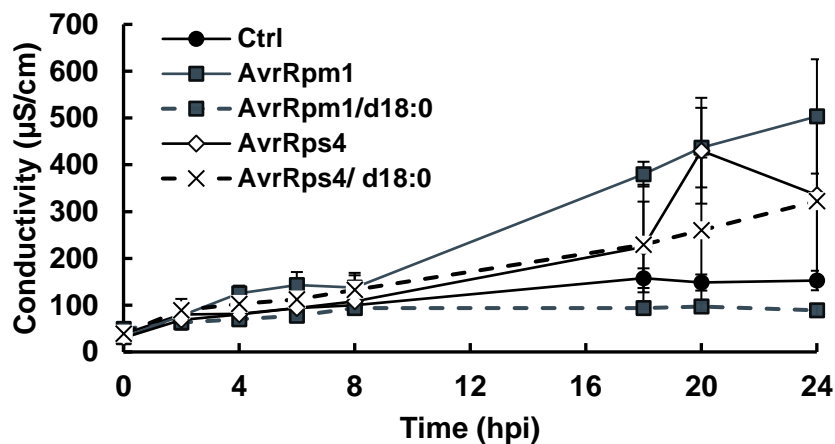
Figure 25. Electrolyte leakage from *Arabidopsis* in response to *Pst*

Conductivity (µS/cm) was measured over 24 hours in solutions containing leaf discs of *Arabidopsis* WT infiltrated with *Pst AvrRpm1* or *Pst AvrRps4* (10^7 CFU/mL, 10 mM $MgCl_2$), either with ethanol (0,1%, v/v) or with d18:0 (100 µM, ethanol 100%). Control inoculations were conducted with 10 mM $MgCl_2$ and ethanol (0,1%, v/v). Data are reported as means ± SD (n=3). The experiment was repeated three times with similar results.

b. Co-infiltration reduces extracellular ROS production by *Arabidopsis* in response to some strains of *Pst*

Experiments performed by Magnin-Robert *et al.* (2015) showed a decreased extracellular ROS production when *Arabidopsis* was co-treated with d18:0 and *Pst* DC3000 or *Pst AvrRpm1* (**Supplemental Figure S5.**). Considering this result, extracellular ROS production by *Arabidopsis* in response to other bacteria was followed (**Figure 26.**). *Pst AvrRpt2* and *Pst AvrB* had to be resuspended at 10^9 CFU/mL to induce ROS production by the plant while all other bacteria were concentrated enough at 10^8 CFU/mL to trigger a response. No significant statistical difference was found between ROS production triggered by bacteria alone or mixed with ethanol (data not shown). Co-treatment of *Pst AvrRpm1*, *Pst AvrRps4*, *Pst AvrB* and *Pst AvrPphB* with d18:0 significantly reduced extracellular ROS production by *Arabidopsis* (**Figure 26A.**). It was reduced by approximatively 6-fold for *Pst AvrRpm1*, 1.7-fold for *Pst AvrRps4*, 1.6-*fold* for *Pst AvrB* and 3-fold for *Pst AvrPphB*. Data obtained for *Pst AvrRpm1* are in accordance with those of Magnin-Robert *et al.* (2015) (**Supplemental Figure S5.**). Interestingly, co-treatment of *Pst AvrRpt2* with d18:0 had no significant impact on ROS production by the plant.

In Chapter 1, we highlighted that the absence of HR was dose dependent, with d18:0 being active up to 10 µM. Extracellular ROS production was therefore measured in response to *Pst AvrRpm1* or *Pst AvrB* without or with d18:0 at various concentrations (**Figure 26B.** and **C.**). Co-treatment of *Pst AvrRpm1* with d18:0 at concentrations ranging from 10 µM to 100 µM resulted in a ~ 6-fold decrease of ROS production which is consistent with symptoms observed on leaves. This effect was however lost when d18:0 concentrations dropped to 5 µM and below. Interestingly, only co-treatment of *Pst AvrB* with d18:0 at 100µM led to a decrease of ROS production (~ 2-fold) (**Figure 26C.**), perhaps because, as previously explained, *Pst AvrB* was used at a higher concentration that *Pst AvrRpm1*.

Considering d18:0 effects on ROS production in response to some of the tested bacteria, further experiments were conducted to determine if the molecule could also impact ROS production in response to another source of elicitation. Hence, the highly conserved and well characterized IP flg22, which is the N-terminal epitope of flagellin which constitutes the bacterial flagella, was used here (Boller and He, 2009). Flg22 was tested on *Arabidopsis*, at several concentrations, with or without d18:0 (**Figure 26C.**). d18:0 did not affect extracellular ROS production by the plant in response to any of the Fgl22 concentrations tested, suggesting that this phenomenon might be specific to bacterial effectors.
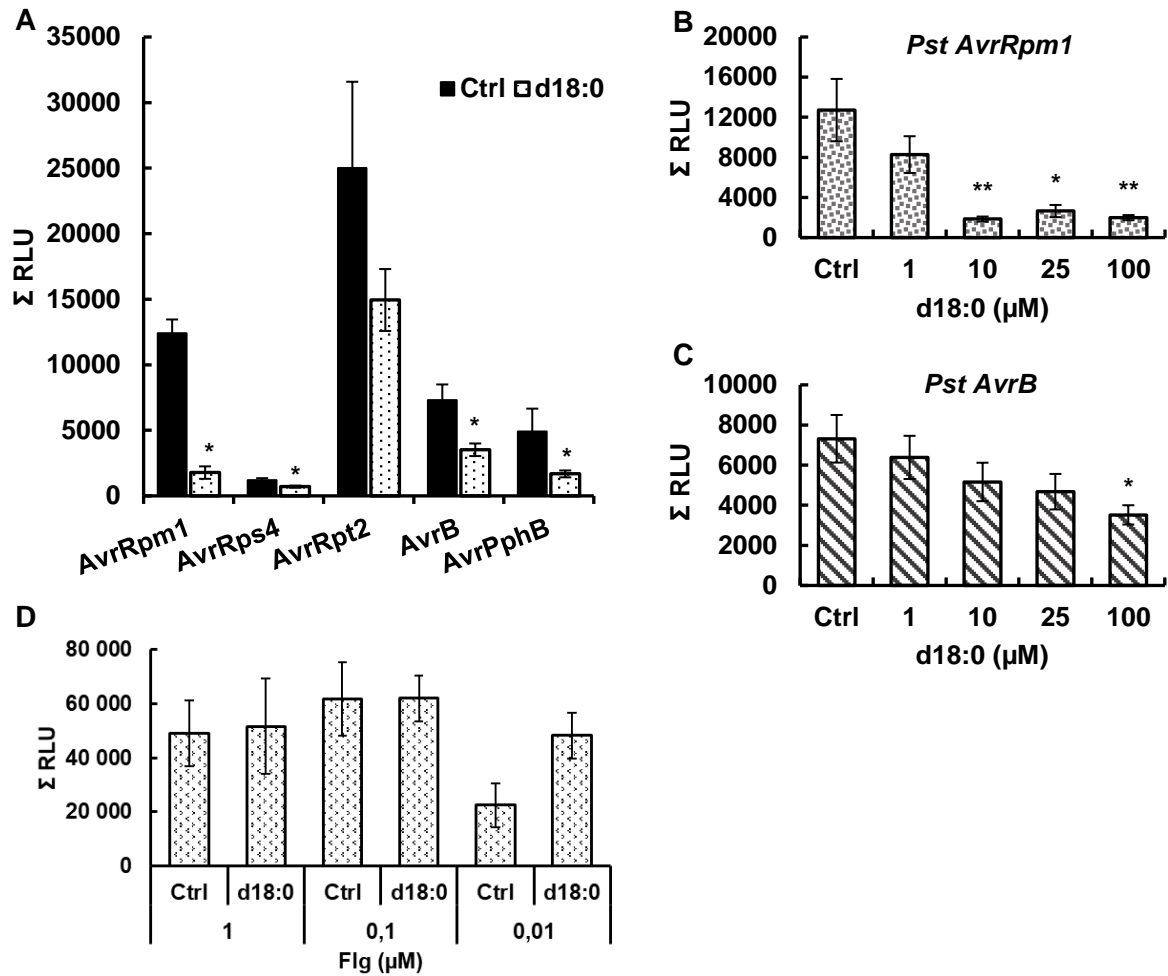
Figure 26. Co-infiltration of d18:0 alters extracellular ROS production by
Arabidopsis* in response to *Pst

Extracellular ROS production was measured by chemiluminescence on petioles of *Arabidopsis* WT (4–5-week-old). **A.** In presence of *Pst AvrRpm1, Pst AvrRps4, Pst AvrRpt2, Pst AvrB* or *Pst AvrPphB* (10^8 or 10^9 CFU/mL in 10 mM MgCl$_2$), with ethanol (Ctrl - 0,1%, v/v) or with d18:0 (100 μM, ethanol 100%) in the medium. **B.** In presence of *Pst AvrRpm1* or **C.** *Pst AvrB* (10^8 CFU/mL, 10 mM MgCl$_2$) with ethanol (Ctrl - 0,1%, v/v) or with d18:0 at various concentrations (ethanol, 100%). Stars indicate statistical differences (Wilcoxon-Mann-Whitney, **, $p<0,01$; *, $p<0,05$). **D.** In presence of flagellin with ethanol (Ctrl – 0,1%, v/v) or d18:0 (100 μM, ethanol 100%). Data were obtained with a Tecan Infinity F200 PRO and represent the sum of RLU (Relative light units) ± SEM (n = 6) over 90 minutes of measurements performed every 2 or 5 minutes. Experiments were performed three times with similar results.

c. Co-infiltration with d18:0 reduces camalexin production by *Arabidopsis* in response to *Pst AvrRpm1*

Control infiltration did not induce camalexin production, at both timings (**Figure 27.**). At 48 hpi, *Pst* DC3000 inoculation triggered camalexin accumulation by *Arabidopsis* up to ~62 nmol/g FW. d18:0 co-infiltration with the same bacteria did not significantly reduce camalexin level. It did however significantly reduce its production in response to *Pst AvrRpm1*. Indeed, at 48 hpi, it decreased from ~250 nmol/g FW to ~3 nmol/g FW (**Figure 27.**).
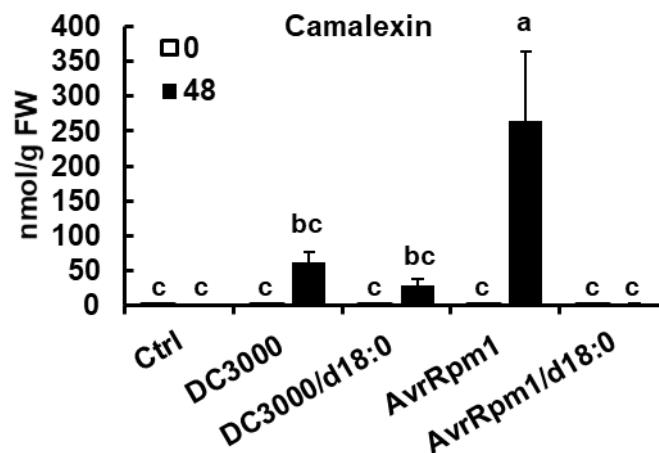
Figure 27. Sphinganine co-infiltration reduces camalexin production by *Arabidopsis* in response to *Pst AvrRpm1*

Camalexin was quantified from leaves harvested either directly or 48 hours post infiltration with *Pst* DC3000 or *Pst AvrRpm1* (10^7 CFU/mL, 10 mM $MgCl_2$), either with ethanol (0,1%, v/v) or with d18:0 (100 μM, ethanol 100%) and analysed with UPLC-nanoESI-QTRAP-MS. Control inoculations were conducted with 10 mM MgCl2 and ethanol (0,1%, v/v). Different letters indicate statistical differences (ANOVA, $p<0,05$, one way, n=5).

d. Co-infiltration with d18:0 provokes changes in stress-related hormone content and gene expression

Considering its effect on ROS production, other markers of plant defence were studied in response to co-infiltration, including the abundance of hormones SA and JA and the expression of *PR1* and *VSP1*, the marker genes of either signalling pathways, respectively. Overexpression of *PR1* was observed 48h after infestation with either *Pst* strains (**Figure 28A.**), which correlated with the accumulation of SA (**Figure 28C.**).

A

B

C
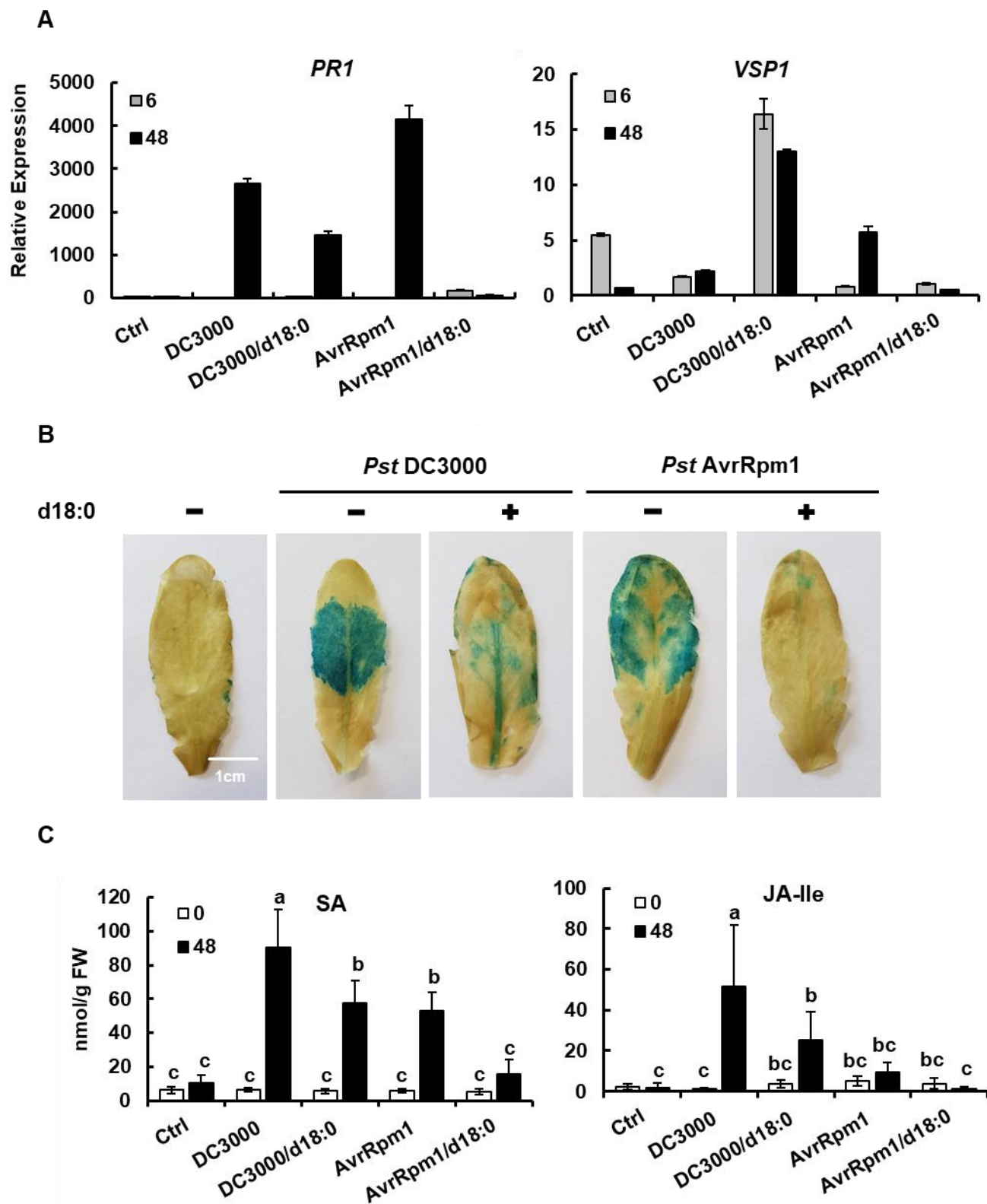
Figure 28. Sphinganine co-infiltration alters the salicylic acid pathway

A. The relative expression of *PR1*, expressed in response to salicylic acid (SA), and *VSP1* expressed in response to jasmonate (JA) was followed. Leaves of *Arabidopsis* were harvested 6 and 48 hours post infiltration with *Pst* DC3000 or *Pst AvrRpm1* (10^7 CFU/mL, 10 mM $MgCl_2$), either with ethanol (0,1%, v/v) or with d18:0 (100 µM, ethanol 100%). Results are normalized upon non-treated leaves. Experiments were repeated 3 times with similar results. **B.** Leaves of *PR1::GUS* were treated as previously described, collected at 48 hpi, placed in a coloration solution, vacuum infiltrated for 5 minutes and incubated for 4 hours at 37°C before being placed in a discoloration solution. **C.** Hormones, SA, and JA-Isoleucine (JA-Ile) were quantified from leaves harvested either directly or 48 hours post infiltration in the same conditions and analysed using UPLC-nanoESI-QTRAP-MS. Different letters indicate statistical differences (ANOVA, $p<0,05$, one way, n=5). For all experiments, control inoculations were conducted with 10 mM $MgCl_2$ and ethanol (0,1%, v/v).

Neither SA accumulation nor *PR1* overexpression was detected at earlier timepoints, which suggests that ETI might indeed be regulated by a concentration gradient of SA (Betsuyaku *et al.*, 2018). The use of an *Arabidopsis* reporter line *PR1::GUS* confirmed the overexpression of *PR1* in treated leaves (**Figure 28B.**). Both SA accumulation and *PR1* overexpression were massively dampened when leaves were co-infiltrated with d18:0 (**Figure 28A-C**.).

VSP1 is weakly expressed in response to *Pst* DC3000 but overexpressed when this bacterium is co-infiltrated with d18:0 (~ 9-fold and ~ 6-fold more at 6 and 48 hpi, respectively) (**Figure 28A.**). JA-Ile levels are however higher with the bacterium alone than co-infiltrated (**Figure 28C.**). When inoculated with *Pst AvrRpm1*, *VSP1* is slightly overexpressed at 48 hpi but repressed in all other conditions (**Figure 28A.**) and JA-Ile levels are concomitantly low (**Figure 28C.**). Globally, co-infiltration with d18:0 tends to lower the amount of both defence hormones for both *Pst* DC3000 and *Pst AvrRpm1*.

3. Co-infiltration of *Pst AvrRpm1* with d18:0 down-regulates *NMT1* relative expression

We used qRT-PCR to determine expression patterns of *NMT1* in response to infiltration of *Arabidopsis* WT leaves with *Pst* DC3000 or *Pst AvrRpm1*, either alone or with d18:0. This gene is one of the two genes encoding for the NMT, responsible for N-myristoylation in *Arabidopsis*, (**Figure 29.**). At 24 hpi, *NMT1* expression is reduced in the control plants but is not significantly changed compared to non-treated plants. At 6 and 24 hpi *NMT1* expression is similar to that of non-treated samples for plant infiltrated with *Pst DC3000* alone or with d18:0.

At 48 hpi, when compared to its relative expression at 6 hpi, *NMT1* appeared overexpressed in all tested conditions, except when plants are co-infiltrated with *Pst AvrRpm1* and d18:0. Similarly, it increased ~ 2-fold for *Pst DC3000* both without and with d18:0. For plants treated with *Pst AvrRpm1* alone, *NMT1* relative expression increased ~2.2-fold but is mostly similar when co-infiltrated with d18:0 (**Figure 29.**). Thus, a decrease of ~1.7-fold could be observed between *Pst AvrRpm1* infiltrated alone and with d18:0.

Overall, it would seem that co-infiltration could slightly modify *NMT1* expression although drawing conclusions with such small induction factors can be troublesome. However, since myristoylation is a key process for plant cells, as demonstrated by the hardly growing corresponding mutant, it should be fine-tuned regulated.
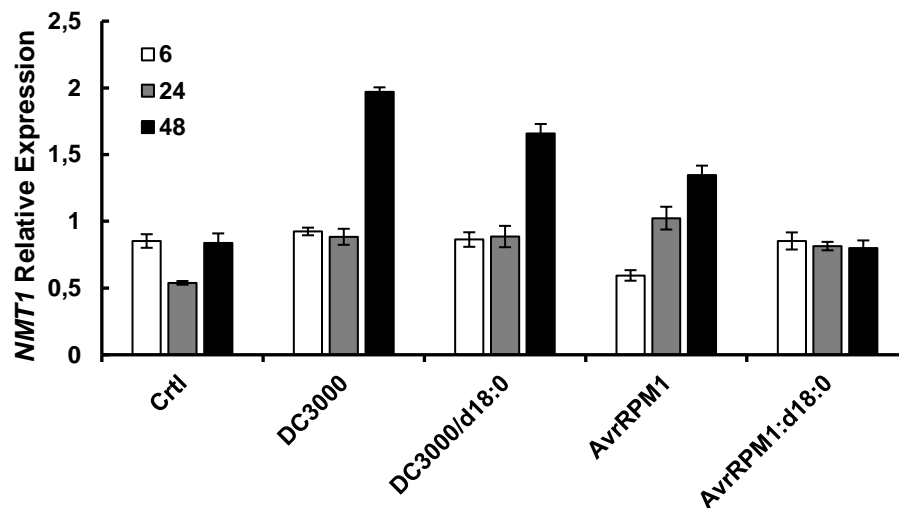
Figure 29. Sphinganine co-infiltration with *Pst AvrRpm1* down-regulates *NMT1* expression

The relative expression of *AtNMT1*, (*N-myristoyltransferase 1*) was followed. Leaves of *Arabidopsis* were harvested 6, 24 and 48 hours post infiltration with *Pst* DC3000 or *Pst AvrRpm1* (10^7 CFU/mL, 10 mM $MgCl_2$), either with ethanol (0,1%, v/v) or with d18:0 (100 µM, ethanol 100%). Control inoculations were conducted with 10 mM $MgCl_2$. Experiments were repeated two times with similar results.

IV. Discussion - Conclusion

Experiments presented in Chapter 1. hinted that the absence of HR was probably not linked to RIN4. To further elucidate the rsole of proteins RPM1 and RIN4 in this phenomenon, mutants of their corresponding genes were infiltrated with *Pst AvrRpm1* and d18:0 or not. Once again, co-infiltrated leaves did not display a visible HR. Moreover, while RPM1-myc is supposed to be degraded 4 to 6 hours after *Pst AvrRpm1* infection, corresponding to the onset of the HR (Boyes *et*

al., 1998; Mackey *et al.*, 2002), the protein was still detected by its corresponding antibody 24 hours after the co-infiltration. Taken collectively, these data suggest that neither RPM1 nor RIN4 are directly involved in the absence of HR and that the mechanism underlying the absence of HR must occur upstream of RPM1 degradation.

Various markers have been evaluated to quantify plant defence responses following pathogen elicitation, such as electrolyte leakage, extracellular ROS production, which are considered as early defence events, expression of PR genes and stress-related hormone accumulation.

The PCD induced by the HR is intimately associated with loss of electrolytes from dying cells due to PM perturbations (Kawasaki *et al.*, 2005). Such measurements were therefore conducted to determine if the absence of visible HR observed when *Pst AvrRpm1* is co-infiltrated with d18:0 was correlated with an absence of quantifiable cell death. The same experiments were performed with *Pst AvrRps4* to highlight if such phenomenon was specific to the effector AvrRpm1. *Pst DC3000* was not tested here as previous experiments already showed the rapid growth of virulent *Pst DC3000* causes necrotic host cell death and therefore electrolyte loss (Grant *et al.*, 1995; Magnin-Robert *et al.*, 2015). Effectors AvrRpt2 and AvrRps4 are known to induce slower HR responses than AvrRpm1 (Johansson *et al.*, 2015). This tendency was confirmed by our data where delayed electrolyte leakage was observed in samples inoculated with *Pst AvrRps4* compared to *Pst AvrRpm1*. Furthermore, co-infiltration with d18:0 had no impact on electrolyte leakage caused by *Pst AvrRps4,* coinciding with the cell death previously observed on leaves. Cell death can be observed as soon as 3 hpi in *Pst AvrRpm1* vacuum infiltrated *Arabidopsis* (Johansson *et al.*, 2015). Here, infiltration of this bacteria alone started to increase medium conductivity as soon as 4 hpi. However, co-infiltration of the pathogen with d18:0 drastically reduced electrolyte leakage. Overall, our results suggest that the absence of visual HR in this condition is corroborated with an absence of cell death.

ROS production can be detected during both PTI and ETI (Torres, 2010). Previous results showed that co-treatment of d18:0 with *Pst* DC3000 or with *Pst AvrRpm1* drastically reduced extracellular ROS production by *Arabidopsis* (Magnin-Robert *et al.,* 2015). In light of this and the results presented in Chapter 1, further experiments were undertaken to elucidate the impact of d18:0 on this production, notably in response to bacteria carrying effectors other than AvrRpm1. Our results demonstrate that d18:0 reduces ROS production in response to bacterium that do induce symptoms *in planta* (*Pst AvrRps4*) and bacteria that do not (*Pst AvrRpm1, Pst AvrB* and *Pst AvrPphB*). This production remained unchanged between plants treated with *Pst AvrRpt2* alone or co-treated with d18:0. The hypothesis that LCBs could impact ROS production by plants has already been put forward in several studies, although some of them are somewhat contradictory.

Coursol *et al.* (2015), for example, showed that exogenous addition of LCBs (20 µM) reduced ROS production by *Arabidopsis* in response to cryptogein. But it has also been postulated that they were able to induce intracellular ROS production at low concentrations (0.5-2 µM) (Shi *et al.*, 2007), as well as extracellular ROS at high concentrations (100 µM) over long periods of time (> 90 min) (Peer *et al.*, 2011). Here, ROS production was significantly decreased in response to *Pst AvrRpm1* when d18:0 was added to a final concentration up to 10 µM. This result matches the studies performed in Chapter 1, where plants co-infiltrated with d18:0 at concentration lower than 10 µM started to exhibit a HR while higher concentrations did not. Similar results were obtained with *Pst AvrB* but only when d18:0 was at 100 µM. As previously suggested, this could be because *Pst AvrB* had to be used at a higher concentration than *Pst AvrRpm1* to be able to trigger a HR. Taken together, these data hint that d18:0 effect on extracellular ROS production in response to *Pst AvrRpm1*, *Pst AvrRps4*, *Pst AvrB*, *Pst AvrPphB* and *Pst* DC3000 is dose dependent but that this phenomenon cannot be solely responsible for the absence of visible HR.

In most plants, including *Arabidopsis*, perception of flagellin initiates the interaction of the RLK FLS2 (Flagellin sensing 2) with the RLK BAK1 (Brassinosteroid insensitive 1 – associated kinase 1). This recognition then triggers a plethora of signalling response including rapid production of ROS by NADPH oxidases (Chinchilla *et al.*, 2006; Chinchilla *et al.*, 2007; Jeworutzki *et al.*, 2010). Our results show that no matter the concentration of elicitor tested, d18:0 had no impact on ROS production in response to flg22. It has been shown that *Pst*-elicited ROS was only partly dependent of BAK1 (Smith and Heese, 2014). Furthermore, some studies point that *fls2* null mutants are still able to elicit signalling cues, including ROS production, in response to crude boiled *Pst* DC3000 extracts (Zipfel *et al.*, 2004; Gimenez-Ibanez *et al.*, 2009). Interestingly, another study showed that FLS2 is the predominant host receptor responsible for initiating early ROS production in response to *Pst* DC3000 (Smith and Heese, 2014). ROS production following a biotic interaction or contact with an isolated elicitor differs in term of perception and response. Indeed, several studies have hinted the existence of functional perception systems for IPs other than flagellin (Zipfel *et al.*, 2004; Gimenez-Ibanez *et al.*, 2009). This suggests that biotic interactions are much more complex and involve not only flagellin perception but also other external components of the bacterial surface (LPS, harpins or peptidoglycanes) (Torres, 2010). This difference could explain why d18:0 can reduce ROS production in response to some bacteria but not in response to flg22, although the underlying mechanism is not yet understood.

How d18:0 can disrupt ROS production is still unknown, but a hypothesis can be put forward. As previously mentioned, ROS production in *Arabidopsis* is mainly related to RbohD, located at the plant PM and more particularly into lipid rafts (Mongrand *et al.*, 2004; Yu *et al.*, 2017). Hao *et al.* (2014) notably showed that RbohDs are organised as clusters at the PM by using GFP-RbohD transformed *Arabidopsis*. They also demonstrated that GFP-RbohD is internalized via clathrin-

dependent and membrane raft-associated pathways following salt stress. A number of studies have suggested that RbohD-derived ROS production is not directly involved in plant cell death, but is rather involved in the signalling pathways associated with plant defence responses (Torres *et al.*, 2005; Lherminier *et al.*, 2009). Indeed, mutation of *AtRbohD* eliminated pathogen-induced ROS production but had only a modest effect on the HR (Torres *et al.*, 2005). This means that even though d18:0 can perturbate ROS production, this activity may not have any impact on PCD and would therefore not be responsible for the absence of HR previously observed. Concerning its mode of action, another lipidic elicitor, the fungal sterol ergosterol, has been proven to modify H^+ flux by inhibiting H^+-ATPase activity in *Beta vulgaris*, due to its interaction with lipid rafts (Rossard *et al.*, 2010). It could therefore be assumed that LCBs might interact with the PM of *Arabidopsis* and have a similar effect on the Rboh proteins it harbours. The effect of d18:0 on plant and bacterial PM will be approached in Chapter 4.

Some studies suggest a link between sphingolipid metabolism, SA levels and other plant defence markers such as camalexin production. For instance to study plant defence in response to herbivory, Begum *et al.* (2016) showed that overexpression of *OsLCB2a* in *Arabidopsis* led to the accumulation of LCBs and ceramides compared to the WT. These plant also exhibited an increased callose and wax deposition, an induction of SA-dependent and camalexin-dependent genes, a reduction of JA-dependent genes and a lower aphid infestation (Begum *et al.*, 2016; Huby *et al.*, 2020). It was also demonstrated that, when challenged with *Pst*, *Atdpl1* (*Dihydrosphingosine-1-phosphate lyase1*) mutant exhibited higher t18:0-P accumulation than the WT, as well as repressed expression of SA-dependent genes and increased JA-dependent gene expression. This mutant consequently was more sensitive to *Pst* (Magnin-Robert *et al.*, 2015). Moreover, FB1, the d18:1 analogue that causes LCB accumulation (Abbas *et al.*, 1994; Saucedo-García *et al.*, 2011; Gutiérrez-Nájera *et al.*, 2020), also triggers HR-like lesions accompanied by callose deposition, ROS and camalexin production and expression of *PR* genes in *Arabidopsis* (Stone *et al.*, 2000). Here, *Arabidopsis* challenged with *Pst* DC3000 accumulated less camalexin at 48 hpi than those inoculated with *Pst AvrRpm1*, which is consistent with previous findings (Qiu *et al.*, 2008). d18:0 co-infiltration appeared to significantly diminish camalexin accumulation in response to *Pst AvrRpm1*. Since no HR is visible on leaves receiving this co-treatment, one could argue that this lower accumulation of camalexin is somewhat involved in this phenomenon. Camalexin biosynthesis is induced by a wide variety of plant pathogens, including *P. syringae*, but its growth-inhibiting capacities have been so far reported for a much narrower range of species (Glawischnig, 2007). More specifically, *Arabidopsis* mutants *pad1, pad2* and *pad3* (Phytoalexin deficient), impaired in camalexin synthesis, were equally capable of restricting the growth of avirulent *Pst* as the WT was (Glazebrook and Ausubel, 1994). This strongly suggests that camalexin biosynthesis is

not required for resistance to avirulent *Pst* (Glazebrook and Ausubel, 1994). Therefore, since lower camalexin accumulation is not believed to mediate plant resistance to *Pst*, it is here probably not the cause for the absence of HR but rather a consequence of it.

Hormonal crosstalk are vital regulators of plant response to pathogens (Shigenaga *et al.*, 2017). As previously stated, SA and its signalling pathways are triggered in response to a hemibiotrophic pathogen, such as *Pst*, whereas JA, and its active form, JA-Ile, are involved in infection by necrotrophic pathogens (Li *et al.*, 2019). In *Arabidopsis*, the two pathways antagonize each other (Mur *et al.*, 2006; Li *et al.*, 2019). Higher SA quantities in plants infected with virulent bacteria than with avirulent one are consistent with previous findings (Heck *et al.*, 2003). It would seem here that d18:0 co-infiltration negatively impacts *PR1* relative expression in response to *Pst* DC3000 and even more drastically in response to *Pst AvrRpm1*. This coincides with lower SA accumulation. Considering these results, it may be conceivable that d18:0 repressed, directly or not, the SA pathway particularly in response to avirulent bacteria. However, SA repression is commonly associated with promotion of bacterial development (Moore *et al.*, 1989; Zhou *et al.*, 1998; Brooks *et al.*, 2005). Indeed, *P. syringae* produces coronatine, a phytotoxin that mimics JA-Ile and acts by inhibiting the accumulation of SA in order to promote bacterial growth (Zheng *et al.*, 2012). This is therefore contradictory with the absence of HR observed on leaves when d18:0 is co-infiltrated with *Pst AvrRpm1*. Moreover, in *Arabidopsis*, coronatine insensitive mutants that are resistant to *Pst,* display higher levels of SA (Block *et al.*, 2005). Besides, still in *Arabidopsis*, mutants deficient in SA-induction genes tend to accumulate camalexin after *Pst* inoculation (Nawrath and Métraux, 1999), which was not the case in our conditions. Furthermore, in the same mutants, only the expression of *PR1* was diminished and not *PR5* following *Pst* infection (Nawrath and Métraux, 1999), whereas both gene expressions are reduced in our conditions (**Supplemental Figure S6.**).

Plants co-infiltrated with d18:0 and *Pst* DC3000 showed an increased *VSP1* expression and slightly, but not significantly, more elevated levels of JA-Ile compared to the infiltration of the bacteria alone. Considering its role in defence against necrotrophic pathogens (Li *et al.*, 2019), low quantities of JA-Ile are expected upon infiltration of *Pst*. In plants co-inoculated with *Pst* DC3000 and d18:0, the repression of the SA pathway could be the reason why *VSP1* is overexpressed, because of the antagonistic effects between these hormones (Leon-Reyes *et al.*, 2010). This overexpression however does not modify the symptoms observed on treated leaves.

Interestingly, it is unclear whether decreased SA accumulation and SA-dependent gene expression are the result of a direct action of d18:0 on the plant, or whether they are the consequences of a more upstream action of the molecule, such as a lowered bacterial virulence, a decreased susceptibility or an altered perception of the pathogen.

As previously mentioned, co-infiltration of *Pst AvrRpm1*, *Pst AvrB* or *Pst AvrPphB* with d18:0 did not induce a visible HR on *Arabidopsis* leaves. Moreover, all effectors possess a consensus N-terminal fatty acylation sequence (Nimchuk *et al.*, 2000). Therefore, our first hypothesis was that d18:0 co-infiltration would provoke a decrease in NMT activity and possibly the relative expression of *NMT1* & *2*. This would supposedly interfere with AvrRpm1, AvrB and AvrPphB myristoylation, preventing them from being redirected to the PM where they should be active, consequently reducing the effect the bacteria had on *Arabidopsis*. Indeed, site-specific amino acid substitution in the fatty acylation sequence in both AvrRpm1 and AvrB (particularly residues G2A and S6A, see **Figure 15.** for the sequence) proved that myristoylation sites are required for maximal avirulence function in plant cells. Indeed, plants inoculated with these mutated bacteria showed fewer responding leaves (Nimchuk *et al.*, 2000). This suggest that when the myristoylation process is perturbated, the HR also is. Due to difficulties finding efficient *NMT2* primers, the relative expression of only *NMT1* was followed here. Interestingly, whereas its expression is induced when plants are infiltrated with *Pst AvrRpm1* alone, no significant change could be observed after co-infiltration with the SL. Thus, *NMT1* expression is slightly reduced at 24 hpi with a more pronounced effect at 48 hpi compared to infection with bacteria alone. Only a limited set of data is available on *NMT1* expression in the literature and is primarily linked to investigations of NMT roles in *Arabidopsis* (Pierre *et al.*, 2007). Furthermore, to the best of our knowledge, none actually studied the response to *P. syringae* or even a pathogen, so data comparison was not possible in this case. Myristoylation is a fine-tuned process so small variations in *NMT1* expression could be significant. To confirm this, studying NMT enzymatic activity would help figuring out its role in the absence of HR. This aspect will notably be further developed in the General Discussion - Perspective section of this manuscript.

Chapter 3 - Main Results

- ✓ RPM1 and RIN4 are not directly involved in the absence of HR when *Pst AvrRpm1* is co-infiltrated with d18:0
- ✓ No increase in medium conductivity was observed in this condition suggesting the infiltration of the bacteria did not lead to cell death
- ✓ Co-treatment of *Pst AvrRpm1*, *Pst AvrRps4*, *Pst AvrB,* and *Pst AvrPphB* with d18:0, but not *Pst AvrRpt2*, significantly reduced ROS production by *Arabidopsis*
- ✓ Co-infiltration of d18:0 and *Pst AvrRpm1* reduced SA levels and lowered *PR1* expression, an SA related gene expression
- ✓ Co-infiltration of d18:0 and *Pst AvrRpm1* slightly reduced *NMT1* expression compared to the infiltration of the bacteria alone

4

Biophysical investigation of the interaction of sphinganine with plant and bacterial membrane lipids

I. Context

PMs, whether of plants or of bacteria, are paramount in a variety of phenomenon connected to cell survival such as cell protection, nutrient exchanges regulation and signal perception and transduction. They are extremely complex and harbour many molecular species of lipids and proteins (Mamode Cassim *et al.*, 2019). Many of their roles are sustained by their proteinaceous content but their lipid components are just as important. Indeed, the composition and physical state of the lipid bilayer greatly impact lipid-protein and protein-protein interactions, membrane bound enzyme activity and membrane transport capacity (Furt *et al.*, 2011).

Plant PM is the most diversified membrane in the plant cell, composed of three main types of lipids: glycerophospholipids (mainly phospholipids such as PC, PE or PG), sterols (mainly sitosterol, stigmasterol, campesterol but also conjugated sterols) and SLs (mainly GIPC and GluCer) (Furt *et al.*, 2011; Cacas *et al.*, 2012; Mamode Cassim *et al.*, 2019) (see **Introduction. II.** for further information). SLs are critical components of this PM in plants, acting as structural elements, PCD regulators or signalling messenger in stress responses (Huby *et al.*, 2020). However, only few researches have reported their mechanism of action and effects when applied exogenously (Saucedo-García *et al.*, 2011; Glenz *et al.*, 2019; Gutiérrez-Nájera *et al.*, 2020). Few studies suggest that lipidic elicitors are actually perceived, not by PRRs, but by plant PM lipids (Cordelier *et al.*, 2021). For instance, ergosterol, the main sterol of fungi, is described as a general elicitor of plant defences (Klemptner *et al.*, 2014). LCB effect on animal membranes has already been demonstrated in a few studies. d18:1, for example, has been shown to increase the permeability of liposomes and erythrocyte ghost membranes to aqueous solutes (Contreras *et al.*, 2006). Also, adding d18:1 to healthy Chinese Hamster Ovary cells resulted in a rapid decrease in PM and lysosome membrane fluidity, which was linked to a direct impact of the LCB (Carreira *et al.*, 2021).

Bacterial membranes are also extremely diverse, especially for Gram-negative bacteria like *Pst*. They possess two membranes, separated by a middle layer of peptidoglycan in the periplasmic space. The outer membrane (OM), which is mainly made up of LPS and some glycerophospholipids, the inner membrane (IM), composed of glycerophospholipids (mainly PE, PG and CL) (Lohner, 2009). SLs are only present in a subset of bacteria and have, so far, not been described in *Pst*. However, the effects of sphingosine on bacterial PMs of human pathogenic bacteria, such as *P. aeruginosa* or *S. aureus*, have already been investigated. Its biocidal activity against such bacteria was notably explained by its binding to CL in the PM, causing membrane permeabilization and ultimately bacterial death (Parsons *et al.*, 2012; Verhaegh *et al.*, 2020).

Previous findings in this work suggested that sphinganine could possibly interact with or trigger changes in the plant PM. This hypothesis was prominently advanced with the lowering of

extracellular ROS production by *Arabidopsis* in response to *Pst* and d18:0 co-infiltration. As such, complementary *in vitro* and *in silico* biophysical approaches have been used to unravel the relations between plant or bacterial PM lipids and d18:0. Indeed, biophysical approaches using simplified PM lipid models that imitate a desired membrane without its protein content (see **Introduction. V.** for further information) can help in understanding at a molecular level the interactions between plant or bacterial PM lipids and a molecule of interest. Using commercially available model lipids, complex membrane models mimicking plant PM are commonly composed of palmitoyl-linoleoyl-phosphatidylcholine (PLPC), as model phospholipid, GluCer, as model sphingolipid and sitosterol (sito) as model sterol (Deleu *et al.*, 2014). Similarly for bacteria, palmitoyl-oleoyl-phosphatidylethanolamine (POPE), palmitoyl-oleoyl-phosphatidylglycerol (POPG) and CL are often used as model lipids to represent the IM (Le *et al.*, 2011).

II. Materials and methods

1. Chemicals

Sphinganine (d18:0) was purchased from Avanti Polar Lipids, dissolved in ethanol (100%) or DMSO (100%), as later precised, and used without further purification. Palmitoyl-2-linoleoyl-sn-glycero-3-phosphocholine (PLPC), sitosterol (sito), D-glucosyl-ß-1,1′-N-palmitoyl-D-erythro-sphingosine (d18:1/16:0 - GluCer or Glucosylceramide), palmitoyl-oleoyl-phosphatidylethanolamine (POPE), palmitoyl-oleoyl-phosphatidylglycerol (POPG) and cardiolipin (CL) were purchased from Avanti Polar Lipids and used without further purification. Calcein and laurdan were obtained from Sigma-Aldrich.

2. Lipid composition for plant and bacterial biomimetic membranes

To mimic the lipid composition of plant PM, PLPC, sito and GluCer were used, either in a mix (60:20:20, molar ratio) or alone, depending on the experiment. For bacterial PM, POPE, POPG and CL were used, either mixed (65:23:12, molar ratio) or alone. These lipid compositions were previously used to mimic plant and *Arabidopsis* PM (Deleu *et al.*, 2014, 2019; Deboever *et al.*, 2022) and bacterial PM, including that of *P. aeruginosa* (Mary *et al.*, 2011; Rivera-Sanchez *et al.*, 2022).

3. Determination of the CAC of d18:0

Determination of the CAC by tensiometry with Langmuir trough

CAC and adsorption experiments at constant surface area were performed in a KSV (Helsinki, Finland) Minitrough (190 cm3) placed on a vibration-isolated table and equipped with a Wilhelmy plate as previously described (Nasir *et al.*, 2016). Experiments were performed in the absence of lipids to determine the CAC of d18:0. To that end, d18:0 was injected at various concentrations in the subphase (10 mM Tris buffer, pH 7.4). For each concentration, the surface pressure increase induced by d18:0 adsorption at the air-water interface was recorded over time until a plateau was reached.

Determination of the CAC by DLS

A d18:0 stock solution was diluted at various concentrations in filtered buffer (Tris-HCl, 10mM, pH 7.4) and samples were placed in a dry bath at 25°C. Each sample was then run through the DLS, and the light scattering was measured between 20 and 100 times for each sample. The data was then processed to obtain a normalised intensity which reflects the scattered intensity of the molecules allowing the determination of their CAC and therefore their state in solution as a function of their concentration.

4. Adsorption of d18:0 onto lipid monolayers using Langmuir trough

Adsorption experiments at constant surface area were performed in a KSV (Helsinki, Finland) Minitrough (190 cm3) placed on a vibration-isolated table and equipped with a Wilhelmy plate as previously described (Nasir *et al.*, 2016). Lipids of either plant or bacteria were prepared individually or mixed in chloroform/methanol (2:1, v:v). Solutions were spread at the air-subphase interface to reach the desired initial surface pressure. After a 15 minutes wait for solvent evaporation and film stabilization, d18:0 was injected in the subphase (10 mM Tris buffer, pH 7.4), underneath the pre-formed lipid monolayer to a final concentration of 1.25 µM. The adsorption of d18:0 to the lipid monolayer was followed with the increase of surface pressure as previously described (Nasir *et al.*, 2016; Deleu *et al.*, 2019).

For all experiments, injection of ethanol (0,1%) was used as control. The maximal insertion pressure (MIP) and the differential Π_0 ($d\Pi_0$) were determined, indicating the penetration power of d18:0 into the lipid monolayer and the attracting effect the lipids have on d18:0, respectively. The MIP was obtained by linear regression of the plot $\Delta\Pi$ *vs* Π_i, $d\Pi_0$ was calculated as follow:

$d\Pi_0 = \Delta\Pi_0 - \Pi_e$

$\Delta\Pi_0$ corresponds to the y-intercept of the linear regression of the plot, and Π_e is the surface pressure of d18:0 at the equilibrium when there is no lipid at the interface.

5. MLVs and liposome preparation

Multilamellar vesicles

Multilamellar vesicles (MLVs) were prepared as follow, with lipid mixtures of either plant or bacteria lipids. They were dissolved in a chloroform/methanol mix (2:1, v:v). Solvents were evaporated and maintained under vacuum overnight to obtain a dry lipid film. Tris-HCl buffer (10 mM, pH 7.4) was then added to hydrate the lipid film. The lipid dispersion was maintained at 37°C for 1 h, vortexed every 10 min followed by 5 cycles of freeze-thawing.

Small unilamellar vesicles

To obtain small unilamellar vesicles (SUVs), this suspension was sonicated to clarity (10 cycles of 2 min) using a titanium probe with 400 W amplitude. Leftover titanium particles were removed from the solution by centrifugation, 10 min at 6200 rpm. Unencapsulated calcein was removed from the SUV solution by the Sephadex G65 mini-column separation technique (Fu and Singh, 1999).

Large unilamellar vesicles

To obtain LUVs, the MLV suspension was extruded 13 times through a 0,1 µM membrane filter using Liposofast extruder (AVESTIN®). Diameter and stability of the LUVs were confirmed by DLS measurements.

6. Membrane permeabilization

MLVs of plant or bacterial lipids (see **Chapter 4. II.2**) were prepared as previously described except that film hydration was performed using 10 mM calcein in Tris-HCl buffer (10 mM, pH 7.4) (see **Chapter 4. II.5**). SUVs were obtained as previously described (see **Chapter 4. II.5**) and their concentration was adjusted for each experiment to 15 µM in Tris-HCl buffer (10 mM, pH 7.4).

Calcein fluorescence was measured as previously described (Bartlett, 1958) with a Perkin Elmer (model LS50B) fluorescence spectrometer. Excitation and emission wavelengths set at 467 nm and 517 nm, respectively. d18:0, dissolved in ethanol (100%) was added to the SUV solution at various concentrations without ever exceeding 0,1% of the final volume. Ethanol (0,1%) was used as

control. Maximal calcein release was determined by adding Triton-X100 (0.2%) to the SUV suspension which dissolved the lipid membrane without interfering with the fluorescence signals. The amount of calcein released or RF was calculated according to Shimanouchi *et al.*, 2009:

$$RF\ (\%) = 100\ (I_t - I_o)/(I_{max} - I_o)$$

where I_t corresponds to the fluorescence intensity measured over three minutes after sphinganine addition, and I_o and I_{max} the fluorescence intensities of the negative control and of the maximal calcein release after Triton-X100 addition, respectively. All experiments were carried out at least three times, each time with freshly prepared SUVs.

7. Measurement of PM fluidity

For Laurdan generalized polarization experiments, LUVs of either plant or bacterial lipids were prepared (see **Chapter 4. II.2 & 5**). LUVs were resuspended to reach a final concentration of 50 µM in Tris-HCl buffer (10 mM, pH 7.4)

Laurdan was dissolved in DMSO and added to the LUV solution (750 µl) at a final concentration of 0,75 mM. d18:0, dissolved in ethanol (100%) was added at various concentrations up to a ratio lipid/sphinganine of 5/1, without ever exceeding 0,1% of the final volume. Ethanol (0,1%) was used as a control. Fluorescence of Laurdan in LUVs was monitored at 20°C with a Perkin Elmer LS50B fluorescence spectrometer. Samples were placed in 10 mm pathlength quartz cuvettes under continuous stirring and the cuvette holder was thermostated with a circulating bath. Samples were equilibrated at 20°C for 10-15 min prior to the measurements. The excitation wavelength was set to 360 nm (slit = 2,5 nm), and at least 10 measurements of emission intensities at 440 nm and 490 nm were recorded and averaged for each sample and the control. Generalized polarization (GP) of Laurdan was then calculated according to (Harris *et al.*, 2002)):

$$GP = I_{440} - I_{490}/I_{440} + I_{490}$$

where I_{440} and I_{490} are the control-subtracted emission intensities at 440 nm and 490 nm, respectively. All experiments were carried out at least three times, each time with freshly prepared LUVs.

8. Thermodynamic parameters of d18:0 interaction with lipid bilayers by isothermal titration calorimetry

For ITC measurements, LUVs were prepared with lipids of either plant or bacteria as previously described (see **Chapter 4. II.2 & 5**). and resuspended to reach a final concentration of 1 mM in

Tris-HCl buffer (10 mM, pH 7.4). A VP-ITC microcalorimeter (Microcal Inc., Northampton, MA, USA) was used for all measurements. d18:0 was dissolved in DMSO (100%). All previous experiments were performed with ethanol as solvent but interactions between water and ethanol are exothermic and would have temper with the results, hence its dissolution in DMSO here. All experiments were performed at 26°C. The reference cell was filled with degassed mQ water. The sample cell (V= 1,4565 mL) was filled either with buffer (blank - Tris-HCl, 10 Mm, pH 7.4), buffer + d18:0 (at a final concentration of 20 μM) or buffer + DMSO (control − 0,01%). This cell is continuously stirred at 305 rpm. The syringe (V= 300 μL) was filled with the LUV suspension + DMSO (1 mM in buffer + 0.01%). Both the LUV solution and the content of the sample cell were degassed by ultrasonication before use. The first injection of LUVs suspension was 2 μL and was not used in data analysis. Then, every 600 s, 10 μL of the suspension were injected in the sample cell. ITC data were analysed using Origin 7.0 (Microcal) software following a previously described method (Heerklotz and Seelig, 2000; Lebecque *et al.*, 2018).

9. Propensity of d18:0 to insert into a bilayer determined by the Impala procedure

First, the structure of d18:0 was constructed using HyperChem software (Hypercube, Inc.). The molecular geometry was optimized by systematic analysis of the torsion angles using the structure tree method as previously described (Lins *et al.*, 1995). The most probable structure corresponding to the lowest conformational energy was used.

The Impala procedure uses a Monte Carlo approach to simulate the insertion of d18:0 in an implicit lipid bilayer, as previously described (Ducarme *et al.*, 1998; Franche *et al.*, 2020). Briefly, this method employs an empirical forcefield to depict membrane physicochemical features while taking into account two types of restraints, the hydrophobic effect and lipid disturbances. The Z axis is assumed to be the only variable in membrane properties. The two restraints were calculated at each place by moving the d18:0 molecules the Z axis by 1 Å steps from one side of the implicit membrane to the other and later added to determine the total energy restraint.

10. Interaction energies between d18:0 and lipids determined by the Hypermatrix docking method

The hypermatrix docking method was employed, as previously described (Deleu *et al.*, 2014; Deleu *et al.*, 2019) in order to dock a molecule of sphinganine to a lipid system composed of either

plant or bacterial lipids. Briefly, a molecule of d18:0 is fixed at the centre of the system and oriented at the hydrophilic/hydrophobic interface. The lipid molecules, which are also orientated at the interface, are positioned around the centre molecule and over 10^7 positions (translations and rotations) are tested. Interactions such as Van der Waals, electrostatic, and hydrophobic are all taken into account when calculating the interaction energies. The energy of interaction along the coordinates of all assembly are gathered in a matrix and sorted according to decreasing values. The assembly with the lowest energy value is considered the energetically most stable.

11. Modelling of sphinganine/plant lipids monolayer interactions with Big Monolayer method

The big monolayer method was used as described by Deleu *et al.*, 2019 to visualize lipid domains. Briefly, the initial stage consisted in aligning each pair of molecules in the system at the hydrophilic/hydrophobic interface according to Hypermatrix. Then, their interaction energies were computed, considering Van der Waals, electrostatic, and hydrophobic interactions. The second phase involved creating a grid of 200 × 200 molecules and utilizing a Monte Carlo procedure to minimize the system using the interaction energies computed in the previous step. Each molecule is represented by a pixel, producing an image of the molecular domains formed. Three repetitions of the system were calculated. The simulations were performed using plant or bacterial lipid mixture (see **Chapter 4. II.2**) without or with d18:0 (88% lipids, 12% d18:0).

III. Results

1. Depending on its concentration, d18:0 exists in various forms in solution

As amino alcohols with an unsaturated hydrocarbon chain, LCBs are amphiphilic lipids and as such, are able to form micelles or aggregates above a threshold concentration defined as critical aggregation concentration (CAC) (Brogden *et al.*, 2019; Yi *et al.*, 2021). Experiments were performed to determine the aggregation state of d18:0 in solution at various concentrations, notably to select the appropriate concentration for further biophysical experiments (**Figure 30.**).

To that end, two approaches were employed. The first one used the Langmuir trough to determine the CAC of d18:0 (**Figure 30A.**). The injection of ethanol (0,1%) was used as a control and did not influence surface pressure (data not shown). The injection of the molecule at various concentrations in a buffer modified the measured surface pressure. It reached a plateau for

concentrations of d18:0 over 2 µM. Therefore, with this method, the CAC was estimated between 1,5 and 2 µM. At concentrations above this threshold, d18:0 supposedly forms aggregates.
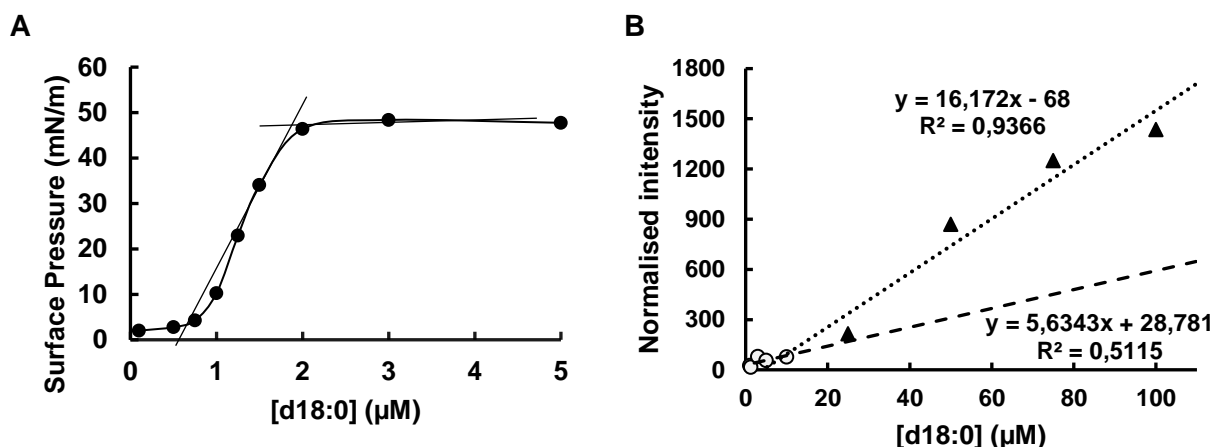
A. DLS size distribution of 100 µM of d18:0 in solution (Tris-HCl, 10 mM, pH=7,4) at 25°C. Particle size is expressed in nm and was around 1 µM. **C.** Estimation of the CAC of d18:0 by tensiometry using the Langmuir trough technique. The molecule is injected at multiple concentrations in a sub-phase (Tris HCl, 10 mM, pH 7,4) without lipids at the interface air-liquid. The resulting surface pressure at the equilibrium is recorded. The CAC is determined by the intersection of the two linear regression curves. This experiment was repeated two times with similar results. **B.** Variation of the normalized intensity as a function of d18:0 concentration in a buffer (Tris-HCl, 10 mM, pH=7,4). Light scattering induced by various concentrations of d18:0 was measured, and the normalised intensity calculated. The CAC is determined by the intersection of two linear regression curves: one for low concentrations where the normalised intensity does not increase and one for higher concentrations where it begins to increase.

The second method used DLS where the normalised intensity is calculated for each concentration of d18:0 tested (**Figure 30B.**). The results allow two linear regression curves to be made, one for low concentrations at which the normalised intensity does not increase and one for higher concentrations, where the normalised intensity starts to increase. The intersection of these two curves allows us to determine the CAC. With this method, the CAC of d18:0 was estimated between 2 and 10 µM. The DLS also allowed to estimate the size of d18:0 aggregates in solution at 100 µM, which was around 1 µm (data not shown). Another measure was performed with d18:0 at 1,25 µM

and it was not possible to determine particle size suggesting d18:0 was not aggregated at this concentration.

2. Interaction of d18:0 with plant plasma membrane-mimicking models

The Impala procedure was used to predict the ability of d18:0 to insert into an implicit model lipid bilayer and to determine the preferable location and positioning of d18:0 within the bilayer (**Figure 31A**.). A sharp drop of energy from the aqueous phase to the membrane surface was observed (up to ~-10 Kcal/mol), which indicates the insertion of d18:0 into membranes is favourable. The energy is approximately 0 Kcal/mol in the hydrophobic region of the membrane which suggested a less favourable interaction than with the hydrophilic region. Nevertheless, the non-positive value of the energy in the hydrophobic region of the bilayer suggests the flip-flop potential of d18:0 between the two bilayer leaflets. The preferable positioning of d18:0 within the membrane, is shown in **Figure 31B.** The lipid chain of d18:0 lies within the hydrophobic part of the membrane while the amine and alcohol groups are located at its hydrophilic part. Altogether, this would indicate that d18:0 can penetrate membranes and possibly cross them.
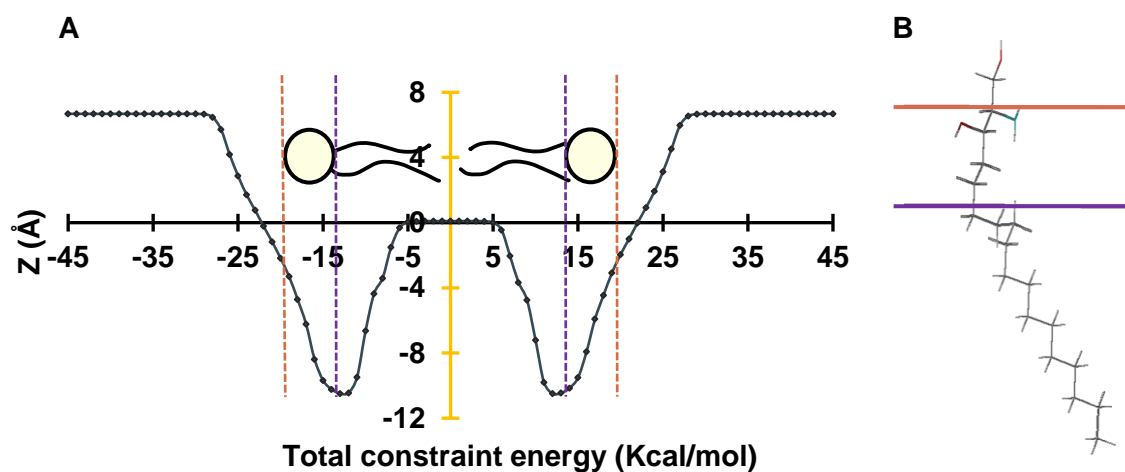
Figure 31. Propensity of d18:0 to insert into an implicit modelled bilayer

A. The Impala simulation calculates the energy restraints of a lipid bilayer as d18:0 goes through it. The X-axis corresponds to the position of the center of mass along the Z-axis. From left to right: the interface between the bilayer and the aqueous phase (orange), the interface between the polar head and the alkyl chain (purple) and the center of the bilayer (yellow). The more the negative the energy is, the more favourable the insertion will be **B.** Modelling of the most probable conformation of d18:0. The lines represent the same planar surfaces as in A.

Simulation results were completed by experimental data using ITC experiments that provided typical raw data (**Figure 32 A.**) and thermodynamic parameters of the interaction between d18:0 and plant PM-mimicking LUVs (**Figure 32 B.**).

The negative and decreasing heat flow observed after each LUV injection into the d18: containing solution indicates that the molecule interacts spontaneously with PM-like lipids (**Figure 32 A.**)

The binding coefficient K was relatively high (>80 m/M) compared to a study on linoleic and linolenic acid hydroperoxides interactions with plant PM-like liposomes (<3 m/M; Deleu *et al.*, 2019), and a study on bolaamphiphiles interaction with mammalian-like liposomes (<25 m/M; Nasir *et al.*, 2016). This suggests d18:0 has a high affinity for plant mimicking lipid membranes. The binding reaction to liposomes was spontaneous as the molar free energy ΔG was negative, exothermic as the molar enthalpy change ΔH was negative and generated a positive change of the molar entropy (TΔS>0). These interactions are mostly of hydrophobic nature since the value of the molar entropy (TΔS>0) is greater than the value of the molar enthalpy change (ΔH), indicating the interactions are entropy driven. Altogether, these results suggest that d18:0 is attracted by and can interact with plant lipid membranes.
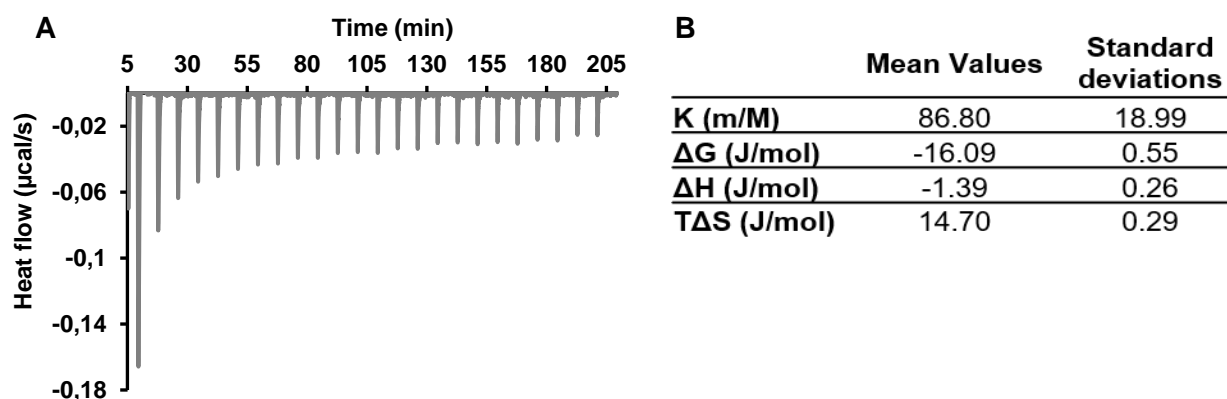
Figure 32. Ability of d18:0 to interact with plant liposomes determined by isothermal titration calorimetry

A. Raw data from ITC experiments at 26°C, each peak corresponds to a single injection of a 1 mM PLPC, GluCer and sito (60:20:20, molar ratio) LUV suspension to a solution containing 20 µM of d18:0. **B.** Calculated thermodynamic parameters for this interaction. These values are means of two independent experiments. K represents the binding coefficient (the affinity of d18:0 for the LUVs), ΔG represents the molar free energy, ΔH, the molar enthalpy change, and TΔS, the molar entropy change.

3. Lipid specificity of the interaction

The adsorption capacity of sphinganine into monolayer of individual or ternary mixture of lipids representative of the plant or bacterial PM was analysed to determine if lipid specific interactions occurred (**Figure 33A.** and **C.**). To that end, the Langmuir trough technique was used, where a monolayer of lipids is initially formed at an air-water interface, and d18:0 is injected into the subphase. The adsorption of d18:0 at into the lipid monolayer at different initial surface pressures (Π_i) was monitored by the increase of the surface pressure ($\Delta\Pi_0$) at a constant trough area (**Figure 33B.** and **D.**). The differential Π ($d\Pi_0$) gives information on the attractive effect of the lipids on d18:0, and the maximal insertion pressure (MIP), reflects the penetration capacity of d18:0 into the lipid monolayer (Deleu *et al.*, 2014; see **II.4** for calculation details).

Upon addition of d18:0 to monolayers formed with plant PM lipids, $d\Pi_0$ values were all positive and similar for all tested compositions, indicating that all tested lipids exert a comparable attraction on d18:0 (**Figure 33A.**).

MIP values were all higher than the lateral pressure supposed to prevail into biological membranes (30 – 35 mN/m) (Marsh, 1996), meaning that d18:0 could possibly adsorb onto natural plant membranes. MIP value is higher for GluCer, but the wide standard deviation does not allow to conclude on a specific interaction of d18:0 with this lipid (68 mN/m ± 17,5)" (**Figure 33A.**). Collectively, these data suggest that d18:0 is attracted by and can adsorb onto monolayers of plant mimicking PM lipids, without a particular affinity for any lipid tested.

$d\Pi_0$ values were also similar upon addition of d18:0 on monolayers formed with bacterial PM lipids (**Figure 33B.**), which once again indicates that all lipid tested attract d18:0 in a similar way. The MIP values were also above the threshold of 30-35 mN/m meaning that d18:0 has a propensity to insert into a natural bacterial membrane (Marsh, 1996).

The comparison between data on bacterial and plant model membranes indicates that although d18:0 is more attracted by bacterial lipids than plant lipids, it is more able to insert into plant membrane than bacterial membrane.
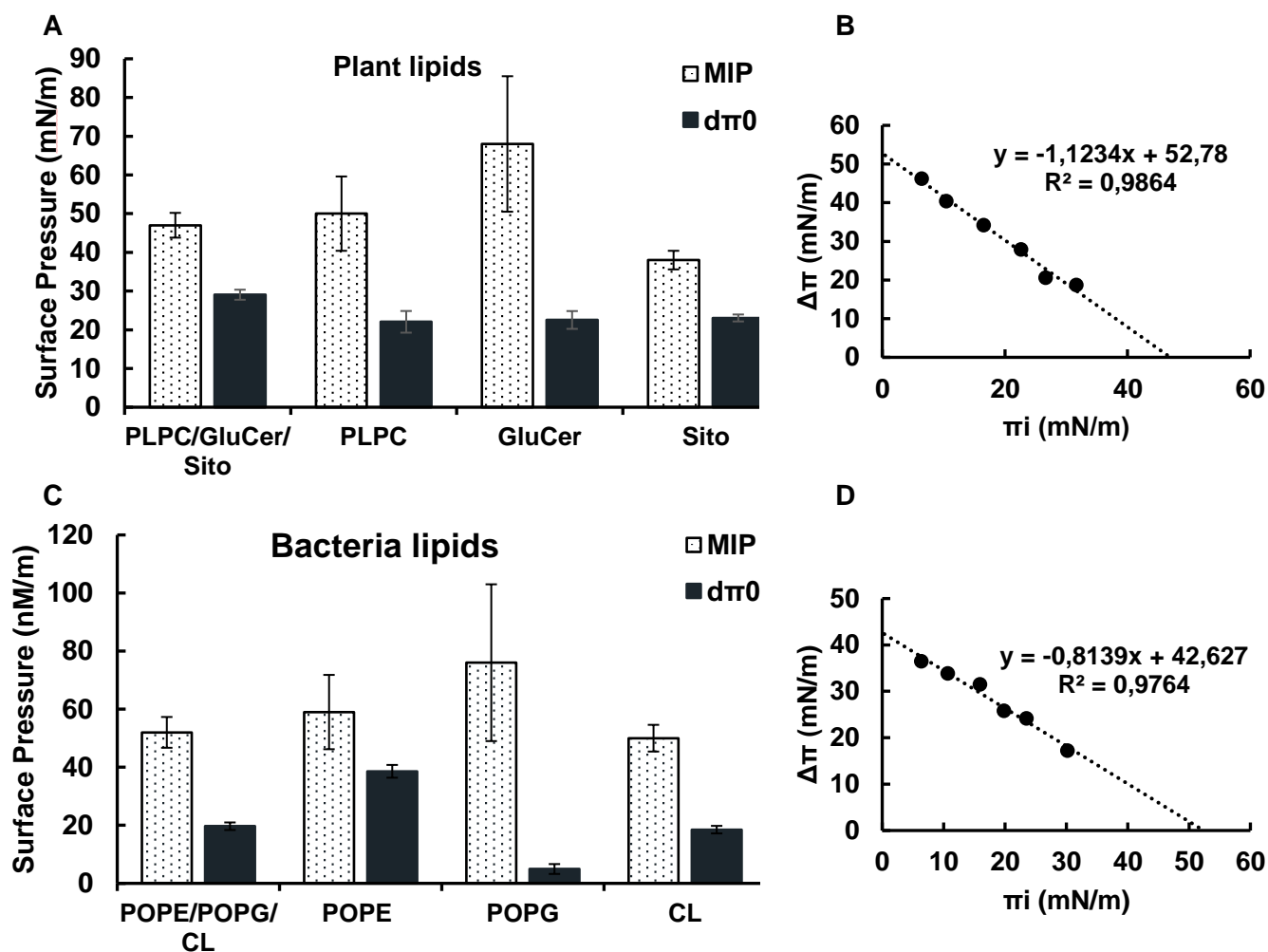
Figure 33. Lipid specificity of the interaction between d18:0 and lipids representative of plant and bacterial plasma membrane

A. Adsorption of d18:0 into monolayers of plant PM lipids: PLPC, GluCer and sito, either pure or mixed (60:20:20, molar ratio). **B.** Plot of the maximal surface pressure variation (ΔΠ) *vs* the initial pressure upon d18:0 addition into a PLPC:GluCer:sito monolayer. **C.** Adsorption of d18:0 into monolayers of bacterial PM lipids: POPE, POPG and CL, pure or mixed (65:23:12, molar ratio). **D.** Plot of the maximal surface pressure variation (ΔΠ) *vs* the initial pressure upon d18:0 addition into a POPE:POPG:CL monolayer. d18:0 was injected at 1,25 µM in a subphase (Tris HCl, 10 mM, pH 7,4), underneath the lipid monolayer. The maximal insertion pressure (MIP) reflects the penetration power of the sphinganine into the lipid monolayer and the differential Π (dΠ0) indicates the attracting effect the lipids have on the molecule.

Lipid specificity of the interaction was further studied by an *in silico* approach using the Hypermatrix docking method. This method is used to calculate the energy of interaction between d18:0 and plant or bacterial individual lipids at an hydrophilic/hydrophobic interface, and to help determine whether this interaction is favourable or not (Brasseur *et al.*, 1987; Deleu *et al.*, 2014).

The results obtained (**Figure 34.**) show that the interaction between d18:0 and all plant or bacterial lipids was favourable as all interaction energies are negative. These interactions are more favourable than the interaction of d18:0 with itself as the energy values are lower (higher negative value) with lipids than with d18:0 itself (represented by the dashed line in **Figure 34.**). However, it can be seen that the interaction between d18:0 and PLPC and GluCer, for plants, and POPG and particularly CL, for bacteria, appeared more favourable than with other lipids.

Altogether, these data show that d18:0 is attracted by and can interact with lipids of both plants and bacteria. There is however no clear trend in the data to determine a preferential interaction of d18:0 with a particular lipid.
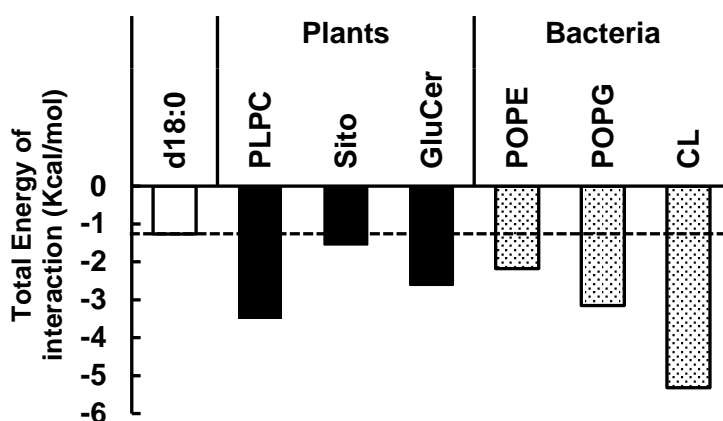
Figure 34. Total energies of interaction of d18:0 with itself or with representative lipids of the plant and bacterial plasma membrane

The total energies of interaction were calculated with the Hypermatrix docking method. Lipids representative of the plant PM are PLPC, sito and GluCer. Lipids representative of bacteria are POPE, POPG and CL.

4. Effect of d18:0 on the structure and organization of plant and bacterial PM

After determining if d18:0 could interact with lipids of plant or bacterial PM, further experimentations were employed to elaborate on the effects these interactions could have on the structure and organization of the model PMs.

First, the Big Monolayer simulation was used to examine the behaviour of a molecule in a lipid monolayer. Each pixel represents a molecule. For the plant lipid composition: PLPC in green, sito in orange and GluCer in blue. For bacterial lipid composition: POPE in yellow, POPG in black and CL in red. The representations are either without d18:0 in pink (100% lipids) (**Figure 35A. and C.**) or with (88% lipids, 12% d18:0) (**Figure 35B. and D.**).

As suggested by the previous results, d18:0 is predicted to interact with lipids from plants and bacteria. Interestingly, it seemed to interact preferentially with the lipid domains formed by sito and GluCer and caused their fragmentation (**Figure 35B.**).

Concerning bacterial lipids, d18:0 is predicted to interact preferentially with POPG and CL (**Figure 35D.**), as suggested by the Hypermatrix results (**Figure 34.**). Without completely disrupting these lipid domains, it nevertheless appeared to be able to remodel them by inducing POPE entry into the CL domains.
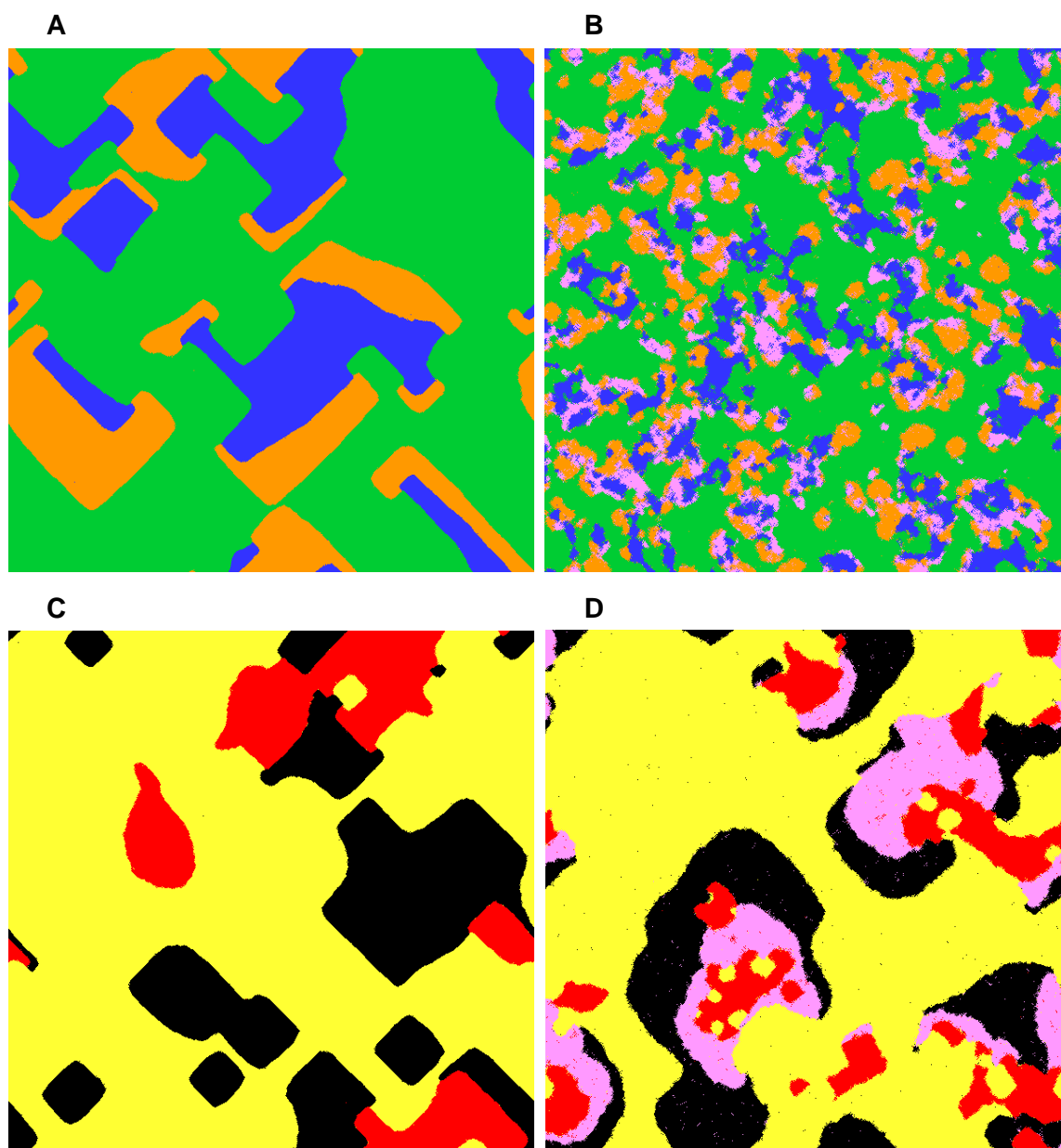
Figure 35. Modulation of membrane organization by d18:0

Monolayer simulations of lipid-d18:0 interactions performed with Big Monolayer where each pixel represents a molecule. **A.** Plant lipid model with PLPC in green, GluCer in blue and sito in orange (60:20:20, molar ratio). **B.** The same lipids after addition of d18:0 in pink (88% lipids, 12% d18:0). **C.** bacterial lipid model with POPE in yellow, POPG in black and CL in red (65:23:12, molar ratio). **D.** The same lipids after addition of d18:0 in pink (88% lipides, 12% d18:0).

Bacterial membrane lipids are one of the target of choice for antimicrobial agents (Epand and Epand, 2011), and many of them are of amphiphilic nature (Jung *et al.*, 1999; Verhaegh *et al.*, 2020). Furthermore, some amphiphilic plant defence elicitors are able to interact with the plant PM (Furlan *et al.*, 2020; Cordelier *et al.*, 2021). This led us to investigate the capacity of d18:0 to permeabilize artificial plant and bacterial model membranes (**Figure 36.**). To that end, liposomes in which the fluorescent probe calcein had been previously encapsulated were used. Our results showed that d18:0 is able to induce an increase in the permeability of bacterial liposomes, up to 60% for a concentration of 13 μM (**Figure 36A.**). For plant liposomes, we first observed a liposome permeabilization (~10% at 1,3 μM) then a slight negative permeability for concentrations ranging from 5 to 15μM (**Figure 36 A. and B.**). There is no increased leakage observed at the estimated CAC (between 2 and 10 μM). In this experiment, when d18:0 is concentrated at 15 μM, the ratio is already 1, which is not very representative of the biological reality and such results are therefore to be taken with caution.
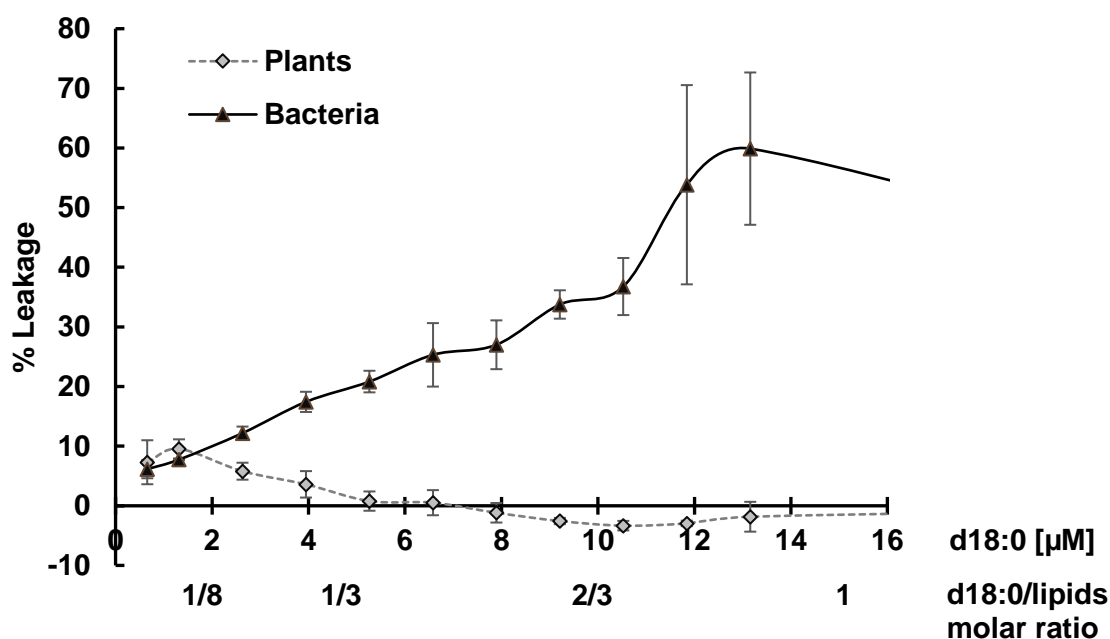
Figure 36. Leakage properties of d18:0 on liposomes mimicking plant or bacterial plasma membrane

Mean relative calcein leakage plant PM-like liposomes composed of PLPC, sito and GluCer (60:20:20, molar ratio), or bacteria PM-like liposomes composed of POPE, POPG, and CL (65:23:12, molar ratio) induced by a range of sphinganine concentrations. Experiments were repeated 3 times.

Finally, the effect of d18:0 on membrane order was measured by evaluating the fluidity of the bilayer with Laurdan (**Figure 37.**). The shift in the maximum emission wavelength of this solvatochromic probe can be attributed to membrane fluidity. A more ordered lipid environment causes a blue shift in the maximum Laurdan emission wavelength while in the presence of more fluid lipid environments, a red shift in the maximum Laurdan emission is observed. Such modifications can be quantified by calculating the Laurdan GP, where the greater the GP values, the higher the order of the membranes (Deleu *et al.*, 2014; Carreira *et al.*, 2021). On both plant and bacterial liposomes, our findings revealed that d18:0 addition at very high concentrations (80 µM) increased the GP value, translating to an increased membrane order. One could link this increase to the state of d18:0 in solution since this concentration is above its CAC, but another factor is to be considered. Indeed, at this concentration, the ratio d18:0/lipids reached 8/5 and d18:0 which could temper with the results (**Figure 37A. and B.**). At lower concentration, there is no change in the GP value, even at the supposed CAC of d18:0 (2 or 10 µM), which suggests d18:0 does not have an impact on membrane fluidity of both plant PM-like and bacterial PM-like liposomes.
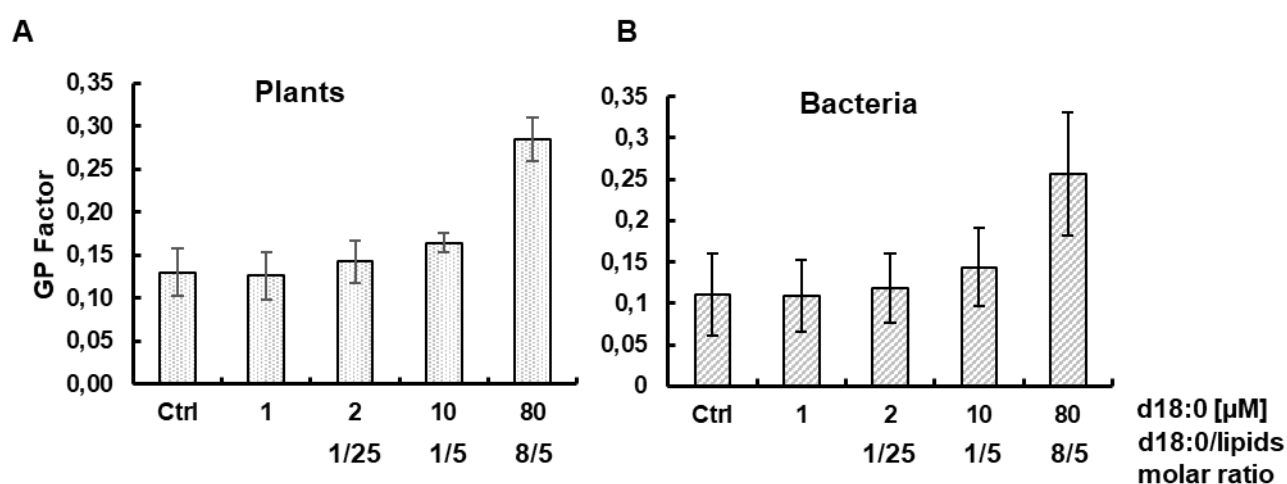
Figure 37. Effect of d18:0 on the order and fluidity of the bilayer

Laurdan generalized polarization (GP) on **A.** plant PM-like liposomes composed of plant lipids: PLPC, sito and GluCer (60:20:20, molar ratio), or **B.** bacteria PM-like liposomes composed of: POPE, POPG, and CL (65:23:12, molar ratio). The temperature was fixed at 20°C. The GP of the control is measured with ethanol (0,1%).

IV. Discussion

Discrepancies can be found in the literature as to whether or not LCBs can cause cell death, and if so, at which concentrations. For instance, low concentrations of d18:0 and t18:0 (between 0.5 and 2 µM) could induce ROI production and cell death in *Arabidopsis* leaves (Shi *et al.*, 2007). Interestingly, 5 µM of d18:0 on *Arabidopsis* seedlings could induce cell death while the same concentration of t18:0 could not (Saucedo-García *et al.*, 2011). However, high concentrations of d18:0, d18:1 and t18:0 (20 µM) had no effect on the viability of BY-2 cells (Coursol *et al.*, 2015) and similarly, infiltration on *Arabidopsis* leaves of d18:0 at 100 µM did not lead to cell death (Magnin-Robert *et al.*, 2015a). Our results, presented in Chapter 1., also show that infiltration of d18:0 at concentrations between 1 to 100 µM did not cause cell death. Some studies also reported their bactericidal effects: d18:1 (1-10 µM) was reported to have such effect on *P. aeruginosa* and t18:0 (25 to 50 µM) on *Pst* (Glenz *et al.*, 2022). Our results, presented in Chapter 2, show however no clear antibacterial effect of d18:0 at 100 µM on *Pst*, both *in vivo* and *in vitro*. Considering the amphiphilic nature of LCBs and their capacities to form aggregates, one could think that these differences could be ascribed to the aggregation state of the LCBs in solution and that their CAC can differ with the experimental setup (i.e., buffer, pH, biological model).

Multiple CAC have been reported for d18:1 in the literature, ranging from 18 µM (Contreras *et al.*, 2006) to 112 µM (Deguchi *et al.*, 2004). These CAC have been previously estimated through fluorescence measurements, which involves the partitioning of fluorophores into micelles. These types of techniques possess however a few limitations including the assumptions that the fluorophore and the molecule mix ideally and that the fluorophore does not perturbate the CAC itself (Sasaki *et al.*, 2009). Furthermore, it has been highlighted that the aggregation behaviour of d18:1 was pH dependent. Its CAC was estimated at 0,99 ±0,12 µM at physiological pH and could range from 0,70 ±0,02 µM to 1,71 ±0,24 µM when deprotonated and protonated, respectively (Sasaki *et al.*, 2009). These data are somewhat closer to our findings for d18:0. Indeed, our experiments with DLS estimated a CAC between 2 and 10 µM while the ones with tensiometry placed it around 2 µM. It is however noteworthy that DLS measurements with low d18:0 concentrations were quite difficult, as correlated by the low R^2 (R^2= 0.51) and must therefore be taken with caution. Cryogenic transmission electron microscopy has previously been used to image structure formed by amphiphile molecule in aqueous environments (Almgren *et al.*, 1996; Almgren *et al.*, 2000) and could help here to determine the aggregation state (aggregated structure) of d18:0 in solution at different concentrations.

The final localization of d18:0 when exogenously applied to *Arabidopsis* by infiltration is so far still unknown. Glenz *et al.*, (2019) suggested that t18:0 crossed the PM by passive diffusion. This

phenomenon is propelled by the solute concentration and electric gradient and does not require energy. In its most basic form, passive diffusion is a three-step process in which the permeant partitions into the membrane, diffuses across it, and is released into the cytosol (Yang and Hinner, 2015). This hypothesis was tested using *in vitro* tests in which t18:0 partitioning between an aqueous and organic phase was quantified using HPLC-MS/MS and showed t18:0 was more present in the aqueous medium. Other studies have proven that ceramides can induce a generalized flip-flop motion in model and cell membranes (Goñi and Alonso, 2006). Here, the data obtained by the Impala simulation suggested the flip-flop potential of d18:0 between the two bilayer leaflets, which means that on top of perturbating the PM, exogenous d18:0 could also be added to the intracellular LCB pool and modify the SL metabolism.

Monolayer adsorption experiments showed that d18:0 could interact with bacterial model lipids without highlighting a preferential attraction from any of the lipids tested. Hypermatrix simulations however, hinted a preferential interaction of d18:0 with CL. This was already reported to explain the bactericidal effect of d18:1 on *P. aeruginosa*, where the NH_2 group of the LCB is thought to bind to the highly negatively charged CL in bacterial membranes (Verhaegh *et al.*, 2020). They notably showed that the binding of d18:1 led to the permeabilization of the PM, and we did observe a similar pattern for low concentrations of d18:0. Indeed, here the permeabilization was maximal when d18:0 reached 13 µM. This concentration is not only higher than the estimated CAC but also corresponds to a ratio d18:0/lipid of almost 1, which is really elevated. It is also noteworthy that concentration below and above the estimated CAC did not impact the fluidity of bacterial PM-like liposomes, meaning that even though d18:0 permeabilized the liposomes and modified the lipid organization, according to the Big Monolayer data, this did not affect the global order of the PM.

Concerning plant model lipids, unlike what is usually found for detergents (Helenius and Simons, 1975), no increase in calcein efflux was observed at the assumed CAC. A drop of the leakage percentage can be observed for values above 1,5 µM, even reaching low negative values for concentrations above 7 µM. It could be assumed that this phenomenon is due to d18:0, forming aggregates above its CAC and re-encapsulating leaked calcein from the plant PM-like liposomes. However, this does not seem to apply to bacterial PM-like liposomes. Contreras *et al.*, 2006 reported that d18:1 could permeabilize liposomes and erythrocytes ghost membranes due to its capacity to stabilize gel domains in membranes. According to them, it is "structural defects" between the "more rigid" and "less rigid" part of the membrane that likely are the sites of leakage. It could therefore also be assumed that d18:0 could create such structural defect within the plant PM-like liposomes which would lead to a slight leaking of calcein. This could be correlated by the

simulations we performed on Big Monolayer. Indeed, while the data obtained by tensiometry and Hypermatrix showed that d18:0 could interact with plant PM lipids without showing a preference for any of the lipids tested, the Big Monolayer simulation showed d18:0 could interact more specifically with its microdomain (composed of sterol and SL), notably by disorganizing and fractioning them. This interaction could eventually perturbate defence related proteins located within these domains. Indeed, following the CW, the PM is the first point of contact between plant cells and pathogens and many proteins involved in plant defence are embedded in it. Furthermore, the dynamic between membrane microdomains, and the stress-related proteins they harbour appears crucial for immunity (Gronnier *et al.*, 2016; Nagano *et al.*, 2016; Gronnier *et al.*, 2018; Mamode Cassim *et al.*, 2019; Huby *et al.*, 2020). Among these proteins, RbohD, involved in ROS production, has previously been localized to microdomains in tobacco (Lherminier *et al.*, 2009). It could therefore be hypothesized that d18:0, by interacting with these microdomains, would perturbate the activity of RbohD which explain the absence of extracellular ROS production we observed in response to *Pst* (see **Chapter 2.**).

   Overall, our results showed that d18:0 can interact with lipids of the plant PM. Other amphiphilic-lipid-based molecules are also thought to be recognized by the plant PM's lipid fraction, such as rhamnolipids or surfactins, iturins, and fengycins, which are cyclic lipopeptides generated by *Bacillus subtilis* and are known to activate plant defences and interact with membrane lipids (Deleu *et al.*, 2008; Nasir *et al.*, 2010; Vatsa *et al.*, 2010; Henry *et al.*, 2011; Deleu *et al.*, 2013). Further linking biophysical data, obtained from biomimetic membranes, with biological ones, obtained from living plant cells or tissues harbouring complex dynamic PM and CW, appears to be of major interest to the scientific community. To that end, plant protoplasts have emerged as a potential medium to experiment with. Indeed, plant protoplasts are cells devoid of CW and as such, offer an interesting point of view on the PM (see the review - Protoplasts: a valuable toolbox to investigate plant stress perception and response - in the **Annex**). This aspect will be further developed in the Chapter "General Discussion – Perspectives"

Chapter 4 - Main Results

- ✓ Depending on its concentration d18:0 exists in various forms in solution
- ✓ Its activity might vary based on its state in solution
- ✓ d18:0 can interact with both plant and bacterial representative PM lipids
- ✓ d18:0 could act by disorganizing and fractioning membrane microdomains which could eventually perturbate defence related proteins located within these domains, including RbohD, involved in extracellular ROS production.

General Discussion, Conclusions & Perspectives

I. Thesis Overview

As sessile organisms, plants are exposed to myriads of potential stresses that can be harmful to their development. These adverse environmental conditions include both biotic and abiotic stresses that increasingly threaten agricultural plant productivity at a worldwide scale. In response, plants have developed an array of mechanisms to survive tough environmental conditions such as drought, heat, cold, nutrient deficiency, pollutants, pathogens, and herbivore attacks.

Among the different actors of the plant immune system, SLs have fundamental functions. They form a significant proportion of the lipids present in higher plants. Studies suggest they constitute up to 40% of lipids in the PM of plant cells (Cacas *et al.*, 2016). More comprehensive extraction techniques have been developed over recent years that, when coupled with technological advances in mass spectrometry and chromatography, have allowed improved SL identification and the discovery of novel structures from smaller quantities of material (Cacas *et al.*, 2016). This has enabled researchers to determine the contribution of SL metabolites in different cellular processes. Among them, the existence of a rheostat between ceramides/LCBs and their phosphorylated counterparts, already described in animal cells, is thought to exist in plants to control cell fate. According to this model, ceramides and LCBs are able to trigger cell death, whereas ceramide phosphates and LCB-Ps promote cell survival (Shi *et al.*, 2007; Alden *et al.*, 2011; Huby *et al.*, 2020). Plant LCBs are therefore increasingly studied (Shi *et al.*, 2007; Chen *et al.*, 2008; Saucedo-Garcia *et al.*, 2015; Glenz *et al.*, 2019; Glenz *et al.*, 2022).

Previous research in our lab showed that co-infiltration of *Pst AvrRpm1* with the LCB d18:0 on *Arabidopsis* leaves resulted in an unusual phenotype. Indeed, instead of developing an HR on the infiltrated leaves, they showed no evidence of cell death, indicating that the plant PM was still intact and that there was no cell lysis (Magnin-Robert *et al.*, 2015a).

This thesis aimed to characterize the role of d18:0 in the interaction between bacteria and plants, and more specifically in the *Pst* DC3000 - *Arabidopsis* pathosystem. This work required the use of a wide range of complementary techniques, mixing both biological and biophysical studies, therefore giving an original overview on this interaction.

Some key factors in the absence of HR observed when *Pst AvrRpm1* is co-infiltrated with d18:0 were put forward (**Figure 36.**). First, the method of choice for bacterial inoculation appeared to be co-infiltration. Then, the specificity of LCBs (d18:0, d18:1 and t18:0) in this phenomenon was also reported, along with their range of concentration for optimum results (10 - 100 µM). Other effectors producing similar results as the ones described with effector AvrRpm1 were put forward, namely AvrB and AvrPphB. The impact of d18:0 directly on *Pst* was also explored. More specifically, it was demonstrated that d18:0 had no impact on the morphology, motility, mannitol fermentation capacities and EPS production of *Pst* DC3000 and *Pst AvrRpm1*. *In vitro* tests

showed that the LCB did not have an antibacterial effect on *Pst AvrRpm1*, *Pst AvrB* and *Pst AvrPphB*. It was also showed that d18:0 co-infiltration with multiple bacteria, including ones triggering symptoms, reduced extracellular ROS production by *Arabidopsis*. The investigation of the plant defence mechanisms in response to co-infiltration of *Pst AvrRpm1* with d18:0 has notably shown that RIN4 and RPM1 were probably not directly involved in the absence of HR. This co-infiltration also negatively impacted camalexin production, SA levels and SA related gene expression. It remains however unclear whether those phenomena are the causes or the consequences of the absence of HR. Finally, the co-infiltration of d18:0 with *Pst AvrRpm1* down-regulated the expression of *NMT1*. In *Arabidopsis*, the NMT is responsible for the N-myristoylation of effectors AvrRpm1, AvrB and AvrPphB which relocates them at the PM where they can be actives, this down-regulation could therefore mean that the enzymatic activity of NMT is also perturbated by d18:0 addition, therefore altering the virulence of bacteria carrying these effectors.

Such activity of d18:0 would suppose that the molecule can interact with the plant cell. Considering the amphiphilic nature of d18:0 it was hypothesized that it could be recognized by the lipid fraction of the PM, as already suggested for other molecules such as fatty acid hydroperoxides, rhamnolipids, surfactins, iturins, and fengycins that interact with lipids of plant PMs (Deleu *et al.*, 2008; Nasir *et al.*, 2010; Vatsa *et al.*, 2010; Henry *et al.*, 2011; Deleu *et al.*, 2013; Deboever *et al.*, 2022). Biophysical studies have shown that d18:0 was attracted by and could interact with biomimetic PMs of both plants and bacteria. These findings were subsequently supported by *in silico* analyses that notably showed d18:0 could perturbate the lateral organization of these mimetic membranes and more specifically of its microdomain. While it was suggested that exogenous LCB could cross the PM by passive diffusion (Glenz *et al.*, 2019), our results suggested d18:0 actually possessed a flip-flop potential meaning that exogenous addition of d18:0 could perturbate the PM and/or this d18:0 could be added to the intracellular LCB pool and/or modify the plant SL metabolism. As previously stated, this interaction could eventually perturbate defence related proteins located within these domains (Gronnier *et al.*, 2016; Nagano *et al.*, 2016; Gronnier *et al.*, 2018; Mamode Cassim *et al.*, 2019; Huby *et al.*, 2020). Indeed, RbohD, involved in ROS production, has previously been localized to microdomains in tobacco (Lherminier *et al.*, 2009). It was therefore hypothesized that d18:0, by interacting with these microdomains, could perturbate the activity of RbohD, which could possibly explain the absence of extracellular ROS production we observed in response to *Pst*.
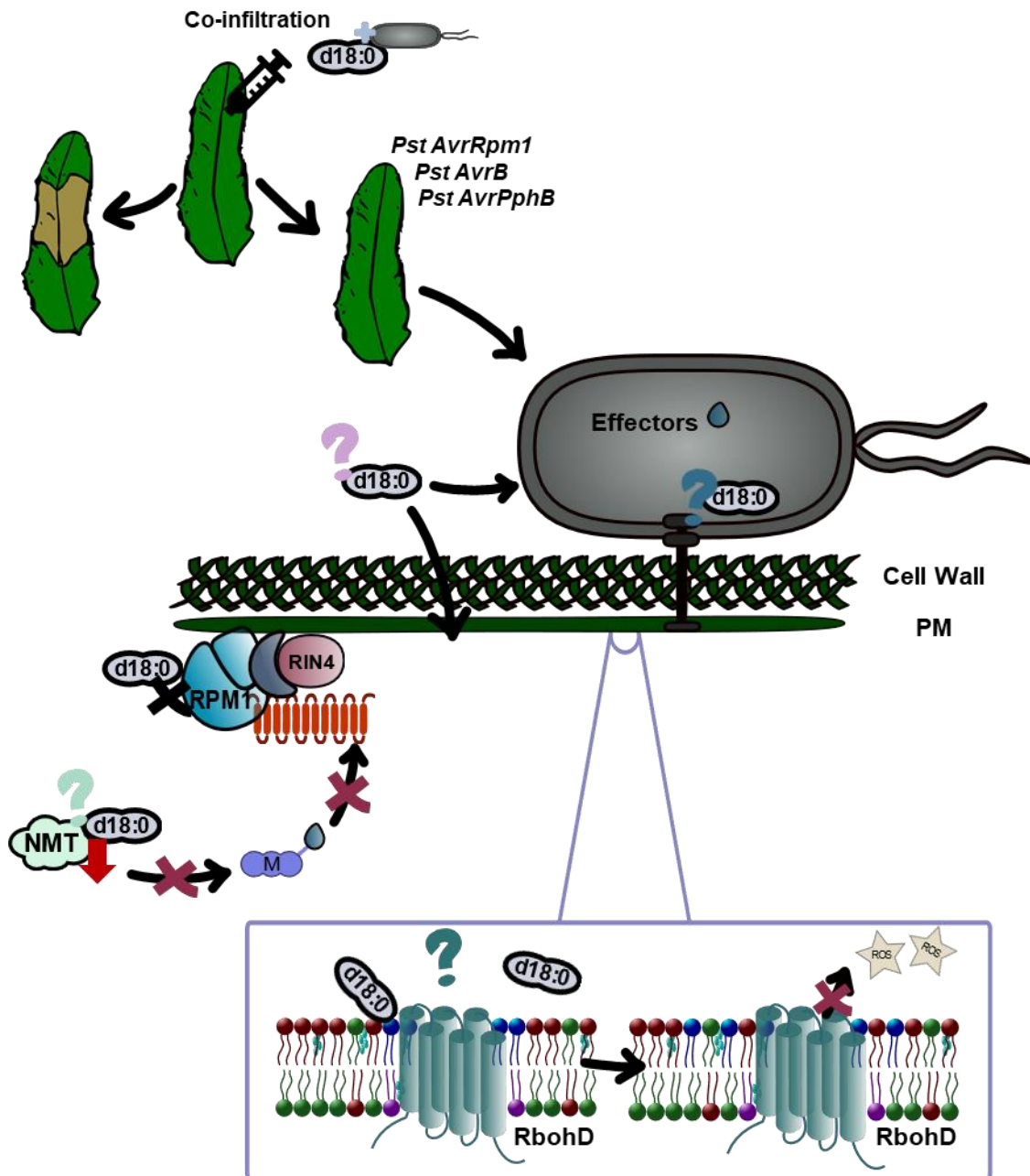
Figure 38. Working hypothesis: effects of d18:0 when co-infiltrated with
Pst

The co-infiltration of d18:0 with *Pst AvrRpm1*, *Pst AvrB* or *Pst AvrPphB* does not induce an HR on treated *Arabidopsis* leaves. It is unclear whether d18:0 could have an effect by directly targeting the bacteria or its T3SS. It is however clear that it has no effect on the RPM1/RIN4 complex in *Arabidopsis*. Preliminary data suggests that d18:0 down-regulated the *NMT1* gene and therefore might impact the activity of NMT. This could stop or reduce the addition of myristate (M) to the effectors AvrRpm1, AvrB and AvrPphB in the cytoplasm, blocking their relocalisation to the PM and therefore preventing their perception by *Arabidospis*. Whether d18:0 can interact with PM or relocate within plant or bacterial cells remains to be determined. Biophysical studies have however shown d18:0 can interact with lipids of both plant and bacterial PM. More specifically, it was supposed that it could disorganise plant PM microdomains. It remains to be determined whether d18:0, through this interaction, could disturb the activity of membrane proteins such as RbohD, partly responsible for extracellular ROS production.

This study has shed light on the absence of HR and provided some leads to explain it, it has also raised questions that could be worth investigating (**Figure 38.**). Indeed, while biophysical studies have brought some insight on the mode of action of d18:0, further linking these data obtained with biomimetic PM with biological ones could bring even more explanation on the absence of HR. In this direction, protoplasts could be at the crossroads of biophysical and biological studies as they retain the complexity of living cells while being less complex that whole tissues or plants.

II. How much further can we go to elucidate the absence of HR?

1. Plant protoplasts as an innovative tool to connect the biophysical and biological effect of d18:0 on PMs?

(Partially adapted from Protoplasts: a valuable toolbox to investigate plant stress perception and response, Gilliard *et al*., 2021)

Single cell approaches, including live-cell imaging methods, have advanced rapidly in recent years. Single-cell systems are a simplified model for studying the function of mechanical forces *in vivo*, removing the added complexity of the tissue context (e.g., chemical signals, impact of neighbouring cells, complex mechanical stress patterns) (Colin *et al*., 2022).

There are many ways to study elicitor perception and stress signals in plant, and among them, protoplasts appear to provide a unique experimental system (see the review - Protoplasts: a valuable toolbox to investigate plant stress perception and response - in the **Annex**.). As plant cells devoid of CW, protoplasts allow observations at the individual cell level. They also offer a prime access to the PM and an original view on the inside of the cell. In this regard, protoplasts could be valuable plant PM models to study the perception of bioactive molecules such as d18:0 by plant cells that are supposed to directly interact with the PM. Indeed, as previously mentioned, they could link data obtained by biophysics studies on biomimetic PM models containing representative lipids with the ones provided by biological assays on living plant cells or tissues with complex dynamic PM and CW (Gilliard *et al*., 2021).

During this thesis, a number of effects of d18:0 on plant and bacterial biomimetic PM were determined, but many parameters remain to be determined on plant protoplasts. Several experiments using *Arabidopsis* protoplasts were therefore engaged. The viability of these protoplasts when in contact with d18:0 was first determined in order to assert which concentration of the molecule would best suit our experiments (**Supplemental Information** &

Supplemental Figure S3.). These results are obtained after a 15 min incubation period that has now been reduced to minimize d18:0-related cell death.

Some tests were carried out but were unfortunately unsuccessful and would require deep equipment and protocol adaptations to potentially work. For instance, Laurdan was added to protoplasts and fluorescence measurements were conducted with a spectrofluorometer to study the impact of d18:0 on PM fluidity. However, protoplasts were too dense and not staying in suspension long enough for proper measurement. Even though the machine offered a setting for light vortexing, which could have kept the protoplasts in suspension, it would often result in membrane breakage and protoplast death which would highly temper with the results.

Two other approaches have been undertaken with protoplasts. The first involved AFM measurements to examine whether d18:0 is capable of deforming membranes and thus to assess its effect on the mechanical properties of the membrane (e.g., Young's modulus, viscoelastic properties) (Alessandrini and Facci, 2005). Many studies are available on model membranes (Morandat *et al.*, 2013), animal cells (Francis *et al.*, 2010), live thylakoids (Clausen *et al.*, 2014), dead plant protoplasts (Yang *et al.*, 2015) and more recently on live plant cell wall (Pu *et al.*, 2021). To the best of our knowledge, there is no mention in the literature of AFM conducted on living protoplasts which renders this work all the more interesting. The second approach was confocal microscopy of living protoplasts with the fluorescent dye Laurdan, previously used in this thesis to assess membrane fluidity by spectrophotometer. Indeed, the absence of CW makes possible the accurate visualisation of events at the protoplast PM using fluorescent probes. Such experiments have already been implemented in living protoplasts (Blachutzik *et al.*, 2012) but were only recently developed in our laboratory.

On top of Laurdan, other fluorescent probes could be used on protoplast and monitored with confocal microscopy to further determine the effect of d18:0 on plant PMs. However, while a lot of probes exist to study lipid organisation and dynamics into artificial model membranes which are deprived of proteins, they often cannot be directly applied to living cell and protoplast PMs which are far more complex and require deep protocol adaptations in terms of concentration and incubation time (Klymchenko and Kreder, 2014). Every probe will have its specificities and are used by themselves or combined. For instance, FM4-64 ((N-(3-Triethylammoniumpropyl)-4-(6-(4-(Diethylamino) Phenyl) Hexatrienyl) Pyridinium Dibromide) and LRB-PE (Lissamine Rhodamine B-Phosphoethanolamine) have been employed to specifically stain phospholipid enriched areas of protoplast PM and BD-SM (Bodipy Sphingomyelin FL C$_{12}$) has been used to stain sphingolipid enriched domains (Blachutzik *et al.*, 2012). FM4-64 and BD-SM were also used in combination with FRAP (Fluorescence Recovery After Photobleaching) experiments to visualise lipid redistribution. Similarly to Laurdan, the solvatochromic dye di-4-ANEPPDHQ can

distinguish the ordered from the disordered domains of the PM by a change of its fluorescence colour (Blachutzik *et al.*, 2012; Klymchenko, 2017). Di-4-ANEPPDHQ has notably been used on protoplasts from rice transgenic plants that lack FAH1/2, enzymes responsible for the formation of 2-hydroxy sphingolipids (2-OH-SL), precursors of GIPC, that are both located at the PM in *Arabidopsis*. They notably demonstrated that a disordered PM was concomitant with a lower amount of 2-OH-SL and less abundant microdomains which gave rise to an increased sensibility to rice blast fungus infection (Nagano *et al.*, 2016). The probes Rhod-PE (Lissamine rhodamine B sulfonyl) and NBD- PE (N-(7-Nitrobenz-2-Oxa-1,3-Diazol-4-yl)-1,2-Dihexadecanoyl-sn-Glycero-3-Phosphoethanolamine) can also mark the disordered and ordered phases of the PM, respectively (Verstraeten *et al.*, 2019). Finally, advanced solvatochromic probes based on DMA-3HF and Nile Red can simultaneously stain the outer leaflet of PMs while reporting its lipid order (Niko and Klymchenko, 2021).

Tracking the fate of the exogenous d18:0 within the cell could also provide valuable information and help determine if d18:0 actually penetrates the cell and incorporates its pre-existing SL pool. A commercially available fluorescent d18:0 (nitrobenzoxadiazole-sphinganine) could be used although this probe is usually dissolved in chloroform, a solvent with which protoplasts do not cope well. Deuterated probes could also be considered as they distinguish between endogenous and exogenous SLs using mass spectrometry (Murai *et al.*, 2022).

There are still a few challenges for live plant cell imaging. Indeed, while there are many advantages to use fluorescent probes directly on protoplasts, its PM remains an active, dynamic structure, which can cause issues. It has been reported that some probes could be internalized in the cytoplasm, such as DiIC12 (1,1'-Didodecyl-3,3,3',3'-Tetramethylindocarbocyanine Perchlorate) and DiIC18 (1,1'-Dioctadecyl-3,3,3',3'-Tetramethylindodicarbocyanine-5,5'-Disulfonic Acid) , which stains phospholipids, leading to a decrease of fluorescence in the PM (Blachutzik *et al.*, 2012).

Finally, using protoplasts, or even whole plants to follow effector (AvrRpm1, AvrB or AvrPphB) secretion from *Ps*t to the cytoplasm of *Arabidopsis* could be envisaged to determine if they actually are delivered in the cell and if they are redirected to the PM. Despite the importance of bacterial effectors and their delivery by the T3SS in host-microbe interaction, direct effector secretion has only recently been achieved. Fluorescent protein-based approach to monitor this secretion directly from bacteria to host cells appears impossible because the size of fluorescent proteins would prevent effector delivery through the T3SS (Park *et al.*, 2017). Spatiotemporal monitoring of effectors was however possible using effectors fused to the 11th β-strand of super folder GFP and plant cells expressing 1-10 β strand of super-folder GFP. When delivered into plant cells,

interaction of both GFP proteins reconstituted its fluorescence (Henry *et al.*, 2017; Park *et al.*, 2017).

2. Is the NMT really involved in the absence of HR and how to determine it?

In the present study, we began investigating the implication of the NMT in the absence of HR when d18:0 is co-infiltrated with *Pst AvrRpm1*. No data concerning the activity of *NMT2* is available in the literature, and this enzyme appears to only accumulates in only small amounts (Pierre *et al.*, 2007) which makes it challenging to study. Our data showed that co-infiltration of d18:0 and *Pst AvrRpm1* had a significant impact on the expression levels of *NMT1*. The fact that effectors AvrB and AvrPphB also possess a N-myristoylation sequence and that their co-infiltration does not trigger a HR in *Arabidopsis* strongly suggests that investigating this lead could provide significant breakthrough in this research.

Several approaches could be considered to see if LCB could interrupt this myristoylation process. First, testing other bacterial effectors that possess the specific myristoylation sequence could be interesting, such as AvrC, AvrPto (Nimchuk *et al.*, 2000), or HopF2, which causes an avirulent reaction in tobacco (Robert-Seilaniantz *et al.*, 2006). A mutant approach could also be considered but *NMT1* was found to be essential throughout organ development, at both early and later stages so *NMT1*-null mutants are excluded, inducible *NMT1* mutants could therefore be considered. *NMT2* was found to be essential only for the transition to flowering but is supposedly not the main responsible for N-myristoylation (Pierre *et al.*, 2007).

It is relatively difficult to detect the addition of a fatty acid to a protein. A method, however, employs a new, rapid, and efficient technique for detecting myristoylation of a protein *in planta*, which could potentially be applied to the current study. This method, described by Boyle *et al.* (2016), uses a plant cell, typically a protoplast, that has been transformed to express an epitope-tagged metabolite of interest which is expected to undergo myristoylation *in planta*. The cells are then treated with a myristate analogue, and the metabolite is extracted using affinity chromatography. A "click" chemistry step follows, which involves a biocompatible reaction between the myristate analogue and a reporter. Electrophoresis is then used to detect metabolites that have been myristoylated and thus carry the reporter (Boyle *et al.*, 2016).

The mechanisms by which d18:0 exogenous application could perturbate the myristoylation process is so far still unknown. Particularly since, in plants, it would seem the myristoylation process is independent of the SL metabolism. However, it can be noted that in humans, part of the

cardiac pool of SLs, d16:0, is synthesised from myristoyl-CoA instead of palmitoyl-CoA (Russo *et al.*, 2013).

3. How much is the SL metabolism implicated in the absence of HR and could exogen application of d18:0 disrupt it?

LCB accumulation has been previously linked to cell death (Berkey *et al.*, 2012; Yanagawa *et al.*, 2017; Zienkiewicz *et al.*, 2020). Glenz *et al.* (2022) hypothesised that LCB treatment could induce cell death by blocking SL biosynthesis, leading to increased cellular levels of LCB. Here, LCB treatment did not lead to cell death, but it is still possible that it had an effect on the SL metabolism. Indeed, other studies suggested exogenously added LCBs could cross the PM by passive diffusion (Glenz *et al.*, 2019). Our results showed d18:0 could interact with plant biomimetic PMs, possibly rearrange them before crossing them. This could suggest that once infiltrated in leaves, d18:0 might end up in *Arabidopsis* cytoplasm and therefore join its free LCB pool. It would therefore be interesting to determine if d18:0 infiltration, with or without *Pst*, could have affected free LCB levels in *Arabidopsis* leaves. Other SLs, such as ceramides, are also suspected to play a role in cell death induction (Huby *et al.*, 2020; Zienkiewicz *et al.*, 2020), it could therefore be interesting to quantify them as well.

Many studies have used mutants of the SL pathway to study their implication in plant defence mechanisms (Shi *et al.*, 2007; Nagano *et al.*, 2012; König *et al.*, 2012; Nagano *et al.*, 2016; Li *et al.*, 2016; König *et al.*, 2021). *loh* and *fah* mutants are most commonly used since deregulation of SL synthesis in other part of the pathway often leads to SA-related cell death (Wang *et al.*, 2008; Li *et al.*, 2016; Yanagawa *et al.*, 2017; Zienkiewicz *et al.*, 2020) and this mutations often leads to modifications of the plant PM. Indeed, in *Arabidopsis* the double mutant *fah1fah2* appeared to have modified nanodomain organization, leading to a decreased expression level of several defence related proteins including RbohD (Ukawa *et al.*, 2022). Di-4-ANEPPDHQ has been used in these mutants, to show a lower order of the PM compared to the WT, suggesting an altered PM organization when its content in GIPC is low (Lenarčič *et al.*, 2017). Here, they could be employed to determine if d18:0 co-infiltration with *Pst* DC3000 in PM-altered and sphingolipidome-altered plants would still not induce an HR.

Alternatively, chemical inhibitors (**Table III.**), such as FB1 (Tsegaye *et al.*, 2007; Luttgeharm *et al.*, 2016; Yanagawa *et al.*, 2017), could be used to strategically modify *in vivo* the plant lipid pool (Mamode Cassim *et al.*, 2019).

Table III. Examples of inhibitors used to modify *in vivo* the pools of lipids and some recent related references (from Mamode-Cassim *et al*. 2019).

The used concentration of the inhibitors is indicative and must be tested for each plant species or tissues. To address the modification of the PM lipid pool, a phase partition to purify PM vesicles must be conducted coupled with a dedicated lipidomic approach. PLD, Phospholipase D; PLC, Phospholipase C, DAG, Diacylglycerol; VLCFAs, Very Long Chain Fatty Acids; HMG-CoA reductase, 3-hydroxy-3-methyl-glutaryl-coenzyme A reductase.

	Inhibitors of:	Name	References
Phosphoinositides	PI3-Kinase (50–100 µM)	LY-294002	[398]
	PI3P 5-Kinase (1 µM)	YM-201636	[399]
	PI4-Kinase (30–60 µM)	Phenylarsine oxide (PAO)	[117,398]
	PI3-Kinase (1 µM)	Wortmannin	[283,31]
	PI3-Kinase + PI4-Kinase (30 µM)	Wortmannin	
Sphingolipids	Ceramide synthase (1 µM)	Fumonisin B1 (1 mg)	[400,401]
	Glucosylceramide synthase (50 µM)	DL-THREO-PDMP	[402]
	VLCFAs/sphingolipid (50–100 nM)	Metazachlor	[235]
	Serine palmitoyltransferase (SPT)	Myriocin	[56,403]
	Inositol phosphorylceramide synthase (fungi)	Aureobasidin A	[404]
Diacylglycerol/phosphatidic acid	Lyso PA Acyl transferase	CI-976	[405–407]
	PLD-derived PA formation (50 µM)	(R)-(+)-Propanolol hydrochloride	[408]
	PLD-derived PA formation (0.2–0.4%)	1- butanol	[409,410]
	PLC-derived DAG formation (5 µM)	U73122 (active analog)	[31,411]
	PLC-derived DAG formation (5 µM)	U73343 (inactive analog)	[411]
	PLC-derived DAG formation (50 µM)	Edelfosine	[283]
	DAG-Kinase (50 µM)	R59022	[283]
Sterols	Cyclopropylsterol isomerase 1, CPI1	Fenpropimorph	[7,175,162]
	HMG-CoA reductase	Lovastatin	[7]

4. Other aspects worth considering

The targeting of effectors to specific targets within plant cells, particularly the internal face of the host PM, is critical for their virulence function. But *Pst* DC3000, even transformed to express *AvrRpm1*, still produces no less than 29 other effectors along with toxins such as coronatine (Cunnac *et al*., 2011). Therefore, elucidating the specific role of each effector independently, in the same genetic background appeared important, especially since all tested strains were provided by different laboratories and constructed differently. Based on advice and strains given by Dr. Laurent Deslandes (CNRS-INRA - Laboratoire des interactions plantes-microbes-environnement), we used *P. fluorescens* strain *Pfo-1* possessing a stably integrated T3SS-encoding region to perform bacterial transformations. This strain is devoid of any endogenous type-III effector genes and lacks most, if not all, necessary virulence factors required for *in planta* growth. Thus, any observed phenotypes can be attributed to the delivered type-III effector protein of interest (Thomas *et al*., 2009). Co-infiltrations were carried out with *Pfo-1* transformed to express *AvrRpm1* and yielded the same results as the ones obtained with *Pst AvrRpm1*, as no HR was observable on leaves (data not shown). It would be interesting to test *Pfo-1* expressing effectors *AvrB*, *AvrPphB* and *AvrRpt2* (that would be used as positive control for HR).

Finally, the mitogen-activated protein kinase MPK6 and the calcium-dependent protein kinase the calcium-dependent protein kinase CPK3 have also been identified as possible signalling components of LCB-mediated programmed cell death in plants (Lachaud *et al.*, 2013; Saucedo-García *et al.*, 2011). Furthermore, considering the mutual interplay between calcium and ROS signalling in plant immune response (Marcec *et al.*, 2019), the study of calcium fluxes could be considered. Measurement of calcium after infiltration of d18:0 with or without *Pst* could be performed using aequorin technology based on bioluminescence (Mithöfer and Mazars, 2002; Jeworutzki *et al.*, 2010; Coursol *et al.*, 2015).

III. Concluding remarks

Throughout this thesis, we have addressed various aspects of the effect of d18:0 on both *Pst* and *Arabidopsis.* Our research ranged from investigating its bactericidal and its effect on plant defences to determining how it can interact with plants and bacteria through their PM. This has allowed to narrow down the possible explanations for the absence of HR when d18:0 is co-infiltrated with *Pst AvrRpm1*. It notably paved the way for future experimentations on the role of NMT in this phenomenon and the impact d18:0 can have on membranes, and more specifically on microdomains, organisation and function, including the protein it harbours.

Supplemental Data

Supplemental Table S1. Strains of *P. syringae* (Hwang *et al.*, 2005)

Pathovar	Designation	Strain name	Place of isolation[b]	Yr of isolation	Host	Source[a]	Accession no.
aceris	ATCC10853	Pac A10853			Maple	J. Dangl	ATCC 10853
actinidiae	FTRS_L1	Pan FTRS_L1	Japan	1984	Kiwi	MAFF	MAFF302091
aesculi	0893_23	Pae 0893_23	US		Horse chestnut	D. Cooksey	
apii	1089_5	Pap 1089_5	US		Celery	D. Cooksey	
aptata	601	Ptt 601		1966	Sugar beet	MAFF	MAFF301008
aptata	DSM50252	Ptt DSM5022			Wheat	J. Dangl	
aptata	G733	Ptt G733		1976	Brown rice	MAFF	MAFF302831
atrofaciens	DSM50255	Paf DSM5025			Wheat	J. Dangl	
broussonetiae	KOZ8101	Pbr KOZ8101	Japan	1980	Paper mulberry	MAFF	MAFF810036
cilantro	0788_9	Pci 0788_9	US		Cilantro	D. Cooksey	
coronafaciens	3113	Pcn 3113	UK	1958	Oats	D. Arnold	ICMP3113
coronafaciens	KN221	Pcn KN221		1984	Oats	MAFF	MAFF302787
glycinea	BR1	Pgy BR1		1989	Soybean	MAFF	MAFF210373
glycinea	KN127	Pgy KN127		1982	Soybean	MAFF	MAFF302751
glycinea	KN166	Pgy KN166		1982	Soybean	MAFF	MAFF302770
glycinea	KN28	Pgy KN28		1981	Soybean	MAFF	MAFF302676
glycinea	KN44	Pgy KN44	Japan	1981	Soybean	MAFF	MAFF301683
glycinea	LN10	Pgy LN10		1989	Soybean	MAFF	MAFF210389
glycinea	MAFF301765	Pgy M301765		1982	Soybean	MAFF	MAFF301765
glycinea	MOC601	Pgy MOC601		1994	Soybean	MAFF	MAFF311113
glycinea	R4a	Pgy R4a			Soybean	J. Dangl	
glycinea	UnB647	Pgy UnB647			Kidney bean	MAFF	MAFF210405
japonica	MAFF301072	Pja M301072	Japan	1951	Barley	MAFF	MAFF301072
lachrymans	107	Pla 107			Cucumber	J. Dangl	MAFF301315
lachrymans	3988	Pla 3988	US	1935	Cucumber	D. Arnold	ICMP3988
lachrymans	1188_1	Pla 1188_1	US		Zucchini	D. Cooksey	
lachrymans	ATCC7386	Pla A7386			Cucumber	J. Dangl	MAFF302278
lachrymans	N7512	Pla N7512	Japan	1975	Cucumber	MAFF	MAFF301315
lachrymans	YM7902	Pla YM7902		1979	Cucumber	MAFF	MAFF730057
lachrymans	YM8003	Pla YM8003		1980	Cucumber	MAFF	MAFF730069
maculicola	4981	Pma 4981	Zimbabwe		Cauliflower	D. Cuppels	
maculicola	AZ85297	Pma AZ85297		1985	Chinese cabbage	MAFF	MAFF302539
maculicola	ES4326	Pma ES4326		1965	Radish	J. T. Greenberg	
maculicola	H7311	Pma H7311	Japan	1973	Chinese cabbage	MAFF	MAFF301174
maculicola	H7608	Pma H7608		1976	Chinese cabbage	MAFF	MAFF301175
maculicola	KN203	Pma KN203		1983	Chinese cabbage	MAFF	MAFF302783
maculicola	KN84	Pma KN84		1982	Radish	MAFF	MAFF302724
maculicola	KN91	Pma KN91		1982	Radish	MAFF	MAFF302731
maculicola	M4a	Pma M4a			Radish	J. Dangl	
maculicola	M6	Pma M6	UK	1965	Cauliflower	J. Dangl	
maculicola	YM7930	Pma YM7930		1979	Radish	MAFF	MAFF301419
mellea	N6801	Pme N6801		1968	Tobacco	MAFF	MAFF302303
mori	MAFF301020	Pmo M301020	Japan	1966	Mulberry	MAFF	MAFF301020
morsprunorum	19322	Pmp 19322			European plum	J. Dangl	ATCC 19322
morsprunorum	FTRS_U7805	Pmp FTRS_U7	Japan	1978	Japanese apricot	MAFF	MAFF301436
myricae	AZ84488	Pmy AZ84488		1984	Bayberry	MAFF	MAFF302460
myricae	MAFF302941	Pmy M302941		1989	Bayberry	MAFF	MAFF302941
oryzae	36_1	Por 36_1		1983	Rice	MAFF	MAFF301538
oryzae	1_6	Por 1_6		1991	Rice	MAFF	MAFF311107
phaseolicola	1302A	Pph 1302A	Ethiopia	1984	Kidney bean	D. Arnold	
phaseolicola	1449B	Pph 1449B	Ethiopia	1985	Hyacinth bean	D. Arnold	
phaseolicola	HB10Y	Pph HB10Y			Snap bean	P. Turner	ATCC 21781
phaseolicola	KN86	Pph KN86	Japan	1982	Kidney bean	MAFF	MAFF301673
phaseolicola	NPS3121	Pph NPS3121			Kidney bean	J. T. Greenberg	
phaseolicola	NS368	Pph NS368		1992	Kidney bean	MAFF	MAFF311004
phaseolicola	R6a	Pph R6a			Kidney bean	J. Dangl	
phaseolicola	SG44	Pph SG44	US	1980	Snap bean	S. Hirano	
phaseolicola	Y5_2	Pph Y5_2			Kudzu	MAFF	MAFF311162
pisi	895A	Ppi 895A			Pea	D. Arnold	
pisi	H5E1	Ppi H5E1		1993	Pea	MAFF	MAFF311141
pisi	H5E3	Ppi H5E3		1993	Pea	MAFF	MAFF311143
pisi	H6E5	Ppi H6E5		1994	Pea	MAFF	MAFF311144
pisi	H7E7	Ppi H7E7		1995	Pea	MAFF	MAFF311146
pisi	PP1	Ppi PP1	Japan	1978	Pea	MAFF	MAFF301208
pisi	R6a	Ppi R6a			Pea	J. Dangl	
savastanoi	4352	Psv 4352	Yugoslavia		Olive	A. Colmer	
sesami	HC_1	Pse HC_1			Sesame	MAFF	MAFF311181
syringae	1212R	Psy 1212R			Pea	D. Arnold	
syringae	A2	Psy A2			Ornamental pear	C. Bender	
syringae	B48	Psy B48	US		Peach	T. Denny	
syringae	B64	Psy B64	US		Wheat	T. Denny	
syringae	B728A	Psy B728A	US		Snap bean	S. Hirano	
syringae	B76	Psy B76	US		Tomato	T. Denny	
syringae	FF5	Psy FF5	US	1998	Ornamental pear	C. Bender	
syringae	FTRS_W6601	Psy FTRS_W6		1966	Japanese apricot	MAFF	MAFF301429
syringae	FTRS_W7835	Psy FTRS_W7		1978	Japanese apricot	MAFF	MAFF301430
syringae	L177	Psy L177		1983	Lilac	MAFF	MAFF302085
syringae	LOB2_1	Psy LOB2_1	Japan	1986	Lilac	MAFF	MAFF301861
syringae	NCPPB281	Psy NCPPB28	UK		Lilac	B. Hancock	ATCC 19310
syringae	Ps9220	Psy Ps9220		1992	Spring onion	MAFF	MAFF730125
syringae	PSC1B	Psy PSC1B	US		Corn	T. Denny	
tabaci	6606	Pta 6606	Japan	1967	Tobacco	MAFF	MAFF301612
thea	K93001	Pth K93001		1993	Tea	MAFF	MAFF302851
tomato	487	Pto 487	Greece		Tomato	D. Cuppels	
tomato	1318	Pto 1318	Switzerland		Tomato	D. Cuppels	
tomato	2170	Pto 2170		1984	Tomato	MAFF	MAFF301591
tomato	DC3000	Pto DC3000	UK		Tomato	J. T. Greenberg	
tomato	DC84_1	Pto DC84_1	Canada		Tomato	D. Cuppels	
tomato	DC89_4H	Pto DC89_4H	Canada		Tomato	D. Cuppels	
tomato	DCT6D1	Pto DCT6D1	Canada		Tomato	D. Cuppels	
tomato	KN10	Pto KN10		1981	Tomato	MAFF	MAFF302665
tomato	PT23	Pto PT23	US	1986	Tomato	N. T. Keen	
tomato	TF1	Pto TF1	US	1997	Tomato	S. Hirano	
—[c]	Cit7	Ps Cit7			Navel orange	S. Lindow	
—[c]	TLP2	Ps TLP2			Potato	S. Lindow	

[a] MAFF, Japanese Ministry of Agriculture, Forestry, and Fisheries; ATCC, American Type Culture Collection; ICMP, International Collection of Micro-organisms from Plants (New Zealand).
[b] US, United States; UK, United Kingdom.
[c] —, no pathovar designation.

Supplemental Table S2. Composition of media and solutions used in this study

Bacterial Culture

King's B medium

	C (g/L)
Peptone	10
KH2PO4	1,5
MgSO4 + 7 H2O	1,5
Agar	15
H2O	qsp

Lysogeny Broth medium (LB)

	C (g/L)
Peptone	10
Yeast Extract	5
NaCl	10
Agar	15
H2O	qsp

Minimal medium m9

	C (g/L)	Cf (mM)
KH2PO4	15	
Na2HPO4	64	
NaCl	2,5	
NH4Cl	5	
Glucose 20%	20%	
MgSO4		2
CaCl2		0,1
H2O		qsp

Yeast extract medium (YEM)

	C (g/L)
NaCl	50
MgCl2	9
MgSO4 + 7 H2O	13
CaCl2	0,2
KCl	1,3
NaHCO3	0,05
NaBr	0,15
FeCl3	0,005
Glucose	10
Yeast Extract	3
Malt Extract	3
Peptone	5
H2O	qsp

Mannitol motility medium
pH = 7,6

	C (g/L)
Peptone	10
Mannitol	7,5
KNO3	1
Phenol red	0,04
Agar	4
H2O	qsp

Protoplasts formation

Enzymatic solution

	Cf (mM)		%
MES	20	BSA	0,1
Mannitol	400	Cellulase	1,5
KCl	20	Maceroenzyme	0,4
CaCl2	10		

Washing solution

	Cf (mM)
MES	2
NaCl	154
KCl	5
CaCl2	125

Storage solution

	Cf (mM)
MES	4
Mannitol	400
MgCl2	15

Supplemental Table S3. Primers used in this study

Gene	Accession	Forward Primer	Reverse Primer	Ref
PsOprF	PSPTO_2299	TGCTGCGTCCATACGTTTCT	TCGGTGAAGTACAGCTTGGC	This study
PsLeuD	PSPTO_2174	AGCCTTTACCCAGCACAATG	CGCTTGATCGACTTGAGAAACT	Smith *et al.*, 2018
PsHrpA	PSPTO_1381	GTGTCAACACGGTTGCTTCC	TGGCGTCGGACTCTTTACTG	This study
PsHopB1	PSPTO_1406	ATGGACAGTTGTCTGGGGAC	CTCAGGTAACTTTTGCGCGT	This study
PsHrcC / SctC	PSPTO_1389	GCAATGGTTCTGCGTCAGTC	AAGTGGCCGTCAGGTATTCG	This study
PsHrpJ	PSPTO_1391	AAAATCGTCGCTCCGCCTAT	GCGAAGTCCCTGAATTGTGC	This study
AtUBQ5	NM_116090.3	GGAAGAAGAAGACTTACACC	AGTCCACACTTACCACAGTA	This study
AtPR1	NM_127025	AACTACGCTGCGAACACGTG	TCACTTTGGCACATCCGAGTC	
AtPR5	NM_106161	GACTCCAGGTGCTTCCCGACAG	ACTCCGCCGCCGTTACATCTT	Magnin-Robert *et al.*, 2015
AtVSP1	NM_0011258 01	GGATCGAAGTTGACGCAAGTG	CTCAACCAAATCAGCCCATTG	
AtNMT1	NM_125084.3	TCCTTCTGTTTACGAGTGGACG ACATGT	CTCCAATATGCCAGCTCTGGTA ATAACC	Pierre *et al.*, 2007

Supplemental Table S4. T3SS genes of *Pst*

T3SS Gene	Locus tag	Replicon	Localisation	Role of the protein	Source
hrpA1	PSPTO_1381	Chromosome	Extracellular	Responsible for pilus formation	Jin *et al.* (2001)
hrpZ1	PSPTO_1382	Chromosome	Extracellular	Harpin, forms ion channels in the PM of the host	Kvitko *et al.* (2007); Lee *et al.* (2001)
hrpK1	PSPTO_1405	Chromosome	Extracellular	Harpine, participates in the formation of translocon in the PM of the host	Kvitko *et al.* (2007) Petnicki-Ocwieja *et al.* (2005)
hrpL	PSPTO_1404	Chromosome	Cytoplasmic	RNA polymerase sigma 70 family factor, essential for the expression of genes in the *hrp/hrc* system. A *hrpL* mutant will no longer be able to produce coronatin	Fouts *et al.* (2001)
hrcC	PSPTO_1389	Chromosome	Outer membrane	Required for secretion of *hrpZ*	Deng *et al.* (1999)
hrpV	PSPTO_1391	Chromosome	Unknown	Hydrophilic protein, this gene is in the same cluster as *hrcC* but its mutation does not induce modification of the virulence of the bacterium	Deng *et al.* (1998)
hrcN	PSPTO_1400	Chromosome	Membrane	ATPase activity, catalyzes protein translocation by T3SS	Pozidis *et al.* (2003), Rezzonico *et al.* (2004)
hrpJ	PSPTO_1403	Chromosome	Inner and outer membrane	Required for virulence and secretion of *hrpZ*	Deng *et al.* (1999), Fu *et al.* (2006)
hopB1	PSPTO_1406	Chromosome	Extracellular	Effector, interaction with the host PM	Petnicki-Ocwieja *et al.* (2005)
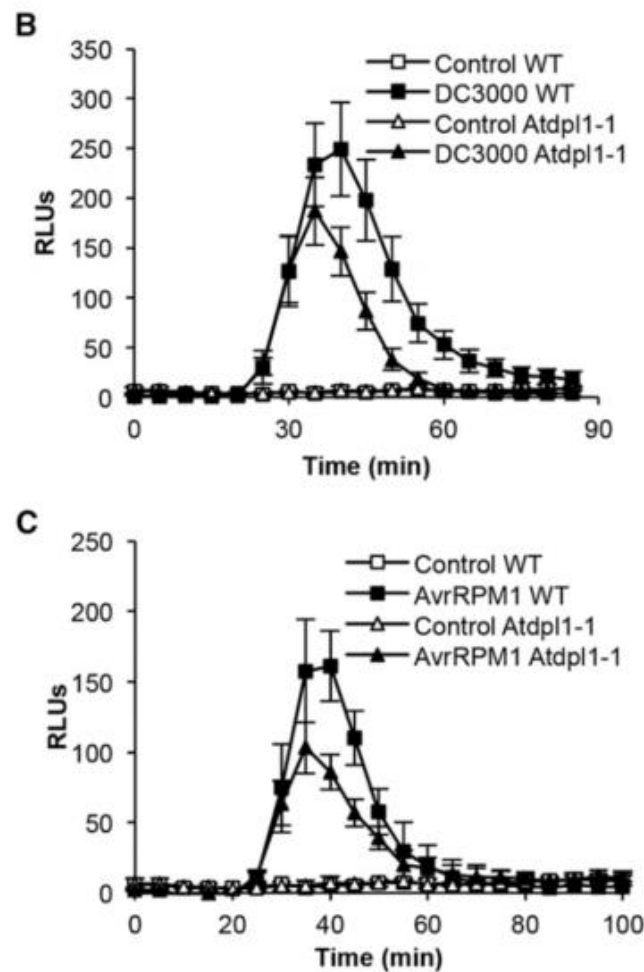
Supplemental Figure S1. Transient ROS production in response to pathogen infection in wild-type and *Atdpl1-1* mutant plants (from Magnin-Robert *et al*., 2014)

Transient ROS production in response to pathogen infection in wild-type (WT) and the *Arabidopsis* mutant *Atdpl1-1* (*Dihydrosphingosine-1-phosphate lyase1* mutant that exhibit susceptibility to *Pst*). The time course of ROS production in wild type and *Atdpl1-1* mutant plants is shown in response to **B.** *Pst* DC3000, or **C.** *Pst AvrRpm1* infection. Leaf discs were immersed in a solution containing either 10^5 spores/mL *B. cinerea* or 10^8 CFU/mL *Pst*. Error bars represent SE from 12 biological repetitions. Three independent experiments were performed with similar results. RLUs, Relative light units.
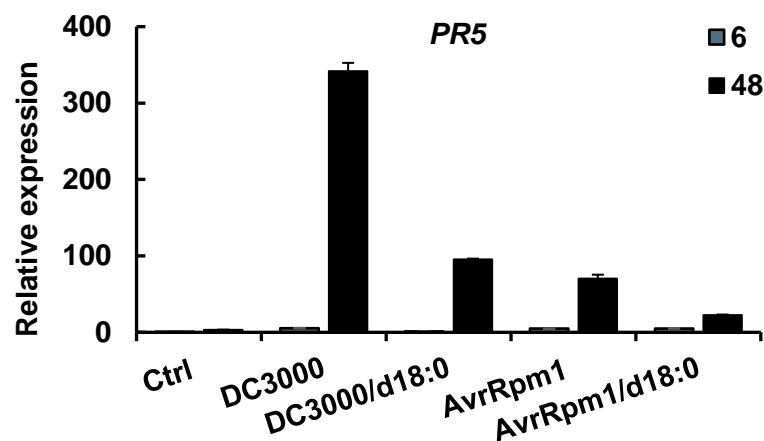
Supplemental Figure S2. Expression of *PR5* in response to *Pst* DC3000 and *Pst AvrRpm1* infiltrated alone or with d18:0

The expression of *PR5*, expressed in response to salicylic acid (SA) was followed. Leaves of *Arabidopsis* were harvested 6 and 48 hours post infiltration with *Pst* DC3000 or *Pst AvrRpm1* (10^7 CFU/mL,10 mM $MgCl_2$), either with ethanol (0,1%, v/v) or with d18:0 (100 μM, ethanol 100%). Results are normalized upon non treated leaves. Experiments were repeated 3 times with similar results. Control inoculations were conducted with 10 mM $MgCl_2$ and ethanol (0,1%, v/v).

Supplemental Information. Protoplasts formation and viability tests in presence of d18:0

Plant material and growth conditions

Seeds of *Arabidopsis thaliana* WT Columbia-0 were obtained from the Nottingham *Arabidopsis* Stock Center (http://*Arabidopsis*.info) and grown in soil under 12 h-light/12 h-dark conditions (150 µmol/m²/s, 20°C, and 60% humidity) for 5 weeks.

Protoplast formation and viability tests

The composition of all solutions used are described in **Supplemental data 2.** Leaves of *Arabidopsis* were harvested, their abaxial side abrased with a scalpel blade and place abaxial face down in an enzymatic solution. They were left overnight, at room temperature, and in the dark in this solution. The next day the digested solution was filtrated with a gauze and centrifuged at 300g for 2 minutes. The supernatant was removed, and a rinsing solution was added. This operation was repeated two times. The last supernatant was discarded, and the protoplasts were resuspended at 10^6 protoplast/mL in the storage solution until further use.

Protoplast's viability was estimated with fluorescein diacetate (FDA). The dye, which highlights living cells, was prepared by diluting 2 mg of FDA in 1 mL of acetone in a glass vial covered with foil. In the dark, 1 µL of this mixture was added to 1 mL of protoplasts. Images were observed with a fluorescence microscope with a maximum excitation wavelength of 490 nm and a maximum emission wavelength of 526 nm.
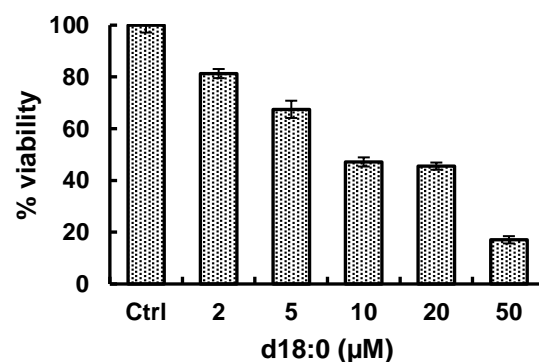
Supplemental Figure S3. Viability of *Arabidopsis* protoplasts in presence of d18:0

5-week-old *Arabidopsis* leaves were harvested and digested to obtain protoplasts that were resuspended at 10^6 protoplast/mL. d18:0 was prepared at various concentrations in ethanol 100%. Protoplasts were consequently treated with either ethanol 100% (Ctrl) or with d18:0. Viability was estimated by adding fluorescein diacetate to the medium and counting living cells under a fluorescence microscope after addition of d18:0.

References

Abbas, H. K., Tanaka, T., Duke, S. O., Porter, J. K., Wray, E. M., Hodges, L., Sessions, A. E., Wang, E., Merrill Jr, A. H., and Riley, R. T. (1994). Fumonisin-and AAL-toxin-induced disruption of sphingolipid metabolism with accumulation of free sphingoid bases. *Plant Physiology* 106:1085–1093.

Afzal, A. J., Kim, J. H., and Mackey, D. (2013). The role of NOI-domain containing proteins in plant immune signalling. *BMC Genomics* 14:1471–2164.

Alden, K. P., Dhondt-Cordelier, S., McDonald, K. L., Reape, T. J., Ng, C. K.-Y., McCabe, P. F., and Leaver, C. J. (2011). Sphingolipid long chain base phosphates can regulate apoptotic-like programmed cell death in plants. *Biochemical and Biophysical Research Communications* 410:574–580.

Alessandrini, A., and Facci, P. (2005). AFM: a versatile tool in biophysics. *Measurement Science and Technology* 16:R65–R92.

Alfano, J. R., and Collmer, A. (1997). The type III (Hrp) secretion pathway of plant pathogenic bacteria: trafficking harpins, Avr proteins, and death. *Journal of Bacteriology* 179:5655–5662.

Alfano, J. R., and Collmer, A. (2004). Type III secretion system effector proteins: double agents in bacterial disease and plant defence. *Annual Review of Phytopathology* 42:385–414.

Alfano, J. R., Charkowski, A. O., Deng, W.-L., Badel, J. L., Petnicki-Ocwieja, T., van Dijk, K., and Collmer, A. (2000). The *Pseudomonas syringae* Hrp pathogenicity island has a tripartite mosaic structure composed of a cluster of type III secretion genes bounded by exchangeable effector and conserved effector loci that contribute to parasitic fitness and pathogenicity in plants. *Proceedings of the National Academy of Sciences* 97:4856–4861.

Ali, U., Li, H., Wang, X., and Guo, L. (2018). Emerging roles of sphingolipid signalling in plant response to biotic and abiotic stresses. *Molecular Plant* 11:1328–1343.

Almgren, M., Edwards, K., and Gustafsson, J. (1996). Cryotransmission electron microscopy of thin vitrified samples. *Current Opinion in Colloid & Interface Science* 1:270–278.

Almgren, M., Edwards, K., and Karlsson, G. (2000). Cryo transmission electron microscopy of liposomes and related structures. *Colloids and Surfaces A: Physicochemical and Engineering Aspects* 174:3–21.

Anantharajah, A., Mingeot-Leclercq, M.-P., and Van Bambeke, F. (2016). Targeting the type three secretion system in *Pseudomonas aeruginosa*. *Trends in Pharmacological Sciences* 37:734–749.

Arrebola, E., Carrión, V. J., Gutiérrez-Barranquero, J. A., Pérez-García, A., Rodríguez-Palenzuela, P., Cazorla, F. M., and de Vicente, A. (2015). Cellulose production in *Pseudomonas syringae* pv. *syringae* : a compromise between epiphytic and pathogenic lifestyles. *FEMS Microbiology Ecology* 91:fiv071.

Asai, T., Tena, G., Plotnikova, J., Willmann, M. R., Chiu, W.-L., Gomez-Gomez, L., Boller, T., Ausubel, F. M., and Sheen, J. (2002). MAP kinase signalling cascade in *Arabidopsis* innate immunity. *Nature* 415:977–983.

Bacete, L., Mélida, H., Miedes, E., and Molina, A. (2018). Plant cell wall-mediated immunity: cell wall changes trigger disease resistance responses. *Plant Journal* 93:614–636.

Bargmann, B. O. R., and Munnik, T. (2006). The role of phospholipase D in plant stress responses. *Current Opinion in Plant Biology* 9:515–522.

Bari, R., and Jones, J. D. G. (2009). Role of plant hormones in plant defence responses. *Plant Molecular Biology* 69:473–488.

Bauer, Z., Gómez-Gómez, L., Boller, T., and Felix, G. (2001). Sensitivity of Different Ecotypes and Mutants of *Arabidopsis thaliana* toward the Bacterial Elicitor Flagellin Correlates with the Presence of Receptor-binding Sites. *Journal of Biological Chemistry* 276:45669–45676.

Baxter, A., Mittler, R., and Suzuki, N. (2014). ROS as key players in plant stress signalling. *Journal of Experimental Botany* 65:1229–1240.

Beattie, G. A., and Lindow, S. E. (1995). The Secret Life of Foliar Bacterial Pathogens on Leaves. *Annual Review of Phytopathology*. 33:145–172.

Becam, J., Walter, T., Burgert, A., Schlegel, J., Sauer, M., Seibel, J., and Schubert-Unkmeir, A. (2017). Antibacterial activity of ceramide and ceramide analogs against pathogenic Neisseria. *Scientific Report* 7:17627.

Beckers, G. J. M., Jaskiewicz, M., Liu, Y., Underwood, W. R., He, S. Y., Zhang, S., and Conrath, U. (2009). Mitogen-activated protein kinases 3 and 6 are required for full priming of stress responses in *Arabidopsis thaliana*. *The Plant Cell* 21:944–953.

Begum, M. A., Shi, X.-X., Tan, Y., Zhou, W.-W., Hannun, Y., Obeid, L., Mao, C., and Zhu, Z.-R. (2016). Molecular characterization of rice OsLCB2a1 gene and functional analysis of its role in insect resistance. *Frontiers in Plant Science* 7-1789.

Bennett, R. N., and Wallsgrove, R. M. (1994). Secondary metabolites in plant defence mechanisms. *New Phytologist* 127:617–633.

Bentham, A. R., De la Concepcion, J. C., Mukhi, N., Zdrzałek, R., Draeger, M., Gorenkin, D., Hughes, R. K., and Banfield, M. J. (2020). A molecular roadmap to the plant immune system. *Journal of Biological Chemistry* 295:14916–14935.

Berkey, R., Bendigeri, D., and Xiao, S. (2012). Sphingolipids and plant defence/disease: The "death" connection and beyond. *Frontiers in Plant Science* 3-68.

Betsuyaku, S., Katou, S., Takebayashi, Y., Sakakibara, H., Nomura, N., and Fukuda, H. (2018). Salicylic acid and jasmonic acid pathways are activated in spatially different domains around the infection site during effector-triggered immunity in *Arabidopsis thaliana*. *Plant and Cell Physiology* 59:8–16.

Bigeard, J., Colcombet, J., and Hirt, H. (2015). Signalling mechanisms in pattern-triggered immunity (PTI). *Molecular Plant* 8:521–539.

Bjornson, M., and Zipfel, C. (2021). Plant immunity: Crosstalk between plant immune receptors. *Current Biology* 31:R796–R798.

Blachutzik, J. O., Demir, F., Kreuzer, I., Hedrich, R., and Harms, G. S. (2012). Methods of staining and visualization of sphingolipid enriched and non-enriched plasma membrane regions of *Arabidopsis thaliana* with fluorescent dyes and lipid analogues. *Plant methods* 8:28.

Block, A., and Alfano, J. R. (2011). Plant targets for *Pseudomonas syringae* type III effectors: virulence targets or guarded decoys? *Current Opinion in Microbiology* 14:39–46.

Block, A., Schmelz, E., Jones, J. B., and Klee, H. J. (2005). Coronatine and salicylic acid: the battle between *Arabidopsis* and *Pseudomonas* for phytohormone control. *Molecular Plant Pathology* 6:79–83.

Boller, T., and He, S. Y. (2009). Innate immunity in plants: an arms race between pattern recognition receptors in plants and effectors in microbial pathogens. *Science* 324:742–744.

Bolwell, G. P., and Wojtaszek, P. (1997). Mechanisms for the generation of reactive oxygen species in plant defence – a broad perspective. *Physiological and Molecular Plant Pathology* 51:347–366.

Bonet, R., Simon-Pujol, M. D., and Congregado, F. (1993). Effects of nutrients on exopolysaccharide production and surface properties of *Aeromonas salmonicida*. *Applied and Environmental Microbiology* 59:2437–2441.

Bostock, R. M., Kuc, J. A., and Laine, R. A. (1981). Eicosapentaenoic and arachidonic acids from phytophthora infestans elicit fungitoxic sesquiterpenes in the potato. *Science* 212:67–69.

Bostock, R. M., Savchenko, T., Lazarus, C., and Dehesh, K. (2011). Eicosapolyenoic acids: Novel MAMPs with reciprocal effect on oomycete-plant defence signalling networks. *Plant Signalling & Behavior* 6:531–533.

Boureau, T., Routtu, J., Roine, E., Taira, S., and Romantschuk, M. (2002). Localization of hrpA-induced *Pseudomonas syringae* pv. *tomato* DC3000 in infected tomato leaves. *Molecular Plant Pathology* 3:451–460.

Boyes, D. C., Nam, J., and Dangl, J. L. (1998). The *Arabidopsis thaliana* RPM1 disease resistance gene product is a peripheral plasma membrane protein that is degraded coincident with the hypersensitive response. *Proceedings of the National Academy of Sciences* 95:15849–15854.

Boyle, P. C., Schwizer, S., Hind, S. R., Kraus, C. M., De la Torre Diaz, S., He, B., and Martin, G. B. (2016). Detecting N-myristoylation and S-acylation of host and pathogen proteins in plants using click chemistry. *Plant Methods* 12:38.

Brasseur, R., Killian, J. A., De Kruijff, B., and Ruysschaert, J. M. (1987). Conformational analysis of gramicidin-gramicidin interactions at the air/water interface suggests that gramicidin aggregates into tube-like structures similar as found in the gramicidin-induced hexagonal HII phase. *Biochimica et Biophysica Acta (BBA) - Biomembranes* 903:11–17.

Bredow, M., and Monaghan, J. (2019). Regulation of plant immune signalling by calcium-dependent protein kinases. *Molecular Plant Microbe Interactions* 32:6–19.

Breslow, D. K., and Weissman, J. S. (2010). Membranes in balance: mechanisms of sphingolipid homeostasis. *Molecular Cell* 40:267–279.

Brogden, G., Husein, D. M., Steinberg, P., and Naim, H. Y. (2019). Isolation and quantification of sphingosine and sphinganine from rat serum revealed gender differences. *Biomolecules* 9:459.

Brooks, D. M., Bender, C. L., and Kunkel, B. N. (2005). The *Pseudomonas syringae* phytotoxin coronatine promotes virulence by overcoming salicylic acid-dependent defences in *Arabidopsis thaliana*. *Molecular Plant Pathology* 6:629–639.

Buell, C. R., Joardar, V., Lindeberg, M., Selengut, J., Paulsen, I. T., Gwinn, M. L., Dodson, R. J., Deboy, R. T., Durkin, A. S., Kolonay, J. F., *et al.* (2003). The complete genome sequence of the *Arabidopsis* and tomato pathogen *Pseudomonas syringae* pv. *tomato* DC3000. *Proceedings of the National Academy of Sciences* 100:10181–10186.

Butsenko, L., Pasichnyk, L., Kolomiiets, Y., and Kalinichenko, A. (2020). The effect of pesticides on the tomato bacterial speck disease pathogen *Pseudomonas syringae* pv. *tomato*. *Applied Sciences* 10:3263.

Cacas, J. L., Furt, F., Le Guédard, M., Schmitter, J.-M., Buré, C., Gerbeau-Pissot, P., Moreau, P., Bessoule, J.-J., Simon-Plas, F., and Mongrand, S. (2012). Lipids of plant membrane rafts. *Progress in Lipid Research* 51:272–299.

Cacas, J.-L., Buré, C., Grosjean, K., Gerbeau-Pissot, P., Lherminier, J., Rombouts, Y., Maes, E., Bossard, C., Gronnier, J., Furt, F., *et al.* (2016). Revisiting plant plasma membrane lipids in tobacco: a focus on sphingolipids. *Plant Physiology*. 170:367–384.

Carmona-Salazar, L., El Hafidi, M., Enríquez-Arredondo, C., Vázquez-Vázquez, C., González de la Vara, L. E., and Gavilanes-Ruíz, M. (2011). Isolation of detergent-resistant membranes from plant photosynthetic and non-photosynthetic tissues. *Analytical Biochemistry* 417:220–227.

Carreira, A. C., Pokorna, S., Ventura, A. E., Walker, M. W., Futerman, A. H., Lloyd-Evans, E., de Almeida, R. F. M., and Silva, L. C. (2021). Biophysical impact of sphingosine and other abnormal lipid accumulation in Niemann-Pick disease type C cell models. *Biochimica et Biophysica Acta (BBA) - Molecular and Cell Biology of Lipids* 1866:158944.

Chen, M., Han, G., Dietrich, C. R., Dunn, T. M., and Cahoon, E. B. (2006). the essential nature of sphingolipids in plants as revealed by the functional identification and characterization of the *Arabidopsis* LCB1 subunit of serine palmitoyltransferase. *The Plant Cell* 18:3576–3593.

Chen, M., Markham, J. E., Dietrich, C. R., Jaworski, J. G., and Cahoon, E. B. (2008). Sphingolipid long-chain base hydroxylation is important for growth and regulation of sphingolipid content and composition in *Arabidopsis*. *The Plant Cell* 20:1862–1878.

Chinchilla, D., Bauer, Z., Regenass, M., Boller, T., and Felix, G. (2006). The *Arabidopsis* receptor kinase FLS2 binds flg22 and determines the specificity of flagellin perception. *The Plant Cell* 18:465–476.

Chinchilla, D., Zipfel, C., Robatzek, S., Kemmerling, B., Nürnberger, T., Jones, J. D. G., Felix, G., and Boller, T. (2007). A flagellin-induced complex of the receptor FLS2 and BAK1 initiates plant defence. *Nature* 448:497–500.

Choi, M.-S., Kim, W., Lee, C., and Oh, C.-S. (2013). Harpins, multifunctional proteins secreted by gram-negative plant-pathogenic bacteria. *Molecular Plant Microbe Interactions* 26:1115–1122.

Chung, E.-H., da Cunha, L., Wu, A.-J., Gao, Z., Cherkis, K., Afzal, A. J., Mackey, D., and Dangl, J. L. (2011). Specific threonine phosphorylation of a host target by two unrelated type III effectors activates a host innate immune receptor in plants. *Cell Host & Microbe* 9:125–136.

Clausen, C. H., Brooks, M. D., Li, T.-D., Grob, P., Kemalyan, G., Nogales, E., Niyogi, K. K., and Fletcher, D. A. (2014). dynamic mechanical responses of *Arabidopsis* thylakoid membranes during PSII-specific illumination. *Biophysical Journal* 106:1864–1870.

Coca, M., and San Segundo, B. (2010). AtCPK1 calcium-dependent protein kinase mediates pathogen resistance in *Arabidopsis*: AtCPK1 is involved in pathogen resistance. *The Plant Journal* 63:526–540.

Colin, L., Martin-Arevalillo, R., Bovio, S., Bauer, A., Vernoux, T., Caillaud, M.-C., Landrein, B., and Jaillais, Y. (2022). Imaging the living plant cell: From probes to quantification. *The Plant Cell* 34:247–272.

Coll, N. S., Epple, P., and Dangl, J. L. (2011). Programmed cell death in the plant immune system. *Cell Death Differ* 18:1247–1256.

Contreras, F.-X., Sot, J., Alonso, A., and Goñi, F. M. (2006). Sphingosine increases the permeability of model and cell membranes. *Biophysical Journal* 90:4085–4092.

Cook, D. E., Mesarich, C. H., and Thomma, B. P. H. J. (2015). Understanding plant immunity as a surveillance system to detect invasion. *Annual Review of Phytopathology.* 53:541–563.

Cordelier, S., Crouzet, J., Gilliard, G., Dorey, S., Deleu, M., and Dhondt-Cordelier, S. (2022). Deciphering the role of plant plasma membrane lipids in response to invasion patterns: how could biology and biophysics help? *Journal of Experimental Botany* 73:9.

Cornelis, G. R. (2006). The type III secretion injectisome. *Nature Reviews Microbiology* 4:811–825.

Coursol, S., Fromentin, J., Noirot, E., Brière, C., Robert, F., Morel, J., Liang, Y.-K., Lherminier, J., and Simon-Plas, F. (2015). Long-chain bases and their phosphorylated derivatives differentially regulate cryptogein-induced production of reactive oxygen species in tobacco (*Nicotiana tabacum*) BY-2 cells. *New Phytologist* 205:1239–1249.

Couto, D., and Zipfel, C. (2016). Regulation of pattern recognition receptor signalling in plants. *Nature Review Immunology* 16:537–552.

Cukkemane, N., Bikker, F. J., Nazmi, K., Brand, H. S., Sotres, J., Lindh, L., Arnebrant, T., and Veerman, E. C. I. (2015). Anti-adherence and bactericidal activity of sphingolipids against *Streptococcus mutans*. *European Journal of Oral Science* 123:221–227.

Cunnac, S., Lindeberg, M., and Collmer, A. (2009). *Pseudomonas syringae* type III secretion system effectors: repertoires in search of functions. *Current Opinion in Microbiology* 12:53–60.

Cunnac, S., Chakravarthy, S., Kvitko, B. H., Russell, A. B., Martin, G. B., and Collmer, A. (2011). Genetic disassembly and combinatorial reassembly identify a minimal functional repertoire of type III effectors in *Pseudomonas syringae*. *Proceedings of the National Academy of Sciences* 108:2975–2980.

Cuppels, D. A. (1986). Generation and characterization of Tn5 insertion mutations in *Pseudomonas syringae* pv. *tomato*. *Applied and Environmental Microbiology* 51:323–327.

Dangl, J. L., and Jones, J. D. G. (2001). Plant pathogens and integrated defence responses to infection. *Nature* 411:826–833.

Debener, T., Lehnackers, H., Arnold, M., and Dangl, J. L. (1991). Identification and molecular mapping of a single *Arabidopsis thaliana* locus determining resistance to a phytopathogenic *Pseudomonas syringae* isolate. *The Plant Journal* 1:289–302.

Debenert, T., Lehnackers, H., Arnold, M., and Dangl, J. L. (1991). Identification and molecular mapping of a single *Arabidopsis thaliana* locus determining resistance to a phytopathoggenic *Pseudomonas syringae* isolate. *The Plant Journal* 1:299–302.

Deboever, E., Van Aubel, G., Rondelli, V., Koutsioubas, A., Mathelie-Guinlet, M., Dufrene, Y. F., Ongena, M., Lins, L., Van Cutsem, P., Fauconnier, M., *et al.* (2022). Modulation of plant

plasma membrane structure by exogenous fatty acid hydroperoxide is a potential perception mechanism for their eliciting activity. *Plant Cell & Environment* 45:1082–1095.

Deguchi, H., Yegneswaran, S., and Griffin, J. H. (2004). Sphingolipids as Bioactive Regulators of Thrombin Generation. *Journal of Biological Chemistry* 279:12036–12042.

Deleu, M., Paquot, M., and Nylander, T. (2005). Fengycin interaction with lipid monolayers at the air–aqueous interface—implications for the effect of fengycin on biological membranes. *Journal of Colloid and Interface Science* 283:358–365.

Deleu, M., Paquot, M., and Nylander, T. (2008). Effect of fengycin, a lipopeptide produced by *Bacillus subtilis*, on model biomembranes. *Biophysical Journal* 94:2667–2679.

Deleu, M., Lorent, J., Lins, L., Brasseur, R., Braun, N., El Kirat, K., Nylander, T., Dufrêne, Y. F., and Mingeot-Leclercq, M.-P. (2013). Effects of surfactin on membrane models displaying lipid phase separation. *Biochimica et Biophysica Acta (BBA) - Biomembranes* 1828:801–815.

Deleu, M., Crowet, J.-M., Nasir, M. N., and Lins, L. (2014). Complementary biophysical tools to investigate lipid specificity in the interaction between bioactive molecules and the plasma membrane: A review. *Biochimica et Biophysica Acta (BBA) - Biomembranes* 1838:3171–3190.

Deleu, M., Deboever, E., Nasir, M. N., Crowet, J.-M., Dauchez, M., Ongena, M., Jijakli, H., Fauconnier, M.-L., and Lins, L. (2019). Linoleic and linolenic acid hydroperoxides interact differentially with biomimetic plant membranes in a lipid specific manner. *Colloids and Surfaces B: Biointerfaces* 175:384–391.

Delledonne, M., Zeier, J., Marocco, A., and Lamb, C. (2001). Signal interactions between nitric oxide and reactive oxygen intermediates in the plant hypersensitive disease resistance response. *Proceedings of the National Academy of Sciences* 98:13454–13459.

Deng, W.-L., and Huang, H.-C. (1999). Cellular locations of *Pseudomonas syringae* pv. *syringae* HrcC and HrcJ Proteins, required for harpin secretion via the type III Pathway. *Journal of Bacteriology*. 181:2298–2301.

Deslandes, L., and Rivas, S. (2012). Catch me if you can: bacterial effectors and plant targets. *Trends in Plant Science* 17:644–655.

Diepold, A., and Armitage, J. P. (2015). Type III secretion systems: the bacterial flagellum and the injectisome. *Philosophical Transactions of the Royal Society: Biological Sciences* 370:20150020.

Diepold, A., and Wagner, S. (2014). Assembly of the bacterial type III secretion machinery. *FEMS Microbiology Reviews* 38:802–822.

Diepold, A., Wiesand, U., and Cornelis, G. R. (2011). The assembly of the export apparatus (YscR,S,T,U,V) of the *Yersinia* type III secretion apparatus occurs independently of other structural components and involves the formation of an YscV oligomer: Assembly of the *Yersinia* injectisome export apparatus. *Molecular Microbiology* 82:502–514.

Domínguez, E., Heredia-Guerrero, J. A., and Heredia, A. (2017). The plant cuticle: old challenges, new perspectives. *Journal of Experimental Botany* 68:5251–5255.

Dongfack, M. D. J., Lallemand, M.-C., Kuete, V., Mbazoa, C. D., Wansi, J.-D., Trinh-van-Dufat, H., Michel, S., and Wandji, J. (2012). A New Sphingolipid and Furanocoumarins with Antimicrobial Activity from *Ficus exasperata*. *Chemical and Pharmaceutical Bulletin* 60:1072–1075.

Ducarme, P., Rahman, M., and Brasseur, R. (1998). IMPALA: A simple restraint field to simulate the biological membrane in molecular structure studies. *Proteins: Structure, Function and Genetics* 30:357-371.

Eeman, M., and Deleu, M. (2010). From biological membranes to biomimetic model membranes. *Biotechnology Agronomy Society and Environment* 14:719-736.

El Kasmi, F., Chung, E.-H., Anderson, R. G., Li, J., Wan, L., Eitas, T. K., Gao, Z., and Dangl, J. L. (2017). Signalling from the plasma-membrane localized plant immune receptor RPM1 requires self-association of the full-length protein. *Proceedings of the National Academy of Sciences* 114:E7385–E7394.

Epand, R. M., and Epand, R. F. (2011). Bacterial membrane lipids in the action of antimicrobial agents. *Journal of Peptide Science* 17:298–305.

Farias, G. A., Olmedilla, A., and Gallegos, M. T. (2019). Visualization and characterization of *Pseudomonas syringae* pv. *tomato* DC3000 pellicles. *Microbial Biotechnology*. 12:688–702.

Feil, H., Feil, W. S., Chain, P., Larimer, F., DiBartolo, G., Copeland, A., Lykidis, A., Trong, S., Nolan, M., Goltsman, E., *et al.* (2005). Comparison of the complete genome sequences of *Pseudomonas syringae* pv. *syringae* B728a and pv. *tomato* DC3000. *Proceedings of the National Academy of Sciences* 102:11064–11069.

Fett, W. F., and Dunn, M. F. (1989). Exopolysaccharides produced by phytopathogenic *Pseudomonas syringae* pathovars in infected leaves of susceptible hosts. *Plant Physiology*. 89:5–9.

Fischer, C. L., Drake, D. R., Dawson, D. V., Blanchette, D. R., Brogden, K. A., and Wertz, P. W. (2012). Antibacterial activity of sphingoid bases and fatty acids against gram- positive and Gram- negative bacteria. *Antimicrobial Agents and Chemotherapy* 56:1157–1161.

Franche, A., Fayeulle, A., Lins, L., Billamboz, M., Pezron, I., Deleu, M., and Léonard, E. (2020). Amphiphilic azobenzenes: Antibacterial activities and biophysical investigation of their interaction with bacterial membrane lipids. *Bioorganic Chemistry* 94:103399.

Francis, L. W., Gonzalez, D., Ryder, T., Baer, K., Rees, M., White, J. O., Conlan, R. S., and Wright, C. J. (2010). Optimized sample preparation for high-resolution AFM characterization of fixed human cells: cell sample preparation for AFM characterization. *Journal of Microscopy* 240:111–121.

Furlan, A. L., Buchoux, S., Miao, Y., Banchet, V., Létévé, M., Lambertyn, V., Michel, J., Sarazin, C., and Bonnet, V. (2018). Nanoparticles based on lipidyl-β-cyclodextrins: synthesis, characterization, and experimental and computational biophysical studies for encapsulation of atazanavir. *New Journal of Chemistry*. 42:20171–20179.

Furlan, A. L., Laurin, Y., Botcazon, C., Rodríguez-Moraga, N., Rippa, S., Deleu, M., Lins, L., Sarazin, C., and Buchoux, S. (2020). Contributions and limitations of biophysical approaches to study of the interactions between amphiphilic molecules and the plant plasma membrane. *Plants* 9:648.

Furt, F., Simon-Plas, F., and Mongrand, S. (2011). Lipids of the plant plasma membrane. In *The Plant Plasma Membrane* (ed. Murphy, A. S.), Schulz, B., and Peer, W., pp. 3–30. Berlin, Heidelberg: Springer Berlin Heidelberg.

Gassmann, W., Hinsch, M. E., and Staskawicz, B. J. (1999). The *Arabidopsis* RPS4 bacterial-resistance gene is a member of the TIR-NBS-LRR family of disease-resistance genes. *The Plant Journal* 20:265-277.

Gerbeau-Pissot, P., Der, C., Thomas, D., Anca, I.-A., Grosjean, K., Roche, Y., Perrier-Cornet, J.-M., Mongrand, S., and Simon-Plas, F. (2014). Modification of plasma membrane organization in tobacco cells elicited by cryptogein. *Plant Physiology* 164:273–286.

Ghai, R., Falconer, R. J., and Collins, B. M. (2012). Applications of isothermal titration calorimetry in pure and applied research-survey of the literature from 2010: survey of recent applications of ITC. *Journal of Molecular Recognition*. 25:32–52.

Gilliard, G., Huby, E., Cordelier, S., Ongena, M., Dhondt-Cordelier, S., and Deleu, M. (2021). Protoplast: A valuable toolbox to investigate plant stress perception and response. *Frontiers in Plant Science*. 12:749581.

Gimenez-Ibanez, S., Ntoukakis, V., and Rathjen, J. P. (2009). The LysM receptor kinase CERK1 mediates bacterial perception in *Arabidopsis*. *Plant Signalling & Behavior* 4:539–541.

Ginocchio, C., Olmsted, S., Wells, C., and Galan, J. (1994). Contact with epithelial cells induces the formation of surface appendages on Salmonella typhimurium. *Cell* 76:717–724.

Glawischnig, E. (2007). Camalexin. *Phytochemistry* 68:401–406.

Glazebrook, J. (2005). Contrasting mechanisms of defence against biotrophic and necrotrophic pathogens. *Annual Review of Phytopathology* 43:205–227.

Glazebrook, J., and Ausubel, F. M. (1994). Isolation of phytoalexin-deficient mutants of *Arabidopsis thaliana* and characterization of their interactions with bacterial pathogens. *Proceedings of the National Academy of Sciences* 91:8955–8959.

Glenz, R., Schmalhaus, D., Krischke, M., Mueller, M. J., and Waller, F. (2019). Elevated levels of phosphorylated sphingobases do not antagonize sphingobase or fumonisin b1-induced plant cell death. *Plant and Cell Physiology* 60:1109–1119.

Glenz, R., Kaiping, A., Göpfert, D., Weber, H., Lambour, B., Sylvester, M., Fröschel, C., Mueller, M. J., Osman, M., and Waller, F. (2022). The major plant sphingolipid long chain base phytosphingosine inhibits growth of bacterial and fungal plant pathogens. *Sci Rep* 12:1081.

Gomila, M., Busquets, A., Mulet, M., García-Valdés, E., and Lalucat, J. (2017). Clarification of taxonomic status within the *Pseudomonas syringae* species group based on a phylogenomic analysis. *Frontiers in Microbiology*. 8:2422.

Goñi, F. M., and Alonso, A. (2006). Biophysics of sphingolipids. Membrane properties of sphingosine, ceramides and other simple sphingolipids. *Biochimica et Biophysica Acta (BBA) - Biomembranes* 1758:1902–1921.

Govrin, E. M., and Levine, A. (2000). The hypersensitive response facilitates plant infection by the necrotrophic pathogen *Botrytis cinerea*. *Current Biology* 10:751–757.

Grant, M., Godiard, L., Straube, E., Ashfield, T., Lewald, J., Sattler, A., Innes, R., and Dangl, J. (1995). Structure of the *Arabidopsis* RPM1 gene enabling dual specificity disease resistance. *Science* 269:843–846.

Grennan, A. K. (2007). Lipid rafts in plants. *Plant Physiology*. 143:1083–1085.

Gronnier, J., Germain, V., Gouguet, P., Cacas, J.-L., and Mongrand, S. (2016). GIPC: Glycosyl Inositol Phospho Ceramides, the major sphingolipids on earth. *Plant Signalling & Behavior* 11:e1152438.

Gronnier, J., Gerbeau-Pissot, P., Germain, V., Mongrand, S., and Simon-Plas, F. (2018). Divide and rule: plant plasma membrane organization. *Trends in Plant Science* 23:899–917.

Grosjean, K., Mongrand, S., Beney, L., Simon-Plas, F., and Gerbeau-Pissot, P. (2015). Differential effect of plant lipids on membrane organization: specificities of phytosphingolipids and phytosterols. *J. Biol. Chem.* 290:5810–5825.

Guerineau, F., Benjdia, M., and Zhou, D. X. (2003). A jasmonate-responsive element within the *A. thaliana* vsp1 promoter. *Journal of Experimental Botany* 54:1153–1162.

Gullino, M. L., Albajes, R., Al-Jboory, I., Angelotti, F., Chakraborty, S., Garrett, K. A., Hurley, B. P., Juroszek, P., Makkouk, K., Pan, X., *et al.* (2021). *Scientific review of the impact of climate change on plant pests*. FAO on behalf of the IPPC Secretariat.

Gururaj, C., Federman, R., and Chang, A. (2013). Orm proteins integrate multiple signals to maintain sphingolipid homeostasis. *Journal of Biological Chemistry*. 288:20453–20463.

Gutiérrez-Nájera, N. A., Saucedo-García, M., Noyola-Martínez, L., Vázquez-Vázquez, C., Palacios-Bahena, S., Carmona-Salazar, L., Plasencia, J., El-Hafidi, M., and Gavilanes-Ruiz, M. (2020). Sphingolipid effects on the plasma membrane produced by addition of fumonisin b1 to maize embryos. *Plants* 9:150.

Haefele, D. M., and Lindow, S. E. (1987). Flagellar Motility Confers Epiphytic Fitness Advantages upon *Pseudomonas syringae*. *Applied Environmental Microbiology* 53:2528–2533.

Halliwell, B. (2006). Reactive species and antioxidants. redox biology is a fundamental theme of aerobic life. *Plant Physiology* 141:312–322.

Hannun, Y. A., and Obeid, L. M. (2008). Principles of bioactive lipid signalling: lessons from sphingolipids. *Nature Reviews Molecular Cell Biology* 9:139–150.

Hao, H., Fan, L., Chen, T., Li, R., Li, X., He, Q., Botella, M. A., and Lin, J. (2014). Clathrin and membrane microdomains cooperatively regulate RbohD dynamics and activity in *Arabidopsis*. *The Plant Cell* 26:1729–1745.

Harris, F. M., Best, K. B., and Bell, J. D. (2002). Use of laurdan fluorescence intensity and polarization to distinguish between changes in membrane fluidity and phospholipid order. *Biochimica et Biophysica Acta (BBA) - Biomembranes* 1565:123–128.

Hawkins, N. J., Bass, C., Dixon, A., and Neve, P. (2019). The evolutionary origins of pesticide resistance: The evolutionary origins of pesticide resistance. *Biological Review* 94:135–155.

He, S. Y., and Collmer, A. (1993). *Pseudomonas syringae* pv. *syringae* harpin P: A protein that is secreted via the hrp pathway and elicits the hypersensitive response in plants. *Cell* 73:1255–1266.

Heath, M. C. (2000). Nonhost resistance and nonspecific plant defences. *Current Opinion in Plant Biology* 3:315–319.

Heck, S., Grau, T., Buchala, A., Metraux, J.-P., and Nawrath, C. (2003). Genetic evidence that expression of NahG modifies defence pathways independent of salicylic acid biosynthesis in the *Arabidopsis-Pseudomonas syringae* pv. *tomato* interaction. *The Plant Journal* 36:342–352.

Heerklotz, H., and Seelig, J. (2000). Titration calorimetry of surfactant–membrane partitioning and membrane solubilization. *Biochimica et Biophysica Acta (BBA) - Biomembranes* 1508:69–85.

Helenius, A., and Simons, K. (1975). Solubilization of membranes by detergents. *Biochimica et Biophysica Acta (BBA) - Reviews on Biomembranes* 415:29–79.

Henry, G., Deleu, M., Jourdan, E., Thonart, P., and Ongena, M. (2011). The bacterial lipopeptide surfactin targets the lipid fraction of the plant plasma membrane to trigger immune-related defence responses: Surfactin perception by plant cells. *Cellular Microbiology* 13:1824–1837.

Henry, E., Toruño, T. Y., Jauneau, A., Deslandes, L., and Coaker, G. (2017). Direct and indirect visualization of bacterial effector delivery into diverse plant cell types during infection. *Plant Cell* 29:1555–1570.

Herrfurth, C., and Feussner, I. (2020). Quantitative jasmonate profiling using a high-throughput UPLC-NanoESI-MS/MS Method. In *Jasmonate in Plant Biology: Methods and Protocols* (ed. Champion, A.) Laplaze, L., pp. 169–187. New York, NY: Springer US.

Hirano, S. S. (1985). Ecology and physiology of *Pseudomonas syringae. Nature Biotechnology* 3:1073–1078.

Hirano, S. S., and Upper, C. D. (2000). Bacteria in the leaf ecosystem with emphasis on *Pseudomonas syringae*—a pathogen, ice nucleus, and epiphyte. *Microbiology and Molecular Biology Reviews* 64:624–653.

Hojjati, M. R., Li, Z., and Jiang, X.-C. (2005). Serine palmitoyl-CoA transferase (SPT) deficiency and sphingolipid levels in mice. *Biochimica et Biophysica Acta (BBA) - Molecular and Cell Biology of Lipids* 1737:44–51.

Hotinger, J. A., Pendergrass, H. A., and May, A. E. (2021). Molecular Targets and strategies for inhibition of the bacterial type iii secretion system (t3ss); inhibitors directly binding to t3ss components. *Biomolecules* 11:316.

Hu, J., Worrall, L. J., Hong, C., Vuckovic, M., Atkinson, C. E., Caveney, N., Yu, Z., and Strynadka, N. C. J. (2018). Cryo-EM analysis of the T3S injectisome reveals the structure of the needle and open secretin. *Nature Communications* 9:3840.

Huang, H., Ullah, F., Zhou, D.-X., Yi, M., and Zhao, Y. (2019). Mechanisms of ROS Regulation of Plant Development and Stress Responses. *Frontiers in Plant Science* 10:800.

Huby, E., Napier, J. A., Baillieul, F., Michaelson, L. V., and Dhondt-Cordelier, S. (2020). Sphingolipids: towards an integrated view of metabolism during the plant stress response. *New Phytologist* 225:659–670.

Hwang, M. S. H., Morgan, R. L., Sarkar, S. F., Wang, P. W., and Guttman, D. S. (2005). Phylogenetic characterization of virulence and resistance phenotypes of *Pseudomonas syringae. Applied Environmental Microbiology* 71:5182–5191.

Ishikawa, T., Aki, T., Yanagisawa, S., Uchimiya, H., and Kawai-Yamada, M. (2015). Overexpression of BAX INHIBITOR-1 links plasma membrane microdomain proteins to stress. *Plant Physiology* 169:1333–1343.

Islam, S. (2017). Isolation and biochemical characterization of *Pseudomonas syringae* causing citrus blast disease and its sensitivity test against some antibiotics. *International Journal of Scientific & Engineering Research* 8:7.

Jacob, C., Panchal, S., and Melotto, M. (2017). Surface Inoculation and quantification of *Pseudomonas syringae* population in the *Arabidopsis* leaf apoplast. *Bio-protocol* 7.

Jeworutzki, E., Roelfsema, M. R. G., Anschütz, U., Krol, E., Elzenga, J. T. M., Felix, G., Boller, T., Hedrich, R., and Becker, D. (2010). Early signalling through the *Arabidopsis* pattern recognition receptors FLS2 and EFR involves Ca^{2+}-associated opening of plasma membrane anion channels. *The Plant Journal* 62:367–378.

Jiang, G.-F., Jiang, B. L., Yang, M., Liu, S., Liu, J., Liang, X. X., Bai, X.-F., Tang, D. J., Lu, G. T., He, Y. Q., *et al.* (2013). Establishment of an inducing medium for type III effector secretion in *Xanthomonas campestris* pv. *campestris*. *Brazilian Journal of Microbiology* 44:945–952.

Jin, Q., and He, S.-Y. (2001). Role of the Hrp Pilus in Type III Protein Secretion in *Pseudomonas syringae*. *Science* 294:4.

Johansson, O. N., Fahlberg, P., Karimi, E., Nilsson, A. K., Ellerström, M., and Andersson, M. X. (2014). Redundancy among phospholipase D isoforms in resistance triggered by recognition of the *Pseudomonas syringae* effector AvrRpm1 in *Arabidopsis thaliana*. *Frontiers in Plant Science*. 5:639.

Johansson, O. N., Nilsson, A. K., Gustavsson, M. B., Backhaus, T., Andersson, M. X., and Ellerström, M. (2015). A quick and robust method for quantification of the hypersensitive response in plants. *PeerJ* 3:e1469.

Jones, J. D. G., and Dangl, J. L. (2006). The plant immune system. *Nature* 444:323–329.

Jung, B.-O., Kim, C.-H., Choi, K.-S., Lee, Y. M., and Kim, J.-J. (1999). Preparation of amphiphilic chitosan and their antimicrobial activities. *Journal of Applied Polymer Science*. 72:1713–1719.

Kadota, Y., Shirasu, K., and Zipfel, C. (2015). Regulation of the NADPH oxidase RBOHD during plant immunity. *Plant and Cell Physiology* 56:1472–1480.

Kaplan, I., Halitschke, R., Kessler, A., Sardanelli, S., and Denno, R. F. (2008). Constitutive and induced defences to herbivory in above- and belowground plant tissues. *Ecology* 89:392–406.

Kärkönen, A., and Kuchitsu, K. (2015). Reactive oxygen species in cell wall metabolism and development in plants. *Phytochemistry* 112:22–32.

Katagiri, F., Thilmony, R., and He, S. Y. (2002). The *Arabidopsis thaliana-Pseudomonas syringae* interaction. *The Arabidopsis Book* 1:e0039.

Kawasaki, T., Nam, J., Boyes, D. C., Holt, B. F., Hubert, D. A., Wiig, A., and Dangl, J. L. (2005). A duplicated pair of *Arabidopsis* RING-finger E3 ligases contribute to the RPM1- and RPS2-mediated hypersensitive response: Transmembrane RING-E3 ligases and the HR. *The Plant Journal* 44:258–270.

Kim, M. G., da Cunha, L., McFall, A. J., Belkhadir, Y., DebRoy, S., Dangl, J. L., and Mackey, D. (2005). Two *Pseudomonas syringae* Type III Effectors Inhibit RIN4-Regulated Basal Defense in *Arabidopsis*. *Cell* 121:749–759.

Kim, M. G., Geng, X., Lee, S. Y., and Mackey, D. (2009). The *Pseudomonas syringae* type III effector AvrRpm1 induces significant defences by activating the *Arabidopsis* nucleotide-binding leucine-rich repeat protein RPS2. *The Plant Journal* 57:645–653.

Kimberlin, A. N., Han, G., Chen, M., Cahoon, R. E., Luttgeharm, K. D., Stone, J. M., Markham, J. E., Dunn, T. M., and Cahoon, E. B. (2016). ORM expression alters sphingolipid homeostasis and differentially affects ceramide synthase activities. *Plant Physiology* 172:889-900.

Klemptner, R. L., Sherwood, J. S., Tugizimana, F., Dubery, I. A., and Piater, L. A. (2014). Ergosterol, an orphan fungal microbe-associated molecular pattern (MAMP): Ergosterol as a MAMP. *Molecular Plant Pathology* 15:747–761.

Klymchenko, A. S. (2017). Solvatochromic and fluorogenic dyes as environment-sensitive probes : design and biological applications. *Accounts of chemical research* 50:366–375.

Klymchenko, A. S., and Kreder, R. (2014). Fluorescent probes for lipid rafts: From model membranes to living cells. *Chemistry and Biology* 21:97–113.

König, S., Feussner, K., Schwarz, M., Kaever, A., Iven, T., Landesfeind, M., Ternes, P., Karlovsky, P., Lipka, V., and Feussner, I. (2012). *Arabidopsis* mutants of sphingolipid fatty acid α-hydroxylases accumulate ceramides and salicylates. *New Phytologist* 196:1086–1097.

König, S., Gömann, J., Zienkiewicz, A., Zienkiewicz, K., Meldau, D., Herrfurth, C., and Feussner, I. (2021). Sphingolipid-Induced programmed cell death is a salicylic acid and eds1-dependent phenotype in *Arabidopsis*. Bioarchive.

Kutschera, A., Dawid, C., Gisch, N., Schmid, C., Raasch, L., Gerster, T., Schäffer, M., Smakowska-Luzan, E., Belkhadir, Y., Vlot, A. C., *et al.* (2019). Bacterial medium-chain 3-hydroxy fatty acid metabolites trigger immunity in *Arabidopsis* plants. *Science* 364:178–181.

Kvitko, B. H., Ramos, A. R., Morello, J. E., Oh, H.-S., and Collmer, A. (2007). Identification of Harpins in *Pseudomonas syringae* pv. *tomato* DC3000, which are functionally similar to hrpk1 in promoting translocation of type III secretion system effectors. *Journal of Bacteriology* 189:8059–8072.

Lachaud, C., Da Silva, D., Cotelle, V., Thuleau, P., Xiong, T. C., Jauneau, A., Brière, C., Graziana, A., Bellec, Y., Faure, J.-D., *et al.* (2010). Nuclear calcium controls the apoptotic-like cell death induced by d-erythro-sphinganine in tobacco cells. *Cell Calcium* 47:92–100.

Le, M. T., Litzenberger, J., and Prenner, E. (2011). Biomimetic model membrane systems serve as increasingly valuable *in vitro* tools. In *Advances in Biomimetics* (ed. George, A.), p. InTech.

Lebecque, S., Crowet, J.-M., Lins, L., Delory, B. M., du Jardin, P., Fauconnier, M.-L., and Deleu, M. (2018). Interaction between the barley allelochemical compounds gramine and hordenine and artificial lipid bilayers mimicking the plant plasma membrane. *Sci Rep* 8:9784.

Leborgne-Castel, N., Lherminier, J., Der, C., Fromentin, J., Houot, V., and Simon-Plas, F. (2008). The Plant Defense Elicitor cryptogein stimulates clathrin-mediated endocytosis correlated with reactive oxygen species production in bright Yellow-2 tobacco cells. *Plant Physiology* 146:1255–1266.

Lee, C. C., Wood, M. D., Ng, K., Andersen, C. B., Liu, Y., Luginbühl, P., Spraggon, G., and Katagiri, F. (2004). Crystal structure of the type III effector AvrB from *Pseudomonas syringae*. *Structure* 12:487–494.

Lee, D., Bourdais, G., Yu, G., Robatzek, S., and Coaker, G. (2015). Phosphorylation of the plant immune regulator RPM1-INTERACTING PROTEIN4 enhances plant plasma membrane H⁺-ATPase activity and inhibits flagellin-triggered immune responses in *Arabidopsis*. *The Plant Cell* 27:2042–2056.

Lenarcic, T., Albert, I., Böhm, H., Hodnik, V., Pirc, K., Zavec, A. B., Podobnik, M., Pahovnik, D., Ema, Ž., Pruitt, R., *et al.* (2017). Eudicot plant-specific sphingolipids determine host selectivity of microbial NLP cytolysins. *Science* 358:1431–1434.

Lenarčič, T., Albert, I., Böhm, H., Hodnik, V., Pirc, K., Zavec, A. B., Podobnik, M., Pahovnik, D., Žagar, E., Pruitt, R., *et al.* (2017). Eudicot plant-specific sphingolipids determine host selectivity of microbial NLP cytolysins. *Science* 358:1431–1434.

Leon-Reyes, A., Van der Does, D., De Lange, E. S., Delker, C., Wasternack, C., Van Wees, S. C. M., Ritsema, T., and Pieterse, C. M. J. (2010). Salicylate-mediated suppression of jasmonate-responsive gene expression in *Arabidopsis* is targeted downstream of the jasmonate biosynthesis pathway. *Planta* 232:1423–1432.

Lherminier, J., Elmayan, T., Fromentin, J., Elaraqui, K. T., Vesa, S., Morel, J., Verrier, J.-L., Cailleteau, B., Blein, J.-P., and Simon-Plas, F. (2009). NADPH oxidase-mediated reactive oxygen species production: subcellular localization and reassessment of its role in plant defence. *Molecular Plant Microbe Interactions* 22:868–881.

Li, J., and Wang, X. (2019). Phospholipase D and phosphatidic acid in plant immunity. *Plant Science* 279:45–50.

Li, J., Yin, J., Rong, C., Li, K.-E., Wu, J.-X., Huang, L.-Q., Zeng, H.-Y., Sahu, S. K., and Yao, N. (2016). Orosomucoid proteins interact with the small subunit of serine

palmitoyltransferase and contribute to sphingolipid homeostasis and stress responses in *Arabidopsis*. *The Plant Cell* 28:3038–3051.

Li, N., Han, X., Feng, D., Yuan, D., and Huang, L.-J. (2019). Signalling crosstalk between salicylic acid and ethylene/jasmonate in plant defence: do we understand what they are whispering? *IJMS* 20:671.

Liang, H. (2003). Ceramides modulate programmed cell death in plants. *Genes & Development* 17:2636–2641.

Lin, N.-C., and Martin, G. B. (2005). An *AvrPto/AvrPtoB* mutant of *Pseudomonas syringae* pv. *tomato* DC3000 does not elicit pto-mediated resistance and is less virulent on tomato. *Molecular Plant-Microbe Interactions* 18:43–51.

Lindow, S. E., and Brandl, M. T. (2003). Microbiology of the phyllosphere. *Applied environmental microbiology* 69:9.

Lins, L., Brasseur, R., and Malaisse, W. J. (1995). Conformational analysis of non-sulfonylurea hypoglycemic agents of the meglitinide family. *Biochemical Pharmacology* 50:1879–1884.

Liu, J., Elmore, J. M., Fuglsang, A. T., Palmgren, M. G., Staskawicz, B. J., and Coaker, G. (2009). RIN4 functions with plasma membrane H+-ATPases to regulate stomatal apertures during pathogen attack. *PLoS Biology* 7:e1000139.

Liu, Y., Wang, L., Cai, G., Jiang, S., Sun, L., and Li, D. (2013). Response of tobacco to the *Pseudomonas syringae* pv. *tomato* DC3000 is mainly dependent on salicylic acid signalling pathway. *FEMS Microbiology Letters* 344:77–85.

Lohner, K. (2009). New strategies for novel antibiotics: peptides targeting bacterial cell membranes. *Genomics, Proteomics and Bioinformatics* 28:105–116.

Louise Meyer, R., Zhou, X., Tang, L., Arpanaei, A., Kingshott, P., and Besenbacher, F. (2010). Immobilisation of living bacteria for AFM imaging under physiological conditions. *Ultramicroscopy* 110:1349–1357.

Luttgeharm, K. D., Cahoon, E. B., and Markham, J. E. (2016). Substrate specificity, kinetic properties and inhibition by fumonisin B1 of ceramide synthase isoforms from *Arabidopsis*. *Biochemical Journal* 473:593–603.

Lynch, D. V., and Dunn, T. M. (2004). An introduction to plant sphingolipids and a review of recent advances in understanding their metabolism and function. *New phytologist* 161:677–702.

Mackey, D., Holt III, B. F., Wiig, A., and Dangl, J. L. (2002). RIN4 interacts with *Pseudomonas syringae* type III effector molecules and is required for RPM1-mediated resistance in *Arabidopsis*. *Cell* 108:743–754.

Mackey, D., Belkhadir, Y., Alonso, J. M., Ecker, J. R., and Dangl, J. L. (2003). *Arabidopsis* RIN4 is a target of the type III virulence effector AvrRpt2 and modulates RPS2-Mediated resistance. *Cell* 112:379–389.

Magnin-Robert, M., Le Bourse, D., Markham, J. E., Dorey, S., Clément, C., Baillieul, F, and Dhondt-Cordelier, S. (2015). Modifications of sphingolipid content affect tolerance to hemibiotrophic and necrotrophic pathogens by modulating plant defence responses in *Arabidopsis*. *Plant Physiology* 169:2255-2273.

Maherani, B., Arab-Tehrany, E., Kheirolomoom, A., Geny, D., and Linder, M. (2013). Calcein release behavior from liposomal bilayer; influence of physicochemical/ mechanical/ structural properties of lipids. *Biochimie* 95:2018–2033.

Mamode Cassim, A., Gouguet, P., Gronnier, J., Laurent, N., Germain, V., Grison, M., Boutté, Y., Gerbeau-Pissot, P., Simon-Plas, F., and Mongrand, S. (2019). Plant lipids: Key players of plasma membrane organization and function. *Progress in Lipid Research* 73:1–27.

Marcec, M. J., Gilroy, S., Poovaiah, B. W., and Tanaka, K. (2019). Mutual interplay of Ca^{2+} and ROS signalling in plant immune response. *Plant Science* 283:343–354.

Markham, J. E., and Jaworski, J. G. (2007). Rapid measurement of sphingolipids from *Arabidopsis thaliana* by reversed-phase high-performance liquid chromatography coupled to electrospray ionization tandem mass spectrometry. *Rapid Communications in Mass Spectrometry* 21:1304–1314.

Markham, J. E., Lynch, D. V., Napier, J. A., Dunn, T. M., and Cahoon, E. B. (2013). Plant sphingolipids: function follows form. *Current Opinion in Plant Biology* 16:350–357.

Marsh, D. (1996). Lateral pressure in membranes. *Biochimica et Biophysica Acta (BBA) - Reviews on Biomembranes* 1286:183–223.

Martinez-Medina, A., Flors, V., Heil, M., Mauch-Mani, B., Pieterse, C. M. J., Pozo, M. J., Ton, J., van Dam, N. M., and Conrath, U. (2016). Recognizing plant defence priming. *Trends in Plant Science* 21:818–822.

Mary, J. K. L., Le, T., Prenner E. J., (2011). Biomimetic model membrane systems serve as increasingly valuable *in vitro* tools, in: Marko Cavrak (Ed.), *Advances in Biomimetics*, InTech,pp. 252–269

Matteï, P.-J., Faudry, E., Job, V., Izoré, T., Attree, I., and Dessen, A. (2011). Membrane targeting and pore formation by the type III secretion system translocon: Membrane targeting and pore formation by the T3SS. *FEBS Journal* 278:414–426.

Matzrafi, M. (2019). Climate change exacerbates pest damage through reduced pesticide efficacy. *Pest Management Science*. 75:9–13.

McShan, A. C., and De Guzman, R. N. (2015). The bacterial type III secretion system as a target for developing new antibiotics. *Chemical Biology and Drug Design* 85:30–42.

Melotto, M., Underwood, W., Koczan, J., Nomura, K., and He, S. Y. (2006). Plant stomata function in innate immunity against bacterial invasion. *Cell* 126:969–980.

Melotto, M., Underwood, W., and He, S. Y. (2008). Role of Stomata in Plant Innate Immunity and Foliar Bacterial Diseases. *Annual Reviews of Phytopathology*. 46:101–122.

Melotto, M., Zhang, L., Oblessuc, P. R., and He, S. Y. (2017). Stomatal defence a decade later. *Plant Physiology* 174:561–571.

Merrill, A. H. (2011). Sphingolipid and glycosphingolipid metabolic pathways in the era of sphingolipidomics. *Chemical Reviews* 111:6387–6422.

Mithöfer, A., and Mazars, C. (2002). Aequorin-based measurements of intracellular Ca2+- signatures in plant cells. *Biological Procedures Online* 4:105–118.

Miya, A., Albert, P., Shinya, T., Desaki, Y., Ichimura, K., Shirasu, K., Narusaka, Y., Kawakami, N., Kaku, H., and Shibuya, N. (2007). CERK1, a LysM receptor kinase, is essential for chitin elicitor signalling in *Arabidopsis*. *Proc. Natl. Acad. Sci. U.S.A.* 104:19613–19618.

Mongrand, S., Morel, J., Laroche, J., Claverol, S., Carde, J.-P., Hartmann, M.-A., Bonneu, M., Simon-Plas, F., Lessire, R., and Bessoule, J.-J. (2004). Lipid rafts in higher plant cells: purification and characterization of triton x-100-insoluble microdomains from tobacco plasma membrane. *Journal of Biological Chemistry*. 279:36277–36286.

Mongrand, S., Stanislas, T., Bayer, E. M. F., Lherminier, J., and Simon-Plas, F. (2010). Membrane rafts in plant cells. *Trends in Plant Science* 15:656–663.

Monnier, N., Furlan, A., Buchoux, S., Deleu, M., Dauchez, M., Rippa, S., and Sarazin, C. (2019). Exploring the dual interaction of natural rhamnolipids with plant and fungal biomimetic plasma membranes through biophysical studies. *IJMS* 20:1009.

Moore, B. D., and Johnson, S. N. (2017). Get tough, get toxic, or get a bodyguard: identifying candidate traits conferring belowground resistance to herbivores in grasses. *Frontiers in Plant Science*. 7.

Moore, L. W., and Pscheidt, J. W. (2018). Diseases Caused by *Pseudomonas syringae*. *Pacific Northwest Plant Disease Management Handbook*.

Moore, R. A., Starratt, A. N., Ma, S.-W., Morris, V. L., and Cuppels, D. A. (1989). Identification of a chromosomal region required for biosynthesis of the phytotoxin coronatine by *Pseudomonas syringae* pv. *tomato*. *Canadian Journal of Microbiology*. 35:910–917.

Morandat, S., Azouzi, S., Beauvais, E., Mastouri, A., and El Kirat, K. (2013). Atomic force microscopy of model lipid membranes. *Analytical and Bioanalytical Chemistry* 405:1445–1461.

Mudgett, M. B., and Staskawicz, B. J. (1999). Characterization of the *Pseudomonas syringae* pv. *tomato* AvrRpt2 protein: demonstration of secretion and processing during bacterial pathogenesis. *Molecular microbiology* 32:927–941.

Mur, L. A. J., Kenton, P., Atzorn, R., Miersch, O., and Wasternack, C. (2006). The outcomes of concentration-specific interactions between salicylate and jasmonate signalling include synergy, antagonism, and oxidative stress leading to cell death. *Plant Physiology*. 140:249–262.

Murai, Y., Yuyama, K., Mikami, D., Igarashi, Y., and Monde, K. (2022). Penta-deuterium-labeled 4E, 8Z-sphingadienine for rapid analysis in sphingolipidomics study. *Chemistry and Physics of Lipids* 245:105202.

Nagano, M., Takahara, K., Fujimoto, M., Tsutsumi, N., Uchimiya, H., and Kawai-Yamada, M. (2012). *Arabidopsis* sphingolipid fatty acid 2-hydroxylases (AtFAH1 and AtFAH2) are functionally differentiated in fatty acid 2-hydroxylation and stress responses. *Plant Physiology* 159:1138–1148.

Nagano, M., Ishikawa, T., Fujiwara, M., Fukao, Y., Kawano, Y., Kawai-Yamada, M., and Shimamoto, K. (2016). Plasma membrane microdomains are essential for Rac1-RbohB/H-mediated immunity in rice. *The Plant Cell* 28:1966–1983.

Nasir, M. N., Thawani, A., Kouzayha, A., and Besson, F. (2010). Interactions of the natural antimicrobial mycosubtilin with phospholipid membrane models. *Colloids and Surfaces B: Biointerfaces* 78:17–23.

Nasir, M. N., Crowet, J.-M., Lins, L., Obounou Akong, F., Haudrechy, A., Bouquillon, S., and Deleu, M. (2016). Interactions of sugar-based bolaamphiphiles with biomimetic systems of plasma membranes. *Biochimie* 130:23–32.

Nasir, M. N., Lins, L., Crowet, J.-M., Ongena, M., Dorey, S., Dhondt-Cordelier, S., Clément, C., Bouquillon, S., Haudrechy, A., Sarazin, C., *et al.* (2017). Differential Interaction of synthetic glycolipids with biomimetic plasma membrane lipids correlates with the plant biological response. *Langmuir* 33:9979–9987.

Naughton, P. J., Marchant, R., Naughton, V., and Banat, I. M. (2019). Microbial biosurfactants: current trends and applications in agricultural and biomedical industries. *Journal of Applied Microbiology* 127:12–28.

Nawrath, C., and Métraux, J.-P. (1999). Salicylic acid induction–deficient mutants of *Arabidopsis* express PR-2 and PR-5 and accumulate high levels of camalexin after pathogen inoculation. *The Plant Cell* 11:1393–1404.

Ng, D., Abeysinghe, J., and Kamali, M. (2018). Regulating the regulators: the control of transcription factors in plant defence signalling. *IJMS* 19:3737.

Ngou, B. P. M., Ahn, H.-K., Ding, P., and Jones, J. D. G. (2021). Mutual potentiation of plant immunity by cell-surface and intracellular receptors. *Nature* 592:110-115.

Ngou, B. P. M., Ding, P., and Jones, J. D. G. (2022). Thirty years of resistance: Zig-zag through the plant immune system. *The Plant Cell* 34:1447–1478.

Nguyen, Q.-M., Iswanto, A. B. B., Son, G. H., and Kim, S. H. (2021). Recent advances in effector-triggered immunity in plants: new pieces in the puzzle create a different paradigm. *IJMS* 22:4709.

Nicolson, G. L. (2014). The Fluid—Mosaic Model of Membrane Structure: Still relevant to understanding the structure, function and dynamics of biological membranes after more than 40years. *Biochimica et Biophysica Acta (BBA) - Biomembranes* 1838:1451–1466.

Niko, Y., and Klymchenko, A. S. (2021). Emerging solvatochromic push–pull dyes for monitoring the lipid order of biomembranes in live cells. *The Journal of Biochemistry* 170:163–174.

Nimchuk, Z., Marois, E., Kjemtrup, S., Leister, R. T., Katagiri, F., and Dangl, J. L. (2000). Eukaryotic fatty acylation drives plasma membrane targeting and enhances function of several type III effector proteins from *Pseudomonas syringae*. *Cell* 101:353–363.

Nishad, R., Ahmed, T., Rahman, V. J., and Kareem, A. (2020). Modulation of Plant Defense System in Response to Microbial Interactions. *Front. Microbiol.* 11:1298.

O'Brien, J. A., Daudi, A., Butt, V. S., and Paul Bolwell, G. (2012). Reactive oxygen species and their role in plant defence and cell wall metabolism. *Planta* 236:765–779.

Olsen, I., and Jantzen, E. (2001). Sphingolipids in Bacteria and Fungi. *Anaerobe* 7:103–112.

Ongena, M., and Jacques, P. (2008). *Bacillus* lipopeptides: versatile weapons for plant disease biocontrol. *Trends in microbiology* 16:115–125.

Parasassi, T., and Gratton, E. (1995). Membrane lipid domains and dynamics as detected by Laurdan fluorescence. *Journal of Fluorescence* 5:59–69.

Parasassi, T., De Stasio, G., Ravagnan, G., Rusch, R. M., and Gratton, E. (1991). Quantitation of lipid phases in phospholipid vesicles by the generalized polarization of Laurdan fluorescence. *Biophysical Journal* 60:179–189.

Park, E., Lee, H.-Y., Woo, J., Choi, D., and Dinesh-Kumar, S. P. (2017). Spatiotemporal monitoring of *Pseudomonas syringae* effectors via type III Secretion using split fluorescent protein fragments. *The Plant Cell* 29:1571–1584.

Parsons, J. B., Yao, J., Frank, M. W., Jackson, P., and Rock, C. O. (2012). Membrane disruption by antimicrobial fatty acids releases low-molecular-weight proteins from *Staphylococcus aureus*. *Journal of Bacteriology* 194:5294–5304.

Pata, M. O., Hannun, Y. A., and Ng, C. K.-Y. (2010). Plant sphingolipids: decoding the enigma of the Sphinx: Tansley review. *New Phytologist* 185:611–630.

Peck, S. C., Nühse, T. S., Hess, D., Iglesias, A., Meins, F., and Boller, T. (2001). Directed Proteomics Identifies a Plant-Specific Protein Rapidly Phosphorylated in Response to Bacterial and Fungal Elicitors. *The Plant Cell* 13:1467-1471.

Peer, M., Stegmann, M., Mueller, M. J., and Waller, F. (2010). *Pseudomonas syringae* infection triggers de novo synthesis of phytosphingosine from sphinganine in *Arabidopsis thaliana*. *FEBS Letters* 584:4053–4056.

Penninckx, I. A. M. A., Thomma, B. P. H. J., Buchala, A. J., Métraux, J.-P., and Broekaert, W. F. (1998). Concomitant activation of jasmonate and ethylene response pathways is required for induction of a plant defensin gene in *Arabidopsis*. *The Plant Cell* 10:2103–2213.

Petnicki-Ocwieja, T., van Dijk, K., and Alfano, J. R. (2005). The hrpK Operon of *Pseudomonas syringae* pv. *tomato* DC3000 encodes two proteins secreted by the type III (Hrp) protein secretion system: HopB1 and HrpK, a putative type III translocator. *Journal of Bacteriologogy* 187:649–663.

Pewzner-Jung, Y., Tavakoli Tabazavareh, S., Grassmé, H., Becker, K. A., Japtok, L., Steinmann, J., Joseph, T., Lang, S., Tuemmler, B., Schuchman, E. H., *et al.* (2014). Sphingoid long chain bases prevent lung infection by *Pseudomonas aeruginosa*. *EMBO Molecular Medicine* 6:1205–1214.

Pierre, M., Traverso, J. A., Boisson, B., Domenichini, S., Bouchez, D., Giglione, C., and Meinnel, T. (2007). *N* -Myristoylation regulates the SnRK1 pathway in *Arabidopsis*. *Plant Cell* 19:2804–2821.

Pieterse, C. M. J., and van Loon, L. C. (1996). Systemic resistance in *Arabidopsis* induced by biocontrol bacteria is independent of salicylic acid accumulation and pathogenesis-related gene expression. *The Plant Cell* 8:1225–1237.

Pinkart, H. C., and White, D. C. (1998). Lipids of *Pseudomonas*. In *Pseudomonas* (ed. Montie, T. C.), pp. 111–138. Boston, MA: Springer US.

Pottinger, S. E., and Innes, R. W. (2020). RPS5-mediated disease resistance: fundamental insights and translational applications. *Annual Reviews of Phytopathology*. 58:annurev-phyto-010820-012733.

Pruitt, R. N., Gust, A. A., and Nürnberger, T. (2021). Plant immunity unified. *Nat. Plants* 7:382–383.

Qi, J., Wang, J., Gong, Z., and Zhou, J. M. (2017). Apoplastic ROS signalling in plant immunity. *Current Opinion in Plant Biology* 38:92–100.

Qiu, J. L., Fiil, B. K., Petersen, K., Nielsen, H. B., Botanga, C. J., Thorgrimsen, S., Palma, K., Suarez-Rodriguez, M. C., Sandbech-Clausen, S., Lichota, J., *et al.* (2008). *Arabidopsis* MAP kinase 4 regulates gene expression through transcription factor release in the nucleus. *EMBO Journal* 27:2214–2221.

Quiñones, B., Dulla, G., and Lindow, S. E. (2005). Quorum sensing regulates exopolysaccharide production, motility, and virulence in *Pseudomonas syringae*. *Molecular Plant Microbe Interactions* 18:682–693.

Ramstedt, B., and Slotte, J. P. (2002). Membrane properties of sphingomyelins. *FEBS Letters* 531:33–37.

Ranf, S., Gisch, N., Schäffer, M., Illig, T., Westphal, L., Knirel, Y. A., Sánchez-Carballo, P. M., Zähringer, U., Hückelhoven, R., Lee, J., *et al.* (2015). A lectin S-domain receptor kinase mediates lipopolysaccharide sensing in *Arabidopsis thaliana*. *Nature Immunology* 16:426–433.

Reimer-Michalski, E.-M., and Conrath, U. (2016). Innate immune memory in plants. *Seminars in Immunology* 28:319–327.

Rivera-Sanchez, S. P., Ocampo-Ibáñez, I. D., Liscano, Y., Martínez, N., Muñoz, I., Manrique-Moreno, M., Martinez-Martinez, L., and Oñate-Garzon, J. (2022). Integrating In Vitro and In Silico Analysis of a Cationic Antimicrobial Peptide Interaction with Model Membranes of Colistin-Resistant *Pseudomonas* aeruginosa Strains Advance Access published 2022.

Robert-Seilaniantz, A., Shan, L., Zhou, J. M., and Tang, X. (2006). The *Pseudomonas syringae* pv. *tomato* DC3000 Type III Effector HopF2 has a putative myristoylation site required for its avirulence and virulence functions. *Molecular Plant Microbe Interactions* 19:130–138.

Rogers, E., Glazebrook, J., and Ausubel, F. (1996). Mode of action of the *Arabidopsis thaliana* phytoalexin camalexin and its role in *Arabidopsis*-pathogen interactions. *Molecular Plant Microbe Interaction* 9:748–757.

Rolando, M., and Buchrieser, C. (2019). A comprehensive review on the manipulation of the sphingolipid pathway by pathogenic bacteria. *Frontiers in Cell and Developmental Biology* 7:168.

Rossard, S., Roblin, G., and Atanassova, R. (2010). Ergosterol triggers characteristic elicitation steps in *Beta vulgaris* leaf tissues. *Journal of Experimental Botany* 61:1807–1816.

Russo, S. B., Tidhar, R., Futerman, A. H., and Cowart, L. A. (2013). Myristate-derived d16:0 sphingolipids constitute a cardiac sphingolipid pool with distinct synthetic routes and functional properties. *Journal of Biological Chemistry*. 288:13397–13409.

Sabarwal, A., Kumar, K., and Singh, R. P. (2018). Hazardous effects of chemical pesticides on human health–Cancer and other associated disorders. *Environmental Toxicology and Pharmacology* 63:103–114.

Sagi, M., and Fluhr, R. (2006). Production of reactive oxygen species by plant NADPH oxidases. *Plant Physiology* 141:336–340.

Sanchez, L., Courteaux, B., Hubert, J., Kauffmann, S., Renault, J.-H., Clement, C., Baillieul, F., and Dorey, S. (2012). Rhamnolipids elicit defence responses and induce disease resistance against biotrophic, hemibiotrophic, and necrotrophic pathogens that require different signalling pathways in *Arabidopsis* and highlight a central role for salicylic acid. *Plant Physiology* 160:1630–1641.

Sanchez-Rangel, D., Rivas-San Vicente, M., de la Torre-Hernandez, M. E., Najera-Martinez, M., and Plasencia, J. (2015). Deciphering the link between salicylic acid signalling and sphingolipid metabolism. *Frontiers in Plant Science* 6:125.

Sasaki, H., Arai, H., Cocco, M. J., and White, S. H. (2009). pH dependence of sphingosine aggregation. *Biophysical Journal* 96:2727–2733.

Saucedo-García, M., Gavilanes-Ruíz, M., and Arce-Cervantes, O. (2015). Long-chain bases, phosphatidic acid, MAPKs, and reactive oxygen species as nodal signal transducers in stress responses in *Arabidopsis*. *Frontiers in Plant Science* 6:55.

Saucedo-García, M., Guevara-García, A., González-Solís, A., Cruz-García, F., Vázquez-Santana, S., Markham, J. E., Lozano-Rosas, M. G., Dietrich, C. R., Ramos-Vega, M., Cahoon, E. B., *et al.* (2011). MPK6, sphinganine and the LCB2a gene from serine palmitoyltransferase are required in the signalling pathway that mediates cell death induced by long chain bases in *Arabidopsis*. *New Phytologist* 191:943–957.

Schellenberger, R., Touchard, M., Clément, C., Baillieul, F., Cordelier, S., Crouzet, J., and Dorey, S. (2019). Apoplastic invasion patterns triggering plant immunity: plasma membrane sensing at the frontline. *Molecular Plant Pathology* 20:1602–1616.

Schellenberger, R., Crouzet, J., Nickzad, A., Shu, L.-J., Kutschera, A., Gerster, T., Borie, N., Dawid, C., Cloutier, M., Villaume, S., *et al*. (2021). Bacterial rhamnolipids and their 3-hydroxyalkanoate precursors activate *Arabidopsis* innate immunity through two independent mechanisms. *Proc. Natl. Acad. Sci. U.S.A.* 118:e2101366118.

Shahollari, B., Peskan-Berghofer, T., and Oelmuller, R. (2004). Receptor kinases with leucine-rich repeats are enriched in Triton X-100 insoluble plasma membrane microdomains from plants. *Physiologia Plantarum* 122:397–403.

Shi, L., Bielawski, J., Mu, J., Dong, H., Teng, C., Zhang, J., Yang, X., Tomishige, N., Hanada, K., Hannun, Y. A., *et al*. (2007). Involvement of sphingoid bases in mediating reactive oxygen intermediate production and programmed cell death in *Arabidopsis*. *Cell Research* 17:1030-1040.

Shi, C., Yin, J., Liu, Z., Wu, J.-X., Zhao, Q., Ren, J., and Yao, N. (2015). A systematic simulation of the effect of salicylic acid on sphingolipid metabolism. *Frontiers in Plant Science* 6:186.

Shigenaga, A. M., Berens, M. L., Tsuda, K., and Argueso, C. T. (2017). Towards engineering of hormonal crosstalk in plant immunity. *Current Opinion in Plant Biology* 38:164–172.

Shimanouchi, T., Ishii, H., Yoshimoto, N., Umakoshi, H., and Kuboi, R. (2009). Calcein permeation across phosphatidylcholine bilayer membrane: Effects of membrane fluidity, liposome size, and immobilization. *Colloids and Surfaces B: Biointerfaces* 73:156–160.

Simanshu, D. K., Zhai, X., Munch, D., Hofius, D., Markham, J. E., Bielawski, J., Bielawska, A., Malinina, L., Molotkovsky, J. G., Mundy, J. W., *et al*. (2014). *Arabidopsis* accelerated cell Death 11, ACD11, is a ceramide-1-phosphate transfer protein and intermediary regulator of phytoceramide levels. *Cell Reports* 6:388–399.

Simon-Plas, F., Perraki, A., Bayer, E., and Gerbeau-pissot, P. (2011). An update on plant membrane rafts. *Current Opinion in Plant Biology* 14:642–649.

Singer, S. J., and Nicolson, G. L. (1972). The fluid mosaic model of the structure of cell membranes. *Science* 175:720–731.

Singh, K., Foley, R., C., and Oñate-Sánchez, L. (2002). Transcription factors in plant defence and stress responses. *Current Opinion in Plant Biology* 5:430–436.

Singh, A., Sagar, S., and Biswas, D. K. (2017). Calcium dependent protein kinase, a versatile player in plant stress management and development. *Critical Reviews in Plant Sciences* 36:336–352.

Smith, J. M., and Heese, A. (2014). Rapid bioassay to measure early reactive oxygen species production in *Arabidopsis* leave tissue in response to living *Pseudomonas syringae*. *Plant Methods* 10:6.

Smith, A., Lovelace, A. H., and Kvitko, B. H. (2018). Validation of RT-qPCR approaches to monitor *pseudomonas syringae* gene expression during infection and exposure to pattern-triggered immunity. *Molecular Plant Microbe Interactions* 31:410–419.

Sohlenkamp, C., and Geiger, O. (2016). Bacterial membrane lipids: diversity in structures and pathways. *FEMS Microbiology Reviews* 40:133–159.

Sperling, P., and Heinz, E. (2003). Plant sphingolipids: structural diversity, biosynthesis, first genes and functions. *Biochimica et Biophysica Acta (BBA) - Molecular and Cell Biology of Lipids* 1632:1–15.

Stahl, E., Bellwon, P., Huber, S., Schlaeppi, K., Bernsdorff, F., Vallat-Michel, A., Mauch, F., and Zeier, J. (2016). Regulatory and functional aspects of indolic metabolism in plant systemic acquired resistance. *Molecular Plant* 9:662–681.

Stone, J. M., Heard, J. E., Asai, T., and Ausubel, F. M. (2000). Simulation of fungal-mediated cell death by fumonisin B1 and selection of fumonisin B1-resistant (fbr) *Arabidopsis* mutants. *The Plant Cell* 12:1811–1822.

Sułowicz, S., Cycoń, M., and Piotrowska-Seget, Z. (2016). Non-target impact of fungicide tetraconazole on microbial communities in soils with different agricultural management. *Ecotoxicology* 25:1047–1060.

Tang, F. H. M., Lenzen, M., McBratney, A., and Maggi, F. (2021). Risk of pesticide pollution at the global scale. *Nature Geoscience* 14:206–210.

Thomas, W. J., Thireault, C. A., Kimbrel, J. A., and Chang, J. H. (2009). Recombineering and stable integration of the *Pseudomonas syringae* pv. *syringae* 61 hrp/hrc cluster into the genome of the soil bacterium *Pseudomonas* fluorescens Pf0-1: Stable integration of a T3SS-locus into Pf0-1. *The Plant Journal* 60:919–928.

Topel, Ö., Çakır, B. A., Budama, L., and Hoda, N. (2013). Determination of critical micelle concentration of polybutadiene-block-poly(ethyleneoxide) diblock copolymer by fluorescence spectroscopy and dynamic light scattering. *Journal of Molecular Liquids* 177:40–43.

Torres, M. A. (2010). ROS in biotic interactions. *Physiologia Plantarum* 138:414–429.

Torres, M. A., Jones, J. D. G., and Dangl, J. L. (2005). Pathogen-induced, NADPH oxidase–derived reactive oxygen intermediates suppress spread of cell death in *Arabidopsis thaliana*. *Nature Genetic* 37:1130–1134.

Toruño, T. Y., Shen, M., Coaker, G., and Mackey, D. (2019). Regulated disorder: posttranslational modifications control the RIN4 plant immune signalling hub. *Molecular Plant Microbe Interactions* 32:56–64.

Townley, H. E., McDonald, K., Jenkins, G. I., Knight, M. R., and Leaver, C. J. (2005). Ceramides induce programmed cell death in *Arabidopsis* cells in a calcium-dependent manner. *Biological Chemistry* 386.

Tsegaye, Y., Richardson, C. G., Bravo, J. E., Mulcahy, B. J., Lynch, D. V., Markham, J. E., Jaworski, J. G., Chen, M., Cahoon, E. B., and Dunn, T. M. (2007). *Arabidopsis* mutants lacking long chain base phosphate lyase are fumonisin-sensitive and accumulate trihydroxy-18:1 long chain base phosphate. *Journal of Biological Chemistry* 282:28195–28206.

Ukawa, T., Banno, F., Ishikawa, T., Kasahara, K., Nishina, Y., Inoue, R., Tsujii, K., Yamaguchi, M., Takahashi, T., Fukao, Y., *et al.* (2022). Sphingolipids with 2-hydroxy fatty acids aid in plasma membrane nanodomain organization and oxidative burst. *Plant Physiology* Advance Access published March 21, 2022, doi:10.1093/plphys/kiac134.

Umemura, K., Ogawa, N., Koga, J., Iwata, M., and Usami, H. (2002). Elicitor activity of cerebroside, a sphingolipid elicitor, in cell suspension cultures of rice. *Plant and Cell Physiology* 43:778–784.

Umemura, K., Tanino, S., Nagatsuka, T., Koga, J., Iwata, M., Nagashima, K., and Amemiya, Y. (2004). Cerebroside elicitor confers resistance to *Fusarium* disease in various plant species. *Phytopathology* 94:813–818.

van der Burgh, A. M., and Joosten, M. H. A. J. (2019). Plant immunity: thinking outside and inside the box. *Trends in Plant Science* 24:587–601.

van Meer, G., Voelker, D. R., and Feigenson, G. W. (2008). Membrane lipids: where they are and how they behave. *Nature Reviews Molecular Cell Biology* 9:112–124.

VanEtten, H. D., Mansfield, J. W., Bailey, J. A., and Farmer, E. E. (1994). Two classes of plant antibiotics: phytoalexins versus phytoanticipins. *The Plant Cell* Letter to the Editor 1191-1992.

Vatsa, P., Sanchez, L., Clement, C., Baillieul, F., and Dorey, S. (2010). Rhamnolipid biosurfactants as new players in animal and plant defence against microbes. *IJMS* 11:5095–5108.

Verhaegh, R., Becker, K. A., Edwards, M. J., and Gulbins, E. (2020). Sphingosine kills bacteria by binding to cardiolipin. *Journal of Biological Chemistry* 295:7686–7696.

Verstraeten, S. L., Deleu, M., Janikowska-Sagan, M., Claereboudt, E. J. S., Lins, L., Tyteca, D., and Mingeot-Leclercq, M.-P. (2019). The activity of the saponin ginsenoside Rh2 is enhanced by the interaction with membrane sphingomyelin but depressed by cholesterol. *Scientific Report* 9:7285.

Waite, C., Schumacher, J., Jovanovic, M., Bennett, M., and Buck, M. (2017). Evading plant immunity: feedback control of the T3SS in *Pseudomonas syringae*. *Microbial Cell* 4:137–139.

Wang, J., Liu, X., Zhang, A., Ren, Y., Wu, F., Wang, G., Xu, Y., Lei, C., Zhu, S., Pan, T., *et al.* (2019). A cyclic nucleotide-gated channel mediates cytoplasmic calcium elevation and disease resistance in rice. *Cell Res* 29:820–831.

Wang, L., Mitra, R. M., Hasselmann, K. D., Sato, M., Lenarz-Wyatt, L., Cohen, J. D., Katagiri, F., and Glazebrook, J. (2008). The genetic network controlling the *Arabidopsis* transcriptional response to *Pseudomonas syringae* pv. *maculicola*: roles of major regulators and the phytotoxin coronatine. *Molecular Plant Microbe Interactions* 21:1408–1420.

Wang, X., Wang, Y., Xu, J., and Xue, C. (2021). Sphingolipids in food and their critical roles in human health. *Critical Reviews in Food Science and Nutrition* 61:462–491.

Wei, W., Plovanich-Jones, A., Deng, W.-L., Jin, Q.-L., Collmer, A., Huang, H.-C., and He, S. Y. (2000). The gene coding for the Hrp pilus structural protein is required for type III secretion of Hrp and Avr proteins in *Pseudomonas syringae* pv. *tomato*. *Proceedings of the National Academy of Sciences* 97:2247–2252.

Wei, H.-L., Zhang, W., and Collmer, A. (2018). Modular study of the type III effector repertoire in *Pseudomonas syringae* pv. *tomato* DC3000 reveals a matrix of effector interplay in pathogenesis. *Cell Reports* 23:1630–1638.

Whalen, M. C., Innes, R. W., Bent, A. F., and Staskawicz, B. J. (1991). Identification of *Pseudomonas syringae* pathogens of *Arabidopsis* and a bacterial locus determining avirulence on both *Arabidopsis* and soybean. *The Plant Cell* 3:49–59.

Wirthmueller, L., Zhang, Y., Jones, J. D. G., and Parker, J. E. (2007). Nuclear accumulation of the *Arabidopsis* immune receptor RPS4 is necessary for triggering EDS1-Dependent defence. *Current Biology* 17:2023–2029.

Woestyn, S., Allaoui, A., Wattiau, P., and Cornelis, G. R. (1994). YscN, the putative energizer of the *Yersinia* Yop secretion machinery. *Journal of Bacteriology* 176:1561–1569.

Worrall, L. J., Lameignere, E., and Strynadka, N. C. (2011). Structural overview of the bacterial injectisome. *Current Opinion in Microbiology* 14:3–8.

Wu, Y., Liu, Y., Gulbins, E., and Grassmé, H. (2021). The anti-infectious role of sphingosine in microbial diseases. *Cells* 10:1105.

Xin, X.-F., and He, S. Y. (2013). *Pseudomonas syringae* pv. *tomato* DC3000: A model pathogen for probing disease susceptibility and hormone signalling in plants. *Annual Reviews of Phytopathology*. 51:473–498.

Xin, X.-F., Kvitko, B., and He, S. Y. (2018). *Pseudomonas syringae*: what it takes to be a pathogen. *Nature Reviews Microbiology* 16:316–328.

Xu, X., Bittman, R., Duportail, G., Heissler, D., Vilcheze, C., and London, E. (2001). Effect of the Structure of Natural Sterols and Sphingolipids on the Formation of Ordered Sphingolipid/Sterol Domains (Rafts): comparison of cholesterol to plant, fungal, and disease-associated sterols and comparison of sphingomyelin, cerebrosides, and ceramide. *Journal of Biological Chemistry* 276:33540–33546.

Yanagawa, D., Ishikawa, T., and Imai, H. (2017). Synthesis and degradation of long-chain base phosphates affect fumonisin B1-induced cell death in *Arabidopsis thaliana*. *Journal of Plant Research* 130:571–585.

Yang, N. J., and Hinner, M. J. (2015). Getting Across the Cell Membrane: An Overview for Small Molecules, Peptides, and Proteins. *Methods in Molecular Biology* 1266: 29-53.

Yang, S. H., Shrivastav, A., Kosinski, C., Sharma, R. K., Chen, M.-H., Berthiaume, L. G., Peters, L. L., Chuang, P.-T., Young, S. G., and Bergo, M. O. (2005). N-Myristoyltransferase 1 is essential in early mouse development. *Journal of Biological Chemistry* 280:18990–18995.

Yang, Q., Wang, L., Zhou, Q., and Huang, X. (2015). Toxic effects of heavy metal terbium ion on the composition and functions of cell membrane in horseradish roots. *Ecotoxicology and Environmental Safety* 111:48–58.

Yi, Y., Lin, Y., Han, J., Lee, H. J., Park, N., Nam, G., Park, Y. S., Lee, Y.-H., and Lim, M. H. (2021). Impact of sphingosine and acetylsphingosines on the aggregation and toxicity of metal-free and metal-treated amyloid-β. *Chemical Science*. 12:2456–2466.

Yip, C. K., Finlay, B. B., and Strynadka, N. C. J. (2005). Structural characterization of a type III secretion system filament protein in complex with its chaperone. *Nature Structural & Molecular Biology* 12:75–81.

Yu, J., Penaloza-Vazquez, A., Chakrabarty, A. M., and Bender, C. L. (1999). Involvement of the exopolysaccharide alginate in the virulence and epiphytic fitness of *Pseudomonas syringae* pv. syringae. *Molecular Microbiology* 33:712–720.

Yu, X., Feng, B., He, P., and Shan, L. (2017). From chaos to harmony: responses and signalling upon microbial pattern recognition. *Annual Reviews of Phytopathology*. 55:109–137.

Yuan, M., Jiang, Z., Bi, G., Nomura, K., Liu, M., Wang, Y., Cai, B., Zhou, J.-M., He, S. Y., and Xin, X.-F. (2021a). Pattern-recognition receptors are required for NLR-mediated plant immunity. *Nature* 592:105-109.

Yuan, M., Ngou, B. P. M., Ding, P., and Xin, X.-F. (2021b). PTI-ETI crosstalk: an integrative view of plant immunity. *Current Opinion in Plant Biology* 62:102030.

Yun, B.-W., Feechan, A., Yin, M., Saidi, N. B. B., Le Bihan, T., Yu, M., Moore, J. W., Kang, J.-G., Kwon, E., Spoel, S. H., *et al.* (2011). S-nitrosylation of NADPH oxidase regulates cell death in plant immunity. *Nature* 478:264–268.

Zhang, N., Lariviere, A., Tonsor, S. J., and Traw, M. B. (2014). Constitutive camalexin production and environmental stress response variation in *Arabidopsis* populations from the Iberian Peninsula. *Plant Science* 225:77–85.

Zheng, X., Spivey, N. W., Zeng, W., Liu, P.-P., Fu, Z. Q., Klessig, D. F., He, S. Y., and Dong, X. (2012). Coronatine promotes *Pseudomonas syringae* virulence in plants by activating a signalling cascade that inhibits salicylic acid accumulation. *Cell Host & Microbe* 11:587–596.

Zhou, J., and Zhang, Y. (2020). Plant immunity : danger perception and signalling. *Cell* 181:978–989.

Zhou, N., Tootle, T. L., Tsui, F., Klessig, D. F., and Glazebrook, J. (1998). PAD4 functions upstream from salicylic acid to control defence responses in *Arabidopsis*. *The Plant Cell* 10:1021–1030.

Zienkiewicz, A., Gömann, J., König, S., Herrfurth, C., Liu, Y., Meldau, D., and Feussner, I. (2020). Disruption of *Arabidopsis* neutral ceramidases 1 and 2 results in specific sphingolipid imbalances triggering different phytohormone-dependent plant cell death programmes. *New Phytologist* 226:170–188.

Zipfel, C., Kunze, G., Chinchilla, D., Caniard, A., Jones, J. D. G., Boller, T., and Felix, G. (2006). Perception of the Bacterial PAMP EF-Tu by the Receptor EFR Restricts Agrobacterium-Mediated Transformation. *Cell* 125:749–760.

Zipfel, C. (2014). Plant pattern-recognition receptors. *Trends in Immunology* 35:345–351.

Zipfel, C., and Oldroyd, G. E. D. (2017). Plant signalling in symbiosis and immunity. *Nature* 543:328–336.

Zipfel, C., Robatzek, S., Navarro, L., Oakeley, E. J., Jones, J. D. G., Felix, G., and Boller, T. (2004). Bacterial disease resistance in *Arabidopsis* through flagellin perception. *Nature* 428:764–767.

Annex

Research review

Sphingolipids: towards an integrated view of metabolism during the plant stress response

Authors for correspondence:
Sandrine Dhondt-Cordelier
Tel: +33 3 26 91 85 87
Email: sandrine.cordelier@univ-reims.fr

Louise V. Michaelson
Tel: +44 1582 763133
Email: louise.michaelson@rothamsted.ac.uk

Eloïse Huby[1,2], Johnathan A. Napier[3] (iD)**, Fabienne Baillieul[1]** (iD)**,**
Louise V. Michaelson[3]* (iD) **and Sandrine Dhondt-Cordelier[1]*** (iD)

[1]Résistance Induite et Bioprotection des Plantes EA 4707, SFR Condorcet FR CNRS 3417, University of Reims Champagne-Ardenne, BP 1039,F-51687, Reims Cedex 2, France; [2]Laboratoire de Biophysique Moléculaire aux Interfaces, Gembloux Agro-Bio Tech, Université de Liège, 2 Passage des Déportés,B-5030, Gembloux, Belgique; [3]Plant Sciences, Rothamsted Research, West Common, Harpenden, AL5 2JQ, UK

Summary

Plants exist in an environment of changing abiotic and biotic stresses. They have developed a complex set of strategies to respond to these stresses and over recent years it has become clear that sphingolipids are a key player in these responses. Sphingolipids are not universally present in all three domains of life. Many bacteria and archaea do not produce sphingolipids but they are ubiquitous in eukaryotes and have been intensively studied in yeast and mammals. During the last decade there has been a steadily increasing interest in plant sphingolipids. Plant sphingolipids exhibit structural differences when compared with their mammalian counterparts and it is now clear that they perform some unique functions. Sphingolipids are recognised as critical components of the plant plasma membrane and endomembrane system. Besides being important structural elements of plant membranes, their particular structure contributes to the fluidity and biophysical order. Sphingolipids are also involved in multiple cellular and regulatory processes including vesicle trafficking, plant development and defence. This review will focus on our current knowledge as to the function of sphingolipids during plant stress responses, not only as structural components of biological membranes, but also as signalling mediators.

Introduction

The strategies that plants employ to endure stressful conditions are varied and involve a multitude of molecular, metabolic and physiological adaptations. There is now a significant body of work to indicate that sphingolipids are an important part of the arsenal of tools the plant has at its disposal to respond to stress. Sphingolipids are an incredibly diverse group of compounds (Pata *et al.*, 2010) with a vast array of physical properties that facilitate their function in a variety of cellular processes. Sphingolipids form a significant proportion of the lipids present in higher plants. Studies suggest sphingolipids constitute up to 40% of lipids in the plasma membrane of plant cells (Cacas *et al.*, 2016) and are enriched in the endosomes and tonoplasts (Moreau *et al.*, 1998). More comprehensive extraction techniques have been developed over recent

years that, when coupled with technological advances in mass spectrometry and chromatography, have allowed improved sphingolipid identification and the discovery of novel structures from smaller quantities of material (Cacas *et al.*, 2016). This situation has enabled researchers to determine the contribution that sphingolipid metabolites make in different cellular processes.

An overview of the sphingolipid biosynthetic pathway is presented in Fig. 1. The term sphingolipid covers a class of lipids whose defining component is a long-chain or sphingoid base (LCB; for ease of reference, Supporting Information Table S1 lists the abbreviations used in this review). The LCB is a carbon amino-alcohol backbone most commonly of 18 carbons that is synthesised by the condensation of serine and palmitoyl-CoA catalysed by serine palmitoyl transferase (SPT) in the endoplasmic reticulum (ER) (Chen *et al.*, 2006). The product of this reaction, 3-ketosphinganine, is then reduced by the action of the 3-ketosphinganine reductase to sphinganine (d18:0) (Beeler *et al.*, 1998).

The LCB is considered the simplest functional sphingolipid and can have a range of modifications including phosphorylation, desaturation and hydroxylation. It is sometimes referred to as the free LCB. The LCB may be linked to a very-long-chain fatty acid *via* an amide bond to form a ceramide. The fatty acyl component is usually 16–26 carbons. This reaction is catalysed by ceramide synthase. In *Arabidopsis thaliana* (hereafter Arabidopsis) three ceramide synthases have been identified, LOH1–3. Ceramidases catalyse the reverse reaction and are a component in regulating the ceramide pool and sphingolipid homeostasis (Pata *et al.*, 2008). Ceramides can be phosphorylated in the endoplasmic reticulum (ER) by ceramide kinases (CerK) or ACD5 (accelerated cell death 5) or further modified to form the complex sphingolipids glycosylceramides (GlcCers) in the ER and glycosyl inositol phosphorylceramides (GIPCs) by the addition of simple or multiple sugars on ceramide at the C1 position in the Golgi. These reactions are catalysed by glucosylceramide synthase (GCS) and at least three functional IPC-synthases and several glycosyl or glucuronyl transferases (Wang *et al.*, 2008; Mina *et al.*, 2010; Rennie *et al.*, 2014; Msanne *et al.*, 2015). The complex sphingolipids can exhibit very high levels of sugar decoration. One study of 23 plant species identified at least 21 different patterns showing variation in number, type and order of glycan substitutions (Cacas *et al.*, 2013). The biosynthesis of complex sphingolipids is tightly controlled and the GIPC pool is regulated by the hydrolysis of GIPC to phytoceramide-1 phosphate by the action of a phospholipase D (PLD) (Tanaka *et al.*, 2013). Functional characterisations of enzymes of the sphingolipid biosynthetic pathway have also pointed to the controls on the pathway and the specific pool sizes and structures that are generated. This flexibility enables sphingolipids to constitute both a structural membrane component and a signalling molecule from the same basic lipid backbones. For more details about sphingolipid biosynthesis, see the recent reviews by Luttgeharm *et al.*, 2016; Michaelson *et al.*, 2016 and Mamode Cassim *et al.*, 2019.

In plants, the size of the different sphingolipid pools tends to vary in a species-specific and tissue-dependent manner. For example, the occurrence of the LCB d18:2 containing GlcCer in Arabidopsis is mainly confined to floral and pollen tissue (Michaelson *et al.*, 2009) and sphingolipid distribution changes during fruit development and ripening (Ines *et al.*, 2018). However outside the Brassicaceae family d18:2 production occurs throughout the plant and, in species such as tomato and soybean, it is the most abundant GlcCer (Markham *et al.*, 2006). Wheat was found to contain much higher levels of d18:1 in its LCBs when compared with rice (Goto *et al.*, 2012). In addition, the different tissues in rice have been found to contain a similar quantity of sphingolipids, but distribution across the lipid classes was altered. A survey of 21 different plant species from different phylogenetic groups found d18:1$^{\Delta 4}$ to be present in nonseed land plants and monocots but absent from Arabidopsis and soybean (Islam *et al.*, 2012).

The functional significance of variations in sphingolipid chemical diversity and abundance is still in the early stages of investigation. The different classes and modifications offer a variety of differing solubility, charge, shape and size. It is this array of properties that confers the potential of sphingolipids to function both as bio-active components of cells involved in regulating cellular processes and as integral components involved in the structural integrity of the membranes. Regulation of sphingolipid metabolism enables plants to facilitate cell growth and to appropriately respond to stress, both biotic and abiotic, using different metabolites to modulate its response.

Here, we summarise our current knowledge on the role of sphingolipids in plants in response to environmental cues and stress.

Signals in programmed cell death

Recent work utilising genetically altered plants and plants exposed to sphingolipid biosynthesis inhibitors have revealed that sphingolipids are regulators of programmed cell death (PCD) occurring either during plant development or immunity. Perception of a stress often occurs at the plasma membrane level. Therefore its integrity is essential for cell signalling and survival. Sphingolipids are major structural constituents of plant plasma membrane microdomains and their relationship with other components of the plasma membrane is crucial. Changes in sphingolipid biosynthesis therefore affect the microdomain composition and this could affect protein content and distribution due to altered interactions between plasma membrane components. For example, Bax-inhibitor-1 (AtBI-1, an inhibitor of Bax-induced cell death) interacts with both FAH1 and FAH2 (fatty acid 2-hydroxylase). Plants overexpressing AtBI-1 therefore displayed enrichment in 2-hydroxy fatty acid-containing GlcCer in microdomains as well as a loss of two proteins that are usually specifically localised to microdomains (Ishikawa *et al.*, 2015). These two proteins feature in plant defence, both being involved in cell death triggered by salicylic acid (SA) or oxidative stress. This reduction in protein content led to an enhanced tolerance to SA or oxidative stress in AtBI-1-overexpressing plants (Ishikawa *et al.*, 2015). These data suggest that the integrity of microdomains is critical to cell death and sphingolipids are central to these structures.

Sphingolipids are involved in the control of PCD, either as structural components of membranes but also as initiators in the cell death regulatory pathway. The existence of a rheostat between ceramides/LCBs and their phosphorylated counterparts, already described in animal cells, is thought to exist in plants and similarly to control cell fate. According to this model, ceramides and LCBs are able to trigger cell death, whereas ceramide phosphates and LCB-Ps promote cell survival (Shi *et al.*, 2007; Alden *et al.*, 2011) (Fig. 2). The induction of PCD by LCB was based on the activation of protein kinases, MPK6 (Saucedo-Garcia *et al.*, 2011) or 14-3-3-regulated CPK3 (Lachaud *et al.*, 2013). The spontaneous PCD observed in the *acd5* mutant, defective in ceramide kinase and with enhanced levels of ceramides, was due to a strong accumulation of mitochondrial reactive oxygen species (ROS) (Bi *et al.*, 2014). This finding suggests that ROS are a component of sphingolipid-induced PCD. The mycotoxin fumonisin B1 (FB1) has been widely used to study both sphingolipid biosynthesis and PCD. Indeed, FB1 is a strong inhibitor of ceramide synthase and has been shown to induce PCD. When applied to plants, FB1 also triggered
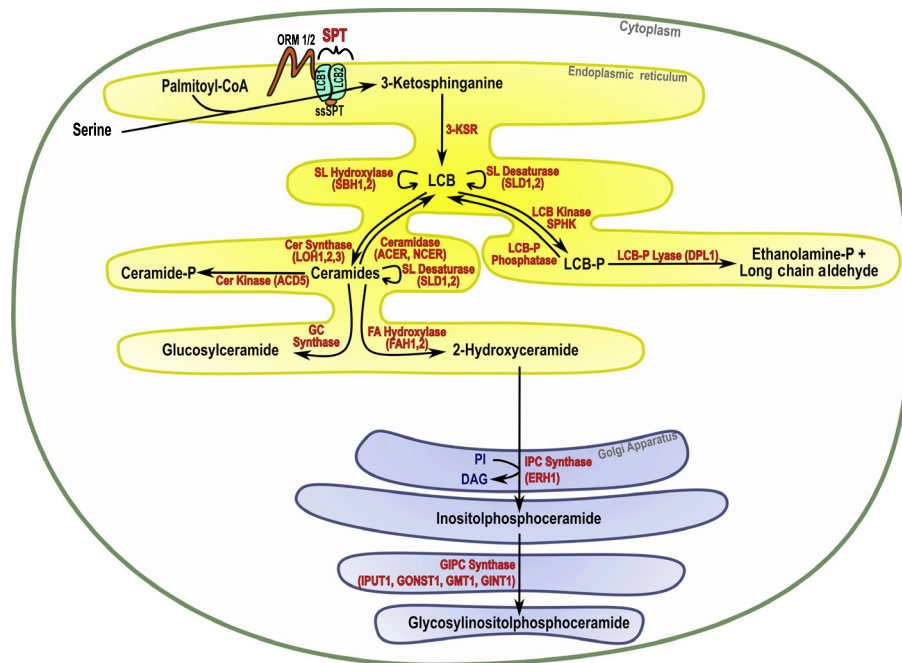
Fig. 1 Schematic representation of the sphingolipid biosynthetic pathway in plants. 3-KSR, 3-ketosphinganine reductase; ACD5, accelerated cell death 5; ACER, alkaline ceramidase; Cer, ceramide; ceramide-P, ceramide-phosphate; CoA, coenzyme A; DAG, diacylglycerol; DPL1, dihydrosphingosine phosphate lyase; ERH1, enhancing RPW8-mediated HR-like cell death; FA, fatty acid; FAH, fatty acid hydroxylase; GC, glucosylceramide; GINT1, glucosamine inositol phosphorylceramide transferase 1; GIPC, glycosyl inositol phosphoceramide; GMT1, GIPC mannosyl-transferase 1; GONST1, Golgi localized nucleotide sugar transporter 1; IPC, inositol phosphorylceramide; IPUT, inositol phosphorylceramide glucuronosyltransferase 1; LCB1,2, subunit of serine palmitoyltransferase 1 and 2; LCB, long-chain base; LCB-P, long-chain base phosphate; LOH, LAG1 homolog; NCER, neutral ceramidase; ORM, orosomucoid-like protein; PI, phosphoinositol; SBH, sphingoid base hydroxylase; SL, sphingolipid; SLD, sphingolipid Δ8 long-chain base desaturase; SPHK, sphingosine kinase; ssSPT, small subunit of serine palmitoyl transferase; SPT, serine palmitoyl transferase.
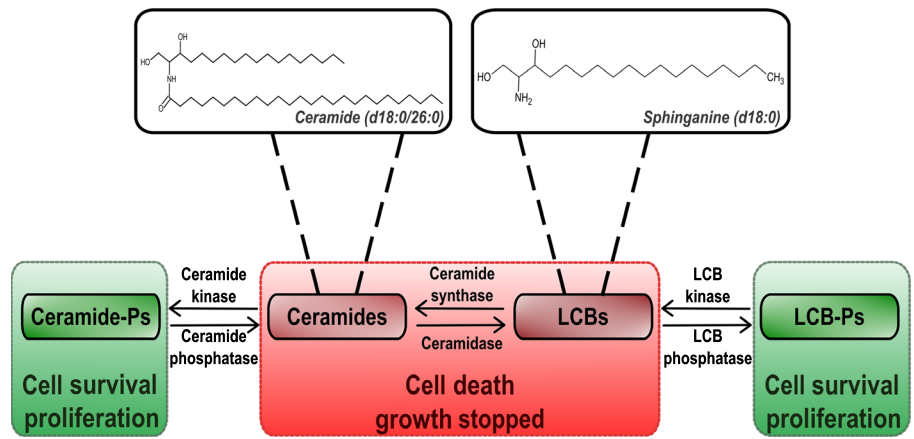
Fig. 2 Sphingolipid rheostat. The equilibrium between ceramides/long-chain bases (LCBs) and ceramide phosphates (ceramide-Ps)/LCB-Ps defines cell fate.

the accumulation of LCBs and LCB-Ps (Shi *et al.*, 2007; Tsegaye *et al.*, 2007; Saucedo-Garcia *et al.*, 2011; Yanagawa *et al.*, 2017). Overexpression of *AtLCBK1* (Arabidopsis sphingoid LCB kinase) in a recent study in plants induced resistance to FB1 treatment and, conversely, *AtLCBK1* knockdown plants exhibited a sensitivity to such a treatment (Yanagawa *et al.*, 2017). Moreover, the authors demonstrated that transgenic alteration of proteins involved in LCB/LCB-P homeostasis (AtLCBK1, AtSPP1 and AtDPL1) resulted in a positive correlation between the levels of free LCBs and the degree of FB1-induced cell death (Yanagawa *et al.*, 2017).

Increase in SPT activity, by overexpression of *AtssSPTa* (small subunit of SPT), resulted in an accumulation of LCBs and reduced tolerance to FB1, whereas *AtssSPTa* suppression lines displayed lower levels of LCBs but enhanced tolerance to FB1 (Kimberlin *et al.*, 2013). It was recently demonstrated by two independent studies that orosomucoid-like proteins AtORM1 and AtORM2 physically interact with the core SPT complex and function as a repressor of SPT activity (Kimberlin *et al.*, 2016; Li *et al.*, 2016). ORM proteins therefore regulate sphingolipid homeostasis by differently modulating functionally different ceramide synthase activities (Kimberlin *et al.*, 2016). *AtORM1* and *AtORM2*

overexpressing plants were more tolerant to FB1 treatment when compared with wild-type (WT) plants. This tolerance is accompanied by a lower accumulation of C16 ceramides, LCBs and their phosphorylated counterparts. Conversely, *AtORM* RNAi lines were more sensitive to such treatment, and displayed higher content of C16 ceramides, LCBs and LCB-Ps (Kimberlin *et al.*, 2016). Similarly, the ceramide synthase *LOH2* overexpressing lines resulted in the accumulation of ceramides containing C16 fatty acids and dihydroxy LCBs and had reduced accumulation of free LCBs and LCB-Ps in response to FB1. This overexpression also resulted in constitutive induction of PCD and increased resistance to FB1 (Luttgeharm *et al.*, 2015). These findings suggested that FB1-induced PCD is primarily due to the accumulation of free LCBs rather than the accumulation of ceramides containing C16 fatty acids/dihydroxy LCBs. Curiously, growth and increased cell division were promoted in *LOH1* and *LOH3* overexpressing plants, which displayed enhanced production of ceramides with very-long-chain fatty acids (VLCFAs) and trihydroxy LCBs (Luttgeharm *et al.*, 2015). These unexpected outcomes for growth and development could be due to a ceramide synthesis with a certain chain length fatty acid and quantity and in response to the correct stimuli. It is also known that VLCFA ceramides are important for Golgi trafficking and cell plate or phragmoplast formation during cell division in Arabidopsis (Molino *et al.*, 2014). It is therefore possible that increased cell expansion could be due to sphingolipid targeting to plant membranes that contributes directly to cell expansion. In addition, the fatty acid hydroxylase double mutant *fah1/fah2* fails to form spontaneous lesions under standard culture conditions, despite an accumulation in free trihydroxy LCBs, C16 ceramides and VLCFA ceramides and SA (König *et al.*, 2012). Moreover, the *gonst1* (Golgi localised nucleotide sugar transporter1, involved in glycosylation of GIPCs) mutant displayed spontaneous hypersensitive reaction (HR)-like lesions but did not accumulate ceramides or LCBs (Mortimer *et al.*, 2013). One potential explanation for these observed differences is that several different mechanisms could be responsible for inducing cell death.

Sphingolipids as structural components in response to abiotic stress

Several studies have recently reported a role for sphingolipids in response to temperature stress. Acclimation capacity was correlated with changes in the content of TAGs (triacylglycerols), MGDG (monogalactosyldiacylglycerol), DGDG (digalactosyldiacylglycerol) and a GlcCer (Degenkolbe *et al.*, 2012). Analysis of oat, rye and Arabidopsis lipid profiles during cold acclimation demonstrated that GlcCer contents decreased in the plasma membrane, whereas they were unchanged in microdomains (Minami *et al.*, 2009; Takahashi *et al.*, 2016). These changes could contribute to a greater hydration of the plasma membrane that could, in turn, increase membrane stability during cold stress. In a study focusing on grapevine leaves, it was found that high levels of t18:1 (8Z) in complex sphingolipids were correlated with freezing tolerance (Kawaguchi *et al.*, 2000). The sphingolipid Δ8 long-chain base desaturases (SLD), which desaturate the LCB at the Δ8 position in both *cis* and *trans* orientations, appear to play a role in cold

tolerance in Arabidopsis (Chen *et al.*, 2012) and tomato (Zhou *et al.*, 2016). In Arabidopsis, the *sld1sld2* double mutant is sensitive to cold stress (Chen *et al.*, 2012). Similarly, *SlSLD* knockdown tomato plants displayed greater membrane damage and physiological indicators of chilling damage after stress than WT plants. Chloroplasts are the main organelle affected by cold and many studies have reported that chloroplast morphology is affected by changes in lipid unsaturation. Chloroplasts in *SlSLD* knockdown were more severely damaged than in WT plants and the surviving organelles were not surrounded by an extra membrane (Zhou *et al.*, 2016). GlcCers, believed to stabilise membranes, were detected in the envelope membrane of chloroplasts (Spassieva & Hille, 2003), suggesting that sphingolipids are structurally important for chloroplast membrane for cold tolerance. This finding illustrated that disrupting *SlSLD* transcript accumulation reduced chilling tolerance of tomato. Lipid desaturation is a way for plants to mitigate the effects of chilling or freezing temperatures. *SlSLD* knockdown plant sensitivity to chilling could therefore be related to membrane properties such as fluidity, which is diminished due to depletion of sphingolipids with unsaturated LCBs. Another explanation for the decrease in cold tolerance could be a change in the formation and content of microdomains in the membrane. It is conceivable that activity of some microdomain-localised proteins important for cold tolerance could be modified in perturbed microdomains (Chen *et al.*, 2012). There has been no characterised function for sphingolipids in tolerance of high temperature by contrast with the high concentration of trienoic fatty acids in the thylakoid membranes that have been shown to be involved in both chilling and high temperature tolerance (Murakami *et al.*, 2000; Routaboul *et al.*, 2012; Tovuu *et al.*, 2016).

Sphingolipids as structural components in response to biotic stress

The rice *Osfah1/2* plants displayed similar SA levels to WT and a decreased tolerance to the hemibiotrophic fungus *Magnaporthe oryzae*. Nagano and colleagues demonstrated that products of these enzymes, 2-hydroxy-sphingolipids, were critical in the formation of microdomains and disruption of OsFah1/2 activity disturbed organisation of defence proteins localized in these microdomains, such as the NADPH oxidase RbohB, required for ROS production involved in rice immunity (Nagano *et al.*, 2016).

Recent work has identified three genes involved in GIPC glycosylation: GONST1, IPUT1 (inositol phosphorylceramide glucuronosyltransferase1) and GMT1 (GIPC mannosyl-transferase1) (Mortimer *et al.*, 2013; Fang *et al.*, 2016; Tartaglio *et al.*, 2017). These three mutants displayed high SA and ROS levels coupled to a constitutive HR and defence-gene induction, suggesting a constitutive biotic stress response. Interestingly, *gmt1* also had a decrease in cellulose accompanied by an increase in lignin content, a well known process in disease resistance.

Eudicot plant-specific GIPCs appeared to act as NLP (necrosis and ethylene-inducing peptide 1-like protein) cytolysin receptors (Lenarcic *et al.*, 2017). NLP are produced by bacterial, fungal and oomycete plant pathogens. Monocots did not develop necrotic lesions upon challenge with NLP. The difference between the two

clades resides in the length of terminal hexose residues in GIPCs (two for eudicots and three for monocots). The GIPC sugar moiety is exposed at the surface of the plasma membrane and is therefore accessible to NLP binding. The presence of a third hexose unit in monocots impeded NLP insertion into the plasma membrane. The structural and molecular consequences for the plasma membrane that could occur downstream of this recognition requires further study. These studies demonstrate that GIPC glycosylation and the identity of the glycan headgroup are important for the plant immune response.

Sphingolipids as signalling messengers in abiotic stress

The sessile nature of plants has driven them to develop a myriad of strategies to resist cell damage. Abiotic stress affects plant growth and development, resulting in loss of vigour and ultimately death. The altered physical and chemical composition of cell membranes under temperature, salt stress or hypoxia is a problem the plant must manage. As a major component of plasma membranes, sphingolipids are significant in mitigating abiotic stress, both in plasma membrane remodelling, and as signal transduction molecules (Ali *et al.*, 2018). A summary of the available data on the enzymes and genes of the sphingolipid pathway involved in response to both abiotic and biotic stress is presented in Table 1.

Temperature stress

Sphingolipids are involved in cold acclimation as structural components of membranes and also as signalling molecules. In Arabidopsis WT plants, low temperatures trigger an accumulation of total sphingolipids, whereas the ratio of unsaturated LCBs is not increased by low temperatures (Nagano *et al.*, 2014). This situation suggests that sphingolipids containing unsaturated LCBs are potential candidates for natural resistance to low temperatures but not for induced tolerance to cold. The cell death suppressor AtBI-1 is involved in sphingolipid synthesis in response to cold by interacting with AtSLD1, AtFAH1, AtSBH2 (a LCB C-4 hydroxylase) and AtADS2 (acyl lipid desaturase 2) through Arabidopsis cytochrome b$_5$ (Nagano *et al.*, 2014). Moreover, chilling induced a decrease in LCB production (especially t18:1) (Guillas *et al.*, 2013). An Arabidopsis mutant exhibiting low levels of nitric oxide (NO) displayed an accumulation of t18:1. A rapid and transient production of t18:0-P and ceramide phosphates is induced by cold. This accumulation was negatively regulated by NO (Cantrel *et al.*, 2011) and was specifically impaired in *lcbk2* (but not in *lcbk1*) or *acd5* mutants, respectively (Dutilleul *et al.*, 2012, 2015). Whether NO is able to directly regulate enzymes involved in LCB/LCB-P and Cer/Cer-P rheostat or their substrate availability is still unknown. *lcbk2* displayed a constitutive activation of a cold-responsive MAPK, AtMPK6, at 22°C. AtMPK6 activation was also stimulated by t18:0-P treatment (Dutilleul *et al.*, 2012). The expression of some cold-responsive genes and phenotypical cold responses were impaired in the *lcbk2* mutant but not in *acd5*. In addition, *acd5* seed germination was hypersensitive to cold and abscisic acid (ABA), however gibberellic acid (GA) treatment

reverted the *acd5* germination phenotype at 4°C. Germination is regulated by ABA and GA, two hormones that function antagonistically. This finding suggests that defects in the ABA/GA balance and CerK activity could be responsible for *acd5* seed hypersensitivity (Dutilleul *et al.*, 2015). Therefore, some responses are regulated by phosphorylated sphingolipids, ABA and NO signalling during cold stress. Recent data have described a role for LCBK1 in Arabidopsis freezing tolerance (Huang *et al.*, 2017). Typical responses including osmolyte accumulation, induction of cold- and membrane lipid-related genes occurring during this abiotic stress are all impaired in the *lcbk1* mutant. This situation suggested a fine-tuned regulation in which LCBK1 acts as a signal in response to freezing temperatures and LCBK2 in response to chilling temperatures.

There are only a small number of studies indicating that sphingolipid metabolism is also involved in heat stress. It was shown that exogenous LCB-phosphate contributed to heat stress tolerance in Arabidopsis cell culture (Alden *et al.*, 2011). Moreover, a recent transcriptome analysis showed that *AtSLD1* expression is significantly decreased in response to a combination of heat wave and drought at ambient and elevated CO_2, mimicking global changes in climate (Zinta *et al.*, 2018).

Hypoxia and oxidative stress

Hypoxia leads to an increase in ceramides, hydroxyceramides, GlcCers and GIPCs (Xie *et al.*, 2015a,b). In hypoxic conditions, GIPCs are elevated in Arabidopsis and increased further in *Atacbp3* (acyl-CoA binding protein 3), whereas AtACBP3-overexpressors were hypersensitive to submergence (Xie *et al.*, 2015b; Lung & Chye, 2019). Similarly, a reduction of unsaturated VLC-ceramides in *loh1*, *loh2* and *loh3* mutants due to the disruption of ceramide synthase is accompanied by an enhanced sensitivity to dark submergence. The *loh1-1 loh3-1* double mutant displayed a reduction in unsaturated very-long-chain (VLC)-ceramides and impaired tolerance to dark and light submergence. Unsaturated VLC ceramides are therefore seen as defence molecules for plant tolerance to hypoxia (Xie *et al.*, 2015a). The mechanism underlying this tolerance involves the modulation of ethylene signalling. These molecules were shown to interact with constitutive triple response1 (CTR1; a negative regulator in ethylene signalling) and to inhibit its kinase activity (Xie *et al.*, 2015a) and subsequent ethylene signalling. Furthermore, the hypersensitivity of *loh* mutants to dark submergence was rescued by introduction of the *crt1-1* mutation that constitutively induces the ethylene response. Overexpression of long-chain base kinase (OsLCBK1) in tobacco led to an increased tolerance to oxidative stress provoked by treatment with either methyl viologen or H_2O_2, accompanied with an induction of oxidative stress-related gene expression (Zhang *et al.*, 2013). *orm1* amiR-*ORM2* plants exhibited an early senescence phenotype accompanied by ROS production and they displayed higher survival rates to oxidative stress (Li *et al.*, 2016). Measurement of sphingolipids showed an increase in LCBs and ceramides and an active vesicular transport that could contribute to the onset of the senescence phenotype and the resistance to oxidative stress. A homolog of human ceramidase, the neutral ceramidase nCer1, was

Table 1 Enzymes and genes of sphingolipid metabolism involved in response to (a)biotic stress.

Enzyme	Name	Mutant/transgenic plants	Phenotype under (a)biotic stress	References
Sphingolipid Δ8 long-chain base desaturases	SLD	*sld1sld2* (Arabidopsis)	Sensitive to cold	Chen *et al.* (2012)
		SlSLD-KD (tomato)	Sensitive to chilling	Zhou *et al.* (2016)
Long-chain base kinase	LCBK1	*lcbk1* (Arabidopsis)	Freezing tolerant	Huang *et al.* (2017)
		lcbk1-KD (Arabidopsis)	Sensitive to FB1 treatment	Yanagawa *et al.* (2017)
		OsLCBK1-OE (rice)	Tolerance to oxidative stress	Zhang *et al.* (2013)
		AtLCBK1-OE (Arabidopsis)	Tolerance to FB1 treatment	Yanagawa *et al.* (2017)
Long-chain base kinase	LCBK2	*lcbk2* (Arabidopsis)	Tolerance to intermediate cold (12°C)	Dutilleul *et al.* (2012)
Long-chain base kinase	SPHK1	*SPHK1*-OE (Arabidopsis)	Sensitive to ABA treatment	Worrall *et al.* (2008)
Ceramide kinase	ACD5	*acd5* (Arabidopsis)	Seed germination sensitive to cold	Dutilleul *et al.* (2015)
			Tolerance to powdery mildew	Wang *et al.* (2008)
			Susceptibility to *B. cinerea*	Bi *et al.* (2014)
Ceramide synthase	LOH1LOH2LOH3	*loh1, loh2, loh3* (Arabidopsis)	Sensitivity to dark submergence	Xie *et al.* (2015a)
		loh1-1 loh3-1 (Arabidopsis)	Sensitivity to dark and light submergence	Xie *et al.* (2015a)
		LOH2-OE (Arabidopsis)	Tolerance to FB1 treatment	Luttgeharm *et al.* (2015)
Neutral ceramidase	nCER1	*ncer1* (Arabidopsis)	Sensitivity to oxidative stress	Li *et al.* (2015)
		nCer1-OE (Arabidopsis)	Tolerance to oxidative stress	Li *et al.* (2015)
Alkaline ceramidase	AtACER	*Atacer* (Arabidopsis)	Sensitive to oxidative stress	Zheng *et al.* (2018)
			Susceptibility to *P. syringae* strain DG3	Wu *et al.* (2015a)
		Atacer, AtACER RNAi (Arabidopsis)	Sensitivity to salinity	Wu *et al.* (2015a)
		AtACER-OE (Arabidopsis)	Tolerance to salinity	Wu *et al.* (2015a)
Sphingosine-1 phosphate lyase	OsSPL1	*OsSPL1*-OE (rice)	Sensitivity to salinity	Zhang *et al.* (2012)
			Susceptibility to *P. syringae* pv. *tabaci*	Zhang *et al.* (2014)
Sphingoid phosphate phosphatase1	AtSPP1	*Atssp1* (Arabidopsis)	Sensitive to ABA treatment	Nakagawa *et al.* (2012)
Dihydrosphingosine-1-phosphate lyase1	AtDPL1	*Atdpl1* (Arabidopsis)	Susceptibility to *P. syringae* pv. *tomato* and tolerant to *B. cinerea*	Magnin-Robert *et al.* (2015)
Fatty acid alpha-hydroxylase	FAH1FAH2	*fah1/fah2* (Arabidopsis)	Tolerance to powdery mildew	König *et al.* (2012)
		OsFah1/OsFah2 (rice)	Susceptibility to *Magnaporthe oryzae*	Nagano *et al.* (2016)
Enhancing RPW8-mediated HR-like cell death	ERH1	*erh1* (Arabidopsis)	Tolerance to powdery mildew	Wang *et al.* (2008)
Glucosamine inositol phosphorylceramide transferase1	AtGINT1	*Atgint1* (Arabidopsis)	Tolerance to moderate salinity	Ishikawa *et al.* (2018)
Serine palmitoyltransferase	SPT	*SPT*-silenced (tobacco)	Susceptibility to *Alternata alternata* f. sp. *lycopersici*	Rivas-San Vicente *et al.* (2013)
Small subunit of serine palmitoyltransferase	ssSPTa	*AtssSPTa*-OE (Arabidopsis)	Sensitivity to FB1 treatment	Kimberlin *et al.* (2013)
		AtssSPTa RNAi (Arabidopsis)	Tolerance to FB1 treatment	Kimberlin *et al.* (2013)
Subunit of serine palmitoyltransferase	LCB2a1	*OsLCB2a*-OE (rice)	Tolerance to *Myzus persicae* infestation	Begum *et al.* (2016)
Orosomucoid-like proteins	ORM1ORM2	*orm1* amiR-*ORM2* (Arabidopsis)	Tolerance to *P. syringae* strain DG3	Li *et al.* (2016)
			Tolerance to oxidative stress	Li *et al.* (2016)
		AtORM1-OE, *AtORM2*-OE (Arabidopsis)	Tolerance to FB1 treatment	Kimberlin *et al.* (2016)
		AtORM1 RNAi, *AtORM2* RNAi (Arabidopsis)	Sensitivity to FB1 treatment	Kimberlin *et al.* (2016)

KD, knocked-down; OE, overexpressing line.

recently characterised. *ncer1* Arabidopsis plants accumulated hydroxyceramides and were more sensitive to oxidative stress. Conversely, *nCer1* overexpressing plants were more tolerant to oxidative stress (Li *et al.*, 2015). Loss of AtACER, encoding an alkaline ceramidase, inhibited autophagy and its overexpression stimulated autophagy under oxidative stress (Zheng *et al.*, 2018). The *Atacer* mutant is highly sensitive to oxidative stress, whereas the complementation line showed a similar tolerance to this stress as the WT plant (Zheng *et al.*, 2018). This result suggests that AtACER improves adaptation to oxidative stress by regulating autophagy.

Salt stress

During the early stage of salt stress in *Carex rigescens,* an iTRAQ-based proteome study showed a reduction of the enzyme that catalyses the second step of the biosynthesis of phytosphingosine, 3-ketosphingosine reductase (KDSR) (Li *et al.*, 2017). Based on work performed in yeast where 3-ketosphinganine reductase suppressed Ca^{2+} sensitivity (Beeler *et al.*, 1998), the authors hypothesised that KDSR acts as a suppressor of the calcium signal during salt stress. Seeds of *Atgint1* (glucosamine inositol phosphorylceramide transferase1, responsible for the glycosylation of some GIPCs) mutants displayed a higher germination rate than WT in response to salt stress, although this difference disappeared at higher salt concentrations (Ishikawa *et al.*, 2018). The *Atacer* mutant and *AtACER* RNAi lines displayed high ceramide levels but reduced LCBs due to a disruption of an alkaline ceramidase gene (Wu *et al.*, 2015a). Whereas these plants showed increased sensitivity to salinity, *AtACER* overexpression led to an increased tolerance to such a stress, highlighting the involvement of ceramides in response to salt stress. More precisely, it has recently been shown that AtACER regulates autophagy induced by high salt stress (Zheng *et al.*, 2018). Overexpression of a rice S1P (sphingosine-1-phosphate) lyase gene in tobacco led to a decrease in tolerance to salt and changes in salt stress related genes (Zhang *et al.*, 2012). By contrast, overexpression of *OsLCBK1* in tobacco plants triggered no alteration in expression of salt stress-related genes or tolerance/sensitivity phenotype compared with control plants in response to salt stress (Zhang *et al.*, 2013), suggesting that this enzyme is not involved in salt stress responses in rice. Bioinformatic analysis supported the hypothesis that there are at least two OsLCBKs (Zhang *et al.*, 2013). No sphingolipidomic analysis has been performed to reveal how the LCB content could vary between these two overexpressing plants. Previously published papers suggested that the sphingolipid metabolism could be adjusted, so that length chain, concentration and threshold are important for sphingolipid function.

Interplay with ABA signalling pathway

ABA has a key function in cold/drought stress responses. Pioneering work on sphingolipids showed that d18:1-P and t18:0-P were rapidly induced by drought and were involved in ABA signalling pathway to control guard-cell turgor and therefore stomatal

aperture (Ng *et al.*, 2001; Coursol *et al.*, 2003, 2005). This sphingolipid signalling pathway involved Ca^{2+} mobilisation, modification of ion channel activity, and heterotrimeric G-protein. Consistent with this, AtLCBK1 was reported to be induced by low-humidity or ABA treatments (Imai & Nishiura, 2005). Moreover, ABA also induces the accumulation of several LCB-Ps (Guo *et al.*, 2012). SPHK1 is an enzyme that phosphorylates d18:1 and t18:0. Stomata of SPHK1-OE and of *Atspp1* mutant (which accumulates d18:1-P) displayed a higher sensitivity than WT to ABA (Worrall *et al.*, 2008; Nakagawa *et al.*, 2012). Therefore, LCB-P content regulated by LCB kinases and phosphatases plays a key role in the ABA signalling pathway.

Interplay with phospholipid metabolism

Similar to sphingolipids, phosphatidic acid (PA) is considered as a lipid messenger involved in plant response to both biotic and abiotic stress. Like sphingolipids, PA interacts with MPK6 during salt stress response in Arabidopsis (Yu *et al.*, 2010) and NADPH oxidase to regulate ROS production during ABA-regulated stomatal closure (Zhang *et al.*, 2009). The PA biosynthetic pathway responds to temperature and salt stress and interacts with sphingosine kinases (Guo *et al.*, 2011). Moreover, addition of exogenous PA induced LCB-P production and LCB-P levels are diminished in *pldα1* in response to ABA (Guo *et al.*, 2012). Overexpression of sphingosine kinase increased PA accumulation. Altogether, the crosstalk between PA and sphingolipids should be a critical point to coordinate a stress response that needs to be elucidated (Fig. 3) (Guo & Wang, 2012; Ng & Coursol, 2012). DAG is a by-product of the IPC synthase and is known to promote stomatal opening (Lee & Assmann, 1991; Peters *et al.*, 2010). Although there is no direct evidence for a relationship between sphingolipids and DAG (Fig. 3), lipidome remodelling under stress could yet prove a link.

Signalling messengers in biotic stress

Biotic stress caused by plant pathogens and insects is a major threat to both plant survival and productivity. Plants have developed a complex set of defences when challenged by pathogens. A successful innate immune response depends on the capability of the plant to recognise its invader and then to translate the different stimuli to an

Fig. 3 Interplay between sphingolipid and phospholipid metabolisms and their involvement in stomatal aperture. Phospholipid compounds are highlighted in blue. Solid arrows represent enzymatic reactions and dashed arrows indicate a stimulation reaction. Cer, ceramide; DAG, diacylglycerol; FA, fatty acid; GIPC, glycosyl inositol phosphoceramide; IPC, inositol phosphorylceramide; LCB, long-chain base; LCB-P, long-chain base phosphate; PA, phosphatidic acid; PI, phosphoinositol.
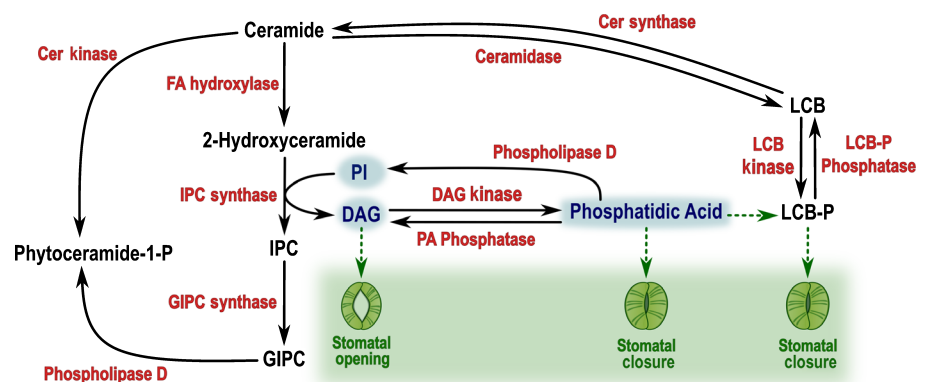
adaptive response. As structural plasma membrane components, sphingolipids are important molecules on the front line of pathogen recognition. Sphingolipid disruption also has an impact on PCD and accumulation of several well known defence molecules (such as ROS, MAPK, and hormones) and sphingolipids therefore act as mediators in the defence signalling cascade.

Very recently, metabolomic profiling identified changes in the sphingolipid pool after exposure to biotic stress. *Xanthomonas campestris* pv. *campestris* infection on *Brassica oleracea* triggered dynamic changes in sphingolipid metabolism including a reduction in the levels of ceramide N-palmitoylsphinganine (Tortosa *et al.*, 2018). Treatment of tomato fruit with the β-aminobutyric acid elicitor increased the detected levels of ceramide phosphatidylinositol (Wilkinson *et al.*, 2017). These metabolomic studies suggested that biotic stresses could impact sphingolipid metabolism.

Interplay with SA signalling pathway

Genetic and biochemical data suggest that sphingolipids are involved in the regulation of SA levels. Several mutants with altered sphingolipid metabolism displayed higher SA content and activation of SA-dependent responses. Conversely, both SA and its analogue benzothiadiazole affected sphingolipid metabolism (Shi *et al.*, 2015). The Arabidopsis *fah1/2* mutant displayed SA accumulation in addition to an increase in ceramides but moderate changes in LCB accumulation (König *et al.*, 2012). This suggests that elevated ceramide levels lead to an increase in salicylate levels. By contrast, the Arabidopsis *loh1* mutant displayed an accumulation of C16-ceramides but no changes in SA levels (Ternes *et al.*, 2011). This discrepancy suggests the sphingolipid trigger for SA accumulation may be more complicated than initially expected. It is noteworthy that these mutants displayed other changes in sphingolipid homeostasis (e.g. *fah1/2* also shows a decrease in glucosylceramides) that maybe have previously been overlooked. The induction of SA could therefore be due to alterations in sphingolipid classes other than LCBs or ceramides. The link between sphingolipid metabolism and SA may rely on MPK6, ROS/NO and/or calcium accumulation but this is still unclear (Sanchez-Rangel *et al.*, 2015). For example, overexpression of LCBK1 in tobacco cell culture triggered the accumulation of ROS in response to cryptogein. Loss of LCBK activity by using inhibitors resulted in a decrease in ROS production in elicited tobacco cells (Coursol *et al.*, 2015).

In conjunction with activation of the SA pathway, several studies revealed that plants disrupted in sphingolipid biosynthesis are also affected in their ability to tolerate biotrophic pathogens. Whereas SA is considered essential for resistance to biotrophic and hemibiotrophic pathogens, it has been demonstrated that jasmonic acid (JA) and ethylene (ET) signalling pathways are important for resistance to necrotrophic pathogens in Arabidopsis (Thomma *et al.*, 2001; Glazebrook, 2005). In Arabidopsis, it is now acknowledged that SA has a reciprocal antagonistic effect on JA signalling (Glazebrook, 2005). Using *orm1* amiR-*ORM2* plants, Li *et al.* (2016) demonstrated that the loss of ORM function triggered a constitutive induction of SA-dependent gene and a tolerance to

Pseudomonas syringae strain DG3 compared with WT plants. *acd5*, *erh1* (enhancing RPW8-mediated HR-like cell death) and *fah1/2* mutants also exhibited a constitutive activation of SA pathway and enhanced resistance to powdery mildew. However, they had a similar phenotype to WT after challenge with the hemibiotrophic pathogens *P. syringae* pv. *maculicola* or *Verticillium longisporum* (Wang *et al.*, 2008; König *et al.*, 2012). Similarly, overexpression of *OsSPL1* in tobacco dramatically reduced SA-dependent gene expression and increased susceptibility to *P. syringae* pv. *tabaci*. Conversely, *PDF1.2*, a JA-dependent gene, expression is slightly enhanced (Zhang *et al.*, 2014). SA-dependent pathogenesis-related (*PR*) gene expressions were constitutively lower in *Atacer-1* plants compared with WT plants. This profile was similar, but enhanced, when these plants were infected by the *P. syringae* strain DG3. As a consequence, *Atacer-1* plants were found to be more susceptible to the biotrophic *P. syringae* strain DG3 (Wu *et al.*, 2015a). In light of the antagonistic relationship between SA and JA, it would be interesting to analyse SA and JA levels alongside JA-responsive genes in *Atacer-1* plants.

Few studies have analysed the role of sphingolipids during plant/necrotrophic pathogen interaction. Tobacco plants in which SPT was silenced accumulated SA, constitutively expressed SA-induced genes and showed an increased susceptibility to the necrotrophic fungus *Alternaria alternata* f. sp. *lycopersici* (Rivas-San Vicente *et al.*, 2013). Similarly, the SA accumulating *acd5* showed increased susceptibility to *B. cinerea* (Bi *et al.*, 2014).

The role of sphingolipid metabolism in response to herbivory has been analysed (Begum *et al.*, 2016). Overexpression of OsLCB2a in Arabidopsis led to the accumulation of LCB and ceramides compared with WT. These transgenic plants also displayed increased callose and wax deposition, an induction of SA-dependent and camalexin-dependent genes but a reduction of JA-related genes, and inhibited aphid infestation (Begum *et al.*, 2016).

Interplay with JA signalling pathway

The *Atdpl1* mutant displayed a sensitivity towards the hemibiotrophic bacterium *Pseudomonas syringae* pv. *tomato* but a tolerance when infected by the necrotrophic fungus *Botrytis cinerea* (Magnin-Robert *et al.*, 2015). However, SA levels were similar or even reduced compared with WT, whereas JA levels and JA-dependent gene expression were higher in the *Atdpl1* infected mutant. This situation suggested a link between the sphingolipid and JA pathway. By using *SPHK1* overexpressing plants, SA production was enhanced in response to FB1 treatment. Conversely *SPHK1*-KD plants displayed an increase in JA-related transcripts and metabolites (Qin *et al.*, 2017). Therefore, it was suggested that the balance between LCBs and LCB-Ps modulated by the activity of SPHK1 acted as a signal upstream of the SA/JA signalling pathways during FB1-induced cell death (Qin *et al.*, 2017).

Interplay with ethylene signalling pathway

It was recently shown that sphingolipid metabolism has connections with not only SA and JA pathways but also with ethylene

signalling. Ethylene or its precursor (1-aminocyclopropane carboxylic acid) inhibits sphingolipid biosynthesis. Mutants disturbed in ethylene biosynthesis or signalling displayed constitutive modifications in sphingolipid content (Wu *et al.*, 2015b). For example, *ctr1-1* mutants, which have enhanced ethylene signalling, contained lower levels of ceramides and hydroxyceramides compared with WT. Some constitutive ethylene response mutants displayed a higher tolerance to FB1, and mutants deficient in ethylene signalling exhibited more sensitivity to FB1, showing that enhanced ethylene signalling rescues FB1-induced cell death.

Conclusions and future directions

Over the last few decades we have learned much about the role of sphingolipids during the plant stress response. Functional analyses have demonstrated that sphingolipids are involved in the response to environmental cues. The role of sphingolipids during PCD is well studied. Significant progress has been made but the precise identity of sphingolipids involved in this process is not clearly defined. It is clear that PCD is tightly regulated and further consideration should be given to the different stresses triggering PCD and also the plant species in question. The plasma membrane mediates contact with the environment and is the likely initial source of signal transduction. Recent evidence has shown that GIPC glycosylation involved different regulation processes in the plasma membrane. The composition, distribution and dynamic association of sphingolipids are therefore of high importance for plasma membrane function. It is essential to unravel the dynamic association between sphingolipids, plasma membrane lipids and proteins to better understand the recognition step of the immune response. While a body of evidence has revealed functions for LCBs/LCB-Ps, ceramides and GIPCs, the roles of GlcCers in plants have yet to be fully investigated, other than the observation that they are essential for normal plant growth and development. The relationship between sphingolipids and SA is long acknowledged and recent studies have shown interconnections with other defence signalling pathways such as JA and ethylene. The regulation of stomatal aperture is of crucial importance during plant defence responses, especially in response to foliar pathogens. ABA-mediated stomatal closure inhibits pathogen penetration to the apoplast. As the sphingolipid signalling pathway has some interconnections during this process in response to drought stress, the relationship between sphingolipids and ABA in response to foliar pathogens remains to be elucidated.

Despite the range of different structures of sphingolipids and differing physical properties they exhibit, understanding sphingolipid regulation and function is not comprehensive. The interactions with other cellular lipids are also yet to be fully resolved but there are known relationships with several other lipid classes. The wider lipidome is subject to remodelling when the plant is under stress and it is likely that sphingolipids form part of a coordinated response. The mechanisms for action and whether sphingolipids regulate stress responsive gene expression or are themselves regulated by stress responsive transcription factors are not yet fully understood. There is still a gap in understanding the role of sphingolipids in the plant stress response, but the advent of genome editing technology opens the possibility to develop crops with a greater ability to tolerate stress based on the manipulation of their sphingolipid biosynthetic pathway.

ORCID

Fabienne Baillieul https://orcid.org/0000-0002-7142-1035
Sandrine Dhondt-Cordelier https://orcid.org/0000-0002-3778-6727
Louise V. Michaelson https://orcid.org/0000-0001-5621-4495
Johnathan A. Napier https://orcid.org/0000-0003-3580-3607

References

Alden KP, Dhondt-Cordelier S, McDonald KL, Reape TJ, Ng CK, McCabe PF, Leaver CJ. 2011. Sphingolipid long chain base phosphates can regulate apoptotic-like programmed cell death in plants. *Biochemical and Biophysical Research Communications* 410: 574–580.

Ali U, Li H, Wang X, Guo L. 2018. Emerging roles of sphingolipid signaling in plant response to biotic and abiotic stresses. *Molecular Plant* 11: 1328–1343.

Beeler T, Bacikova D, Gable K, Hopkins L, Johnson C, Slife H, Dunn T. 1998. The *Saccharomyces cerevisiae* TSC10/YBR265w gene encoding 3-ketosphinganine reductase is identified in a screen for temperature-sensitive suppressors of the Ca^{2+}-sensitive *csg2Delta* mutant. *Journal of Biological Chemistry* 273: 30688–30694.

Begum MA, Shi XX, Tan Y, Zhou WW, Hannun Y, Obeid L, Mao C, Zhu ZR. 2016. Molecular characterization of rice OsLCB2a1 gene and functional analysis of its role in insect resistance. *Frontiers in Plant Science* 7: 1789.

Bi FC, Liu Z, Wu JX, Liang H, Xi XL, Fang C, Sun TJ, Yin J, Dai GY, Rong C, *et al*. 2014. Loss of ceramide kinase in Arabidopsis impairs defenses and promotes ceramide accumulation and mitochondrial H_2O_2 bursts. *Plant Cell* 26: 3449–3467.

Cacas JL, Bure C, Furt F, Maalouf JP, Badoc A, Cluzet S, Schmitter JM, Antajan E, Mongrand S. 2013. Biochemical survey of the polar head of plant glycosylinositolphosphoceramides unravels broad diversity. *Phytochemistry* 96: 191–200.

Cacas JL, Bure C, Grosjean K, Gerbeau-Pissot P, Lherminier J, Rombouts Y, Maes E, Bossard C, Gronnier J, Furt F, *et al*. 2016. Revisiting plant plasma membrane lipids in tobacco: a focus on sphingolipids. *Plant Physiology* 170: 367–384.

Cantrel C, Vazquez T, Puyaubert J, Reze N, Lesch M, Kaiser WM, Dutilleul C, Guillas I, Zachowski A, Baudouin E. 2011. Nitric oxide participates in cold-responsive phosphosphingolipid formation and gene expression in *Arabidopsis thaliana*. *New Phytologist* 189: 415–427.

Chen M, Han G, Dietrich CR, Dunn TM, Cahoon EB. 2006. The essential nature of sphingolipids in plants as revealed by the functional identification and characterization of the Arabidopsis LCB1 subunit of serine palmitoyltransferase. *Plant Cell* 18: 3576–3593.

Chen M, Markham JE, Cahoon EB. 2012. Sphingolipid Delta8 unsaturation is important for glucosylceramide biosynthesis and low-temperature performance in Arabidopsis. *The Plant Journal* 69: 769–781.

Coursol S, Fan LM, Le Stunff H, Spiegel S, Gilroy S, Assmann SM. 2003. Sphingolipid signalling in Arabidopsis guard cells involves heterotrimeric G proteins. *Nature* 423: 651–654.

Coursol S, Fromentin J, Noirot E, Briere C, Robert F, Morel J, Liang YK, Lherminier J, Simon-Plas F. 2015. Long-chain bases and their phosphorylated derivatives differentially regulate cryptogein-induced production of reactive oxygen species in tobacco (*Nicotiana tabacum*) BY-2 cells. *New Phytologist* 205: 1239–1249.

Coursol S, Le Stunff H, Lynch DV, Gilroy S, Assmann SM, Spiegel S. 2005. Arabidopsis sphingosine kinase and the effects of phytosphingosine-1-phosphate on stomatal aperture. *Plant Physiology* 137: 724–737.

Degenkolbe T, Giavalisco P, Zuther E, Seiwert B, Hincha DK, Willmitzer L. 2012. Differential remodeling of the lipidome during cold acclimation in natural accessions of *Arabidopsis thaliana*. *The Plant Journal* 72: 972–982.

Dutilleul C, Benhassaine-Kesri G, Demandre C, Reze N, Launay A, Pelletier S, Renou JP, Zachowski A, Baudouin E, Guillas I. 2012. Phytosphingosine-phosphate is a signal for AtMPK6 activation and Arabidopsis response to chilling. *New Phytologist* 194: 181–191.

Dutilleul C, Chavarria H, Reze N, Sotta B, Baudouin E, Guillas I. 2015. Evidence for ACD5 ceramide kinase activity involvement in Arabidopsis response to cold stress. *Plant, Cell & Environment* 38: 2688–2697.

Fang L, Ishikawa T, Rennie EA, Murawska GM, Lao J, Yan J, Tsai AY, Baidoo EE, Xu J, Keasling JD, et al. 2016. Loss of inositol phosphorylceramide sphingolipid mannosylation induces plant immune responses and reduces cellulose content in Arabidopsis. *Plant Cell* 28: 2991–3004.

Glazebrook J. 2005. Contrasting mechanisms of defense against biotrophic and necrotrophic pathogens. *Annual Review of Phytopathology* 43: 205–227.

Goto H, Nishikawa K, Shionoya N, Taniguchi M, Igarashi T. 2012. Determination of sphingoid bases from hydrolyzed glucosylceramide in rice and wheat by online post-column high-performance liquid chromatography with O-Phthalaldehyde derivatization. *Journal of Oleo Science* 61: 681–688.

Guillas I, Guellim A, Reze N, Baudouin E. 2013. Long chain base changes triggered by a short exposure of Arabidopsis to low temperature are altered by AHb1 non-symbiotic haemoglobin overexpression. *Plant Physiology and Biochemistry* 63: 191–195.

Guo L, Mishra G, Markham JE, Li M, Tawfall A, Welti R, Wang X. 2012. Connections between sphingosine kinase and phospholipase D in the abscisic acid signaling pathway in Arabidopsis. *Journal of Biological Chemistry* 287: 8286–8296.

Guo L, Mishra G, Taylor K, Wang X. 2011. Phosphatidic acid binds and stimulates Arabidopsis sphingosine kinases. *Journal of Biological Chemistry* 286: 13336–13345.

Guo L, Wang X. 2012. Crosstalk between phospholipase D and sphingosine kinase in plant stress signaling. *Frontiers in Plant Science* 3: 51.

Huang X, Zhang Y, Zhang X, Shi Y. 2017. Long-chain base kinase1 affects freezing tolerance in *Arabidopsis thaliana*. *Plant Science* 259: 94–103.

Imai H, Nishiura H. 2005. Phosphorylation of sphingoid long-chain bases in Arabidopsis: functional characterization and expression of the first sphingoid long-chain base kinase gene in plants. *Plant Cell Physiology* 46: 375–380.

Ines C, Parra-Lobato MC, Paredes MA, Labrador J, Gallardo M, Saucedo-Garcia M, Gavilanes-Ruiz M, Gomez-Jimenez MC. 2018. Sphingolipid distribution, content and gene expression during olive-fruit development and ripening. *Frontiers in Plant Science* 9: 28.

Ishikawa T, Aki T, Yanagisawa S, Uchimiya H, Kawai-Yamada M. 2015. Overexpression of BAX INHIBITOR-1 links plasma membrane microdomain proteins to stress. *Plant Physiology* 169: 1333–1343.

Ishikawa T, Fang L, Rennie EA, Sechet J, Yan J, Jing B, Moore W, Cahoon EB, Scheller HV, Kawai-Yamada M, et al. 2018. Glucosamine inositolphosphorylceramide transferase1 (GINT1) is a GlcNAc-containing glycosylinositol phosphorylceramide glycosyltransferase. *Plant Physiology* 177: 938–952.

Islam MN, Jacquemot MP, Coursol S, Ng CK. 2012. Sphingosine in plants–more riddles from the Sphinx? *New Phytologist* 193: 51–57.

Kawaguchi M, Imai H, Naoe M, Yasui Y, Ohnishi M. 2000. Cerebrosides in grapevine leaves: distinct composition of sphingoid bases among the grapevine species having different tolerances to freezing temperature. *Bioscience, Biotechnology, and Biochemistry* 64: 1271–1273.

Kimberlin AN, Han G, Luttgeharm KD, Chen M, Cahoon RE, Stone JM, Markham JE, Dunn TM, Cahoon EB. 2016. ORM expression alters sphingolipid homeostasis and differentially affects ceramide synthase activity. *Plant Physiology* 172: 889–900.

Kimberlin AN, Majumder S, Han G, Chen M, Cahoon RE, Stone JM, Dunn TM, Cahoon EB. 2013. Arabidopsis 56-amino acid serine palmitoyltransferase-interacting proteins stimulate sphingolipid synthesis, are essential, and affect mycotoxin sensitivity. *Plant Cell* 25: 4627–4639.

König S, Feussner K, Schwarz M, Kaever A, Iven T, Landesfeind M, Ternes P, Karlovsky P, Lipka V, Feussner I. 2012. Arabidopsis mutants of sphingolipid fatty acid alpha-hydroxylases accumulate ceramides and salicylates. *New Phytologist* 196: 1086–1097.

Lachaud C, Prigent E, Thuleau P, Grat S, Da Silva D, Briere C, Mazars C, Cotelle V. 2013. 14-3-3-regulated Ca^{2+}-dependent protein kinase CPK3 is required for sphingolipid-induced cell death in Arabidopsis. *Cell Death & Differentiation* 20: 209–217.

Lee Y, Assmann SM. 1991. Diacylglycerols induce both ion pumping in patch-clamped guard-cell protoplasts and opening of intact stomata. *Proceedings of the National Academy of Sciences, USA* 88: 2127–2131.

Lenarcic T, Albert I, Bohm H, Hodnik V, Pirc K, Zavec AB, Podobnik M, Pahovnik D, Zagar E, Pruitt R, et al. 2017. Eudicot plant-specific sphingolipids determine host selectivity of microbial NLP cytolysins. *Science* 358: 1431–1434.

Li J, Bi FC, Yin J, Wu JX, Rong C, Wu JL, Yao N. 2015. An Arabidopsis neutral ceramidase mutant ncer1 accumulates hydroxyceramides and is sensitive to oxidative stress. *Frontiers in Plant Science* 6: 460.

Li J, Yin J, Rong C, Li KE, Wu JX, Huang LQ, Zeng HY, Sahu SK, Yao N. 2016. Orosomucoid proteins interact with the small subunit of serine palmitoyltransferase and contribute to sphingolipid homeostasis and stress responses in Arabidopsis. *Plant Cell* 28: 3038–3051.

Li M, Zhang K, Long R, Sun Y, Kang J, Zhang T, Cao S. 2017. iTRAQ-based comparative proteomic analysis reveals tissue-specific and novel early-stage molecular mechanisms of salt stress response in *Carex rigescens*. *Environmental & Experimental Botany* 143: 99–114.

Lung SC, Chye ML. 2019. Arabidopsis acyl-CoA-binding proteins regulate the synthesis of lipid signals. *New Phytologist* 223: 113–117.

Luttgeharm KD, Chen M, Mehra A, Cahoon RE, Markham JE, Cahoon EB. 2015. Overexpression of Arabidopsis ceramide synthases differentially affects growth, sphingolipid metabolism, programmed cell death, and mycotoxin resistance. *Plant Physiology* 169: 1108–1117.

Luttgeharm KD, Kimberlin AN, Cahoon EB. 2016. Plant sphingolipid metabolism and function. *Sub-Cellular Biochemistry* 86: 249–286.

Magnin-Robert M, Le Bourse D, Markham J, Dorey S, Clement C, Baillieul F, Dhondt-Cordelier S. 2015. Modifications of sphingolipid content affect tolerance to hemibiotrophic and necrotrophic pathogens by modulating plant defense responses in Arabidopsis. *Plant Physiology* 169: 2255–2274.

Mamode Cassim A, Gouguet P, Gronnier J, Laurent N, Germain V, Grison M, Boutte Y, Gerbeau-Pissot P, Simon-Plas F, Mongrand S. 2019. Plant lipids: key players of plasma membrane organization and function. *Progress in Lipid Research* 73: 1–27.

Markham JE, Li J, Cahoon EB, Jaworski JG. 2006. Separation and identification of major plant sphingolipid classes from leaves. *Journal of Bioogical Chemistry* 281: 22684–22694.

Michaelson LV, Napier JA, Molino D, Faure JD. 2016. Plant sphingolipids: their importance in cellular organization and adaption. *Biochimica et Biophysica Acta* 1861: 1329–1335.

Michaelson LV, Zauner S, Markham JE, Haslam RP, Desikan R, Mugford S, Albrecht S, Warnecke D, Sperling P, Heinz E, et al. 2009. Functional characterization of a higher plant sphingolipid Delta4-desaturase: defining the role of sphingosine and sphingosine-1-phosphate in Arabidopsis. *Plant Physiology* 149: 487–498.

Mina JG, Okada Y, Wansadhipathi-Kannangara NK, Pratt S, Shams-Eldin H, Schwarz RT, Steel PG, Fawcett T, Denny PW. 2010. Functional analyses of differentially expressed isoforms of the Arabidopsis inositol phosphorylceramide synthase. *Plant Molecular Biology* 73: 399–407.

Minami A, Fujiwara M, Furuto A, Fukao Y, Yamashita T, Kamo M, Kawamura Y, Uemura M. 2009. Alterations in detergent-resistant plasma membrane

microdomains in *Arabidopsis thaliana* during cold acclimation. *Plant and Cell Physiology* 50: 341–359.

Molino D, Van der Giessen E, Gissot L, Hematy K, Marion J, Barthelemy J, Bellec Y, Vernhettes S, Satiat-Jeunemaitre B, Galli T, *et al.* 2014. Inhibition of very long acyl chain sphingolipid synthesis modifies membrane dynamics during plant cytokinesis. *Biochimica et Biophysica Acta* 1842: 1422–1430.

Moreau P, Bessoule JJ, Mongrand S, Testet E, Vincent P, Cassagne C. 1998. Lipid trafficking in plant cells. *Progress in Lipid Research* 37: 371–391.

Mortimer JC, Yu X, Albrecht S, Sicilia F, Huichalaf M, Ampuero D, Michaelson LV, Murphy AM, Matsunaga T, Kurz S, *et al.* 2013. Abnormal glycosphingolipid mannosylation triggers salicylic acid-mediated responses in Arabidopsis. *Plant Cell* 25: 1881–1894.

Msanne J, Chen M, Luttgeharm KD, Bradley AM, Mays ES, Paper JM, Boyle DL, Cahoon RE, Schrick K, Cahoon EB. 2015. Glucosylceramides are critical for cell-type differentiation and organogenesis, but not for cell viability in Arabidopsis. *The Plant Journal* 84: 188–201.

Murakami Y, Tsuyama M, Kobayashi Y, Kodama H, Iba K. 2000. Trienoic fatty acids and plant tolerance of high temperature. *Science* 287: 476–479.

Nagano M, Ishikawa T, Fujiwara M, Fukao Y, Kawano Y, Kawai-Yamada M, Shimamoto K. 2016. Plasma membrane microdomains are essential for Rac1-RbohB/H-mediated immunity in rice. *Plant Cell* 28: 1966–1983.

Nagano M, Ishikawa T, Ogawa Y, Iwabuchi M, Nakasone A, Shimamoto K, Uchimiya H, Kawai-Yamada M. 2014. Arabidopsis Bax inhibitor-1 promotes sphingolipid synthesis during cold stress by interacting with ceramide-modifying enzymes. *Planta* 240: 77–89.

Nakagawa N, Kato M, Takahashi Y, Shimazaki K, Tamura K, Tokuji Y, Kihara A, Imai H. 2012. Degradation of long-chain base 1-phosphate (LCBP) in Arabidopsis: functional characterization of LCBP phosphatase involved in the dehydration stress response. *Journal of Plant Research* 125: 439–449.

Ng CK, Carr K, McAinsh MR, Powell B, Hetherington AM. 2001. Drought-induced guard cell signal transduction involves sphingosine-1-phosphate. *Nature* 410: 596–599.

Ng CK, Coursol S. 2012. New insights into phospholipase d and sphingosine kinase activation in Arabidopsis. *Frontiers in Physiology* 3: 67.

Pata MO, Hannun YA, Ng CK. 2010. Plant sphingolipids: decoding the enigma of the Sphinx. *New Phytologist* 185: 611–630.

Pata MO, Wu BX, Bielawski J, Xiong TC, Hannun YA, Ng CK. 2008. Molecular cloning and characterization of OsCDase, a ceramidase enzyme from rice. *The Plant Journal* 55: 1000–1009.

Peters C, Li M, Narasimhan R, Roth M, Welti R, Wang X. 2010. Nonspecific phospholipase C NPC4 promotes responses to abscisic acid and tolerance to hyperosmotic stress in Arabidopsis. *Plant Cell* 22: 2642–2659.

Qin X, Zhang RX, Ge S, Zhou T, Liang YK. 2017. Sphingosine kinase AtSPHK1 functions in fumonisin B1-triggered cell death in Arabidopsis. *Plant Physiology and Biochemistry* 119: 70–80.

Rennie EA, Ebert B, Miles GP, Cahoon RE, Christiansen KM, Stonebloom S, Khatab H, Twell D, Petzold CJ, Adams PD, *et al.* 2014. Identification of a sphingolipid alpha-glucuronosyltransferase that is essential for pollen function in Arabidopsis. *Plant Cell* 26: 3314–3325.

Rivas-San Vicente M, Larios-Zarate G, Plasencia J. 2013. Disruption of sphingolipid biosynthesis in *Nicotiana benthamiana* activates salicylic acid-dependent responses and compromises resistance to *Alternaria alternata* f. sp. *lycopersici*. *Planta* 237: 121–136.

Routaboul JM, Skidmore C, Wallis JG, Browse J. 2012. Arabidopsis mutants reveal that short- and long-term thermotolerance have different requirements for trienoic fatty acids. *Journal of Experimental Botany* 63: 1435–1443.

Sanchez-Rangel D, Rivas-San Vicente M, de la Torre-Hernandez ME, Najera-Martinez M, Plasencia J. 2015. Deciphering the link between salicylic acid signaling and sphingolipid metabolism. *Frontiers in Plant Science* 6: 125.

Saucedo-Garcia M, Guevara-Garcia A, Gonzalez-Solis A, Cruz-Garcia F, Vazquez-Santana S, Markham JE, Lozano-Rosas MG, Dietrich CR, Ramos-Vega M, Cahoon EB, *et al.* 2011. MPK6, sphinganine and the LCB2a gene from serine palmitoyltransferase are required in the signaling pathway that mediates cell death induced by long chain bases in Arabidopsis. *New Phytologist* 191: 943–957.

Shi L, Bielawski J, Mu J, Dong H, Teng C, Zhang J, Yang X, Tomishige N, Hanada K, Hannun YA, *et al.* 2007. Involvement of sphingoid bases in mediating reactive oxygen intermediate production and programmed cell death in Arabidopsis. *Cell Research* 17: 1030–1040.

Shi C, Yin J, Liu Z, Wu JX, Zhao Q, Ren J, Yao N. 2015. A systematic simulation of the effect of salicylic acid on sphingolipid metabolism. *Frontiers in Plant Science* 6: 186.

Spassieva S, Hille J. 2003. Plant sphingolipids today - are they still enigmatic? *Plant Biology* 5: 125–136.

Takahashi D, Imai H, Kawamura Y, Uemura M. 2016. Lipid profiles of detergent resistant fractions of the plasma membrane in oat and rye in association with cold acclimation and freezing tolerance. *Cryobiology* 72: 123–134.

Tanaka T, Kida T, Imai H, Morishige J, Yamashita R, Matsuoka H, Uozumi S, Satouchi K, Nagano M, Tokumura A. 2013. Identification of a sphingolipid-specific phospholipase D activity associated with the generation of phytoceramide-1-phosphate in cabbage leaves. *FEBS Journal* 280: 3797–3809.

Tartaglio V, Rennie EA, Cahoon R, Wang G, Baidoo E, Mortimer JC, Cahoon EB, Scheller HV. 2017. Glycosylation of inositol phosphorylceramide sphingolipids is required for normal growth and reproduction in Arabidopsis. *The Plant Journal* 89: 278–290.

Ternes P, Feussner K, Werner S, Lerche J, Iven T, Heilmann I, Riezman H, Feussner I. 2011. Disruption of the ceramide synthase LOH1 causes spontaneous cell death in *Arabidopsis thaliana*. *New Phytologist* 192: 841–854.

Thomma BP, Penninckx IA, Broekaert WF, Cammue BP. 2001. The complexity of disease signaling in Arabidopsis. *Current Opinion in Immunology* 13: 63–68.

Tortosa M, Cartea ME, Rodriguez VM, Velasco P. 2018. Unraveling the metabolic response of *Brassica oleracea* exposed to *Xanthomonas campestris* pv. *campestris*. *Journal of the Science of Food and Agriculture* 98: 3675–3683.

Tovuu A, Zulfugarov IS, Wu G, Kang IS, Kim C, Moon BY, An G, Lee CH. 2016. Rice mutants deficient in omega-3 fatty acid desaturase (FAD8) fail to acclimate to cold temperatures. *Plant Physiology and Biochemistry* 109: 525–535.

Tsegaye Y, Richardson CG, Bravo JE, Mulcahy BJ, Lynch DV, Markham JE, Jaworski JG, Chen M, Cahoon EB, Dunn TM. 2007. Arabidopsis mutants lacking long chain base phosphate lyase are fumonisin-sensitive and accumulate trihydroxy-18:1 long chain base phosphate. *Journal of Biological Chemistry* 282: 28195–28206.

Wang W, Yang X, Tangchaiburana S, Ndeh R, Markham JE, Tsegaye Y, Dunn TM, Wang GL, Bellizzi M, Parsons JF, *et al.* 2008. An inositolphosphorylceramide synthase is involved in regulation of plant programmed cell death associated with defense in Arabidopsis. *Plant Cell* 20: 3163–3179.

Wilkinson SW, Pastor V, Paplauskas S, Pétriacq P, Luna E. 2017. Long-lasting β-aminobutyric acid-induced resistance protects tomato fruit against *Botrytis cinerea*. *Plant Pathology* 67: 30–41.

Worrall D, Liang YK, Alvarez S, Holroyd GH, Spiegel S, Panagopulos M, Gray JE, Hetherington AM. 2008. Involvement of sphingosine kinase in plant cell signalling. *The Plant Journal* 56: 64–72.

Wu JX, Li J, Liu Z, Yin J, Chang ZY, Rong C, Wu JL, Bi FC, Yao N. 2015a. The Arabidopsis ceramidase AtACER functions in disease resistance and salt tolerance. *The Plant Journal* 81: 767–780.

Wu JX, Wu JL, Yin J, Zheng P, Yao N. 2015b. Ethylene modulates sphingolipid synthesis in Arabidopsis. *Frontiers in Plant Science* 6: 1122.

Xie LJ, Chen QF, Chen MX, Yu LJ, Huang L, Chen L, Wang FZ, Xia FN, Zhu TR, Wu JX, *et al.* 2015a. Unsaturation of very-long-chain ceramides protects plant from hypoxia-induced damages by modulating ethylene signaling in Arabidopsis. *PLoS Genetics* 11: e1005143.

Xie LJ, Yu LJ, Chen QF, Wang FZ, Huang L, Xia FN, Zhu TR, Wu JX, Yin J, Liao B, *et al.* 2015b. Arabidopsis acyl-CoA-binding protein ACBP3 participates in plant response to hypoxia by modulating very-long-chain fatty acid metabolism. *The Plant Journal* 81: 53–67.

Yanagawa D, Ishikawa T, Imai H. 2017. Synthesis and degradation of long-chain base phosphates affect fumonisin B1-induced cell death in *Arabidopsis thaliana*. *Journal of Plant Research* 130: 571–585.

Yu L, Nie J, Cao C, Jin Y, Yan M, Wang F, Liu J, Xiao Y, Liang Y, Zhang W. 2010. Phosphatidic acid mediates salt stress response by regulation of MPK6 in Arabidopsis thaliana. *New Phytologist* 188: 762–773.

Zhang H, Huang L, Li X, Ouyang Z, Yu Y, Li D, Song F. 2013. Overexpression of a rice long-chain base kinase gene OsLCBK1 in tobacco improves oxidative stress tolerance. *Plant Biotechnology* 30: 9–16.

Zhang H, Jin X, Huang L, Hong Y, Zhang Y, Ouyang Z, Li X, Song F, Li D. 2014. Molecular characterization of rice sphingosine-1-phosphate lyase gene OsSPL1 and functional analysis of its role in disease resistance response. *Plant Cell Reports* **33**: 1745–1756.

Zhang H, Zhai J, Mo J, Li D, Song F. 2012. Overexpression of rice sphingosine-1-phoshpate lyase gene OsSPL1 in transgenic tobacco reduces salt and oxidative stress tolerance. *Journal of Integrative Plant Biology* **54**: 652–662.

Zhang Y, Zhu H, Zhang Q, Li M, Yan M, Wang R, Wang L, Welti R, Zhang W, Wang X. 2009. Phospholipase dalpha1 and phosphatidic acid regulate NADPH oxidase activity and production of reactive oxygen species in ABA-mediated stomatal closure in Arabidopsis. *Plant Cell* **21**: 2357–2377.

Zheng P, Wu JX, Sahu SK, Zeng HY, Huang LQ, Liu Z, Xiao S, Yao N. 2018. Loss of alkaline ceramidase inhibits autophagy in Arabidopsis and plays an important role during environmental stress response. *Plant, Cell & Environment* **41**: 837–849.

Zhou Y, Zeng L, Fu X, Mei X, Cheng S, Liao Y, Deng R, Xu X, Jiang Y, Duan X, *et al.* 2016. The sphingolipid biosynthetic enzyme Sphingolipid delta8 desaturase is important for chilling resistance of tomato. *Scientific Reports* **6**: 38742.

Zinta G, AbdElgawad H, Peshev D, Weedon JT, Van den Ende W, Nijs I, Janssens IA, Beemster GTS, Han A. 2018. Dynamics of metabolic responses to combined heat and drought spells in *Arabidopsis thaliana* under ambient and rising atmospheric CO_2. *Journal of Experimental Botany* **69**: 2159–2170.

Supporting Information

Additional Supporting Information may be found online in the Supporting Information section at the end of the article.

Table S1 Abbreviations used in this review.

Please note: Wiley Blackwell are not responsible for the content or functionality of any Supporting Information supplied by the authors. Any queries (other than missing material) should be directed to the *New Phytologist* Central Office.

About *New Phytologist*

- *New Phytologist* is an electronic (online-only) journal owned by the New Phytologist Trust, a **not-for-profit organization** dedicated to the promotion of plant science, facilitating projects from symposia to free access for our Tansley reviews and Tansley insights.

- Regular papers, Letters, Research reviews, Rapid reports and both Modelling/Theory and Methods papers are encouraged. We are committed to rapid processing, from online submission through to publication 'as ready' via *Early View* – our average time to decision is <26 days. There are **no page or colour charges** and a PDF version will be provided for each article.

- The journal is available online at Wiley Online Library. Visit **www.newphytologist.com** to search the articles and register for table of contents email alerts.

- If you have any questions, do get in touch with Central Office (np-centraloffice@lancaster.ac.uk) or, if it is more convenient, our USA Office (np-usaoffice@lancaster.ac.uk)

- For submission instructions, subscription and all the latest information visit **www.newphytologist.com**

frontiers
in Plant Science

Protoplast: A Valuable Toolbox to Investigate Plant Stress Perception and Response

Guillaume Gilliard[1†], Eloïse Huby[1,2†], Sylvain Cordelier[2], Marc Ongena[3], Sandrine Dhondt-Cordelier[2‡]* and Magali Deleu[1‡]*

[1] Laboratoire de Biophysique Moléculaire aux Interfaces, SFR Condorcet FR CNRS 3417, Gembloux Agro-Bio Tech, Université de Liège, Gembloux, Belgium, [2] RIBP EA 4707, USC INRAE 1488, SFR Condorcet FR CNRS 3417, Université de Reims Champagne Ardenne, Reims, France, [3] Microbial Processes and Interactions Laboratory, Terra Teaching and Research Center, SFR Condorcet FR CNRS 3417, Gembloux Agro-Bio Tech, Université de Liège, Gembloux, Belgium

Plants are constantly facing abiotic and biotic stresses. To continue to thrive in their environment, they have developed many sophisticated mechanisms to perceive these stresses and provide an appropriate response. There are many ways to study these stress signals in plant, and among them, protoplasts appear to provide a unique experimental system. As plant cells devoid of cell wall, protoplasts allow observations at the individual cell level. They also offer a prime access to the plasma membrane and an original view on the inside of the cell. In this regard, protoplasts are particularly useful to address essential biological questions regarding stress response, such as protein signaling, ion fluxes, ROS production, and plasma membrane dynamics. Here, the tools associated with protoplasts to comprehend plant stress signaling are overviewed and their potential to decipher plant defense mechanisms is discussed.

Keywords: plant stress response, protein signaling, ion fluxes, cell membrane dynamics, plant protoplasts

INTRODUCTION

As sessile organisms, plants are exposed to myriads of potential stresses that can be harmful to their development. These adverse environmental conditions include both biotic and abiotic stresses that increasingly threaten agricultural plant productivity at a worldwide scale. In response, plants have developed an array of mechanisms to survive tough environmental conditions such as drought, heat, cold, nutrient deficiency, pollutants, pathogens, and herbivore attacks. The first crucial step in plant defense is the perception of the stress so that they can respond in a rapid and effective manner (Couto and Zipfel, 2016). While the underlying sensing mechanisms of abiotic stress are not fully elucidated, mostly due to functional redundancy in genes encoding sensor proteins or mutant lethality (Zhu, 2016; Gong et al., 2020), it is believed they are perceived by primary sensory mechanisms (Lamers et al., 2020). Several putative sensors have been ascribed to abiotic stresses perception and are often linked to membrane-associated proteins of the cells, organelles, or nucleus membrane proteins (Zhu, 2016). These sensors will then translate the changing environment into a signaling cascade allowing the plant to coordinate an appropriate response for acclimation. Similarly, plants have evolved an innate immune system to counteract the deleterious effects of biotic stresses (Jones and Dangl, 2006; Saijo and Loo, 2020; Zhou and Zhang, 2020). Once the constitutive plant defenses such

as the cuticle, the cell wall (CW) and other physical and biochemical barriers are overrun, the plant plasma membrane (PM) is then at the frontline of stress perception. Through cell surface and intracellular protein receptors, the plant is capable of sensing multiple molecular stress factors, such as MAMPs (microbe-associated molecular patterns), PAMPs (pathogen-associated molecular patterns), and DAMPs (damage-associated molecular patterns), thus initiating a cascade of signal transduction leading to a rapid and effective response from the plant (Cook et al., 2015; Couto and Zipfel, 2016). Both biotic and abiotic stresses share some early signaling events such as the production of reactive oxygen species (ROS) by NADPH oxidases, activation of protein kinases, receptors, or co-receptors through phosphorylation (Kadota et al., 2015; Yu et al., 2017; Zipfel and Oldroyd, 2017; Bigeard and Hirt, 2018), and rapid and transient change of ion fluxes (Jones and Dangl, 2006; Bigeard et al., 2015; Lamers et al., 2020). These fluxes can act on PM potential regulation and activation of Ca^{2+}-dependent or K^+-dependent enzymes (Jeworutzki et al., 2010; Bose et al., 2011; Demidchik, 2014; Wu et al., 2014b; Zipfel and Oldroyd, 2017; Sze and Chanroj, 2018; Yoshioka and Moeder, 2020). Then, activation of transcription factors (TFs) leads to the production of stress-related hormones such as abscisic acid, salicylic acid, jasmonic acid, and ethylene. Upon pathogen attacks, positive and negative crosstalks (Glazebrook, 2005) between these signaling molecules trigger the accumulation of an array of antimicrobial compounds such as pathogenesis-related proteins and phytoalexins (Delaunois et al., 2014).

How plants perceive and respond to these stress signals are essential biological questions and many of them are now investigated through innovative techniques that employ protoplasts as proxy for whole tissue, or even for whole plants. A protoplast refers to a spherical cell whose CW has been removed by digestive enzymes. The first protoplast isolations were developed in bacteria (Weibull, 1953) and fungi (Eddy and Williamson, 1957; Barbara and Bonner, 1959), before being transposed to plants (Cocking, 1960). They are usually obtained from enzymatic digestion of leaf and root tissues or even from cultured cells of a wide variety of species (Fowke et al., 1983; Yoo et al., 2007; Lin et al., 2018; Sangra et al., 2019; Zhao et al., 2019; Cheng and Nakata, 2020). With transformation methods already developed and microscopy techniques fast expending, the protoplast system could ultimately be considered as convenient screening platform to better target future whole plant analyses (Li et al., 2014). Moreover, freshly isolated mesophyll protoplasts are believed to retain the physiological properties of whole plants (Yoo et al., 2007).

Protoplasts have already been described as a useful and versatile system to study plant cell reprograming during development (Pasternak et al., 2020) and plastid transformation (Yu et al., 2020). In this review, we will focus on the different approaches and techniques that use protoplasts to study plant responses to both biotic and abiotic stresses and particularly on transient expression assays (TEA), on the use of fluorescence probes and on patch-clamp assays (**Figure 1** for an overview). We will also enlighten and discuss the advantages and the limitations of protoplasts as a proxy for whole tissues or plants.

PROTOPLASTS AS TOOLS IN BIOMOLECULAR STUDIES

Protoplasts represent cell populations that are adapted for synchronous pharmacological and biochemical treatments and efficient genetic transformation (Sheen, 2001; Yoo et al., 2007; Xing and Wang, 2015). As TEAs in protoplasts can provide results in less than 36 h (Yoo et al., 2007), they are a useful system to investigate early and transient events in plants during stress response at the biomolecular scale. TEAs are performed by isolating protoplasts from plant tissues, transfecting them in the presence of polyethylene glycol and calcium (Yoo et al., 2007; Lin et al., 2014) or through electroporation (Miao and Jiang, 2007) and incubating them for 2–24 h. They have been developed in several plant species such as *Arabidopsis thaliana* (Asai et al., 2002; Boudsocq et al., 2004, 2010; Bethke et al., 2009; Li et al., 2019), maize (Kovtun et al., 1998), rice (Takai et al., 2007; Wang et al., 2014; Liu et al., 2018), barley (Saur et al., 2019), wheat (Hahn et al., 2020), strawberry (Gou et al., 2020), banana (Wu et al., 2020b), and rubber tree (Zhang et al., 2016). This system can be used for high-throughput analysis of plant signaling pathways and regulatory mechanisms (**Figure 1**).

Functional Screening of Proteins

Plant signaling involves several large protein families which contain many members. For example, in *Arabidopsis*, mitogen-activated protein kinase (MAPK), MAPK kinase (MAPKK), and MAPKK kinase families contain 20, 10, and 60 members, respectively (Bigeard and Hirt, 2018), calcium-dependent protein kinase (CDPK) family has 34 members (Boudsocq et al., 2010), and TFs families such as MYB TFs, WRKY TFs, and basic leucine zipper transcription TFs comprise more than 176, 75, and 78 members, respectively (Dubos et al., 2010; Dröge-Laser et al., 2018; Wani et al., 2021). However, depending on the type of stress, the proteins involved in the signaling cascade may differ and a better understanding of plant defense mechanisms is therefore linked to the identification of its signaling components.

By avoiding time-consuming whole plant transformation, protoplasts offer a useful system to perform functional genomic screen among a group of proteins and determine which of them are able to activate defense genes. The screening is performed with reporter gene assay comprising a number of TEAs equal to the number of proteins or combination of proteins tested. In each TEA, protoplasts are transfected with 2 or 3 vectors simultaneously. One vector expresses the gene coding a protein of interest and has therefore a different sequence in each TEA. Then, a reporter gene often associated with a control gene, both constant between TEAs, can be expressed either in one (Hellens et al., 2005; Liu et al., 2018) or two different vectors (Asai et al., 2002;
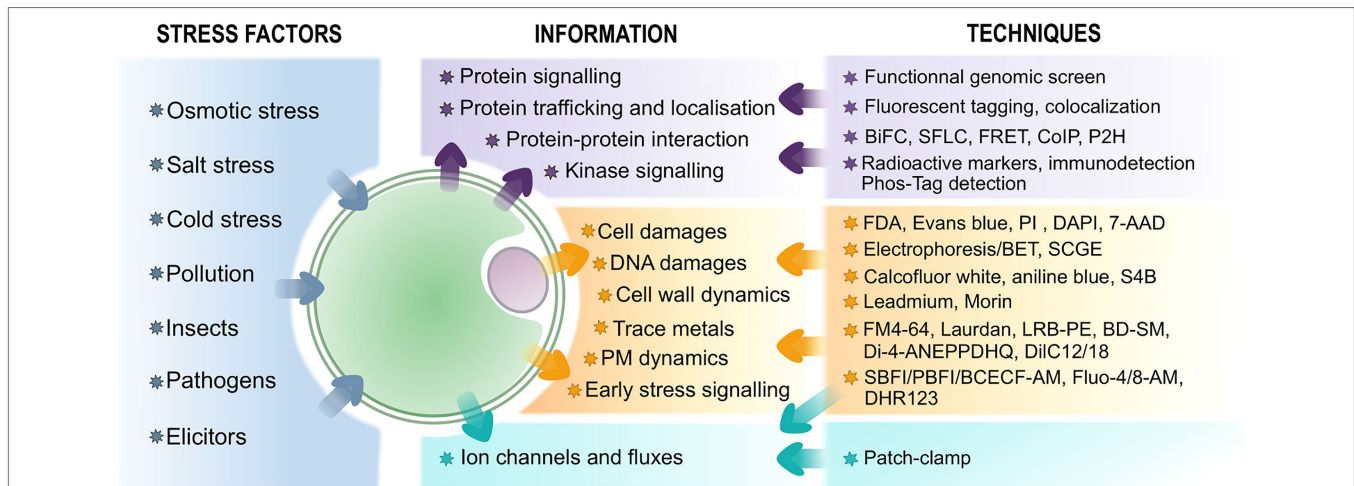
FIGURE 1 | Overview of techniques associated with protoplasts to study plant stress perception and response and the information they provide. The biomolecular-related assays are in purple, fluorescence probes-associated techniques are in orange – see text for further information on the probes, and electrophysiological approaches are in blue.

Boudsocq et al., 2010). The reporter gene is under a stress-inducible promoter that allows the detection of defense gene induction, while the control gene is under a constitutive promoter and allows the normalization of the reporter gene activity by taking into account experimental variation such as differences in cell number, in cell viability, and transformation efficiency (Kovtun et al., 1998). The firefly luciferase or the GFP gene is commonly used as reporter gene, while the ß-glucuronidase (GUS) or the *Renilla* luciferase gene is often used as control gene (Kovtun et al., 1998; Sheen, 2001; Asai et al., 2002; Yoo et al., 2007; Wehner et al., 2011; Thévenin et al., 2012; Liu et al., 2018). The choice of the stress-inducible promoter represents the main limitation of the reporter gene assay as it has to be determined either based on the literature, or by detecting gene activation with PCR (Asai et al., 2002; Boudsocq et al., 2010; Chen et al., 2010). Finally, using the microtiter plate-based protoplast transactivation (PTA) system established by Wehner et al. (2011), high-throughput functional genomic screening can be performed to rapidly analyze up to 96 proteins.

Using this approach, screening of protein kinase families, such as MAPK and CDPK, and TFs has been performed to identify the one(s) involved in plant response to a specific biotic (Asai et al., 2002; Boudsocq et al., 2010; Sheikh et al., 2016) or abiotic stress (Chen et al., 2010; Wehner et al., 2011). When combined with RT-qPCR analysis, TEAs in protoplasts can also reveal potential synergic or antagonist effect between signaling pathways of signaling proteins (Asai et al., 2002; Boudsocq et al., 2010). Moreover, the use of vectors expressing structural variants of the protein of interest could evidence structural motifs compulsory for the signaling function of proteins (Mueller et al., 2012; Pecher et al., 2014). Such variants have provided clues on how allele selection plays a role in climate adaptation of some subspecies (Liu et al., 2018). Reporter gene assays in *Arabidopsis* protoplasts have also demonstrated the complex regulation between catalytic and regulatory subunit

of sucrose non-fermenting1-related Kinase1 (SnRK1), involved in metabolic stress response and development (Ramon et al., 2019).

Protein Location and Trafficking

Besides the functional role of proteins in gene regulation, TEA can also provide information on their subcellular locations and dynamics (i.e., their mobility) into the cell when protoplasts are expressing both the studied protein fused with a fluorescent one, such as YFP, GFP, CFP, or mCherry, and a fluorescent marker specific of a cellular compartment. To that end, several markers have been developed to mark specifically plant organelles (Nelson et al., 2007; Zhang et al., 2021), and their diversity for the different organelles has been recently reviewed (Zhu et al., 2020). These information may help to elucidate protein function (Nelson et al., 2007), since TFs are expected to be found in the nucleus (Asai et al., 2002; Sheikh et al., 2016; Moon et al., 2019), protein receptors in the PM (Li et al., 2017; Liu et al., 2017; Pham et al., 2020), and proteins with a more versatile function can be found both in the cytosol and in cellular organelles (Boudsocq et al., 2010). Fluorescent-tagged proteins in protoplasts have also been used to investigate the influence of the CW on PM protein dynamics (Daněk et al., 2020), the importance of membrane lipid composition in protein cell location (Nagano et al., 2016), and protein trafficking during signaling (Underwood et al., 2017; Menzel et al., 2019). TEA in protoplasts can also bring additional information on protein trafficking with secretion assays to identify and study vacuolar sorting receptor (daSilva et al., 2005; Shen et al., 2013) or signal peptide (Denecke et al., 1990) involved in the regulation of secretory pathways in plant.

Detection of Protein–Protein Interaction

The study of protein–protein interaction (PPI) through TEAs in protoplasts can also bring crucial information to decipher

kinase signaling in plant cells (Pecher et al., 2014; Cheng et al., 2015; Liu et al., 2017; Ye et al., 2019; Li et al., 2020; Takahashi et al., 2020), the activation and interaction of TFs (Pecher et al., 2014; Liu et al., 2018; Ye et al., 2019), or even the interaction between immune receptors and co-receptors (Halter et al., 2014; Yeh et al., 2015; Fliegmann et al., 2016; Gong et al., 2019; Li et al., 2019).

The yeast two-hybrid (Y2H) is a widely used high-throughput method to detect putative PPI and screen a broad range of interactions between proteins (Pecher et al., 2014; Wang et al., 2014; Liu et al., 2017, 2018; Gong et al., 2019; Ye et al., 2019). However, the physiology of the yeast cell differs from that of the plant cell. To get a system more representative of plant cell physiology, a protoplast two-hybrid (P2H) system has been developed. This approach studies PPI by transferring the GAL4-based two-hybrid system into plant protoplasts instead of yeast cells (**Figure 2A**; Ehlert et al., 2006; Iven et al., 2010). Hence, the P2H system identifies PPI between two proteins by fusing one of them with the binding domain (BD) and the second protein with the activation domain (AD) of the transcriptional activator Gal4. With the use of GAL4-UAS4:GUS reporter plasmid, the PPI is detected when a higher GUS activity is observed. When studying interaction between leucine zipper TFs, this method was able to detect some weak interactions not detected in Y2H system, suggesting that P2H studies may be more representative of *in planta* conditions than Y2H (Ehlert et al., 2006; Xing and Wang, 2015). P2H has also been used to analyze PPI involved in the regulation of heat shock response in *Arabidopsis* (Hsu et al., 2010) and in auxin signaling in tobacco (Böttner et al., 2009). Furthermore, in a similar way as it was developed for functional genomic screening, a high-throughput PPI screening can be performed with the combination of P2H and a microtiter plate-based system (Wehner et al., 2011).

Nevertheless, since both Y2H and P2H studies are performed in the nucleus, they are therefore possibly limited to specific classes of proteins such as TFs (Ehlert et al., 2006) and complementary approaches using TEA in protoplasts should be considered to confirm PPI *in planta*. These additional techniques comprise co-immunoprecipitation assays (co-IP; **Figure 2B**; Li et al., 2019; Ye et al., 2019), protein complementation assays (PCA), including bimolecular fluorescence complementation (BiFC; Pecher et al., 2014; Liu et al., 2018; Takahashi et al., 2020; Yang et al., 2020) and split luciferase complementation (SLC; **Figure 2C**; Cheng et al., 2015; Gong et al., 2019) and Förster Resonance Energy Transfer (FRET) experiments (**Figure 2D**; Halter et al., 2014; Fliegmann et al., 2016).

To study PPI with co-IP (**Figure 2B**), protoplasts are transformed with two vectors, each containing one of the proteins of interest fused with a different epitope, such as the hemagglutinin (HA) tag or the FLAG tag (Cheng et al., 2015; Li et al., 2019). The protoplasts are then lysed, and the proteins are immunoprecipitated using one of the two epitopes. The resulting extract is then analyzed by western blot to detect the second epitope and confirm the PPI. This approach has been used in *Arabidopsis* protoplasts to demonstrate the association of the receptor-like kinase (RLK) BAK1 with a calcium channel when studying plant cell death (Yu et al., 2019). Still in *Arabidopsis*, it highlighted the negative effect of the RLK NIK1, involved in antiviral immunity, on bacterial immunity by showing its impact on the formation of the complex between FLS2 and its co-receptor BAK1, paramount in the sensing of the bacterial PAMP flagellin22 (flg22; Li et al., 2019). Co-IP experiments on protoplasts also evidenced the importance of ubiquitination of another RLK, BIK1, for plant immune response regulation (Ma et al., 2020). Nevertheless, co-IP does not provide spatial nor temporal information on PPI. Besides, it is an *in vitro* approach and the lysis process may disrupt weak interaction or induce interaction between proteins that would never be brought together under physiological conditions (Struk et al., 2019). Hence, if the PPI studied is transient, other *in vivo* approaches should be considered such as PCA or FRET (Cui et al., 2019; Struk et al., 2019; Takahashi et al., 2020).

In PCA (**Figure 2C**), one of the studied proteins is fused with the amino-terminal part and the other one with the carboxy-terminal part of a fluorescent protein, such as YFP or mCherry, for BiFC (Pecher et al., 2014; Cheng et al., 2015; Li et al., 2020) or a luciferase enzyme, such as the firefly luciferase, for SLC (Chen et al., 2008; Cheng et al., 2015; Gong et al., 2019). In BiFC, when the two proteins interact, the combination of the two parts of the fluorescent protein restores the fluorescence enabling the visualization and the spatial location of protein complexes. In SLC, the interaction of the two proteins restores the luciferase activity which can be detected in the presence of luciferin by the measurement of chemiluminescence. Thanks to PCA on protoplasts, information on *in vivo* PPI can be obtained, but both techniques have their specificities. With BiFC, the location of both long-standing and transient PPI can be observed, while the high background signal observed with SLC prevents such observation (Fujikawa and Kato, 2007; Cui et al., 2019). In *Arabidopsis*, BiFC has shown the PM location of the interaction between proteins involved in stress response. For instance, it evidenced the interplay between the ATP-recognition receptor DORN1 and the NADPH oxidase RBOHD, involved in ROS production and stomatal closure (Chen et al., 2017). It also showed the nitrate-sensing mechanism where transceptor NRT1.1, that acts as nitrate transporter and sensor, interacts with the calcium channel CNGC15 (Wang et al., 2021). However, the irreversible recombination of fluorescent proteins used in BiFC limits its ability to study PPI dynamics and SLC offers a better alternative in that regard (Kerppola, 2006; Kudla and Bock, 2016; Cui et al., 2019; Struk et al., 2019). Indeed, the reversibility of luciferase recombination allows detection of both the association and dissociation of two proteins in less than 1 min following treatment (Li et al., 2011; Wang et al., 2020b).

Another way to study PPI dynamics and location *in vivo* with protoplasts is the use of FRET. Here, two putative interacting partners are fused with a fluorophore (Halter et al., 2014; Fliegmann et al., 2016; Rios et al., 2017; Long et al., 2018). One partner is fused with a donor fluorophore, while an acceptor fluorophore is fused to the putative interacting partner (**Figure 2D**). The donor fluorophore displays an

FIGURE 2 | Schematic representation of techniques associated with protoplasts to study protein–protein interaction. **(A)** In the protoplast two-hybrid (P2H) system, the protoplasts are transformed with the GAL4-UAS4:GUS reporter plasmid and the two putative interacting partners are fused to the binding domain (BD) and the activation domain (AD) of the transcriptional activator Gal4. An interaction between the partners leads to the transcription of the glucuronidase (GUS) gene and to a higher GUS activity. **(B)** In co-immunoprecipitation (co-IP), the two putative interacting partners are fused to two different epitopes [e.g., hemagglutinin (HA)-tag and FLAG-tag]. The proteins are then extracted from protoplast lysate with a co-IP using one of the two tags (here, the HA-tag). If the proteins are interacting, both HA-tagged and FLAG-tagged proteins are extracted which can be observed with a western blot (WB; upper box). If the proteins do not interact, only the HA-tag is detected in the western blot (bottom box). **(C)** In protein complementation assay (PCA), such as bimolecular fluorescence complementation (BiFC) or split luciferase complementation (SLC) assay, two fragments (the carboxy-terminal and the amino-terminal parts) of a reporter protein are fused to two putative interacting partners. In BiFC, the fragments come from a fluorescent protein and in SLC, from a luciferase enzyme. The interaction between partners leads to the association between the N- and C-ter fragments and restores fluorescence (for BiFC) or luciferase activity detected in the presence of luciferin (for SLC). **(D)** In Förster Resonance Energy Transfer (FRET), each of the two putative interacting partners is fused with one different fluorophore, either a donor or an acceptor. When the partners are interacting, the donor can transfer its energy of excitation to the acceptor, inducing a change in fluorescence intensity of the fluorophores and in the fluorescence lifetime of the donor.

emission spectrum that overlaps with the excitation spectrum of the acceptor fluorophore. When the proteins interact, it brings the donor in close proximity to the acceptor allowing a transfer of energy from the first fluorophore to the second. This leads to a decrease in fluorescence intensity and lifetime of the donor concomitant with an increase in fluorescence intensity of the acceptor. As FRET is based on a remote interaction and not a physical interaction between the tags of the proteins of interest, this approach allows the study of PPI dynamics with information on protein location. It has, for instance, been used in *Arabidopsis* protoplasts to show the early disruption of the interaction between the ethylene factor ERF104 and MAPK6 following treatment with flg22 (Bethke et al., 2009). The implementation of FRET analysis first requires an optimization of the labeling condition. In

this regard, TEAs in protoplast represent a convenient tool to test a large number of FRET pair combinations before transposing it to whole plants or tissues (Long et al., 2018). Nevertheless, FRET measurements require a high accumulation level of the protein of interest and advanced equipment to detect the signal, explaining its limited use in PPI studies (Cui et al., 2019; Struk et al., 2019).

In summary, TEAs in protoplasts associated with the aforementioned techniques provide useful tools to study PPI in plant cells. Each technique has its own characteristics and limitations hence why a complementary use of several of them should be envisaged to get a reliable and comprehensive view of PPI. PPI studies are, however, not restricted to protoplasts, and readers interested in PPI analysis in other systems may refer to recent reviews (Cui et al., 2019; Struk et al., 2019).

Detection of Kinase Activity and Protein Phosphorylation

Following the identification of PPI, one could be interested in understanding its consequences, such as the activation of kinases or protein phosphorylation. To that end, crude or immunoprecipitated protein extracts are collected from lysates of protoplasts or plant seedlings having undergone biotic or abiotic stress. Compared to experiments in plant seedlings which require mutant generation, protoplasts transiently expressing the studied protein(s) provide a high-throughput system to perform explorations as well as hypothesis-driven tests as results can be obtained in a few days (Yoo et al., 2007). For instance, *Arabidopsis* protoplasts have been used to study flg22-induced phosphorylation of the RLK BIK1 (Li et al., 2019) and investigate the importance of amino acid residue for protein phosphorylation in PAMPs-triggered immunity (Menzel et al., 2019) and in cold stress (Ye et al., 2019). The assessment of kinase activation is then performed either by the detection of the kinase activity through the phosphorylation of kinase substrate or by detecting phosphorylated kinases as their activation is linked to their phosphorylation state.

To detect kinase substrate phosphorylation, proteins extracted from protoplasts are incubated with the radioactive marker $\gamma[^{32}P]ATP$ and a substrate, which can be a protein, such as a histone of myelin basic (Asai et al., 2002; Boudsocq et al., 2004, 2010; Liu et al., 2017), a kinase, such as MAPK for MAPKK (Asai et al., 2002; Wang et al., 2014), or even a lipid (Menzel et al., 2019). Once incubated, the kinase activity is determined by measuring the incorporation of the radioactive marker into the kinase substrate. To avoid the use of radioisotopes, an alternative method to measure the phosphorylation of kinase substrate has been developed using a phosphate-binding tag (Phos-Tag) assay (see below; Kinoshita et al., 2006).

Finally, protein phosphorylation can be detected either with specific antibody or by observing mobility shift of proteins with SDS-PAGE (Pecher et al., 2014; Li et al., 2019; Yu et al., 2019; Ma et al., 2020). To perform immunodetection, crude protein extract is analyzed by western blot with a primary antibody recognizing phosphorylated amino acids (Gong et al., 2019; Li et al., 2019) or motifs such as dual phosphorylation specific to active MAPKs detected with anti-pERK antibody (Cheng et al., 2015; Zhang et al., 2016; Gong et al., 2019). For the mobility shift assay, Phos-Tag can be added into the SDS-gel to improve the separation between non-phosphorylated and phosphorylated proteins (Kinoshita et al., 2006; Kinoshita-Kikuta et al., 2007; Bekesová et al., 2015). Thanks to protoplast-associated Phos-Tag mobility shift assay, the phosphorylation of kinases (Bi et al., 2018; Menzel et al., 2019), TFs (Ye et al., 2019), or other proteins (Liu et al., 2017) involved in the signaling process in biotic and abiotic stress has been detected. Hence, while being an alternative to radioisotopes, Phos-Tag assays are also a suitable alternative to antibody recognizing phosphorylated proteins, which are costly or even not always commercially available, to detect protein phosphorylation and kinase activation (Bekesová et al., 2015; Kinoshita et al., 2015). Finally, to confirm that the mobility shift observed is due to phosphorylation, treatment with phosphatase to abrogate the mobility shift is often performed (Pecher et al., 2014; Liu et al., 2017; Bi et al., 2018; Li et al., 2019). Additionally, TEA in protoplasts can also provide information on the consequence of phosphorylation such as the degradation of calcium channels (Yu et al., 2019) or TFs that regulate stress-related genes (Sheikh et al., 2016; Liu et al., 2017).

Complementarity of Biomolecular Assays Performed on Protoplasts and Whole Cells

As presented above, many biomolecular assays have been developed with protoplasts to decipher plant signaling mechanisms in biotic or abiotic stress conditions. All these different types of assays offer a useful toolbox to analyze plant responses and get new insights to better understand the signaling cascade in plants, starting from the perception by a protein receptor to the activation of TFs and genes, passing by the kinase signaling cascade.

The use of these tools is not restricted to protoplasts, and TEA can be performed directly in plant tissues using particle bombardment or *Agrobacterium* infiltration (Cheng et al., 2015; Liu et al., 2017, 2018; Bi et al., 2018; Pham et al., 2020; Takahashi et al., 2020). The latter is used either to transform only specific plant tissue or to produce transgenic plant lines constitutively expressing the gene of interest (Wu et al., 2014a; Sharma et al., 2018). Nevertheless, all these approaches present advantages and limitations. Therefore, TEAs performed in protoplasts are complementary to TEAs performed in intact plant tissues and constitutive expression in mutant plants (Denecke et al., 2012; Sharma et al., 2018). Indeed, protoplasts are obtained from the digestion of tissues containing a mixture of differentiated cell types that can display different locations of specific proteins (Faraco et al., 2011). Even though some protocols exist to isolate protoplasts of specific cell types such as guard cell (Zhao et al., 2019), aleurone layer cell (Daneri-Castro and Roberts, 2016), or from various root tissues (Demidchik et al., 2003), the complementary use of transgenic plants is recommended if a tissue-specific behavior of the process studied is anticipated (Sharma et al., 2018). Instead, if no tissue-specificity is expected, protoplasts offer a valuable model to study physiological processes as it is less time-consuming to obtain than transgenic plant and can be performed in a broad range of plant species, contrary to agroinfiltration in leaves that are mainly restricted to the plant host *Nicotiana benthamiana* (Sharma et al., 2018). Furthermore, in agroinfiltration experiments, the moment when the gene transfer occurs is not well defined. On the contrary, with protoplasts transformation, the moment where the DNA transfer happens is well known and gene products can be detected as early as 4 h after gene transfer (Denecke et al., 2012). Hence, protoplasts are a useful system to perform time-course experiment of gene expression (Babu et al., 2008), which are more difficult to carry out in infiltrated cells (Denecke et al., 2012).

Even though TEA in protoplasts or intact cells can bring precious findings, some cautions must be taken when using these tools. The experiment must be carefully designed to avoid

overexpression artifacts which can lead to artificial cytosolic location, or even aggregation of the protein (Sharma et al., 2018). This can be done by adapting the amount of DNA plasmid used for transformation or the incubation time of protoplasts for gene expression, usually less than 24 h, to obtain low-expressing protoplasts for experimental purpose (Yoo et al., 2007; Denecke et al., 2012). Moreover, the enzymatic CW digestion performed to isolate protoplasts may stress the cell which could alter the expression levels of some genes (Birnbaum et al., 2003; Takai et al., 2007; Jeworutzki et al., 2010). As an example, in a screen of more than 22,000 *Arabidopsis* genes, 356 were found to be induced at least twice more by the CW digestion (Birnbaum et al., 2003) and some flagellin-inducible genes have also shown higher expression following protoplast isolation in rice (Takai et al., 2007). Such induction of genes in protoplasts may alter cell responses to stimulus such as the activation of ion channels (Jeworutzki et al., 2010). In addition to altered gene expression, protoplast isolation can change the sensitivity of cell enzymes to its inhibitor, as shown for phosphoenolpyruvate carboxylase regarding malate inhibition (Petropoulou et al., 1990). It is therefore important to assess that the biological response in protoplasts is not disturbed compared to intact plant cells. Gene induction or protein accumulation similar to whole plants levels (Asai et al., 2002; Boudsocq et al., 2004; Underwood et al., 2017) and the verification with fluorescent probes of protoplast integrity are possible controls.

THE VERSATILITY OF FLUORESCENT PROBES ON PROTOPLASTS

With the advent of cell imaging technologies, fluorescence microscopy has been increasingly used for the visual insight it provides. While many probes can be used on plant tissues, autofluorescence and probe specificity have turned out to be an issue. Some dyes also tend to accumulate within the CW microfibrils, tempering with the imaging process (Blachutzik et al., 2012). Fluorescent probes applications on protoplasts appear then as particularly useful since they allow observations at the single cell level without the issues caused by the presence of the CW (**Figure 1** for an overview).

Cell Viability and DNA Damages
Fluorochromes are often used to discriminate between living and dead protoplasts and to assess their viability and the damages they might have suffered. Indeed, protoplast isolation procedures and the culture conditions that follow, may induce cell stress or damage (Neelakandan and Wang, 2012), which should be avoided if one wants to study the effect of biotic and abiotic stresses. One of the most referenced dyes is FDA (fluorescein diacetate), which highlights living cells (Bertini et al., 2019; Sangra et al., 2019; Qiu et al., 2020) or Evan's blue, which highlights dead ones (Kollárová et al., 2019). Other fluorochromes can be used, such as PI (propidium iodide), DAPI (4'6-diamidino-2-phenylindole, dichloride), and 7-AAD

(7-amino-actinomycin D) that do not cross intact PMs. Issues have previously been raised regarding techniques using fluorescence microscopy, as the quantification is linked to the viewer's perception of fluorescence (Aoyagi, 2011; Badaró Costa et al., 2018). Thus, new automated measurements, such as flow cytometry (FCM; Zhou et al., 2019; González-García et al., 2020) and Muse cell analyzer, a compact FCM, allowing screening and sorting of protoplasts, along with measures on smaller volumes have been developed (Badaró Costa et al., 2018).

DNA damage evaluation is another frequently employed marker to assess protoplast viability or the effect of genotoxicity of environmental pollutants and abiotic stresses on protoplasts. In these procedures, protoplasts are used as a direct source of nuclei to perform gel electrophoresis with ethidium bromide staining in order to detect DNA laddering (Poot-Poot et al., 2016). Identically, single cell gel electrophoresis assay (SCGE), also called Comet assay, allows the study of DNA damage on protoplasts at the single cell or nuclei level (Kuzminsky et al., 2016; Badaró Costa et al., 2018; Choury et al., 2018). While this technique is amply used on animal cell cultures which are easily lysed, the presence of the CW makes it technically difficult to transpose on plant tissue or cell culture. Hence, nuclei isolation through protoplast formation or mechanical destruction of the CW is here preferred (Gichner et al., 2009; Santos et al., 2015; Choury et al., 2018). Finally, DAPI, which has a high affinity for DNA double strand, has also been used to study apoptosis-like cell death and more specifically chromatin condensation and DNA fragmentation in *Brassica napus* leaves (Watanabe et al., 2002).

Cell Wall Dynamics
The CW has a direct role at the frontline of plant defense along with other chemical and physical barriers such as waxes, hairs, and secondary metabolites (Malinovsky, 2014; Engelsdorf et al., 2018). It also possesses an indirect role in plant defense systems, as during a pathogen invasion, cell wall integrity can be modified, parts of the CW can be broken down and their fragments (referenced as DAMPs) can activate plant immune responses (Souza et al., 2020). As protoplasts are cells deprived of CW, they offer a unique point of view on the complete *de novo* synthesis of the CW by providing an excellent support for visualizing its regeneration dynamics and characterizing the cellular proteins involved in the process (Yokoyama et al., 2016). Although changes in CW composition are often studied through biochemical analyses, histochemical staining with fluorochromes is increasingly used to bring a visual insight on these changes. For instance, calcofluor white is employed to preferentially stain cellulose and aniline blue to stain callose (Yokoyama et al., 2016; Kollárová et al., 2019). Using these probes, it has, for instance, been demonstrated that when cultivated in stressful conditions, cellulose microfibrils were not deposited on the surface of white birch protoplasts and only callose deposition could be observed (Tagawa and Kondo, 2018; Tagawa et al., 2019). Calcofluor white has also been used to study the deleterious effect of cadmium on maize protoplast CW regeneration (Kollárová et al., 2019). Another

method also emerged using S4B (Pontamine Fast Scarlet 4 BS) in combination with spinning disk confocal microscopy to stain cellulose patterning on living cells. As calcfluor has toxic properties that might injure cells, this method appears to be more suited to real-time imaging of living protoplasts (Anderson et al., 2010; Yokoyama et al., 2016; Kuki et al., 2017).

Similarly, CW components and callose deposition are known to block the migration of trace metals within cells, such as aluminum which binds to calcium pectate in the CW (Lee et al., 2001). Therefore, protoplasts are often combined with specific fluorochromes to study the effects and uptake of trace metals directly on cells (Krzesłowska, 2011). For instance, Leadmium was used to visualize the uptake of cadmium by protoplasts and its deleterious effects on CW regeneration of wheat (Greger et al., 2016) and maize (Kollárová et al., 2019). Similarly, morin was used to study aluminum toxicity on coffee protoplasts, along with DAPI to monitor its localization into their nuclei (Poot-Poot et al., 2016). It was also used to examine its toxicity on root protoplasts of transgenic camelina (Park et al., 2017).

Plasma Membrane Dynamics

Along with the CW, the PM also plays a major role in plant resistance to both biotic and abiotic stresses. Whether it is by regulation of ion exchanges, perception of PAMPs/MAMPs/DAMPs, or signal transduction, both lipids and proteins of the PM are key players in its physiological function (Lim et al., 2017; Mamode Cassim et al., 2019; Schellenberger et al., 2019; Huby et al., 2020; Saijo and Loo, 2020). Moreover, following the CW, the PM is the first point of contact between plant cells and pathogens and many proteins involved in plant defense are embedded in it. More specifically, the dynamic between membrane microdomains, which are highly ordered domains rich in sphingolipids and sterols, and the stress-related proteins they harbor is crucial for immunity (Gronnier et al., 2016, 2018; Nagano et al., 2016; Mamode Cassim et al., 2019; Huby et al., 2020).

The absence of CW makes possible the accurate visualization of events at the protoplast PM using fluorescent probes. However, while a lot of probes exist to study lipid organization and dynamics into artificial model membranes which are deprived of proteins, they often cannot be directly applied to living cell and protoplast PMs which are far more complex and require deep protocol adaptations in terms of concentration and incubation time (Klymchenko and Kreder, 2014). Every probe will have its specificities and are used by themselves or combined. For instance, FM4-64 [N-(3-Triethylammoniumpropyl)-4-(6-(4-(Diethylamino) Phenyl) Hexatrienyl) Pyridinium Dibromide] and LRB-PE (Lissamine Rhodamine B-Phosphoethanolamine) have been employed to specifically stain phospholipid enriched areas of protoplast PM and BD-SM (Bodipy Sphingomyelin FL C_{12}) has been used to stain sphingolipid enriched domains (Blachutzik et al., 2012). FM4-64 and BD-SM were also used in combination with FRAP (fluorescence recovery after photobleaching) experiments to visualize lipid redistribution. The identification of ordered and disordered regions of the PM is also possible with the solvatochromic dyes di-4-ANEPPDHQ and laurdan that show a shift in emission wavelength when lipids undergo phase transition from gel to fluid state (Blachutzik et al., 2012; Klymchenko, 2017). Di-4-ANEPPDHQ has notably been used on protoplasts from rice transgenic plants that lack fatty acid hydroxylase 1 and 2 (FAH1/2), enzymes responsible for the formation of 2-hydroxy sphingolipids (2-OH-SL), precursors of glycosylinositol phosphorylceramides (GIPC), that are both located at the PM in *Arabidopsis*. They demonstrated that a disordered PM was concomitant with a lower amount of 2-OH-SL which gave rise to an increased sensibility to rice blast fungus infection (Nagano et al., 2016). Di-4-ANEPPDHQ has also been used in *Arabidopsis* FAH1/2 mutants, to show a lower order of the PM compared to the wild type, suggesting an altered PM organization when its content in GIPC is low (Lenarčič et al., 2017).

While there are many advantages to use fluorescent probes directly on protoplasts, its PM remains an active, dynamic structure, which can cause issues. It has been reported that some probes could be internalized in the cytoplasm, such as DiIC12 (1,1'-Didodecyl-3,3,3',3'-Tetramethylindocarbocyanine Perchlorate) and DiIC18 (1,1'-Dioctadecyl-3,3,3',3'-Tetramethylindodicarbocyanine-5,5'-Disulfonic Acid), which stains phospholipids, leading to a decrease in fluorescence in the PM (Blachutzik et al., 2012). By using calcfluor and di-4-ANEPPDHQ on tobacco protoplasts, it has been shown that the absence of a CW does not affect the organization of PM-ordered domains (Grosjean et al., 2018), suggesting that the PM microdomain functions of a protoplast remain highly similar to that of an intact tissue. However, in *Arabidopsis*, FRAP analysis proved that the removal of the CW increased the overall dynamics and mobility of the PM proteins (Martinière et al., 2012), including proteins involved in response to extracellular stimuli flotilin2 proteins (AtFLOT2) and hypersensitive induced reaction proteins (AtHIR1; Daněk et al., 2020).

Detection of Early Stress Signaling Events

Fluorescent probes can also be useful to detect specific early stress signaling events like ROS production and ions fluxes. For instance, in *Arabidopsis*, the molecular probe ContPY1 was used to detect the intracellular accumulation of a ROS, hydrogen peroxide (H_2O_2) in response to the elicitor COS-OGA. The comparison between protoplasts and cell suspensions evidenced the relative contribution of CW peroxidases and membrane dehydrogenases to H_2O_2 production (Ledoux et al., 2014). On maize, the Amplex red reagent, which reacts with H_2O_2 to produce the highly fluorescent resorufin, and the rhodamine dye DHR123 (Dihydrorhodamine 123) were used to measure ROS in both organelles and protoplasts and link their quantities to DNA damage in developing mitochondria and plastids (Tripathi et al., 2020).

Similarly to ROS production, ion fluxes can be easily studied with fluorescent probes associated with protoplasts. For instance, K^+ efflux was monitored with the fluorescent probe PBFI-AM

(Potassium-Binding Benzofuran Isophthalate Acetoxymethyl ester) and cytosol acidification with the pH-sensitive probe BCECF-AM [2',7-Bis-(2-Caboxyethyl)-5-(and-6)-Carboxyfluorescein Acetoxymethyl ester] in wheat and rice protoplasts to study anoxia-induced events (Yemelyanov et al., 2020). Furthermore, protoplasts loaded with the probe SBFI-AM (Sodium Binding Benzofuran Isophthalate Acetoxymethyl ester) were used to study salt stress on wheat. They helped to demonstrate that the application of a moderate amount of K^+ was concomitant with a decrease in cytosolic Na^+ alleviating its toxic effects on cells (Gul et al., 2019). Regarding Ca^{2+} fluxes, their induction has been monitored in elicited protoplasts expressing the genetically encoded reporter system aequorin, a bioluminescent protein (Maintz et al., 2014). This technique can, however, be lengthy, especially for slow growing plants such as fruit trees since it requires plant transformation (Qiu et al., 2020). So small dyes like fluo-8/AM, fluo-4/AM (fluo-8/4 acetoxymethylester) and rhod-2/AM (rhod-2 acetoxymethylester) can be preferred. These molecules are flexible, rapid, and non-cytotoxic. They have been used for calcium imaging on protoplasts of "Fuji" apples (Qiu et al., 2020). Fluo-4/AM has also been used with FCM and confocal microscopy on rice protoplasts to evaluate ceramide-induced programmed cell death (Zhang et al., 2020). While there are many advantages to fluorescent probes to study ion fluxes in protoplasts, there are still some limitations such as the commercial availability of probe sensitive to anions.

PROTOPLASTS AND PATCH-CLAMP ELECTROPHYSIOLOGY

Complementary to fluorescent probes, plant ion fluxes can be studied using patch-clamp electrophysiology that measures ion currents flowing through a membrane (Demidchik et al., 2006; Elzenga, 2012). This technique is a powerful tool to identify and characterize ion channel and non-channel proteins, such as H^+-ATPases, present in biological membranes (Demidchik et al., 2006; Elzenga, 2012; Hamilton et al., 2015). To measure the ionic current with patch clamp, a high resistance contact, the so-called gigaOhm seal, has to be performed between a glass micropipette and a patch of a membrane containing the ion transporter of interest (Demidchik et al., 2006; Elzenga, 2012). The access to a CW-deprived plant cell is particularly important to measure PM ionic current (Elzenga, 2012). Hence, protoplasts are the model of choice to perform patch-clamp electrophysiology on plant.

Four patch-clamp configurations exist, and readers interested in this technique may refer to previous reviews for more details on their specificities (Demidchik et al., 2006; Elzenga, 2012). This technique has provided important insights in the understanding of anion channels involved in immunity (Zheng et al., 2018; Chan et al., 2020) and ABA signaling during osmotic stress (Takahashi et al., 2020). It also contributed to a better comprehension of mechanoperception in plant (Nakagawa et al., 2007; Haswell et al., 2008), potassium and calcium fluxes involved in salt stress (Fuchs et al., 2005; Liya et al., 2012).

It also helped to elucidate calcium fluxes involved in H_2O_2 perception (Demidchik et al., 2007; Tian et al., 2019; Wu et al., 2020a), in extracellular ATP perception (Demidchik et al., 2009), in cold stress (Carpaneto et al., 2007), and in stomatal immunity (Yekondi et al., 2018).

Patch-clamp electrophysiology is the gold standard technique to study ion channels and fluxes even though the process to isolate the cell and remove its CW can be considered a limitation (Demidchik et al., 2006; Hamilton et al., 2015). However, combination of patch clamp with other electrophysiological or physiological techniques using intact plants such as microelectrode ion flux estimation or the use of fluorescent probes can be considered to improve the robustness of the results (Demidchik et al., 2006; Hamilton et al., 2015; Demidchik, 2018).

CHALLENGES AND FUTURE PERSPECTIVES

The current and upcoming rise of pests, diseases, and changes of agricultural practices caused by environmental perturbations will put an increasing pressure on agricultural productivity. This will require specific tools allowing fast, high throughput, or even automated systems, to provide reliable and efficient solutions for crop and genetic engineering.

With the advent of quick and reliable transformation and microscopy methods, protoplasts arise as useful and powerful tools for a wide range of stress-related studies (**Figure 1**). We have argued in this review that the use of protoplasts could turn out to be both an advantage and a limitation (**Figure 3**). While it has been previously stated that protoplasts maintain a similar physiological cellular activity to whole plants (Sheen, 2001; Wang et al., 2020a; Shaw et al., 2021), they ultimately serve as proxy to whole plants studies, implying that complementary experiments are often necessary to connect the phenomena observed on protoplasts to plants. Nonetheless, the single cell level allows for specific, rapid, and high-throughput analysis along with time-course experiments. In addition, even though protoplasts isolation and maintenance require specific conditions that can eventually cause stress, these techniques are improving for a wide range of species or organs (Sangra et al., 2019; Shan et al., 2019; Davis et al., 2020). Furthermore, their formation is still deemed necessary to bypass time-consuming plant culture and whole plant transformation, especially for recalcitrant species or plants with a long reproductive cycle (Du and Bao, 2005). Moreover, somatic hybridization mediated by protoplast fusion has been employed to circumvent sexual incompatibility encountered in plant breeding (Watanabe et al., 2002; Du and Bao, 2005).

Protoplasts possess multiple assets for the upcoming challenges in plant biology. Many technologies employing them are being developed, and these techniques could ultimately facilitate plant stress-related studies. For instance, protoplasts have been employed to assess the efficiency of CRISPR-associated protein 9 (Cas9) mutagenesis, bypassing or preceding stable transformation which can be time-consuming (Lin et al., 2018;

FIGURE 3 | Summary of the advantages and limitations of working with protoplasts to study plant stress perception and response comparatively to whole plants.
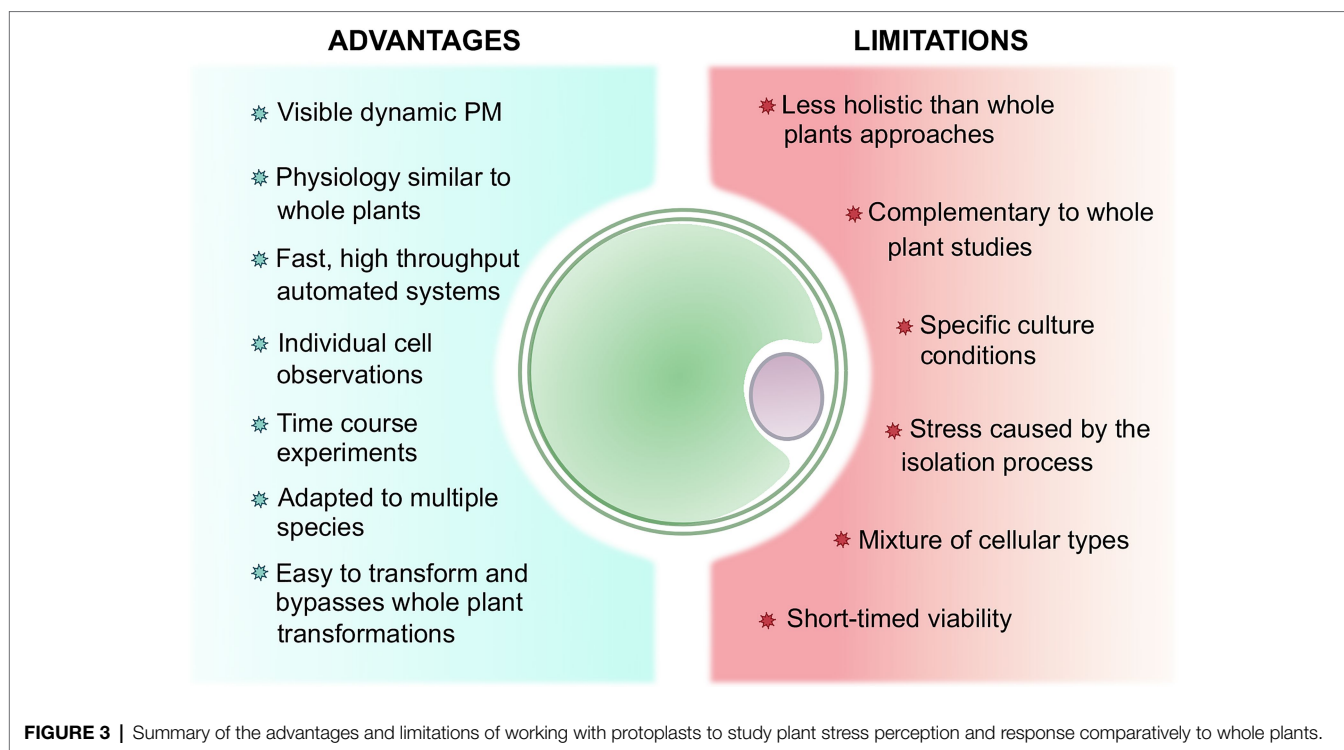
Hahn et al., 2020; Guyon-Debast et al., 2021; Nicolia et al., 2021). Another example is the adaptation of efficient and low-cost microfluidic techniques to perform spatiotemporal studies of plant protoplasts physiology during their development (Sakai et al., 2019) and to apprehend the electrical resistance of CW-regenerated protoplasts (Chen, 2020). Similarly, the usefulness of protoplasts for high-throughput RNA sequencing has also been put forward due to its many advantages over traditional RNA-seq. Indeed, protoplasts being single cells, they can give spatiotemporal information on gene dynamic expression in heterogeneous tissues (Li et al., 2021).

Protoplasts also provide a facilitated access to the plant PM, and pioneering studies have proven their crucial role in growing biotechnologies such as nanoparticles. These particles have the ability to passively penetrate the PM, but their use in plants is limited due to the presence of the CW (Torney et al., 2007; Liu et al., 2009; Lew et al., 2018). As they are believed to have the potential to overcome current limitations in plant genetic transformation, their effect on plants and their PMs are increasingly studied (Lew et al., 2018). With their easily accessible PM, protoplasts can therefore help understand the fundamental interactions between nanoparticles and plants, as such knowledge is of paramount importance for nanoenabled agriculture. Protoplasts have, for instance, been used to determine the impact of nanopesticides or nanofertilizers, on plant photosynthesis (Wang et al., 2020a). Likewise, protoplast cultures have been used to study gold nanoparticles uptake by plants as their use in industrial areas leads to their release into the environment, which can cause an invisible danger to the ecosystem (Milewska-Hendel et al., 2019). Furthermore, nanoparticles have been previously used to deliver drugs,

imaging agents, and DNA for genetic transformation into protoplasts (Torney et al., 2007).

Concomitantly, protoplasts could be valuable plant PM models to study the perception of bioactive molecules such as elicitors by plant cells. Indeed, they could link data obtained by biophysics studies on biomimetic PM models containing representative lipids (Deleu et al., 2014) with the ones provided by biological assays on living plant cells or tissues with complex dynamic PM and CW. Protoplasts-associated technologies and techniques should help improve our fundamental knowledge on plant perception and response to (a)biotic stresses and hence ultimately contribute to develop reliable and efficient solutions for agriculture.

AUTHOR CONTRIBUTIONS

GG, EH, MD, and SD-C designed the outlines of the review and wrote the manuscript with the contribution of SC and MO. All authors contributed to the article and approved the submitted version.

FUNDING

REFERENCES

Anderson, C. T., Carroll, A., Akhmetova, L., and Somerville, C. (2010). Real-time imaging of cellulose reorientation during cell wall expansion in *Arabidopsis* roots. *Plant Physiol.* 152, 787–796. doi: 10.1104/pp.109.150128

Aoyagi, H. (2011). Application of plant protoplasts for the production of useful metabolites. *Biochem. Eng. J.* 56, 1–8. doi: 10.1016/j.bej.2010.05.004

Asai, T., Tena, G., Plotnikova, J., Willmann, M. R., Chiu, W.-L., Gomez-Gomez, L., et al. (2002). MAP kinase signalling cascade in *Arabidopsis* innate immunity. *Nature* 415, 977–983. doi: 10.1038/415977a

Babu, M., Griffiths, J. S., Huang, T. S., and Wang, A. (2008). Altered gene expression changes in *Arabidopsis* leaf tissues and protoplasts in response to *plum pox* virus infection. *BMC Genomics* 9:325. doi: 10.1186/1471-2164-9-325

Badaró Costa, N. L., Carvalho, C. R., and Clarindo, W. R. (2018). Improved procedures to assess plant protoplast viability: evidencing cytological and genomic damage. *Cytologia* 83, 397–405. doi: 10.1508/cytologia.83.397

Barbara, J. B., and Bonner, D. M. (1959). Protoplasts from *Neurospora crassa*. *J. Bacteriol.* 78, 550–556. doi: 10.1128/jb.78.4.550-556.1959

Bekesová, S., Komis, G., Krenek, P., Vyplelovà, P., Ovecka, M., Luptovciak, I., et al. (2015). Monitoring protein phosphorylation by acrylamide pendant Phos-tag in various plants. *Front. Plant Sci.* 6:336. doi: 10.3389/fpls.2015.00336

Bertini, E., Tornielli, G. B., Pezzotti, M., and Zenoni, S. (2019). Regeneration of plants from embryogenic callus-derived protoplasts of Garganega and Sangiovese grapevine (*Vitis vinifera* L.) cultivars. *Plant Cell Tissue Organ Cult.* 138, 239–246. doi: 10.1007/s11240-019-01619-1

Bethke, G., Unthan, T., Uhrig, J. F., Pöschl, Y., Gust, A. A., Scheel, D., et al. (2009). Flg22 regulates the release of an ethylene response factor substrate from MAP kinase 6 in *Arabidopsis thaliana* via ethylene signaling. *Proc. Natl. Acad. Sci. U. S. A.* 106, 8067–8072. doi: 10.1073/pnas.0810206106

Bi, G., Zhou, Z., Wang, W., Li, L., Rao, S., Wu, Y., et al. (2018). Receptor-like cytoplasmic kinases directly link diverse pattern recognition receptors to the activation of mitogen-activated protein kinase cascades in *Arabidopsis*. *Plant Cell* 30, 1543–1561. doi: 10.1105/tpc.17.00981

Bigeard, J., Colcombet, J., and Hirt, H. (2015). Signaling mechanisms in pattern-triggered immunity (PTI). *Mol. Plant* 8, 521–539. doi: 10.1016/j.molp.2014.12.022

Bigeard, J., and Hirt, H. (2018). Nuclear signaling of plant MAPKs. *Front. Plant Sci.* 9:469. doi: 10.3389/fpls.2018.00469

Birnbaum, K., Shasha, D. E., Wang, J. Y., Jung, J. W., Lambert, G. M., Galbraith, D. W., et al. (2003). A gene expression map of the *Arabidopsis* root. *Science* 302, 1956–1960. doi: 10.1126/science.1090022

Blachutzik, J. O., Demir, F., Kreuzer, I., Hedrich, R., and Harms, G. S. (2012). Methods of staining and visualization of sphingolipid enriched and non-enriched plasma membrane regions of *Arabidopsis thaliana* with fluorescent dyes and lipid analogues. *Plant Methods* 8:28. doi: 10.1186/1746-4811-8-28

Bose, J., Pottosin, I. I., Shabala, S. S., Palmgren, M. G., and Shabala, S. (2011). Calcium efflux systems in stress signaling and adaptation in plants. *Front. Plant Sci.* 2:85. doi: 10.3389/fpls.2011.00085

Böttner, S., Iven, T., Carsjens, C. S., and Dröge-Laser, W. (2009). Nuclear accumulation of the ankyrin repeat protein ANK1 enhances the auxin-mediated transcription accomplished by the bZIP transcription factors BZI-1 and BZI-2. *Plant J.* 58, 914–926. doi: 10.1111/j.1365-313X.2009.03829.x

Boudsocq, M., Barbier-Brygoo, H., and Laurière, C. (2004). Identification of nine sucrose nonfermenting 1-related protein kinases 2 activated by hyperosmotic and saline stresses in *Arabidopsis thaliana*. *J. Biol. Chem.* 279, 41758–41766. doi: 10.1074/jbc.M405259200

Boudsocq, M., Willmann, M. R., McCormack, M., Lee, H., Shan, L., He, P., et al. (2010). Differential innate immune signalling via Ca^{2+} sensor protein kinases. *Nature* 464, 418–422. doi: 10.1038/nature08794

Carpaneto, A., Ivashikina, N., Levchenko, V., Krol, E., Jeworutzki, E., Zhu, J. K., et al. (2007). Cold transiently activates calcium-permeable channels in *Arabidopsis* mesophyll cells. *Plant Physiol.* 143, 487–494. doi: 10.1104/pp.106.090928

Chan, C., Panzeri, D., Okuma, E., Töldsepp, K., Wang, Y. Y., Louh, G. Y., et al. (2020). Stress induced factor 2 regulates *Arabidopsis* stomatal immunity through phosphorylation of the anion channel SLAC1. *Plant Cell* 32, 2216–2236. doi: 10.1105/tpc.19.00578

Chen, L. (2020). An impedance-coupled microfluidic device for single-cell analysis of primary cell wall regeneration. *Biosens. Bioelectron.* 165:112374. doi: 10.1016/j.bios.2020.112374

Chen, D., Cao, Y., Li, H., Kim, D., Ahsan, N., Thelen, J., et al. (2017). Extracellular ATP elicits DORN1-mediated RBOHD phosphorylation to regulate stomatal aperture. *Nat. Commun.* 8:2265. doi: 10.1038/s41467-017-02340-3

Chen, H., Lai, Z., Shi, J., Xiao, Y., Chen, Z., and Xu, X. (2010). Roles of *Arabidopsis* WRKY18, WRKY40 and WRKY60 transcription factors in plant responses to abscisic acid and abiotic stress. *BMC Plant Biol.* 10:281. doi: 10.1186/1471-2229-10-281

Chen, H., Zou, Y., Shang, Y., Lin, H., Wang, Y., Cai, R., et al. (2008). Firefly luciferase complementation imaging assay for protein-protein interactions in plants. *Plant Physiol.* 146, 368–376. doi: 10.1104/pp.107.111740

Cheng, Z., Li, J. F., Niu, Y., Zhang, X. C., Woody, O. Z., Xiong, Y., et al. (2015). Pathogen-secreted proteases activate a novel plant immune pathway. *Nature* 521, 213–216. doi: 10.1038/nature14243

Cheng, N., and Nakata, P. A. (2020). Development of a rapid and efficient protoplast isolation and transfection method for chickpea (*Cicer arietinum*). *MethodsX* 7:101025. doi: 10.1016/j.mex.2020.101025

Choury, Z., Meschini, R., Dell'Orso, A., Fardusi, M. J., Mugnozza, G. S., and Kuzminsky, E. (2018). Optimized conditions for the isolation of mesophyll protoplasts along the growing season from *Arbutus unedo* and their use in single cell gel electrophoresis. *Plant Cell Tissue Organ Cult.* 132, 535–543. doi: 10.1007/s11240-017-1349-6

Cocking, E. C. (1960). A method for the isolation of plant protoplasts and vacuoles. *Nature* 187, 962–963. doi: 10.1038/187962a0

Cook, D. E., Mesarich, C. H., and Thomma, B. P. H. J. (2015). Understanding plant immunity as a surveillance system to detect invasion. *Annu. Rev. Phytopathol.* 53, 541–563. doi: 10.1146/annurev-phyto-080614-120114

Couto, D., and Zipfel, C. (2016). Regulation of pattern recognition receptor signalling in plants. *Nat. Rev. Immunol.* 16, 537–552. doi: 10.1038/nri.2016.77

Cui, Y., Zhang, X., Yu, M., Zhu, Y., Xing, J., and Lin, J. (2019). Techniques for detecting protein-protein interactions in living cells: principles, limitations, and recent progress. *Sci. China Life Sci.* 62, 619–632. doi: 10.1007/s11427-018-9500-7

Daněk, M., Angelini, J., Malínská, K., Andrejch, J., Amlerová, Z., Kocourková, D., et al. (2020). Cell wall contributes to the stability of plasma membrane nanodomain organization of *Arabidopsis thaliana* FLOTILLIN2 and HYPERSENSITIVE INDUCED REACTION1 proteins. *Plant J.* 101, 619–636. doi: 10.1111/tpj.14566

Daneri-Castro, S. N., and Roberts, T. H. (2016). Isolation of viable protoplasts from the aleurone layers of commercial barley malting varieties. *J. Inst. Brew.* 122, 693–699. doi: 10.1002/jib.365

daSilva, L. L. P., Taylor, J. P., Hadlington, J. L., Hanton, S. L., Snowden, C. J., Fox, S. J., et al. (2005). Receptor salvage from the prevacuolar compartment is essential for efficient vacuolar protein targeting. *Plant Cell* 17, 132–148. doi: 10.1105/tpc.104.026351

Davis, H. R., Maddison, A. L., Phillips, D. W., and Jones, H. D. (2020). "Genetic transformation of protoplasts isolated from leaves of *Lolium temulentum* and *Lolium perenne*," in *Cereal Genomics Methods in Molecular Biology*. ed. L. M. Vaschetto (New York, NY: Springer US), 199–207.

Delaunois, B., Farace, G., Jeandet, P., Clément, C., Baillieul, F., Dorey, S., et al. (2014). Elicitors as alternative strategy to pesticides in grapevine? Current knowledge on their mode of action from controlled conditions to vineyard. *Environ. Sci. Pollut. Res.* 21, 4837–4846. doi: 10.1007/s11356-013-1841-4

Deleu, M., Crowet, J.-M., Nasir, M. N., and Lins, L. (2014). Complementary biophysical tools to investigate lipid specificity in the interaction between bioactive molecules and the plasma membrane: a review. *Biochim. Biophys. Acta* 1838, 3171–3190. doi: 10.1016/j.bbamem.2014.08.023

Demidchik, V. (2014). Mechanisms and physiological roles of K+ efflux from root cells. *J. Plant Physiol.* 171, 696–707. doi: 10.1016/j.jplph.2014.01.015

Demidchik, V. (2018). ROS-activated ion channels in plants: biophysical characteristics, physiological functions and molecular nature. *Int. J. Mol. Sci.* 19:1263. doi: 10.3390/ijms19041263

Demidchik, V., Shabala, S. N., Coutts, K. B., Tester, M. A., and Davies, J. M. (2003). Free oxygen radicals regulate plasma membrane Ca^{2+}- and K^+-permeable channels in plant root cells. *J. Cell Sci.* 116, 81–88. doi: 10.1242/jcs.00201

Demidchik, V., Shabala, S. N., and Davies, J. M. (2007). Spatial variation in H_2O_2 response of *Arabidopsis thaliana* root epidermal Ca^{2+} flux and plasma membrane Ca^{2+} channels. *Plant J.* 49, 377–386. doi: 10.1111/j.1365-313X.2006.02971.x

Demidchik, V., Shang, Z., Shin, R., Thompson, E., Rubio, L., Laohavisit, A., et al. (2009). Plant extracellular ATP signalling by plasma membrane NADPH oxidase and Ca^{2+} channels. *Plant J.* 58, 903–913. doi: 10.1111/j.1365-313X.2009.03830.x

Demidchik, V., Sokolik, A., and Yurin, V. (2006). "Electrophysiological characterization of plant cation channels," in *Plant Electrophysiology: Theory and Methods*. ed. A. G. Volkov (Berlin, Heidelberg: Springer-Verlag), 173–185.

Denecke, J., Aniento, F., Frigerio, L., Hawes, C., Hwang, I., Mathur, J., et al. (2012). Secretory pathway research: the more experimental systems the better. *Plant Cell* 24, 1316–1326. doi: 10.1105/tpc.112.096362

Denecke, J., Botterman, J., and Deblaere, R. (1990). Protein secretion in plant cells can occur via a default pathway. *Plant Cell* 2, 51–59. doi: 10.1105/tpc.2.1.51

Dröge-Laser, W., Snoek, B. L., Snel, B., and Weiste, C. (2018). The *Arabidopsis* bZIP transcription factor family – an update. *Curr. Opin. Plant Biol.* 45, 36–49. doi: 10.1016/j.pbi.2018.05.001

Du, L., and Bao, M. (2005). Plant regeneration from protoplasts isolated from embryogenic suspension cultured cells of *Cinnamomum camphora* L. *Plant Cell Rep.* 24, 462–467. doi: 10.1007/s00299-005-0969-1

Dubos, C., Stracke, R., Grotewold, E., Weisshaar, B., Martin, C., and Lepiniec, L. (2010). MYB transcription factors in *Arabidopsis*. *Trends Plant Sci.* 15, 573–581. doi: 10.1016/j.tplants.2010.06.005

Eddy, A. A., and Williamson, D. H. (1957). A method of isolating protoplasts from yeast. *Nature* 179, 1252–1253. doi: 10.1038/1791252a0

Ehlert, A., Weltmeier, F., Wang, X., Mayer, C. S., Smeekens, S., Vicente-Carbajosa, J., et al. (2006). Two-hybrid protein-protein interaction analysis in *Arabidopsis* protoplasts: establishment of a heterodimerization map of group C and group S bZIP transcription factors. *Plant J.* 46, 890–900. doi: 10.1111/j.1365-313X.2006.02731.x

Elzenga, J. T. M. (2012). "Patch clamp techniques for plant cells," in *Plant Electrophysiology: Methods and Cell Electrophysiology*. ed. A. G. Volkov (Berlin Heidelberg: Springer-Verlag), 225–243.

Engelsdorf, T., Gigli-Bisceglia, N., Veerabagu, M., McKenna, J. F., Vaahtera, L., and Augstein, F. (2018). The plant cell wall integrity maintenance and immune signaling systems cooperate to control stress responses in *Arabidopsis thaliana*. *Sci. Signal.* 11:eaao3070. doi: 10.1126/scisignal.aao3070

Faraco, M., di Sansebastiano, G. P., Spelt, K., Koes, R. E., and Quattrocchio, F. M. (2011). One protoplast is not the other! *Plant Physiol.* 156, 474–478. doi: 10.1104/pp.111.173708

Fliegmann, J., Jauneau, A., Pichereaux, C., Rosenberg, C., Gasciolli, V., Timmers, A. C. J., et al. (2016). LYR3, a high-affinity LCO-binding protein of Medicago truncatula, interacts with LYK3, a key symbiotic receptor. *FEBS Lett.* 590, 1477–1487. doi: 10.1002/1873-3468.12191

Fowke, L. C., Rennie, P. J., and Constabel, F. (1983). Organelles associated with the plasma membrane of tobacco leaf protoplasts. *Plant Cell Rep.* 2, 292–295. doi: 10.1007/BF00270184

Fuchs, I., Stölzle, S., Ivashikina, N., and Hedrich, R. (2005). Rice K+ uptake channel OsAKT1 is sensitive to salt stress. *Planta* 221, 212–221. doi: 10.1007/s00425-004-1437-9

Fujikawa, Y., and Kato, N. (2007). TECHNICAL ADVANCE: split luciferase complementation assay to study protein–protein interactions in *Arabidopsis* protoplasts. *Plant J.* 52, 185–195. doi: 10.1111/j.1365-313X.2007.03214.x

Gichner, T., Znidar, I., Wagner, E. D., and Plewa, M. J. (2009). "Chapter 4. The use of higher plants in the comet assay," in *Issues in Toxicology*. eds. A. Dhawan and D. Anderson (Cambridge: Royal Society of Chemistry), 98–119.

Glazebrook, J. (2005). Contrasting mechanisms of defense against biotrophic and necrotrophic pathogens. *Annu. Rev. Phytopathol.* 43, 205–227. doi: 10.1146/annurev.phyto.43.040204.135923

Gong, B. Q., Guo, J., Zhang, N., Yao, X., Wang, H. B., and Li, J. F. (2019). Cross-microbial protection via priming a conserved immune co-receptor through juxtamembrane phosphorylation in plants. *Cell Host Microbe* 26, 810–822. doi: 10.1016/j.chom.2019.10.010

Gong, Z., Xiong, L., Shi, H., Yang, S., Herrera-Estrella, L. R., Xu, G., et al. (2020). Plant abiotic stress response and nutrient use efficiency. *Sci. China Life Sci.* 63, 635–674. doi: 10.1007/s11427-020-1683-x

González-García, M. P., Bustillo-Avendaño, E., Sanchez-Corrionero, A., Del Pozo, J. C., and Moreno-Risueno, M. A. (2020). Fluorescence-activated cell sorting using the D-root device and optimization for scarce and/or non-accessible root cell populations. *Plan. Theory* 9:499. doi: 10.3390/plants9040499

Gou, Y.-J., Li, Y.-L., Bi, P.-P., Wang, D.-J., Ma, Y.-Y., Hu, Y., et al. (2020). Optimization of the protoplast transient expression system for gene functional studies in strawberry (*Fragaria vesca*). *Plant Cell Tissue Organ Cult.* 141, 41–53. doi: 10.1007/s11240-020-01765-x

Greger, M., Kabir, A. H., Landberg, T., Maity, P. J., and Lindberg, S. (2016). Silicate reduces cadmium uptake into cells of wheat. *Environ. Pollut.* 211, 90–97. doi: 10.1016/j.envpol.2015.12.027

Gronnier, J., Gerbeau-Pissot, P., Germain, V., Mongrand, S., and Simon-Plas, F. (2018). Divide and rule: plant plasma membrane organization. *Trends Plant Sci.* 23, 899–917. doi: 10.1016/j.tplants.2018.07.007

Gronnier, J., Germain, V., Gouguet, P., Cacas, J. L., and Mongrand, S. (2016). GIPC: Glycosyl inositol phospho ceramides, the major sphingolipids on earth. *Plant Signal. Behav.* 11:e1152438. doi: 10.1080/15592324.2016.1152438

Grosjean, K., Der, C., Robert, F., Thomas, D., Mongrand, S., Simon-Plas, F., et al. (2018). Interactions between lipids and proteins are critical for organization of plasma membrane-ordered domains in tobacco BY-2 cells. *J. Exp. Bot.* 69, 3545–3557. doi: 10.1093/jxb/ery152

Gul, M., Wakeel, A., Steffens, D., and Lindberg, S. (2019). Potassium-induced decrease in cytosolic Na+ alleviates deleterious effects of salt stress on wheat (*Triticum aestivum* L.). *Plant Biol.* 21, 825–831. doi: 10.1111/plb.12999

Guyon-Debast, A., Alboresi, A., Terret, Z., Charlot, F., Berthier, F., Vendrell-Mir, P., et al. (2021). A blueprint for gene function analysis through base editing in the model plant *Physcomitrium (Physcomitrella) patens*. *New Phytol.* 230, 1258–1272. doi: 10.1111/nph.17171

Hahn, F., Korolev, A., Sanjurjo Loures, L., and Nekrasov, V. (2020). A modular cloning toolkit for genome editing in plants. *BMC Plant Biol.* 20:179. doi: 10.1186/s12870-020-02388-2

Halter, T., Imkampe, J., Mazzotta, S., Wierzba, M., Postel, S., Bücherl, C., et al. (2014). The leucine-rich repeat receptor kinase BIR2 is a negative regulator of BAK1 in plant immunity. *Curr. Biol.* 24, 134–143. doi: 10.1016/j.cub.2013.11.047

Hamilton, E. S., Schlegel, A. M., and Haswell, E. S. (2015). United in diversity: mechanosensitive ion channels in plants. *Annu. Rev. Plant Biol.* 66, 113–137. doi: 10.1146/annurev-arplant-043014-114700

Haswell, E. S., Peyronnet, R., Barbier-Brygoo, H., Meyerowitz, E. M., and Frachisse, J.-M. (2008). Two MscS homologs provide mechanosensitive channel activities in the *Arabidopsis* root. *Curr. Biol.* 18, 730–734. doi: 10.1016/j.cub.2008.04.039

Hellens, R. P., Allan, A. C., Friel, E. N., Bolitho, K., Grafton, K., Templeton, M. D., et al. (2005). Transient expression vectors for functional genomics, quantification of promoter activity and RNA silencing in plants. *Plant Methods* 1:13. doi: 10.1186/1746-4811-1-13

Hsu, S.-F., Lai, H.-C., and Jinn, T.-L. (2010). Cytosol-localized heat shock factor-binding protein, AtHSBP, functions as a negative regulator of heat shock response by translocation to the nucleus and is required for seed development in *Arabidopsis*. *Plant Physiol.* 153, 773–784. doi: 10.1104/pp.109.151225

Huby, E., Napier, J. A., Baillieul, F., Michaelson, L. V., and Dhondt-Cordelier, S. (2020). Sphingolipids: towards an integrated view of metabolism during the plant stress response. *New Phytol.* 225, 659–670. doi: 10.1111/nph.15997

Iven, T., Strathmann, A., Böttner, S., Zwafink, T., Heinekamp, T., Guivarc'h, A., et al. (2010). Homo- and heterodimers of tobacco bZIP proteins counteract as positive or negative regulators of transcription during pollen development. *Plant J.* 63, 155–166. doi: 10.1111/j.1365-313X.2010.04230.x

Jeworutzki, E., Roelfsema, M. R. G., Anschütz, U., Krol, E., Elzenga, J. T. M., Felix, G., et al. (2010). Early signaling through the *Arabidopsis* pattern recognition receptors FLS2 and EFR involves Ca^{2+}-associated opening of plasma membrane anion channels. *Plant J.* 62, 367–378. doi: 10.1111/j.1365-313X.2010.04155.x

Jones, J. D. G., and Dangl, J. L. (2006). The plant immune system. *Nature* 444, 323–329. doi: 10.1038/nature05286

Kadota, Y., Shirasu, K., and Zipfel, C. (2015). Regulation of the NADPH oxidase RBOHD during plant immunity. *Plant Cell Physiol.* 56, 1472–1480. doi: 10.1093/pcp/pcv063

Kerppola, T. K. (2006). Design and implementation of bimolecular fluorescence complementation (BiFC) assays for the visualization of protein interactions in living cells. *Nat. Protoc.* 1, 1278–1286. doi: 10.1038/nprot.2006.201

Kinoshita, E., Kinoshita-Kikuta, E., and Koike, T. (2015). Advances in Phostag-based methodologies for separation and detection of the phosphoproteome. *Biochim. Biophys. Acta* 1854, 601–608. doi: 10.1016/j.bbapap.2014.10.004

Kinoshita, E., Kinoshita-Kikuta, E., Takiyama, K., and Koike, T. (2006). Phosphatebinding tag, a new tool to visualize phosphorylated proteins. *Mol. Cell. Proteomics* 5, 749–757. doi: 10.1074/mcp.T500024-MCP200

Kinoshita-Kikuta, E., Aoki, Y., Kinoshita, E., and Koike, T. (2007). Label-free kinase profiling using phosphate affinity polyacrylamide gel electrophoresis. *Mol. Cell. Proteomics* 6, 356–366. doi: 10.1074/mcp.T600044-MCP200

Klymchenko, A. S. (2017). Solvatochromic and fluorogenic dyes as environmentsensitive probes: design and biological applications. *Acc. Chem. Res.* 50, 366–375. doi: 10.1021/acs.accounts.6b00517

Klymchenko, A. S., and Kreder, R. (2014). Fluorescent probes for lipid rafts: from model membranes to living cells. *Chem. Biol.* 21, 97–113. doi: 10.1016/j.chembiol.2013.11.009

Kollárová, K., Kusá, Z., Vatehová-Vivodová, Z., and Lišková, D. (2019). The response of maize protoplasts to cadmium stress mitigated by silicon. *Ecotoxicol. Environ. Saf.* 170, 488–494. doi: 10.1016/j.ecoenv.2018.12.016

Kovtun, Y., Chiu, W. L., Zeng, W., and Sheen, J. (1998). Suppression of auxin signal transduction by a MAPK cascade in higher plants. *Nature* 395, 716–720. doi: 10.1038/27240

Krzesłowska, M. (2011). The cell wall in plant cell response to trace metals: polysaccharide remodeling and its role in defense strategy. *Acta Physiol. Plant.* 33, 35–51. doi: 10.1007/s11738-010-0581-z

Kudla, J., and Bock, R. (2016). Lighting the way to protein-protein interactions: recommendations on best practices for bimolecular fluorescence complementation analyses. *Plant Cell* 28, 1002–1008. doi: 10.1105/tpc.16.00043

Kuki, H., Higaki, T., Yokoyama, R., Kuroha, T., Shinohara, N., Hasezawa, S., et al. (2017). Quantitative confocal imaging method for analyzing cellulose dynamics during cell wall regeneration in *Arabidopsis* mesophyll protoplasts. *Plant Direct* 1:e00021. doi: 10.1002/pld3.21

Kuzminsky, E., Meschini, R., Terzoli, S., Pavani, L., Silvestri, C., Choury, Z., et al. (2016). Isolation of mesophyll protoplasts from mediterranean woody plants for the study of DNA integrity under abiotic stress. *Front. Plant Sci.* 7:1168. doi: 10.3389/fpls.2016.01168

Lamers, J., van der Meer, T., and Testerink, C. (2020). How plants sense and respond to stressful environments. *Plant Physiol.* 182, 1624–1635. doi: 10.1104/pp.19.01464

Ledoux, Q., Van Cutsem, P., Markó, I. E., and Veys, P. (2014). Specific localization and measurement of hydrogen peroxide in *Arabidopsis thaliana* cell suspensions and protoplasts elicited by COS-OGA. *Plant Signal. Behav.* 9:e28824. doi: 10.4161/psb.28824

Lee, Y.-S., Mitiku, G., and Endress, A. G. (2001). Short-term effects of Al3+ on the osmotic behavior of red beet (*Beta vulgaris* L.) protoplasts. *Plant Soil* 228, 223–232. doi: 10.1023/A:1004886115326

Lenarčič, T., Albert, I., Böhm, H., Hodnik, V., Pirc, K., Zavec, A. B., et al. (2017). Eudicot plant-specific sphingolipids determine host selectivity of microbial NLP cytolysins. *Science* 358, 1431–1434. doi: 10.1126/science.aan6874

Lew, T. T. S., Wong, M. H., Kwak, S., Sinclair, R., Koman, V. B., and Strano, M. S. (2018). Rational design principles for the transport and subcellular distribution of nanomaterials into plant protoplasts. *Small* 14:1802086. doi: 10.1002/smll.201802086

Li, Z., Ao, Y., Feng, D., Liu, J., Wang, J., Wang, H. B., et al. (2017). OsRLCK 57, OsRLCK107 and OsRLCK118 positively regulate chitin- and PGN-induced immunity in rice. *Rice* 10:6. doi: 10.1186/s12284-017-0145-6

Li, J.-F., Bush, J., Xiong, Y., Li, L., and McCormack, M. (2011). Large-scale protein-protein interaction analysis in *Arabidopsis* mesophyll protoplasts by split firefly luciferase complementation. *PLoS One* 6:e27364. doi: 10.1371/journal.pone.0027364

Li, H., Dai, X., Huang, X., Xu, M., Wang, Q., Yan, X., et al. (2021). Single-cell RNA sequencing reveals a high-resolution cell atlas of xylem in *Populus*. *J. Integr. Plant Biol.* doi: 10.1111/jipb.13159

Li, B., Ferreira, M. A., Huang, M., Camargos, L. F., Yu, X., Teixeira, R. M., et al. (2019). The receptor-like kinase NIK1 targets FLS2/BAK1 immune complex and inversely modulates antiviral and antibacterial immunity. *Nat. Commun.* 10:4996. doi: 10.1038/s41467-019-12847-6

Li, M., Sun, X., Di, D., Zhang, A., Qing, L., Zhou, T., et al. (2020). Maize AKINβγ proteins interact with P8 of rice black streaked dwarf virus and inhibit viral infection. *Viruses* 12:1387. doi: 10.3390/v12121387

Li, J. F., Zhang, D., and Sheen, J. (2014). Epitope-tagged protein-based artificial miRNA screens for optimized gene silencing in plants. *Nat. Protoc.* 9, 939–949. doi: 10.1038/nprot.2014.061

Lim, G. H., Singhal, R., Kachroo, A., and Kachroo, P. (2017). Fatty acid- and lipid-mediated signaling in plant defense. *Annu. Rev. Phytopathol.* 55, 505–536. doi: 10.1146/annurev-phyto-080516-035406

Lin, H. Y., Chen, J. C., and Fang, S. C. (2018). A protoplast transient expression system to enable molecular, cellular, and functional studies in phalaenopsis orchids. *Front. Plant Sci.* 9:843. doi: 10.3389/fpls.2018.00843

Lin, Y.-C., Li, W., Chen, H., Li, Q., Sun, Y.-H., Shi, R., et al. (2014). A simple improved-throughput xylem protoplast system for studying wood formation. *Nat. Protoc.* 9, 2194–2205. doi: 10.1038/nprot.2014.147

Liu, Q., Chen, B., Wang, Q., Shi, X., Xiao, Z., Lin, J., et al. (2009). Carbon nanotubes as molecular transporters for walled plant cells. *Nano Lett.* 9, 1007–1010. doi: 10.1021/nl803083u

Liu, Z., Jia, Y., Ding, Y., Shi, Y., Li, Z., Guo, Y., et al. (2017). Plasma membrane CRPK1-mediated phosphorylation of 14-3-3 proteins induces their nuclear import to fine-tune CBF signaling during cold response. *Mol. Cell* 66, 117.e5–128.e5. doi: 10.1016/j.molcel.2017.02.016

Liu, C., Ou, S., Mao, B., Tang, J., Wang, W., Wang, H., et al. (2018). Early selection of bZIP73 facilitated adaptation of japonica rice to cold climates. *Nat. Commun.* 9:3302. doi: 10.1038/s41467-018-05753-w

Liya, M., Huan, Z., Lirong, S., Yiheng, J., Guozeng, Z., Chen, M., et al. (2012). NADPH oxidase AtrbohD and AtrbohF function in ROS-dependent regulation of Na$^+$/K$^+$ homeostasis in *Arabidopsis* under salt stress. *J. Exp. Bot.* 63, 305–317. doi: 10.1093/jxb/err280

Long, Y., Stahl, Y., Weidtkamp-Peters, S., Smet, W., Du, Y., Gadella, T. W. J. J., et al. (2018). Optimizing FRET-FLIM labeling conditions to detect nuclear protein interactions at native expression levels in living *Arabidopsis* roots. *Front. Plant Sci.* 9:639. doi: 10.3389/fpls.2018.00639

Ma, X., Claus, L. A. N., Leslie, M. E., Tao, K., Wu, Z., Liu, J., et al. (2020). Ligand-induced monoubiquitination of BIK1 regulates plant immunity. *Nature* 581, 199–203. doi: 10.1038/s41586-020-2210-3

Maintz, J., Cavdar, M., Tamborski, J., Kwaaitaal, M., Huisman, R., Meesters, C., et al. (2014). Comparative analysis of MAMP-induced calcium influx in *Arabidopsis* seedlings and protoplasts. *Plant Cell Physiol.* 55, 1813–1825. doi: 10.1093/pcp/pcu112

Malinovsky, F. G. (2014). The role of the cell wall in plant immunity. *Front. Plant Sci.* 5:178. doi: 10.3389/fpls.2014.00178

Mamode Cassim, A., Gouguet, P., Gronnier, J., Laurent, N., Germain, V., Grison, M., et al. (2019). Plant lipids: key players of plasma membrane organization and function. *Prog. Lipid Res.* 73, 1–27. doi: 10.1016/j.plipres.2018.11.002

Martinière, A., Lavagi, I., Nageswaran, G., Rolfe, D. J., Maneta-Peyret, L., Luu, D. T., et al. (2012). Cell wall constrains lateral diffusion of plant plasma-membrane proteins. *Proc. Natl. Acad. Sci. U. S. A.* 109, 12805–12810. doi: 10.1073/pnas.1202040109

Menzel, W., Stenzel, I., Helbig, L., Krishnamoorthy, P., Neumann, S., Eschen-Lippold, L., et al. (2019). A PAMP-triggered MAPK cascade inhibits phosphatidylinositol 4,5-bisphosphate production by PIP5K6 in *Arabidopsis thaliana*. *New Phytol.* 224, 833–847. doi: 10.1111/nph.16069

Miao, Y., and Jiang, L. (2007). Transient expression of fluorescent fusion proteins in protoplasts of suspension cultured cells. *Nat. Protoc.* 2, 2348–2353. doi: 10.1038/nprot.2007.360

Milewska-Hendel, A., Zubko, M., Stróż, D., and Kurczyńska, E. (2019). Effect of nanoparticles surface charge on the *Arabidopsis thaliana* (L.) roots development and their movement into the root cells and protoplasts. *Int. J. Mol. Sci.* 20:1650. doi: 10.3390/ijms20071650

Moon, S.-J., Min, M. K., Kim, J.-A., Kim, D. Y., Yoon, I. S., Kwon, T. R., et al. (2019). Ectopic expression of OsDREB1G, a member of the OsDREB1 subfamily, confers cold stress tolerance in rice. *Front. Plant Sci.* 10:297. doi: 10.3389/fpls.2019.00297

Mueller, K., Bittel, P., Chinchill, D., Jehle, A. K., Albert, M., Boller, T., et al. (2012). Chimeric FLS2 receptors reveal the basis for differential flagellin perception in *Arabidopsis* and tomato. *Plant Cell* 24, 2213–2224. doi: 10.1105/tpc.112.096073

Nagano, M., Ishikawa, T., Fujiwara, M., Fukao, Y., Kawano, Y., Kawai-Yamada, M., et al. (2016). Plasma membrane microdomains are essential for Rac1-RbohB/H-mediated immunity in rice. *Plant Cell* 28, 1966–1983. doi: 10.1105/tpc.16.00201

Nakagawa, Y., Katagiri, T., Shinozaki, K., Qi, Z., Tatsumi, H., Furuichi, T., et al. (2007). *Arabidopsis* plasma membrane protein crucial for Ca^{2+} influx and touch sensing in roots. *Proc. Natl. Acad. Sci. U. S. A.* 104, 3639–3944. doi: 10.1073/pnas.0607703104

Neelakandan, A. K., and Wang, K. (2012). Recent progress in the understanding of tissue culture-induced genome level changes in plants and potential applications. *Plant Cell Rep.* 31, 597–620. doi: 10.1007/s00299-011-1202-z

Nelson, B. K., Cai, X., and Nebenführ, A. (2007). A multicolored set of in vivo organelle markers for co-localization studies in *Arabidopsis* and other plants. *Plant J.* 51, 1126–1136. doi: 10.1111/j.1365-313X.2007.03212.x

Nicolia, A., Fält, A.-S., Hofvander, P., and Handersson, M. (2021). "Protoplast-based method for genome editing in tetraploid potato," in *Crop Breeding: Genetic Improvement Methods in Molecular Biology*. ed. Tripodi (New York, NY: Springer US), 177–186.

Park, W., Kim, H.-S., Park, T.-W., Lee, Y.-H., and Ahn, S.-J. (2017). Functional characterization of plasma membrane-localized organic acid transporter (CsALMT1) involved in aluminum tolerance in *Camelina sativa* L. *Plant Biotechnol. Rep.* 11, 181–192. doi: 10.1007/s11816-017-0441-z

Pasternak, T., Lystvan, K., Betekhtin, A., and Hasterok, R. (2020). From single cell to plants: mesophyll protoplasts as a versatile system for investigating plant cell reprogramming. *Int. J. Mol. Sci.* 21:4195. doi: 10.3390/ijms21124195

Pecher, P., Eschen-Lippold, L., Herklotz, S., Kuhle, K., Naumann, K., Bethke, G., et al. (2014). The *Arabidopsis thaliana* mitogen-activated protein kinases MPK3 and MPK6 target a subclass of 'VQ-motif'-containing proteins to regulate immune responses. *New Phytol.* 203, 592–606. doi: 10.1111/nph.12817

Petropoulou, Y., Manetas, Y., and Gavalas, N. A. (1990). Intact mesophyll protoplasts from *Zea mays* as a source of phosphoenolpyruvate carboxylase unaffected by extraction: advantages and limitations. *Physiol. Plant.* 80, 605–611. doi: 10.1111/j.1399-3054.1990.tb05685.x

Pham, A. Q., Cho, S.-H., Nguyen, C. T., and Stacey, G. (2020). *Arabidopsis* lectin receptor kinase P2K2 is a second plant receptor for extracellular ATP and contributes to innate immunity. *Plant Physiol.* 183, 1364–1375. doi: 10.1104/pp.19.01265

Poot-Poot, W., Rodas-Junco, B. A., Muñoz-Sánchez, J. A., and Hernández-Sotomayor, S. M. T. (2016). Protoplasts: a friendly tool to study aluminum toxicity and coffee cell viability. *Springerplus* 5:1452. doi: 10.1186/s40064-016-3140-2

Qiu, L., Wang, Y., and Qu, H. (2020). Loading calcium fluorescent probes into protoplasts to detect calcium in the flesh tissue cells of *Malus domestica*. *Hortic. Res.* 7:91. doi: 10.1038/s41438-020-0315-3

Ramon, M., Dang, T. V. T., Broeckx, T., Hulsmans, S., Crepin, N., Sheen, J., et al. (2019). Default activation and nuclear translocation of the plant cellular energy sensor snrk1 regulate metabolic stress responses and development. *Plant Cell* 31, 1614–1632. doi: 10.1105/tpc.18.00500

Rios, A. F., Radoeva, T., De Rybel, B., Weijers, D., and Borst, J. W. (2017). "FRET-FLIM for visualizing and quantifying protein interactions in live plant cells," in *Plant Hormones: Methods and Protocols. Methods in Molecular Biology. Vol. 1497*. eds. J. Kleine-Vehn and M. Sauer (New York, NY: Springer), 135–146.

Saijo, Y., and Loo, E. P. (2020). Plant immunity in signal integration between biotic and abiotic stress responses. *New Phytol.* 225, 87–104. doi: 10.1111/nph.15989

Sakai, K., Charlot, F., Le Saux, T., Bonhomme, S., Nogué, F., Palauqui, J.-C., et al. (2019). Design of a comprehensive microfluidic and microscopic toolbox for the ultra-wide spatio-temporal study of plant protoplasts development and physiology. *Plant Methods* 15:79. doi: 10.1186/s13007-019-0459-z

Sangra, A., Shahin, L., and Dhir, S. K. (2019). Optimization of isolation and culture of protoplasts in alfalfa (*Medicago sativa*) cultivar Regen-SY. *Am. J. Plant Sci.* 10, 1206–1219. doi: 10.4236/ajps.2019.107086

Santos, C. L. V., Pourrut, B., and Ferreira de Oliveira, J. M. P. (2015). The use of comet assay in plant toxicology: recent advances. *Front. Genet.* 6:216. doi: 10.3389/fgene.2015.00216

Saur, I. M. L., Bauer, S., Lu, X., and Schulze-Lefert, P. (2019). A cell death assay in barley and wheat protoplasts for identification and validation of matching pathogen AVR effector and plant NLR immune receptors. *Plant Methods* 15:118. doi: 10.1186/s13007-019-0502-0

Schellenberger, R., Touchard, M., Clément, C., Baillieul, F., Cordelier, S., Crouzet, J., et al. (2019). Apoplastic invasion patterns triggering plant immunity: plasma membrane sensing at the frontline. *Mol. Plant Pathol.* 20, 1602–1616. doi: 10.1111/mpp.12857

Shan, X., Li, Y., Zhou, L., Tong, L., Wei, C., Qiu, L., et al. (2019). Efficient isolation of protoplasts from freesia callus and its application in transient expression assays. *Plant Cell Tissue Organ Cult.* 138, 529–541. doi: 10.1007/s11240-019-01649-9

Sharma, M., Bennewitz, B., and Klösgen, R. B. (2018). Dual or not dual? – comparative analysis of fluorescence microscopy-based approaches to study organelle targeting specificity of nuclear-encoded plant proteins. *Front. Plant Sci.* 9:1350. doi: 10.3389/fpls.2018.01350

Shaw, R., Tian, X., and Xu, J. (2021). Single-cell transcriptome analysis in plants: advances and challenges. *Mol. Plant* 14, 115–126. doi: 10.1016/j.molp.2020.10.012

Sheen, J. (2001). Signal transduction in maize and *Arabidopsis* mesophyll protoplasts. *Plant Physiol.* 127, 1466–1475. doi: 10.1104/pp.010820

Sheikh, A. H., Eschen-Lippold, L., Pecher, P., Hoehenwarter, W., Sinha, A. K., Scheel, D., et al. (2016). Regulation of WRKY46 transcription factor function by mitogen-activated protein kinases in *Arabidopsis thaliana*. *Front. Plant Sci.* 7:61. doi: 10.3389/fpls.2016.00061

Shen, J., Suen, P. K., Wang, X., Lin, Y., Lo, S. W., Rojo, E., et al. (2013). An in vivo expression system for the identification of cargo proteins of vacuolar sorting receptors in *Arabidopsis* culture cells. *Plant J.* 75, 1003–1017. doi: 10.1111/tpj.12257

Souza, C. d. A., Li, S., Lin, A. Z., Boutrot, F., Grossmann, G., Zipfel, C., et al. (2020). Cellulose-derived oligomers act as damage-associated molecular patterns and trigger defense-like responses. *Plant Physiol.* 173, 2383–2398. doi: 10.1104/pp.16.01680

Struk, S., Jacobs, A., Martín-Fontecha, E. S., Gevaert, K., Cubas, P., and Goormachtig, S. (2019). Exploring the protein–protein interaction landscape in plants. *Plant Cell Environ.* 42, 387–409. doi: 10.1111/pce.13433

Sze, H., and Chanroj, S. (2018). Plant endomembrane dynamics: studies of K+/H+ antiporters provide insights on the effects of pH and ion homeostasis. *Plant Physiol.* 177, 875–895. doi: 10.1104/pp.18.00142

Tagawa, S., and Kondo, T. (2018). Secretion of a callose hollow fiber from herbaceous plant protoplasts induced by inhibition of cell wall formation. *J. Wood Sci.* 64, 467–476. doi: 10.1007/s10086-018-1726-8

Tagawa, S., Yamagishi, Y., Watanabe, U., Funada, R., and Kondo, T. (2019). Dynamics of structural polysaccharides deposition on the plasma-membrane surface of plant protoplasts during cell wall regeneration. *J. Wood Sci.* 65:47. doi: 10.1186/s10086-019-1826-0

Takahashi, Y., Zhang, J., Hsu, P. K., Ceciliato, P. H. O., Zhang, L., Dubeaux, G., et al. (2020). MAP3Kinase-dependent SnRK2-kinase activation is required for abscisic acid signal transduction and rapid osmotic stress response. *Nat. Commun.* 11:12. doi: 10.1038/s41467-019-13875-y

Takai, R., Kaneda, T., Isogai, A., Takayama, S., and Che, F. S. (2007). A new method of defense response analysis using a transient expression system in rice protoplasts. *Biosci. Biotechnol. Biochem.* 71, 590–593. doi: 10.1271/bbb.60526

Thévenin, J., Dubos, C., Xu, W., Gourrierec, J. L., Kelemen, Z., Charlot, F., et al. (2012). A new system for fast and quantitative analysis of heterologous gene expression in plants. *New Phytol.* 193, 504–512. doi: 10.1111/j.1469-8137.2011.03936.x

Tian, W., Hou, C., Ren, Z., Wang, C., Zhao, F., Dahlbeck, D., et al. (2019). A calmodulin-gated calcium channel links pathogen patterns to plant immunity. *Nature* 572, 131–135. doi: 10.1038/s41586-019-1413-y

Torney, F., Trewyn, B. G., Lin, V. S.-Y., and Wang, K. (2007). Mesoporous silica nanoparticles deliver DNA and chemicals into plants. *Nat. Nanotechnol.* 2, 295–300. doi: 10.1038/nnano.2007.108

Tripathi, D., Nam, A., Oldenburg, D. J., and Bendich, A. J. (2020). Reactive oxygen species, antioxidant agents, and DNA damage in developing maize mitochondria and plastids. *Front. Plant Sci.* 11:596. doi: 10.3389/fpls.2020.00596

Underwood, W., Ryan, A., and Somerville, S. C. (2017). An *Arabidopsis* lipid flippase is required for timely recruitment of defenses to the host–pathogen

interface at the plant cell surface. *Mol. Plant* 10, 805–820. doi: 10.1016/j.molp.2017.04.003

Wang, X., Feng, C., Tian, L., Hou, C., Tian, W., Hu, B., et al. (2021). A transceptor–channel complex couples nitrate sensing to calcium signaling in *Arabidopsis*. *Mol. Plant* 14, 774–786. doi: 10.1016/j.molp.2021.02.005

Wang, A., Jin, Q., Xu, X., Miao, A., White, J. C., Gardea-Torresdey, J. L., et al. (2020a). High-throughput screening for engineered nanoparticles that enhance photosynthesis using mesophyll protoplasts. *J. Agric. Food Chem.* 68, 3382–3389. doi: 10.1021/acs.jafc.9b06429

Wang, F., Jing, W., and Zhang, W. (2014). The mitogen-activated protein kinase cascade MKK1-MPK4 mediates salt signaling in rice. *Plant Sci.* 227, 181–189. doi: 10.1016/j.plantsci.2014.08.007

Wang, F.-Z., Zhang, N., Guo, Y.-J., Gong, B.-Q., and Li, J.-F. (2020b). Split Nano luciferase complementation for probing protein-protein interactions in plant cells. *J. Integr. Plant Biol.* 62, 1065–1079. doi: 10.1111/jipb.12891

Wani, S. H., Anand, S., Singh, B., Bohra, A., and Joshi, R. (2021). WRKY transcription factors and plant defense responses: latest discoveries and future prospects. *Plant Cell Rep.* 40, 1071–1085. doi: 10.1007/s00299-021-02691-8

Watanabe, M., Setoguchi, D., Uehara, K., Ohtsuka, W., and Watanabe, Y. (2002). Apoptosis-like cell death of *Brassica napus* leaf protoplasts. *New Phytol.* 156, 417–426. doi: 10.1046/j.1469-8137.2000.00536.x

Wehner, N., Hartmann, L., Ehlert, A., Böttner, S., Oñate-Sánchez, L., and Dröge-Laser, W. (2011). High-throughput protoplast transactivation (PTA) system for the analysis of *Arabidopsis* transcription factor function. *Plant J.* 68, 560–569. doi: 10.1111/j.1365-313X.2011.04704.x

Weibull, C. (1953). The isolation of protoplasts from *bacillus megaterium* by controlled treatment with lysozyme. *J. Bacteriol.* 66, 688–695. doi: 10.1128/jb.66.6.688-695.1953

Wu, F., Chi, Y., Jiang, Z., Xu, Y., Xie, L., Huang, F., et al. (2020a). Hydrogen peroxide sensor HPCA1 is an LRR receptor kinase in *Arabidopsis*. *Nature* 578, 577–581. doi: 10.1038/s41586-020-2032-3

Wu, H. Y., Liu, K. H., Wang, Y. C., Wu, J. F., Chiu, W. L., Chen, C. Y., et al. (2014a). AGROBEST: an efficient *agrobacterium*-mediated transient expression method for versatile gene function analyses in *Arabidopsis* seedlings. *Plant Methods* 10:19. doi: 10.1186/1746-4811-10-19

Wu, S., Shan, L., and He, P. (2014b). Microbial signature-triggered plant defense responses and early signaling mechanisms. *Plant Sci.* 228, 118–126. doi: 10.1016/j.plantsci.2014.03.001

Wu, S., Zhu, H., Liu, J., Yang, Q., Shao, X., Bi, F., et al. (2020b). Establishment of a PEG-mediated protoplast transformation system based on DNA and CRISPR/Cas9 ribonucleoprotein complexes for banana. *BMC Plant Biol.* 20:425. doi: 10.1186/s12870-020-02609-8

Xing, T., and Wang, X. (2015). Protoplasts in plant signaling analysis: moving forward in the omics era. *Botany* 93, 325–332. doi: 10.1139/cjb-2014-0219

Yang, J., Liu, S., Ji, L., Tang, X., Zhu, Y., and Xie, G. (2020). Identification of novel OsCML16 target proteins and differential expression analysis under abiotic stresses in rice. *J. Plant Physiol.* 249:153165. doi: 10.1016/j.jplph.2020.153165

Ye, K., Li, H., Ding, Y., Shi, Y., Song, C., Gong, Z., et al. (2019). BRASSINOSTEROID-INSENSITIVE2 negatively regulates the stability of transcription factor ICE1 in response to cold stress in *Arabidopsis*. *Plant Cell* 31, 2682–2696. doi: 10.1105/tpc.19.00058

Yeh, Y.-H., Chang, Y.-H., Huang, P.-Y., Huang, J.-B., and Zimmerli, L. (2015). Enhanced *Arabidopsis* pattern-triggered immunity by overexpression of cysteine-rich receptor-like kinases. *Front. Plant Sci.* 6:322. doi: 10.3389/fpls.2015.00322

Yekondi, S., Liang, F.-C., Okuma, E., Radziejwoski, A., Mai, H.-W., Swain, S., et al. (2018). Nonredundant functions of *Arabidopsis* LecRK-V.2 and LecRK-VII.1 in controlling stomatal immunity and jasmonate-mediated stomatal closure. *New Phytol.* 218, 253–268. doi: 10.1111/nph.14953

Yemelyanov, V. V., Chirkova, T. V., Shishova, M. F., and Lindberg, S. M. (2020). Potassium efflux and cytosol acidification as primary anoxia-induced events in wheat and rice seedlings. *Plan. Theory* 9:1216. doi: 10.3390/plants9091216

Yokoyama, R., Kuki, H., Kuroha, T., and Nishitani, K. (2016). *Arabidopsis* regenerating protoplast: a powerful model system for combining the proteomics

of cellwall proteins and the visualization of cell wall dynamics. *Proteomes* 4:34. doi: 10.3390/proteomes4040034

Yoo, S. D., Cho, Y. H., and Sheen, J. (2007). *Arabidopsis* mesophyll protoplasts: a versatile cell system for transient gene expression analysis. *Nat. Protoc.* 2, 1565–1572. doi: 10.1038/nprot.2007.199

Yoshioka, K., and Moeder, W. (2020). Calcium channel helps shut the door on intruders. *Nature* 585, 507–508. doi: 10.1038/d41586-020-02504-0

Yu, X., Feng, B., He, P., and Shan, L. (2017). From chaos to harmony: responses and signaling upon microbial pattern recognition. *Annu. Rev. Phytopathol.* 55, 109–137. doi: 10.1146/annurev-phyto-080516-035649

Yu, X., Xu, G., Li, B., de Souza Vespoli, L., Liu, H., Moeder, W., et al. (2019). The receptor kinases BAK1/SERK4 regulate Ca^{2+} channel-mediated cellular homeostasis for cell death containment. *Curr. Biol.* 29, 3778.e8–3790.e8. doi: 10.1016/j.cub.2019.09.018

Yu, Y., Yu, P.-C., Chang, W.-J., Yu, K., and Lin, C.-S. (2020). Plastid transformation: how does it work? Can it be applied to crops? What can it offer? *Int. J. Mol. Sci.* 21:4854. doi: 10.3390/ijms21144854

Zhang, M., Hu, S., Yi, F., Gao, Y., Zhu, D., Wang, Y., et al. (2021). Organelle visualization with multicolored fluorescent markers in bamboo. *Front. Plant Sci.* 12:552. doi: 10.3389/fpls.2021.658836

Zhang, Q.-F., Li, J., Bi, F.-C., Liu, Z., Chang, Z.-Y., Wang, L.-Y., et al. (2020). Ceramide-induced cell death depends on calcium and caspase-like activity in rice. *Front. Plant Sci.* 11:145. doi: 10.3389/fpls.2020.00145

Zhang, X., Wang, L., He, C., and Luo, H. (2016). An efficient transient mesophyll protoplast system for investigation of the innate immunity responses in the rubber tree (*Hevea brasiliensis*). *Plant Cell Tissue Organ Cult.* 126, 281–290. doi: 10.1007/s11240-016-0997-2

Zhao, C., Randall, D., Holford, P., Haigh, A. M., and Chen, Z. H. (2019). Isolation of high purity guard cell protoplasts of *Arabidopsis thaliana* for omics research. *Plant Growth Regul.* 89, 37–47. doi: 10.1007/s10725-019-00520-3

Zheng, X., Kang, S., Jing, Y., Ren, Z., Li, L., Zhou, J. M., et al. (2018). Danger-associated peptides close stomata by OST1-independent activation of anion channels in guard cells. *Plant Cell* 30, 1132–1146. doi: 10.1105/tpc.17.00701

Zhou, Q., Jiang, Z., Li, Y., Zhang, T., Zhu, H., Zhao, F., et al. (2019). Mesophyll protoplast isolation technique and flow cytometry analysis of ancient *Platycladus orientalis* (Cupressaceae). *Turk. J. Agric. For.* 43, 275–287. doi: 10.3906/tar-1805-62

Zhou, J., and Zhang, Y. (2020). Plant immunity: danger perception and signaling. *Cell* 181, 978–989. doi: 10.1016/j.cell.2020.04.028

Zhu, J. (2016). Review abiotic stress signaling and responses in plants. *Cell* 167, 313–324. doi: 10.1016/j.cell.2016.08.029

Zhu, D., Zhang, M., Gao, C., and Shen, J. (2020). Protein trafficking in plant cells: tools and markers. *Sci. China Life Sci.* 63, 343–363. doi: 10.1007/s11427-019-9598-3

Zipfel, C., and Oldroyd, G. E. D. (2017). Plant signalling in symbiosis and immunity. *Nature* 543, 328–336. doi: 10.1038/nature22009